การแปรผันปริมาณอิเล็กตรอนรวมเนื่องจากหมอกแม่เหล็กและปรากฏการณ์ต่างๆ

นายสรสิช ถนอมพลกรัง

วิทยานิพนธ์นี้เป็นส่วนหนึ่งของการศึกษาตามหลักสูตรปริญญาวิทยาศาสตรมหาบัณฑิต
สาขาวิชาโลกศาสตร์ ภาควิชาธรณีวิทยา
คณะวิทยาศาสตร์ จุฬาลงกรณ์มหาวิทยาลัย
ปีการศึกษา 2556

TOTAL ELECTRON CONTENT VARIATION RESULTING FROM MAGNETIC CLOUD WITH VARIOUS PHENOMENA

Mr. Sorasit Thanomponkrang

A Thesis Submitted in Partial Fulfillment of the Requirements
for the Degree of Master of Science Program in Earth Sciences
Department of Geology
Faculty of Science
Chulalongkorn University
Academic Year 2013

Thesis Title	TOTAL ELECTRON CONTENT VARIATION RESULTING FROM MAGNETIC CLOUD WITH VARIOUS PHENOMENA
By	Mr. Sorasit Thanomponkrang
Field of Study	Earth Sciences
Thesis Advisor	Paisan Tooprakai, Ph.D.
Thesis Co-Advisor	Sathon Vijarnwannaluk, Ph.D.

Accepted by the Faculty of Science, Chulalongkorn University in Partial Fulfillment of the Requirements for the Master's Degree

....Dean of the Faculty of Science

(Professor Supot Hannongbua, Ph.D.)

THESIS COMMITTEE

....Chairman

(Assistant Professor Sombut Yumuang, Ph.D.)

....Thesis Advisor

(Paisan Tooprakai, Ph.D.)

....Thesis Co-Advisor

(Sathon Vijarnwannaluk, Ph.D.)

....Examiner

(Assistant Professor Srilert Chotpantarat)

....External Examiner

(Nithiwatthn Choosakul, Ph.D.)

สรสิช ถนอมพลกรัง : การแปรผันปริมาณอิเล็กตรอนรวมเนื่องจากหมอกแม่เหล็กและปรากฏการณ์ต่างๆ. (TOTAL ELECTRON CONTENT VARIATION RESULTING FROM MAGNETIC CLOUD WITH VARIOUS PHENOMENA) อ.ที่ปรึกษาวิทยานิพนธ์หลัก: ดร. ไพศาล ตู้ประกาย, อ.ที่ปรึกษาวิทยานิพนธ์ร่วม: ดร. สธน วิจารณ์วรรณลักษณ์, 259 หน้า.

หมอกแม่เหล็ก (MCs) และปรากฏการณ์ต่างๆปะทะชั้นไอโอโนสเฟียร์ทุกวัน ปริมาณอิเล็กตรอนรวม (TEC) ในชั้นไอโอโนสเฟียร์ส่งผลต่อการแพร่กระจายคลื่นวิทยุผ่านไอโอโนสเฟียร์ อันตรกิริยาระหว่างหมอกแม่เหล็ก ปรากฏการณ์ต่างๆ และปริมาณอิเล็กตรอนรวมยังไม่รู้อย่างชัดเจน จุดมุ่งหมายสองข้อของการวิจัยครั้งนี้คือ (1) ศึกษาการแปรผันปริมาณอิเล็กตรอนรวมที่เป็นผลจากหมอกแม่เหล็กและปรากฏการณ์อื่น ๆ โดยใช้ร้อยละการเบี่ยงเบนของปริมาณอิเล็กตรอนรวม (2) หมอกแม่เหล็ก ตัวแปรของปรากฏการณ์อื่น ๆ และสัมประสิทธิการแปรผันปริมาณอิเล็กตรอนรวมปริมาณอิเล็กตรอนรวมภายใต้หมอกแม่เหล็ก (MCs) 6 เหตุการณ์ คลื่นกระแทกระหว่างดาวเคราะห์ (ISs) 5 เหตุการณ์ บริเวณอันตรกิริยา 2 เหตุการณ์ ชีธ 2 เหตุการณ์ กระแสอัตราเร็วสูง(HSSs) 10 เหตุการณ์ และกระแสคอโรนา (CSs) 5 เหตุการณ์ ได้จากสถานีจีพีเอสในทวีปอเมริกาเหนือและใต้เพื่อใช้ประมาณค่าการเบี่ยงเบนของปริมาณอิเล็กตรอนรวมดังนั้นโปรแกรมคอมพิวเตอร์จึงถูกสร้างขึ้นเพื่อตอบโจทย์นี้ การเคลื่อนที่ของหมอกแม่เหล็กชีธ และคลื่นกระแทกระหว่างดาวเคราะห์ทำให้ปริมาณอิเล็กตรอนรวมเพิ่มขึ้นกลายเป็นความผิดปกติของชั้นไอโอโนสเฟียร์บริเวณศูนย์สูตร แต่เปอร์เซ็นต์เบี่ยงเบนปริมาณอิเล็กตรอนรวมเนื่องจากเมฆแม่เหล็กและปรากฏการณ์ต่างๆไม่สามารถประมาณในการศึกษานี้ตัวแปรของหมอกแม่เหล็กและปรากฏการณ์ต่างๆ และปริมาณอิเล็กตรอนรวมสามารถหาการสอดคล้องโดยการถดถอยเชิงเส้นละติจูดแต่ละเส้นมีสมการของแต่ละเส้น และในละติจูดเดียวกันของเหตุการณ์ที่ต่างกันจะมีสมการที่ต่างกัน สัมประสิทธิการแปรผันของปริมาณอิเล็กตรอนรวมภายใต้การเคลื่อนที่เหล่านี้ไม่ขึ้นกับละติจูดภูมิมาตรศาสตร์

ภาควิชา	ธรณีวิทยา	ลายมือชื่อนิสิต	....
สาขาวิชา	โลกศาสตร์	ลายมือชื่อ อ.ที่ปรึกษาวิทยานิพนธ์หลัก	....
ปีการศึกษา	2556	ลายมือชื่อ อ.ที่ปรึกษาวิทยานิพนธ์ร่วม	....

5372352423 : MAJOR EARTH SCIENCES
KEYWORDS: 11 / TOTAL ELECTRON CONTENT (TEC) / MAGNETIC CLOUD / INTERPLANETARY SHOCK (IS)

SORASIT THANOMPONKRANG: TOTAL ELECTRON CONTENT VARIATION RESULTING FROM MAGNETIC CLOUD WITH VARIOUS PHENOMENA. ADVISOR: PAISAN TOOPRAKAI, Ph.D., CO-ADVISOR: SATHON VIJARNWANNALUK, Ph.D., 259 pp.

Magnetic clouds (MCs) and various phenomena hit the ionosphere every day. Total electron contents (TEC) in the ionosphere influence on trans-ionospheric radio propagation. The interaction between MCs, phenomena, and TEC was not clearly known. Two aims of this research are to (1) study TEC variation resulting from MC and other phenomena by using percent deviation of TEC, (2) MC,parameters of the other phenomena, and TEC variation coefficients. TEC under 6 magnetic clouds (MCs), 5 interplanetary shocks (ISs), 2 interaction regions (IRs), 2 sheathes, 10 high speed streams (HSSs), and 5 coronal streams (CSs) derived from GPS stations in north and south America for estimated deviation of TEC. Therefore the computer program was constructed to answer this question. The motion of MC, sheathes, and ISs made TEC increase to be the equatorial ionospheric anomaly (EIA) but dTEC% resulting from MC and various phenomena can't estimate in this study. Parameters of MC and various phenomena, and TEC can be fitted by the linear regression. Each latitude has its equation, andin the same latitude of different events, will have the different equations. Coefficients of variation of TEC under these motions do not depend on geodetic latitude.

Department:	Geology	Student's Signature	....
Field of Study:	Earth Sciences	Advisor's Signature	....
Academic Year:	2013	Co-Advisor's Signature	....

ACKNOWLEDGEMENTS

I would like to express my deepest sincere appreciation to Dr.Paisan Tooprakai and Dr.Sathon Vijarnwannaluk for their expert advice in physics, computer programming and research methodology, encouragement and the second language improvement. I would like to thank committee for instrument experience, effective comments and cheerful encouragement.

The success of this thesis can be attentively data and program supported by following providers: ACE measurements from Los Alamos National laboratory and Sandia National laboratories; Neutron measurement from the Bartol Research Institute, at the University of Delaware, and GPS observations from the International GPS Service (IGS) and thank Dr.Gopi Seemala for version 2.2 RINEX GPS-to-TEC program.

I would like to express my deepest sincere appreciation to Miss Witchuda Ponsai, Miss Porntip Jaiman, Miss Sutipa Arsiraroj and Miss Wilairat Khositchaisri for powerful encouragement, E-thesis processes, hardcopy thesis, and facilitation and I would like to Miss Bussarasiri Thana, Dr.Parichat Wetchayont and Miss Parisa Nimnate and colleages in Earth Sciences and Geology program, and also department of Geology stuffs for convenient opportunities and support me.

This project would have been impossible without the Mr.Kanokwat Wannasorn and families, namely, mother, sister and brother warmly afford and support me in last semester.

CONTENTS

Page

Page

Page

Page

LIST OF TABLE

Page

LIST OF FIGURE

Page

LIST OF ABBREVIATIONS

AU	Astronomical Unit
CME	Coronal Mass Ejection
CS	the High Solar Speed Stream associated with the Coronal Hole
EUV	Extreme Ultraviolet
FFS	the Fast Forward Shock
FGS	the High Solar Speed Stream associated with the Solar Flare
FRS	the Fast Reverse Shock
GEO	the Geographic Coordinate System
GPS	Global Positioning System
GSE	the Geocentric Solar Ecliptic Coordinate System
HSS	the High Solar Speed Stream
ICME	Interplanetary Coronal Mass Ejection
IGS	The International GNSS Service
IMF	the Interplanetary Magnetic Field
ISs	the Sudden Impulse
LASCO	Large Angle and Spectrometric Coronagraph
LF	Low Frequency
LIC	the Local Interstellar Cloud
MC	Magnetic Cloud
MCL	Magnetic Cloud-liked Structure
MF	Medium Frequency
PDL	the Plasma Depleion Layer
SA	Selective Availability
SAP	the Subauroral Polarization Stream
SFS	the Slow Forward Shock
SID	Sudden Ionospheric disturbance
SOHO	the Solar and Heliospheric Observatory
SRS	the Slow Reverse Shock
STEC	Slant Total Electron Content
TEC	Total Electron Content
TID	the Travelling ionospheric Disturbance
UV	Ultraviolet
VLF	Very Low Frequency
VTEC	Vertical Total Electron Content

CHAPTER I
INTRODUCTION

1.1 Motivation

Magnetic clouds (MCs) are subset of the interplanetary coronal mass ejections (ICMEs), one variety of the various solar activities influencing on the earth and human technologies. MCs and ICMEs main sources originate close to the solar disk center (Gopalswamy, Yashiro et al. 2007). Coronal mass ejection (CMEs) are observed by white-light serial imaginary with coronagraphs obtain from the Large Angle and Spectrometric Coronagraphs (LASCO) inboard installed on the Solar and Heliospheric Observatory (SOHO) as a distinctively movable magnetized plasma structure from the occulting disk in frame series (Hundhausen 1993, Kahler and Vourlidas 2005, Kunow, Crooker et al. 2006). Thence, the CMEs propagating in the planetary medium named as the ICMEs travel radially outward from closed magnetic field regions to the heliospheric boundary, hit the Earth and the magnetosphere. The Specific ICMEs present 3 following signatures, a smooth rotation in their magnetic field (B) with low variance, a low proton temperature, and a low plasma beta, are called MCs (Burlaga, Hundhausen et al. 1981, Klein and Burlaga 1982, Burlaga 1991).

CMEs occurrence vary accordingly to the phase of solar cycle. There are 2 to 5 CMEs present daily during the solar maximum whiles there is a one CME presents in a couple of days during the solar minimum (Hundhausen 1993, St. Cyr, Howard et al. 2000, Yashiro, Gopalswamy et al. 2004). Approximately 200 pairs of CMEs and ICMEs were presented at the solar cycle 23 (Gopalswamy, Yashiro et al. 2007). Roughly 30% – 40% of ICMEs are MCs (Cargill and Harra 2007) and 85% of MCs have effect with the Earth. 79% of MCs associate with shock. SN- and S-types MCs following shocks are more able to lead to intense geomagnetic storms (Kumar and Raizada 2010). An existence of the high solar speed stream (HSS) following MCs enhances an additionally storm duration (Badruddin and Singh 2009) MCs dimension at 1 AU are 0.2 – 0.3 AU. They usually trigger 25 - 100 hours geomagnetic disturbances (Lepping, Jones et al. 1990, Badruddin and Singh 2009), causing ionospheric disturbances as plasma bubble disturbing GPS signals, also damage to spacecrafts, satellites, telecommunication, power grid and pipeline systems.

Magnetic Storms influence on the magnetosphere and the equatorial ionosphere noticeably, as a key factor in the magnetosphere - ionosphere coupling indicator, namely, the specific electron density along satellite's orbits called the total electron content (TEC) (Beloff, Denisenko et al. 2004). The ionosphere is the solar – terrestrially environmental by – product. Solar radiation in the ultraviolet (UV) and extreme ultraviolet (EUV) imposes the ionospheric conditions (Chian and Kamide 2007). Solar photoionization in the wavelengths turns the neutral components of the upper atmosphere at the altitude roughly below 90 – 300 km into partially ionized plasma and becomes ionosphere.

The ionosphere obtains heat and accelerating particles from the magnetosphere with their thermal and kinetic energy gradients. The thermospheric wind is a origin of the eastward equatorial electrojet and drives the equatorial ionosphere electrodynamic (Blelly and Alcayde 2007). The electrojet behaves like the eastward electric field and then uplifts the ionospheric plasma. As the consequence of this fountain-like uplift and the gravity force interaction, the plasma, also called TEC in case of using GPS measurement, accumulates at about 10-20 latitudes in both hemispheres. The ionospheric TEC variations depend on solar radiative intensity and the solar cycle as a diurnal, a seasonal and the 11 years periodic variation (Cai 2007).

TEC also responses to the magnetic storm and indicates the ionospheric storm. The result of penetrative electric field from the storm increase a large - range latitude TEC on the dayside simultaneously and create the enhance TEC band which extended from the dusk sector through the cusp to the polar cap (Nsumei, Reinisch et al. 2008). In the cases of storm caused by the transient of MCs, the decrease in magnetospheric convection generates the rapid increasing of the TEC below *F* layer indicates the abnormal descent of *F* layer on the post-sunset sector (Sastri, Rao et al. 1993). TEC during storms also indicates the position and shape of the travelling ionospheric disturbance (TID) and the ionospheric trough (Beloff, Denisenko et al. 2004).

This thesis uses ionospheric total electron contents (TEC) calculated from the GPS signals in IGS network as evidence to investigate the relation between the geoeffectiveness of magnetic clouds and the ionospheric variation. The analyses of characteristics of the interplanetary magnetic field (IMF) parameters and TEC variations allow us to reconstruct the magnetic clouds–magnetosphere–ionosphere coupling processes. TTEC can therefore be an important archive that being convenient to use without converting slant TEC to vertical TEC (Huang and Reinisch 2001, Belehaki and Tsagouri 2002). Previous works by Belehaki and Tsagouri (2002) indicated that the magnetic activity effects intensely on the top side electron content of ionosphere much more than the bottom side electron content. In addition, Gradual driven storms cause ionization depletion on the dayside, but ionization enhancements on the nightside instead.

This thesis also presents IMF and the solar wind parameters variation, magnetic cloud and other features identifications, as well as MCs and TEC correlation test. These give a better understanding of the large latitude magnetosphere-ionosphere coupling processes and also the global geospace–ionosphere coupling processes.

1.2 Objectives

The purpose of this thesis is to investigate the influences of the magnetic cloud and the various phenomena on TEC variation via percentage deviated TEC, the relationship of between MCs and the global TEC.

1.3 Scope and Limitation

The scope and limitation of this thesis are:

- The study area is the global ionosphere at a height of 350 km mostly above North and South America.
- Percentage in deviated TEC under the MCs and various phenomenal circumstances estimation.

- Analyses of MCs and other various phenomena parameters –TEC variation correlation.

1.4 Location of Study area

The GPS stations in this study located extending over North and South America. The network of GPS in this study (see Figure 1-1) covers the latitude between 54°49'55"N and the 53°8'12"S and the longitude between 63°53'45"W and 83°28'22"W. Intensive stations are to substitute for other near stations when the others are not available.

The reason that the study area should be on these stations are the stations most stably work compared with other parts of the world like Sumatran GPS network were devastated by Tsunami in 2006. Although, Japan has many station networks but they are not available to public. The GPS stations, where we selected, are nearly located along the longest latitudinal transaction. This transaction is useful to explain TEC variation in the global scale.

1.5 Expected output

The expected outputs of this thesis consist of:

- TEC variation resulting from MC and other phenomena in percent.
- MC and other phenomena parameters and TEC variation coefficients

1.6 Research methodology

Four sequential steps were designed to achieve the aims of this thesis. Each of which is described as follows:

1.6.1 Preparation

- Literature review of the related research in magnetic clouds, MCs and various phenomena identification, responses of the ionosphere to geomagnetic storms and TEC measurement.
- Station Selection from the IGS network and neutron monitor database.

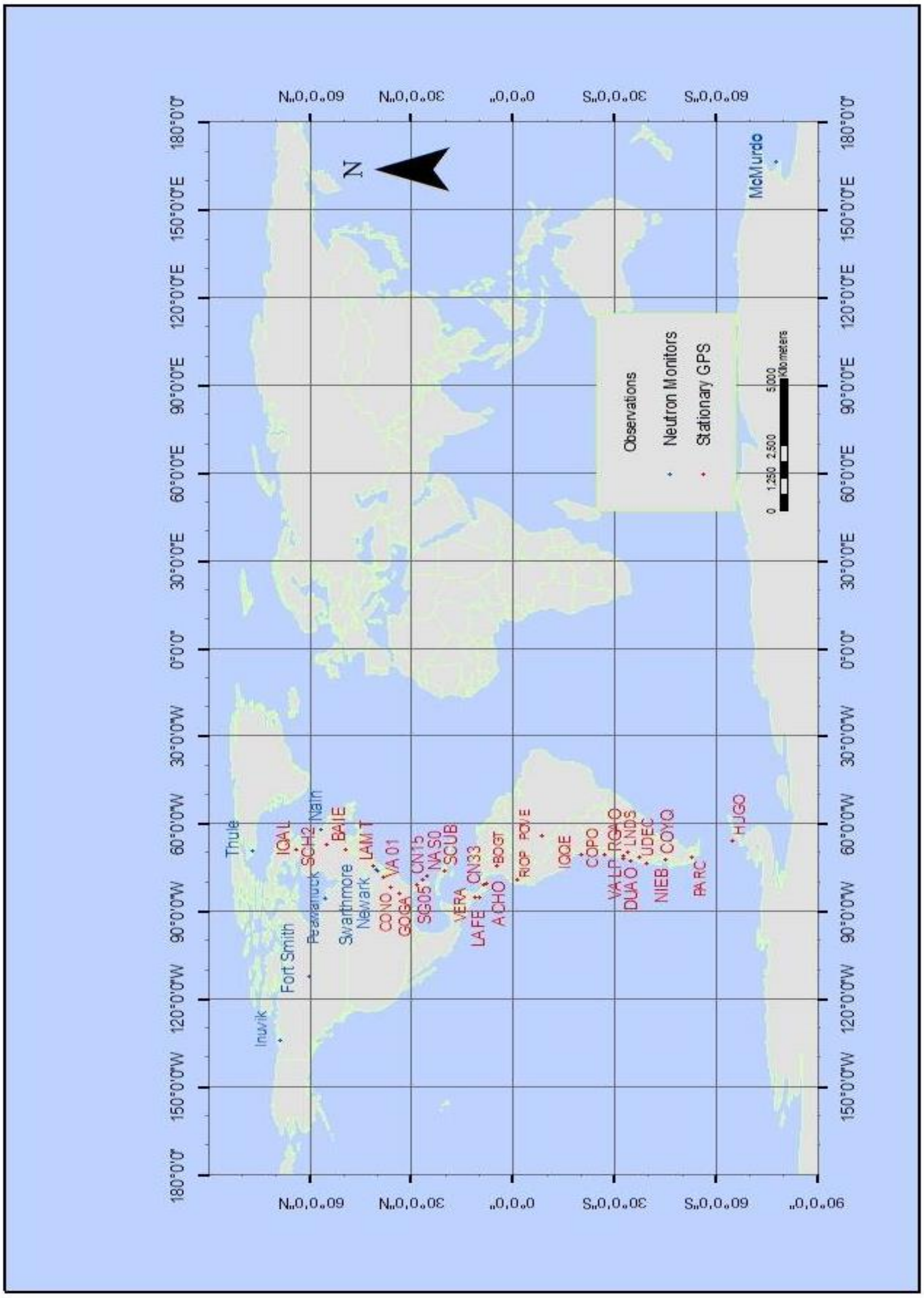

Figure 1.1 GPS station location in the study.

1.6.2 Magnetic cloud identification

- Data collection of an available online data on the ACE spacecraft website. The parameters used in this study, namely, magnetic field components in GSE (B_x, B_y, B_z and B), latitude (Θ) and longitude (φ) of the interplanetary magnetic field (IMF), plasma parameters as proton temperature (T_p), proton density (N_p), flow speed (V) and also derived parameter as plasma beta (β).
- MC identification Programming. The selective program consists of 3 concurrent processes based 3 signatures of MC.
- Coordination Transformation between the Geocentric solar ecliptic coordinate (GSE) system, Geographic coordinate (GEO) system and the Geocentric equatorial Inertial (GEI) system

1.6.3 TEC and percentage of deviation in TECU (*dTEC%*) estimation

- TEC calculation with GOPI program at 350 km.
- Average TEC in 27 days period and dTEC% estimation

1.6.4 MCs and various properties – *dTEC%* correlation analyses

- Regression analyses. A simple regression correlation was used to study their relativistic.

1.7 Components of the thesis

This thesis is composes of 6 chapters, starting first with motivation and introduction as Chapter 1. Reviews of previous studies of magnetic clouds, various phenomena and TEC variations are briefly summarized and reported. Chapter 2 presents basics in MCs, various phenomena, the ionosphere and TEC in detail. The data descriptions of space – based and ground – based measurement are obtained from chapter 3. Chapter 4 provides all methods used in this study, respectively, magnetic cloud – phenomena identification, classification, infirming their arrival at the Earth. All results and their discussions are provided in chapter 5 and finally, the conclusion are presented in chapter 6.

CHAPTER II

LITERATURE REVIEW

2.1 The solar-terrestrial environment

Satellite in geospace, the environment near earth influences telecommunications and transportations, thus the solar-terrestrial environment comes closer to everyday life. The solar-terrestrial environment refers to: the geospace, such as, the Earth's magnetosphere; and the Earth's atmosphere, the ionosphere. These regions are controlled by the physical conditions in the solar interior and atmosphere. The change in the conditions and the solar wind are known as space weather. Space weather is sometimes unstable and disturbs human's space technologies.

Geomagnetic storms and substorms are generally transient disturbances. They are the resultants of the interaction between solar wind and magnetosphere. The geomagnetic storms are a geomagnetic disturbance in global scale. The average instantaneous longitude of the mid-latitude magnetic disturbance, so-called $D\mathrm{st}$ index, is to display their storm magnitude intensities simpliestly.

The storm-time duration generally consists of the continuous series of 3 phases: the sudden commencement phase, the enhancement of the $D\mathrm{st}$ at the Earth's surface typically last for several hours; the main phase, is duration following decrease in $D\mathrm{st}$ drastically; and the recovery phase, the duration that the $D\mathrm{st}$ raises back to the quiet-time condition.

Substorms are transient magnetospheric process formed by the dissipation of the energies of interaction between solar wind and magnetosphere, mainly on the nightside auroral ionosphere (Akasofu 1964, Rostoker, Akasofu et al. 1980).

Substorms sometimes independently occurred to geospace environment, but geomagnetic storms are always caused by the disturbance in the solar magnetic field. The magnetic explore ejects the mass of the Sun's atmosphere which can interrupt the Earth's upper atmosphere.

2.2 The solar interior and atmosphere

The solar magnetohydrodynamics drives our 4.6 billion years. Then, the G2V star drives planets, their interplanetary space and Earth. The Sun consists of two electrically conducting fluids plasma. The chemical compositions are a mixture of 75% hydrogen, 24% helium, and about 1% of all heavier elements. The convection and the rotation of the Sun both force, move the conductive components as an induce current, and also generate and change magnetic field itself. The solar interior is composed of three layers namely, the core, the radiative zone and the convection zone.

Hydrogen nuclei in the core converted themselves into 4.3 million tons of helium nuclei and generate energy at 380 yottawatts (3.8×10^{26} watts) per second. Those energies transfer outward continually as photon. Particles scatter and absorb each other and are finally shifted to the longer wavelength.

A convection process raises the hot ionized gas at the convection zone, the less dense layer. The hot ionized gas raises, cools and falls down on the top of the radiative zone again as the convection current. The process still repeats and manifests as the visible structure called granule (as seen in the Figure 2.1).

The solar atmospheric observations with helioseismologic techniques effect in the forecast of changing environmental conditions in near-Earth space, called space weather. Three layers of the solar atmosphere (e.g. photosphere, chromospheres and corona) are monitored at multi-wavelength.

The photosphere is the lowest atmosphere of the Sun and emits the white light which is the highest percentage of the sunlight. A white-light image reveals dark spots and the brighter area surrounded there. They are called sunspots and the active regions. Different wavelengths is suitable to monitor specific layers (as shown in the Figure 2.2), as well as displaying differently tectonic structures. X-ray and UV show the solar flares always occur within the active region as a sudden brightening.

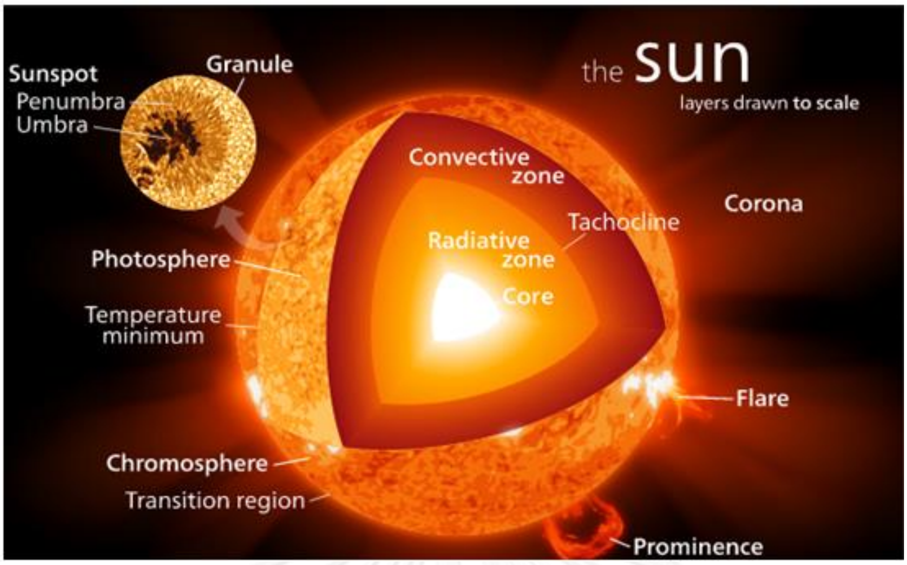

Figure 2.1 The Granule, the solar interiors and the solar atmospheres. Kelvinsong, Sun [online], 24 July 2004.

Source http://en.wikipedia.org/wiki/Sun#mediaviewer/File:Sun_poster.svg

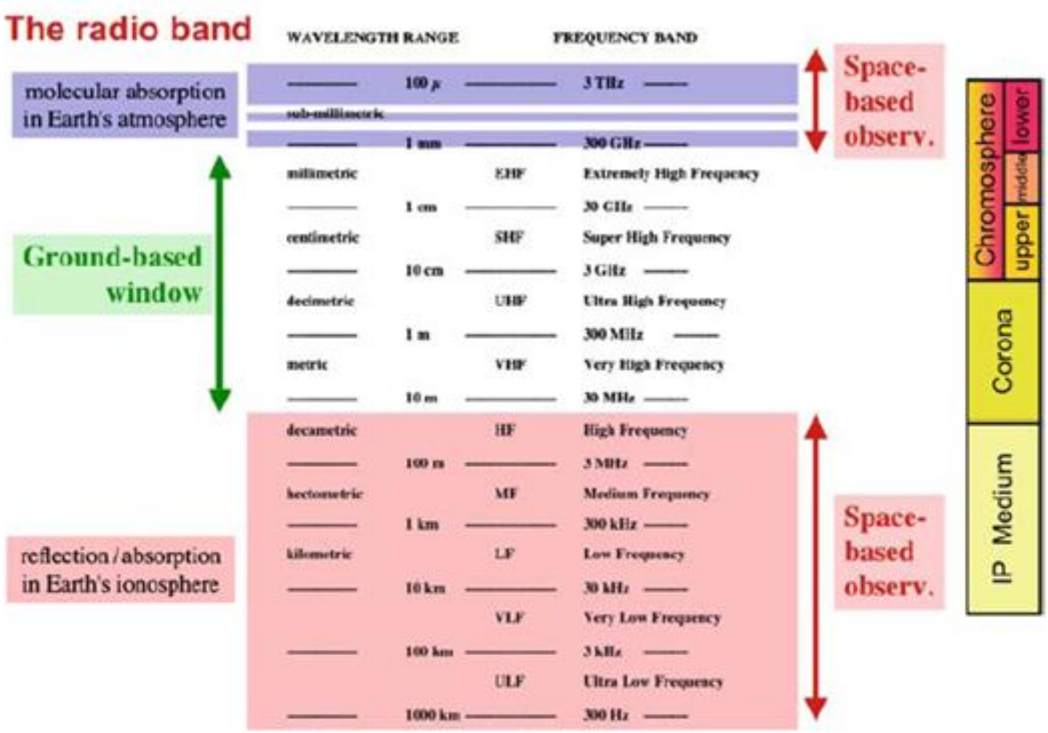

Figure 2.2 Solar environments, their detective wavelength in the radio range and their observing locations. Image credit (Bougeret and Pick, 2007)

Any dark structure indicates an area having a lower temperature compared to its surrounding due to an intense magnetic activity. Hα or a deep visible red is usable to monitor the hue pink-to-red colored generating layer, called the chromospheres. The Hα visualizes the prominence, which is another dark feature extending vertically as a ribbon. The loop rises up through this very low-density layer up to the outermost layer, called corona.

The corona is only seen with the unaided eye during a total eclipse, but the soft X-ray is capable of detecting the coronal tectonic. Active regions are also appear and are more-well seen in this wavelength, as ensembles of closed-coronal flux loops connecting two opposite magnetic polarities consisted of hot gasses. These hot currents containing magnetic field are able to guide, hold, shape and erect themselves of the photosphere.

Another appearance manifests itself as the global-scaled dark band in the soft X-ray image. It often prolongs from the Sun's equator to one magnetic pole and sometimes lay across two poles. Magnetic field lines, within this region, open and allow steady streams of the solar materials straight into interplanetary space. Therefore these regions have a lower density, so it is cooler and finally darker than other general regions as shown in Figure 2.3.

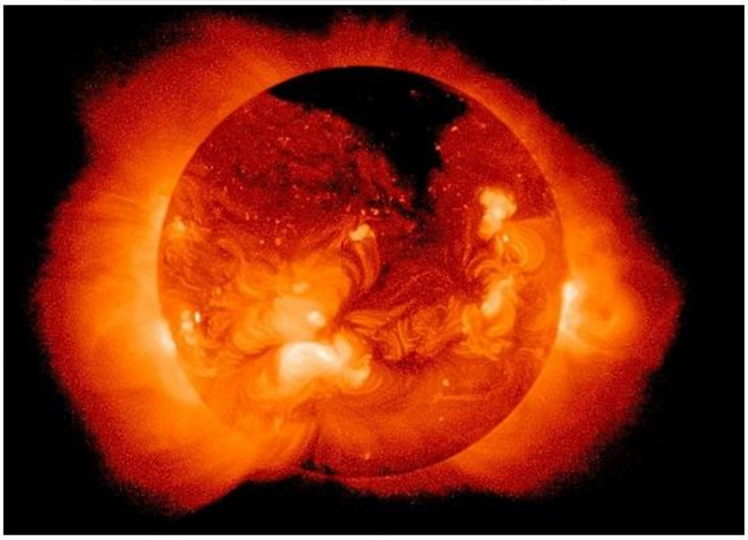

Figure 2.3 X-ray image pictured by Yohkoh satellite. The image shows two global-scaled features: active regions (the bright colored region) on the great circle; and the coronal holes (the dark region) at the solar pole. Kenneth, The X-ray Sun [Online], 24 July 2004. Source http://ase.tufts.edu/cosmos/view_picture.asp?id=559

Coronal hole are an important precursor of the space weather disturbance. Those bad conditions might be the gust of solar wind and the high speed streams. Conversely, active regions are also the origin of 79% of CMEs (Zhou et al., 2003) and 88% of the halo CME directed to the Earth are associated with flare.

2.3 The coronal mass ejection and the interplanetary coronal mass ejection

Monitoring CMEs and their ICMEs arrival times to the Earth forecast are important as near earth asteroids monitor. Several days after CMEs glowed, ICMEs caution would be warned, because the ICMEs directed to the Earth often trigger geomagnetic storm disturbance.

2.3.1 The coronal mass ejection

CMEs are a spectacularly photographic phenomenon in astronomic imagine. The Large Angle Spectrometric Coronagraph (LASCO) installed on the Solar and Heliospheric Observatory (SOHO) spacecraft detected first CME in 1971.

CMEs appear in white light as a large animated feature of discrete brightness. It emerges from an occulting disk and change in individual sequence of frames. Hundhausen gave two properties of CME in 1993: that is the observable change in the coronal structure (1) whose the duration of its occurrence is between a few minutes and several hours and (2) a white-light feature discretises into a new bright appearance in the coronagraph field of view.

August 5^{th} and 18^{th}, 1980 CME was the morphological paradigm of the CME, because the CME had three parts of complete CME configuration. A large helmet streamer (the most outside structure), the prominence (the middle structure) and the prominence cavity (dark region) appeared at the pre-eruption state and were moving away from the Sun (e.g. Hundhausen (1993)) as seen in the Figure 2.4.

The filament eruption causes CMEs. Magnetic forces suspend cool ($<10^4$ K) plasma, above the surface of the Sun. Streamers of plasma twist as an s-shaped and have more complex magnetic field. The more curves they were, the more complex magnetic fields were generated. These twisted complexities can store magnetic energy gradually.

New magnetic flux, from the photosphere, destabilizes of the former filament, reconnects together and following flare-like brightening occurs. Gary and Moore (2004) suggested that reconnection occurred initially at above base. After that the overlying magnetic field is removed and allows the existing filament to erupt.

Youhei (2008) described mechanism of the solar-type magnetic reconnection as four continual phases (Figure 2.5): (a) Precursor phase, the magnetic energy stores in the lower atmosphere; (b) Quiescent phase, the reconnection releases the energy and is transfered by photon flux to the coronal surface and heats it on the sudden, then the coronal plasma pressure increases significantly and creates a hot dense with the upward evaporation flow mass; (c) Main burst phase, The magnetic flux lifts the evaporate matter, then two separated structures are formed, the upper baryon rich prominence (filament and prominence are a same structure) and the lower baryon-poor magnetized corona, the prominence erupts, reconfigurates the field globally and magnetic reconnection; and (d) Mass ejection phase, magnetic energy in main phase converted into the kinetic energy of the trapped mass ejecta.

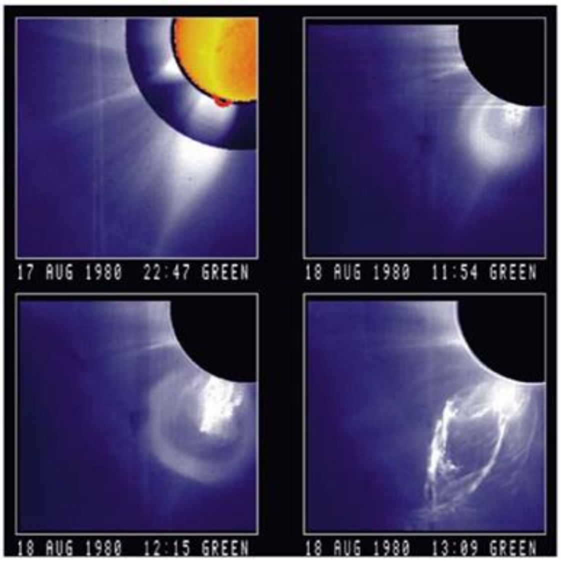

Figure 2.4 coronographs on 18 August 1980. The series starts with the pre-eruption helmet streamer, then, a trailing cavity at an initial eruption, after that the full 3-part structure; the leading bright edge, the cavity, and the prominence, the last image depicts the post-eruption prominence material. Image credit [Figure courtesy of HAO]

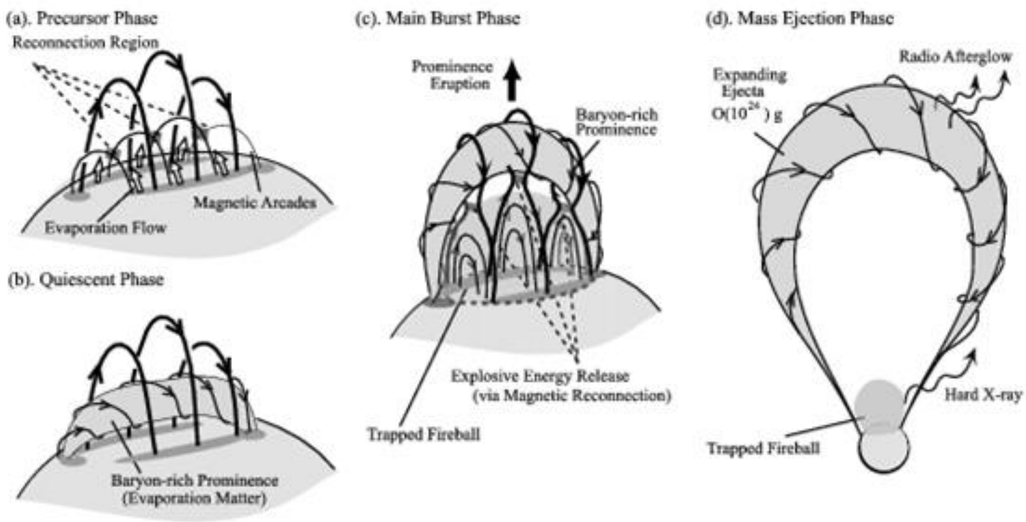

Figure 2.6 Four phase of a mass ejection from the theoretical model for giant flare based on the solar flare, CME theory by Youhei (2008)

The latitude distribution of CME doesn't correspond to sunspots or flares, but does correspond to streamers and prominences. The rate of CMEs at solar minimum is less than four or ten times the rate of CMEs at solar maximum (Hundhausen 1993, St. Cyr, Howard et al. 2000, Yashiro, Gopalswamy et al. 2004). The origins of CMEs are different within a solar cycle. CMEs originate in the equator of the Sun at solar minimum and extend over wider latitudes within solar maximum.

The daily total solar wind mass loss is about 10^{14} kg. Estimates of the daily average mass of a CME from Solwind and SMM were less than fifty billion kg Hundhausen (1993). That was a little percentage in daily loss.

2.3.2 Interplanetary coronal mass ejection

A photographic technique uses to detect CME at the Sun, and in situ interplanetary medium measurement detect CME further away from the Sun. The observed CME with magnetic field and medium measurements in the interplanetary medium, typically at L1, is called the interplanetary coronal mass ejection (ICME). Any ICME identification, an observer must detects the specific plasma and magnetic signals of the ICME at the beginning and rechecks back the CME data.

ICME carries coronal materials into the interplanetary space. The discontinuous enhancements and a depression of some chemical species abundance identify ICME presence. First two primary composers of the solar wind are light elements, namely, hydrogen nuclei (protons) and electron. Heavier species are also found as few quantities in a quiet-solar wind condition. Within ejecta, some anomalous signals of the heavier to the lighter isotopes or species ratio increase. Those significantly twofold anomalies are O^{7+}/O^{6+}, Mg/O and Ne/O. He to proton proportion within CME to normal condition is more than or equals 0.06. The ratio of He^{3}/He^{4} inside CMEs is thousand fold less than a quiet-time He^{3}/He^{4}. Charge state ratio enhancement is related to a greater variation in the local magnetism in the fast solar wind than the slow wind.

The pressure inside ICMEs is higher than the ambient solar wind and drive radial evolution of themselves. The difference between the speed at leading edges and their trailing edges and the pressure gradient expand their dimension. The average expansion speed between 0.3 and 5.4 AU is gradually lower from 65 to 45 km/s. Moreover, ICME velocity is clearly ordered by associated flare magnitude. Seven tenth of ICME are to decelerate in the planetary medium rapidly (Yashiro, Gopalswamy et al. 2004).

The arrival of ICME at the Earth is able to detect by the more than 4% decrease in the galactic cosmic ray, which is known as the Forbush’s decrease. The suppression is able to observe with networks of the neutron monitors.

The ICME contains dense twisted filaments from the Sun, so the internal magnetism in the ICME is greater than its surrounding IMF. The radial ICME expansion also extends its magnetic field as an oval-rope shape.

2.4 Magnetic clouds

Some of ICMEs containing a low proton temperature because of expansion and its magnetic field component rotating smoothly (Burlaga, Hundhausen et al. 1981) through a large angle (about 180°) are so-called the Magnetic cloud. Magnetic cloud (hereafter MC) is a common type of interplanetary ejecta.

2.4.1 Magnetic cloud identification

There are three schemes of the IMF and the solar wind condition most accepted to identify the MCs: (1) the IMF rotates smoothly wider than 30º; (2) the discontinuous enhancement in IMF strength and be higher than the ambient solar wind; and (3) the ratio of the proton pressure to the magnetic pressure is less than 1 (the detail in MC identification is to describe in section 4.2). Some of observed CMEs are not MCs, but pass the acceptably additional test in the magnetic cloud model is so-called the magnetic cloud-liked structure (hereafter MCLs).

2.4.2 Magnetic cloud model

A magnetic cloud was empirically modeled with tens parameters by Burlaga in 1988 and satisfied a MC identification. He assumed the MC was force-free so that

$$\nabla \times B = J = \alpha B \quad (2.1)$$

Goldstein proposed a variable α in 1983 and be used by Marubashi first in 1986 to fit magnetic clouds. Two year after, Burlaga considered the α as a constant, so can describe magnetic clouds to first order with equation (2.1) as

$$\nabla\times(\nabla\times B)=\alpha(\nabla\times B)=\alpha^2 B \quad (2.2)$$

Equation 2.2 production is

$$(\nabla^2 B) = -\alpha^2 B \quad (2.3)$$

Lundquist (1950) defined MCs as a cylinder and $\nabla \cdot B$ equals 0, so any MC is projected in cylindrical coordinate in term of zeroth- and first-order Bessel functions as follows:

Axial component

$$B_A=B_0J_0(\alpha R) B_A = B_0 J_0(\alpha R) \quad (2.4a)$$

Where R is the radial distance from the cloud axis.

Tangential component

$$B_T = B_0 H J_1(\alpha R) B_T = B_0 H J_1(\alpha R) \quad (2.4b)$$

Where $B_0$is the estimated amplitude of the field at maximum strength (assumed as the cloud's axis). The variable H is the handedness if MC field helicity. H equals +1 when a magnetic rope lying on a right-handed (RH) and equals -1 when a magnetic rope lying on a left-handed (LH).

Radial component

$$B_R = 0 \quad (2.4c)$$

These three magnetic field components were used to fit magnetic cloud quite imperfect, so others team propose extra parameters. Ivanov et al. (1989) used a constant-α as toroidally symmetric solution.

The least square fit of the model to the data in the variance coordinate system or $\chi^2 \chi^2$ can be determined with equation (2.5).

$$\chi^2 = \sum \left[\left(B^0_{xv} - B^M_{xv}\right)^2 + \left(B^0_{yv} - B^M_{yv}\right)^2 + \left(B^0_{zv} - B^M_{zv}\right)^2 \right] / N \quad (2.5)$$

Where a subscript *v* and two superscripts, *0* and *M* refer to the variance coordinate system, observed fields and the model. *N* is the number of hourly average field vectors.

The seven proposed extra parameters can provide more cloud's characteristics.

2.4.3 Magnetic cloud's characteristics

Magnetic cloud's characteristics were described and classified finally with determined spacecraft independences. These common eight parameters are as follow:

1. The latitude of the cloud's axis with respect to the ecliptic plane, θ.

$$\theta = \sin^{-1}(B_z/B) \qquad \boldsymbol{\theta = \sin^{-1}(B_z/B)}\theta = \boldsymbol{sin^{-1}(B_z/B)}$$

(2.6)

2. The longitude of the cloud's axis with respect to the ecliptic plane, ϕ.

$$\boldsymbol{\phi = \tan^{-1}(B_Y/B_Z)}\phi = \boldsymbol{tan^{-1}(B_Y/B_Z)}$$

(2.7)

3. The distance from closest cloud's axis to the approach spacecraft point, Y_0.
4. The magnetic field magnitude at the cloud's axis, B_0.
5. Related to the size of the cloud, α^{-1}.
6. The sign of the helicity, H.
7. The time at the closest approach to the cloud's axis, T_0.
8. The radial distance, T_0 and the diameter of cloud, T_0.

Eight parameters allow illustrate and model the paradigm of the MC as the cylindrical object as shown in Figure 2.6.

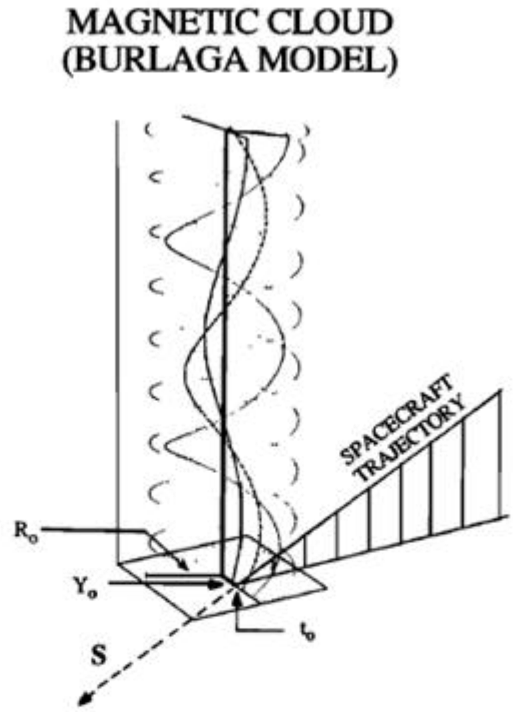

Figure 2.7 A computer simulation based on the Lundquist (1950) of the field lines in a MC, list of variables was declared following; R_0 is the radius of the cloud, *S* is a unit vector parallel to the spacecraft intersecting the cloud at the closest-approach distance Y_0 at time T_0

2.4.4 Magnetic cloud classification

Classification of MCs ICMEs classification) with their magnetic field directions encountered to the observing spacecraft divides MCs into 8 magnetic clouds types. Three parameters needed to classify MCs are leading field (and also trailing field) direction, axial field direction and helicity. The leading field is the field encountered with a spacecraft first at the leading edge. The axial field is the dominance field at the MC axis. The leading and the axial field direction direct perpendicularly to the solar wind flow direction. The helicity used is the helicity in those two orthogonal directions. Figure 2-7 illustrates paradigms of 8 types from MCs classified with three parameters.

Research reveals that clouds had mainly horizontal axes during the cycle 22.

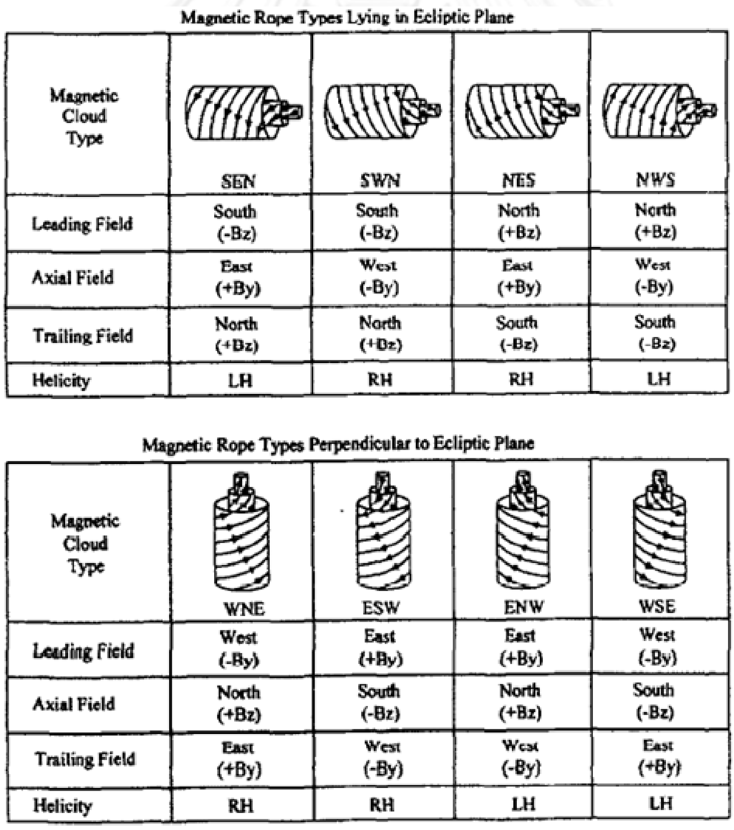

Magnetic Rope Types Lying in Ecliptic Plane

Magnetic Cloud Type	SEN	SWN	NES	NWS
Leading Field	South (-Bz)	South (-Bz)	North (+Bz)	North (+Bz)
Axial Field	East (+By)	West (-By)	East (+By)	West (-By)
Trailing Field	North (+Bz)	North (+Bz)	South (-Bz)	South (-Bz)
Helicity	LH	RH	RH	LH

Magnetic Rope Types Perpendicular to Ecliptic Plane

Magnetic Cloud Type	WNE	ESW	ENW	WSE
Leading Field	West (-By)	East (+By)	East (+By)	West (-By)
Axial Field	North (+Bz)	South (-Bz)	North (+Bz)	South (-Bz)
Trailing Field	East (+By)	West (-By)	West (-By)	East (+By)
Helicity	RH	RH	LH	LH

Figure 2.8 8 types of MC classification with field directions and their helicity can be grouped into two groups respected with the direction that the magnetic rope to the ecliptic plane. (Mulligan, Russel, and Luhmann, 2000)

2.5 MC associated phenomena

Fast moved MCs often don't travel and expand into the heliosphere alone. The fast MC always drives the interplanetary shock in front of them. Area between the interplanetary shocks and MCs had a large swing in proton density and the magnetic magnitude is called sheaths. The solar high speed stream may catches up with slow MCs and causes the interaction region between slow MC and fast stream as shown in Figure 2-8.

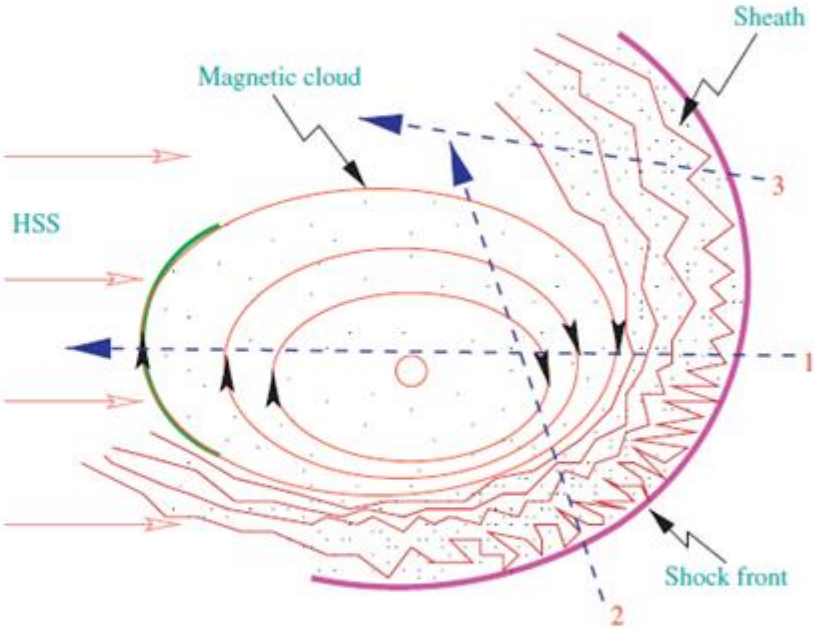

Figure 2.9 Magnetic cloud and structure formed in the interplanetary space likes sheath, shock, high solar speed stream (HSS) and Interaction region (IR) as curve green line. Numbers are spacecraft positions. Diagram from Badruddin and Singh (2009).

2.5.1 Magnetic cloud-like structure

Scheme in automatic identification of MC program provides another type of false positive MC which pass the additional test of $(\chi_M/\langle B\rangle \chi_M/\langle B\rangle) < 0.42$ (Lepping, Jones et al. 1990). It is acceptable as MCLs.

Where χ_M^2 is the Pythagorean mean in which can determine with equation 2.7.

$$\chi_M = \sqrt{\chi_M^2} = \sqrt{(\chi_x^2 + \chi_y^2 + \chi_z^2)} \tag{2.7}$$

For $\chi_x^2, \chi_y^2, \chi_z^2$ $\chi_x^2, \chi_y^2, \chi_z^2$ are chi-squared values of the quadratic fits to the field components.

The occurrence frequency of MCLs is correlated with solar activity. Nearly half of MCLs induced weak geomagnetic storms and around eight percent of MCLs induced strong geomagnetic storms. Anyway, MCLs are generally less geoeffective than MCs.

2.5.2 Interplanetary shock and its classification

Interplanetary shocks are a type of the interplanetary discontinuities. Discontinuities manifest themselves as the discontinuous mathematical jump conditions in spatial change in magnetic fields and plasma parameters.

ICMEs are main IP-shock drivers. The shocks occur when the driver propagate in space plasma at speeds higher than the upstream magnetosonic speed relative to the ambient solar wind. Shock speeds depend on their drivers speeds. The Alfven Mach number and the MHD equations categorize shocks into three categories. The three categories are fast shock (Fs), intermediate shock (IS) and slow shock (Rostoker, Akasofu et al.).

Petschek (1958) and Kennel et al. (1985) detail those the different properties of various shock are: FS has steepening speeds greater than the upstream magnetosonic wave speed, IS has steepening speeds than acoustic wave speed and fast as an Alfven wave, and SS propagate at speed faster than the thermal sonic speed. Further identification and classification with wave modes processes are to describe in detail in section 4.3, in the chapter IV. However, slow ICME does not have a FS when it propagates at a speed less than magnetosonic speed.

Shock subcategorization is related to shock-driver direction. Forward shocks (FSs) (often called as planetary bow shocks) propagate in the same direction to their drivers and reverse shocks (RSs) propagate oppositely to their drivers. Magnetic field intensities, number intensities and sheath plasma temperature in fast forward shocks (FFSs) increase downstream and these three observations present reversely in the sheath after fast reverse shocks (FRSs).

The number densities and plasma temperatures in slower shocks variance consistently as FFSs and FRSs, but the magnetic field intensities decrease in SFSs and increase in SRSs.

The enhanced plasma densities downstream of FFSs sometimes impact the Earth magnetosphere. The impingement enhances the Chapman-Ferraro magnetopause current and trigger the sudden positive variation in the horizontal component at the low-latitude geomagnetic field (also called Sudden impulses, ISs).

Shocks pass the ACE and reach the Earth within 5 minutes. The shock arrival time is calculated from time difference of ACE observation and the onset of the positive sudden impulse (SI^{+}s). The compactions of the FFSs onto the magnetosphere trigger substorms and nightside geomagnetic activity. Energy storage in the ionosphere occurs even during the northward IMF intervals. The lower bound or maximum negative excursion of horizontal component (Auroral electrojet index, AL index) coincides to the magnetosonic Mach number of the precursor shock.

2.5.3 Sheathes and their characteristics

Sheathes are the region contained shocked plasma between a shock and obstacle to a supersonic flow. There are two quasi-stationary shocks producer in the solar wind. These are a planetary magnetosphere and the local interstellar cloud (LIC) shock ahead of the high-speed ICME. ICME sheathes evolve with distance, because their ICME drivers expand with distance.

Characteristics of sheathes depend on the in shock driver. A spatial width of the exhaust region was found at about 80,000 km. Energetic electrons have energy up to 400 keV and able to reconnect to Earth’s magnetic fields. Another configuration found in the sheath is a plasma depletion layer (PDL). The PDLs is unstable to electron ion cyclotron wave, but it is stable to mirror mode wave. Near a half of sheath occurrences show the density decreases.

A mirror mode wave is defined by a large amplitude magnetic field perturbation. The wave mode is found as an anti-correlated with the density fluctuation. The wave period at Earth was about 20 seconds.

Mirror mode waves grow well in high β plasma when $T > T - 1 > \frac{1}{\beta}$. The condition often been in sheathes behind quasi-perpendicular shocks.

2.5.4 Solar high speed streams, co-rotating interaction regions and their identification

High solar speed streams (HSSWS) are defined as the quiet stream emanated from near equatorial hole, and identified as a period as one having a rapidly rising increase in the solar wind speed (V_{sw}) over a short period, registering a maximum speed over and equally 450 and persist at least 5 days after its start.

Two main HSSWS origins provide HSSWS into two types. The first category is the HSSWS associated with solar flare (FGS) and another type is the HSSWS associated with coronal holes (CS).

The solar wind flows out from the Sun in radial direction and drags the magnetic fields from the Sun to space. When the Sun rotates, the magnetic field line will have spiral shape called Archimedean spiral. A fast solar wind (typically > 600 kms^{-1}), emanated from open magnetic field structure (coronal hole), has greater speed than the slow solar wind (typically < 400 kms^{-1}), emanated the closed magnetic structures (loop structures). Fast winds collide with its former slow wind from solar minimum, then, develop a co-rotating interaction region (CIR) between fast and slow wind.

2.6 Ionosphere

Gauss (1839) proposed the existence of a conductive layer in the atmosphere to help interpretating how external sources effect on the diurnal variation of the Earth’s magnetic field. Stewart had proposed the theory of the solar terrestrial dynamo in 1882 before Thomson discovered the electron in 1987. Reflection of the waves in the atmosphere and the curvature of the Earth allowed Marconi to succeed in the first radio transmission across the Atlantic in 1901. Kennely and Heaviside

(1902) cited to Stewarts idea and assured the existence of the ionosphere, a conduction layer.

Ionosphere is an atmosphere where can reflect a HF radio wave (from 3 to 30 MHz). The Ionospheric base lays on the upper atmosphere at the altitude close to (about 50 km above the Earth's surface) the thermosphere. Main components in the ionosphere are free electron, atomic ion and molecular ion. Free electron charges in the layer are the electromagnetic wave mirror. Those three compositions are converted from their neutrally parental specie into an ion with two mechanisms, namely, charge exchange and ion charge exchange. On the other hands, positive ions can combine with the electron and turn back into their neutral species with dissociative electron recombination.

The Sun forms the ionosphere and controls quantities of neutral molecules, positive ions and free electron in the ionosphere. If we assume the ionosphere consists of M neutral molecules like A, B and C. The EUV continuously emitted from the Sun chases the dayside ionosphere and is absorbed by species. The neutral species then turn into positive charges and emit free electrons as the equations below.

$$M + h\nu \longrightarrow M^{+} + e^{-}$$

Then the collision allows the primary products (atomic ions and molecular ions) to exchange their charges with other neutral species as three equations below.

$$A^{+} + B \longrightarrow A + B^{+} \qquad \text{(charge exchange)}$$

$$A^{+} + BC \longrightarrow AB^{+} + C \qquad \text{(ion charge exchange)}$$

$$AB^{+} + C \longrightarrow A + BC^{+} \qquad \text{(ion charge exchange)}$$

The dissociative recombination of molecular ions and free electrons allows the layer losses ions (As shown in the equation below).

$$AB^{+} + e^{-} \longrightarrow A + B \qquad \text{(dissociative recombination)}$$

Free electrons from ionization absorb enough energy (above the thermal energy) to produce primary and sometimes secondary ionization. The suprathermal electron is important, because the secondary product of the photoelectron is one-third composition above the second lowest layer of the ionosphere, called E region.

2.6.1 Ionospheric layers

Breit and Tuve surveyed the ionosphere with an interferometric technique by generating the radio pulse and measurement. The experiment provided detection the electron density of Ionospheric plasma as a function of height.

The gravitational force exerts on variance charges in the atmosphere and charges have different weights, so any specie of charges doesn't distribute equally along the Ionospheric column. The lighter species stay on the higher altitude and molecular charges having more masses appear oppositely in descending order. Dominant chemical process and species distribution of charge allows assort the ionosphere into 5 generally stratified regions, namely, *D, E,* F_1, F_2 region and the topside ionosphere.

The topside ionosphere is the outermost atmosphere facing with the geospace. It is defined to be the region lay above the F_2 peak, where the atomic oxygen ion (O^+) decreases (Nicolet, 1961) to near F_2 base concentration and stops being prominent most (as shown in the Figure 2.9). The mid-latitudinal topside ionosphere extends from 600 to 1,500 km. Because of a very high altitude, the atomic hydrogen ion (H^+) becomes predominant ion on this layer. The photon spheric state is controlled by the diffusion along field aligned transport process.

The *F* region is a less dense ionosphere. It can be divided into 2 vertical layers: *F1* and F_2 region. Above 180-300 km altitude, F_2 region is the place where O^+ presents dominantly. The above 150 to below 200 km altitude is the F_1 region.

The F_2 region is the transition zone of the diffusion equilibrium region (from the topside ionosphere) to the chemical equilibrium region (*F* regions). The ambipolar diffusion still controls region dominantly. The photochemical process is getting more frequent in the lower altitude in descending order, but is not significant. Making electron-ion pairs by the diffusion of the ionized particles through atmosphere constituents, keeps the overall electrical state neutrally.

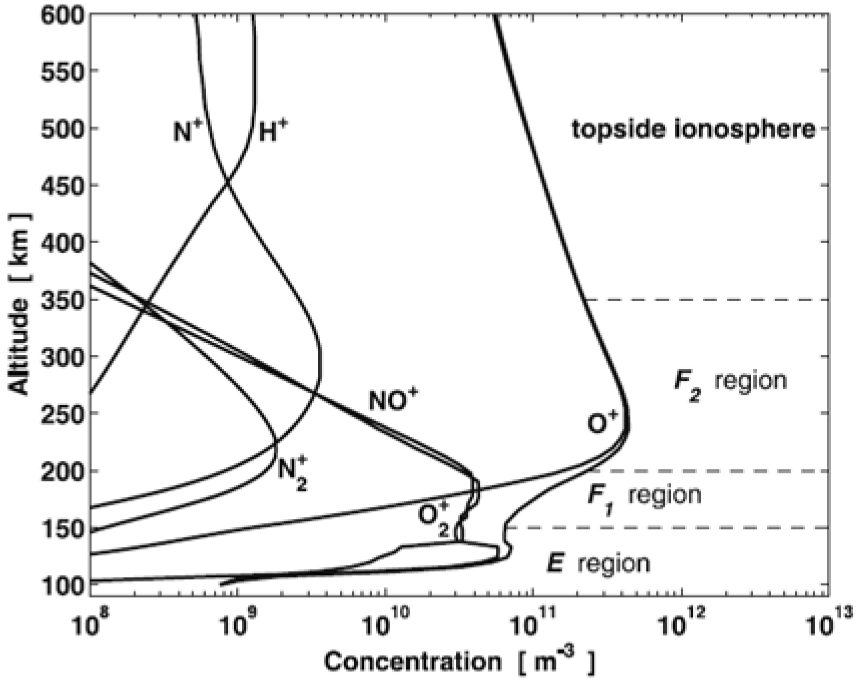

Figure 2.10 Ion species distribution in the ionosphere from E to the topside Ionospheric region

(Blelly and Alcayde 2007)

The *F* region is a less dense ionosphere. It can be divided into 2 vertical layers: *F1* and *F2* region. Above 180-300 km altitude, F_2 region is the place where O^+ presents dominantly. The above 150 to below 200 km altitude is the F_1 region.

The F_2 region is the transition zone of the diffusion equilibrium region (from the topside ionosphere) to the chemical equilibrium region (*F* regions). The ambipolar diffusion still controls region dominantly. The photochemical process is getting more frequent in the lower altitude in descending order, but is not significant. Making electron-ion pairs by the diffusion of the ionized particles through atmosphere constituents, keeps the overall electrical state neutrally.

The photochemical process at the EUV wavelength controls the *F1* region, but the ion-electron recombination process of NO^+ and O_2^+ species balance the molecular ions. In summer daytime, the F1 region moves down to the lower altitude.

The *E* region of the ionosphere presents as a 90 km to 150 km altitude layer. A high ion-neutral collision frequent is the characteristics of this layer. The EUV absorption ionizes different species within the upper regions. The O^+ and O_2^+ are still two main ions of this region. Aside the charge exchange reaction from O_2 with NO^+, another species producing O^+ and O_2^+ participatively in this region, is N_2^+.

The *D* region is the lowest layer of the ionosphere. The region extends approximately from 60 to 80 km above the Earth surface. At 90 km height in the region, the nitric oxide (NO) is just a minor constituent, but its product (NO^+) and by-product (O^+_2) is vastly created as a significantly comparable level. Another identity of the region is the hydrate molecules, so the main primary products of the layer are significantly contributed by hydrate parents.

The sunlight in X-rays and Lyman α emission (the X-rays emitted by solar flares) controls the *D* region principally. The sunlight ionizes hydrate, nitrate and carbonate species, then generates negative, positive charges and electrons in daytime. Ozone and electrons in the layer is the production of the negative charges of oxygen-atomic oxygen charge exchange.

2.6.2 Various temporal-scaled variations in the Ionosphere

Variations in the ionosphere can be classified by frequency of occurrence into two classes: regular variations and irregular variations. Irregular variations are transient variation (the detail of irregular variations is to detail in section 2.6.4). Regular variations are a variation occurred in circles or can be predicted in advance with a reasonable accuracy.

Regular variations can be sub classified into four subsclasses by length of the cycle period. Four regular variations in the ionosphere are daily variation, 27-day variation, seasonal variation and 11-year period variation.

Diurnal variation

The angle of the Sun controls the ionization rate and the 24-hour rotation of the Earth allows any place on the Earth surface moves from a position to another exact location, where gain different angle of the Sun. Daily variation in the ionosphere effects on Ionospheric layers differently.

Structure and density of all Ionospheric layers depends on the time of the day. The *D* region disappears at night. The E region at night has a greatly less ionization than the daytime *E* region. The *F1* and *F2* regions unify as one layer during the night and separate back to be two layers again in daylight.

Seasonal variation

The Earth revolves about the Sun. The axial tilt of the Earth moves the relative position of the Sun from one hemisphere to the others and the seasonal variations of the ionosphere happen. Seasonal variations in all regions, except the *F2* and the topside regions, corresponds to the highest angle of the Sun.

The *F2* region and the topside ionosphere propagate the higher operating frequencies in the winter than in the summer. The electron density in the topside ionosphere is the highest at the winter solstice and lowest at the summer solstice. The subauroral polarization stream (SAP) and the ion upward velocities are largest in winter and smallest in summer.

27-day variation

The Sun rotates around the axis with a differential rotation. One rotation at the solar poles makes every 34.3 days, while one rotation at the equator makes every 25.05 days. Their whole approximately making rotation time is 27 days and equals the sunspot cycle intervals. The sunspot cycle means any one times a sunspot presents, exists, changes, disappears, and new one emerges.

Fluctuation of the ionization density in the *F2* region is greater than other regions. The critical frequency prediction in the region couldn’t be done with day-to-day basis precisely. The limitation is not to bad much, the longer-period based prediction allows forecasters to calculate frequencies for long-distance communications.

11-year variation

An appearance and disappearance of sunspot are called sunspot activity and also be observed. The activity makes a cycle every 11 years. There are a minimum and a maximum level of sunspot activity within one cycle. The ionization density of all Ionospheric regions increases in a maximum sunspot activity.

2.6.3 Application in Ionosphere

Refraction of radio wave allows a trans-ionospheric propagation and a large-distance communication becomes possible. The trans-ionospheric propagation, including a skywave propagation GPS and navigation signal transmissions, makes an amateur radio operation, commercial marine and communications, shortwave broadcast and even in everyday life technologies available.

Skywave propagation is any mode of radio waves that rely on property of refraction in the ionospheric plasma. Telecommunication between two large-distance locations needs *F2* region to be connected each other. The operating frequencies increase with the higher altitude. Classes of radio waves, their specific frequency, wavelength and energy is to describe in the Figure 2-10.

The *D* region reflects very low frequency (VLF), refracts low frequency (LF) and medium frequency (MF), however the *D* region disappears at night. The dayside *E* region refracts high frequency (HF) within 20 MHz to the distance of about 1,930 km. The operating frequencies in *E* region are smaller at night and the maximum usable frequency registers at 4 MHz and above whether it would block the higher frequency signals to reach at *F2* region. Since the F2 region presents through day and night (as *F* region), it is the most appropriate region for radio wave refraction.

The ionosphere in under regular variations like a daily and 27-days variations, is able to predict the optimal frequencies each layers. The abrupt variations have their precursors to forewarn occurrences. Unfortunately, the alert retard or some ionospheric disturbance spreads widely several days. The ionospheric disturbance does interfere in the signals and damages many commercial activities and businesses.

Figure 2.11 Rays and radio waves: EHF = extreme high frequency (Microwave), SHF = super high frequency (Microwaves), UHF = ultrahigh frequency, VHF = very high frequency, HF = high frequency, MF = medium frequency, LF = low frequency, VLF = very low frequency, VF = voice frequency and ELF = extremely low frequency Bjankuloski06en, Electromagnetic radiation [Online], 18 April 2011. Source http://en.wikipedia.org/wiki/Electromagnetic_radiation#mediaviewer/File:Light_spectrum.svg

2.6.4 Ionospheric affects on trans-ionospheric propagations

Ionospheric irregularities cause the absence in selective availability (SA) in the ionosphere effect on trans-ionospheric propagations. The wave transmission allows radiowave propagation, which is available on skywave communications, GPS positioning and navigations. The absence in SA disturbs the activities with wave absorption, refraction and scintillation. The effects produce fluctuating signals, delays, phase shift and errors.

The sporadic *E* region, sudden Ionospheric disturbances (hereafter SIDs), and Ionospheric storms are common irregular variations in the ionosphere. The ionospheric instabilities lead unreliability in different signals specifically.

The sporadic *E* region

A thin layer of high electron density region appears as a cloud irregularly within the *E* region. Its name following its characteristics is the sporadic *E* layer. The cloud appears most frequently in summer months, when an eastward flowing neutral thermospheric wind crosses with the magnetic field. The morphology of the sporadic *E* region depending on latitude and can be classified into three types: an equatorial, middle-latitude and polar (auroral) type. Occurrence of the region allows a long-distance communication with transmitting a very high frequency (VHF) band.

Sudden Ionospheric disturbances

The SIDs is the Ionospheric irregularities which often occurred. The SID durations are from a few minute to several hours. The SID origins are usually an intense burst of EUV and UV likes solar flares. Both of wavelengths are not absorbed by the *F2*, *F1*, and *E* regions, but in been absorbed greatly by the *D* region. The burst instead causes a sudden abnormal increase in the ionization density in the region, thus the 1 to 2 MHz wave are usually completely absorbed and are unable penetrate by the region.

The Ionospheric storms

Ionospheric storms are disturbances associated with the planet's magnetic field and correspond to the interplanetary electric field in dawn-to-dusk axis. The strong eastward electric fields penetrate into the evening Ionospheric sector resulting from the southward IMF.

The ionospheric storms are described with increases and decreases in the Ionospheric electron density into two phases. Positive plasma density increases are related to gravity wave. Global scaled gravity wave launches in the daytime auroral zone, travels to the middle latitude (20°-40°) ionosphere and then lifts the *F* regions ionization upward to higher altitude.

The ionosphere at any latitudinal zone reacts to a storm differently. The middle latitude ionospheric regions increase in ionization plasma significantly. The negative storms are caused by neutral composition change. Chao-Song Huang suggested in 2008 that the plasma density is deeply depleted over the equatorial region ($\sim 20°$) in the evening sector.

Ionospheric affects on skywave propagations

The quiet-time ionosphere also degrades radio signals. Regular and irregular ionizations within the lower ionosphere, especially D region, like absorbing the HF and VHF radio. The present in daytime D region causes significant amount of signal loss.

Ionospheric irregularities sometimes distort the path of radio wave but the irregularities often fade (absorb) signals and shift amplitude of the signals. A signal fluctuation phenomenon is known as scintillation.

Solar wind streams convey very energetic particles which travel at near the speed of light. The energetic particles induce ionizations in the upper atmosphere (the ionosphere) near the magnetic pole. The intensive ionization can make a deep absorption of the HF and VHF signals. The great absorption is called the polar cap absorption (PCA). The HF radio communication is not available when the PCA events occur. Magnetic storms and substorms sometimes extend the PCA out of the polar cap to the auroral zone, such as over Canada and Northern USA.

Ionospheric affects on GPS

The ionosphere mirrors below 30 MHz radio waves back toward to the Earth and allows waves at higher frequencies pass right though. The wave used in the GPS is in the higher frequency wave. The electron density in the ionosphere determines the speed of propagation of a radiowave. The greater density of the electron contributes to the greater speed of the propagation, so the net effect GPS signal is the integration of the electron density along a satellite-to-receiver path.

If the speed of the propagation is to greater than the speed of its signal generator does, the signal traveled from satellite may be completely vacuum. The sinusoid phase of carrier arrived at the receiver earlier is called a phase advance.

The ionosphere doesn't only trigger a phase advance, but also trigger a group delay in radio wave propagation. The ionosphere delay signals modulating the GPS carrier, such as, the navigation massage and the pseudorandom noise codes. The modulating carrier signals are formed with the superposition of a large group of pure sinusoids of slightly different frequencies. The group delay is the delay of the modulation. The phase advance causes pseudorange error and the group delay causes range-rate errors.

The multiplication of a group delay size and the speed of light (about 300,000 km per second) is the pseudorange error. Hence, the ionospheric range error is proportional to secant of the satellite zenith angle. The pseudorange of the dual frequencies can be corrected by the range by L1 and L2 combination. The pseudorange observed with C/A code receivers can be corrected by the ionosphere model with root-mean square correction. Generally, the range error on horizontal coordinate is cancelled by the opposite path of satellite, so the range error occurs in the height coordinate (altitude).

The measurement of the observed carrier phases allows operators to know how much the GPS signals are contaminated by the ionosphere. Moreover the measurement allows operators to convert carrier phases into the carrier range. The carrier range error size equal its carrier range, but is opposite in sign. These range-rage errors are caused by the scintillation effects of the total number of electrons along the signal path, which is called the slant total electron contents (STEC).

2.7 Total electron contents

The counting the number of electrons in the vertical column with a cross-sectional area of 1 m^2 is quantify the electron density. The count is known as the total electron content (hereafter TEC).

2.7.1 Global TEC and its variation

The quantity of TEC relays on spatial and temporal variation. TEC is globally observed at the centroid height of the ionosphere. The height is approximately 400 kilometers above the Earth's surface. All TEC is determined at the same height, but the quantities of TEC in the different latitudes are unequal.

TECU is generally accepted TEC unit, 1 TECU = $10^{16} m^{-2}$. Although TEC observed at the same location, the quantities of daytime and nighttime TEC are different. Since the nighttime electrons are not generated much, moreover the electrons like combining with positive ions. Daytime sunlight and its absence cause a strong swing in TEC as diurnal variation.

TEC starts to increase when the local F_2 ionosphere chases the sunlight. Generally, the rising time for TEC is between 5 to 6 in the morning depend on a season. TEC rises gradually and is most registered at approximately between 14 to 15 LT (the maximum TEC registered period also be suggested by Mansilla *et al*. in 2010, between 14:00-18:00 LT over a South-American section), then the local TEC drops continually and stop at the minimum content at approximate 3:00 LT (Wu *et al.,* 2006).

The daytime TEC maximum at the equatorial (0-20°), middle (40-55°) and high latitudes (60-87.5°) are 38±5, 14±2 and 10±2 TECU respectively. The nighttime TEC minimum is within 5-7 TECU and regardless of season, latitude and longitude. The amplitude of diurnal variation of TEC is the largest (20-35 TECU) at the equatorial latitudes and smallest (2-6 TECU) at high latitudes.

A seasonal variation in TEC between two hemispheres is asymmetrical. The maximum TEC are found in the equinoxes. The minimum TEC is in the summer solstice, but the minimum is also found in winter solstice at low latitudes in very low solar acidity phase.

The largest and the smallest amplitude of diurnal variation are in March and December respectively. There is an asymmetrical behavior in the northern and the southern hemispheres during two equinoxes: the amplitude in the southern hemisphere is higher in autumn than in spring.

TEC variation doesn't not correspond to only the solar cycle as a regular variation, but also correspond to the transient phenomena as an irregular variation. The irregular variation in TEC is often caused by the disturbance in the space weather condition, such geomagnetic storm and solar flare. The irregular variation in TEC is quantified as the percentage deviation in TEC.

2.7.2 The irregular TEC variation

Latitudes play a key role on variation in the Ionospheric parameter under the stormy condition.

The dominant positive storm over the equatorial latitude oppose to predominantly negative storm effect over the midlatitudes. The positive and negative storm variance, both coincide to O/N_2 ratio. Daytime short-lived electron density enhancement is able to track travelling atmospheric disturbances (TAD).

Deviation in TEC (dTEC) and Percentage deviation in TEC (hereafter dTEC%) are generally accepted in a TEC anomaly study.

The deviation in TEC is deviation from the quiet-time TEC which is prefer as the TEC during the A_p index equals or less than 25. The dTEC% exceeds 30% during the storm.

The positive and negative deviations in TEC don't correspond to the severity of the storm. The largest deviation in TEC occurs around the main phase of the magnetic storm. The decrement in TEC occurs in recovery phase of the storm. It is due to prompt penetration electric fields. The penetrating field corresponds well to MC structure interval.

Predominantly negative deviation in TEC in midlatitudes oppose to the dominant positive deviation over the equatorial latitudes. The positive and negative deviations in TEC are parts of TADs.

Nighttime positive deviation in EIA depends a season and greatest in the equinox month.

Percentage deviation in TEC also is found in a pre-storm, post-storm and even in quiet time TEC. Day-to-day deviation in TEC manifests typically approximately 20% in daytime and 33% at night.

Pre-storm TEC enhancement is over equatorial and low latitudes. The pre-storm enhancement at low latitude is caused by the vertical plasma drift or zonal electric field.

Post-storm TEC enhancements are part of equatorial crest region and extend poleward during the late evening and nighttime hours. Daytime TEC enhancements are not confined to the equatorial crest region, but occupy the whole of the latitude range considered in their study. The well-developed positive and negative storm occurs at low and equatorial latitude may represent the strong electric field originated from the magnetosphere.

CHAPTER III
INSTRUMENTS AND DATA DISCRIPTIONS

3.1 Introduction

In studying the interaction between the outer Earth variables and the Earth dependents response, requires the space-based measurements and the ground measurements. The space measurement is needed to confirm an existence of the ICMEs and that doesn't mean the ejection will reach and attack the Earth always, so a neutron monitor is required to assure that the structures have already reached the Earth. The TEC variation will be investigated then whether the structures miss the Earth. There are 4 main required instruments in this study, so the chapter 4 is meant to explain them and their operating owner, including their data used in this investigation, respectively.

3.2 Space-based measurement

The interesting in heliospheric and galactic composition launched a 785 kg of the 1.6 m across and 1 m high octagonal object at Cape Canaveral, Florida, the United Stated at 14:39 UTC in August 25, 1997 with the Delta II 7920, to study the interplanetary medium matters at geospace L1 Earth – Sun libration point. The object is the Explorer-71 named Advanced Composition Explorer (ACE). This unmanned spacecraft designed, built at Johns Hopkins University (JHU) and the Applied Physics Laboratory (APL) is purposed to operate 12 experiments until 2024.

Nine instruments maintained carry on 9 experimental mission of ACE utterly: the Solar Wind Ion Mass Spectrometer (SWIMS) to measure mass and energy of solar wind ions and isotopes; the Solar Wind Ion Composition Spectrometer (SWICS) to determine elemental and ionic composition, it's temperatures and mean speeds; Ultra-Low Energy Isotope Spectrometer (ULEIS) to measure energetic ion fluxes between He and Ni range (from about 20 keV/ nucleon to 10 MeV/nucleon); the Solar Energetic Particle Ionic Charge Analyzer (SEPICA) to measure properties of above 0.2 MeV/ nucleon energetic ion, namely, kinetic energy, ionic charge state and nuclear charge; the Solar Isotope Spectrometer (SIS) to measure isotope from *Z* equal to 2 (Li) though 31 (Zn) at energies from 10 to 100 MeV/nucleon; the Cosmic Ray Isotope Spectrometer (CRIS) to measure to measure isotope from *Z* equal to 2 (Li) though 31 (Zn) at energies from 100 to 600 MeV/nucleon and besides ultra-heavy nuclei measurement from *Z* equal to 31 (Ga) though 40 (Zr); the Solar Wind Electron, Proton and Alpha Monitor (SWEPAM) to measure solar wind electrons and ions at 1 - 900 eV and 0.26 – 35 keV respectively; the Electron, Proton and Alpha Particle Monitor (EPAM) to measure wide range of the solar and interplanetary particle fluxes concluding electrons; the Magnetometer (MAG) to measure three vectors of the interplanetary magnetic field component and the last one is the ACE real time solar wind operated by NOAA to transmit telemetry real-time to NASA's deep space network, 21 hours a day to monitor and predict the change of space weather. All instruments are shown in Figure 3-1.

In situ digital parameters collected from all the analog sensors are assembled together in an onboard solid state data recorder (SSDR) which can store data continuously more than 50 hours long in cast of necessary. Then, the data are flown under the spacecraft command and data handling (C&DH) and formatted into a minor and a major frame. The C&DH system reads one frame spacing 996 bytes out a second. A major frame contains 16 minor frames.

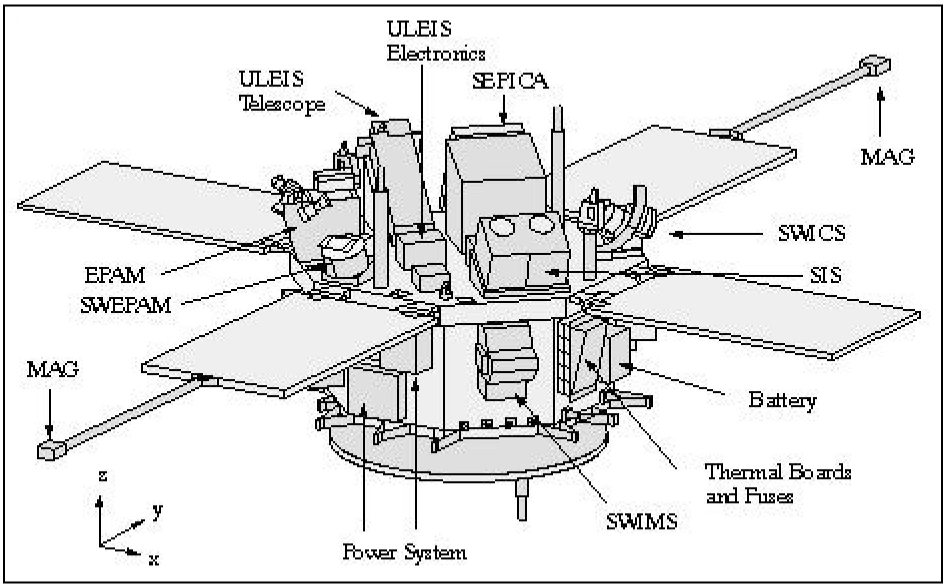

Figure 3.1 The ACE spacecraft illustration (OMNIWeb website, 2013).

3.2.1 Magnetometer, MAG

A twin of tri-axial arrangement fluxgate magnetometer monitors its surrounding IMF representative as the locally magnetic field direction, the magnetic magnitude and provides an effective studying in the fluctuation characteristics of IMF at 1 AU, including, a large-scale structure.

Working principle of MAG is like a normal fluxgate magnetometer. A twin of closed ferromagnetic cores has its susceptibility enough to be saturated magnetically with a weak surrounding IMF. The primary coil winds around two cores oppositely (as a Figure 3-2) and is excited by a kilohertz of alternating current (Beloff, Denisenko et al.) to saturate cores at the same strength but opposite orientation during each half-cycle of excitation. The cores are winded once more with a secondary coil, which get a voltage potential from the primary coil. If there is no external magnetic field, an amp meter connected to the secondary coil should detect and find zero voltage. On the other hand, when there is an external magnetic field, the field will reinforce magnetic field to a core which have the same field direction, but produce a smaller induced field, because of the opposite direction. The difference of measurable voltages in the secondary coil between no-external fielded existence and external field (as Figure 3-2) existence can derive the strength of the environment magnetic field in the direction of the core proportionally.

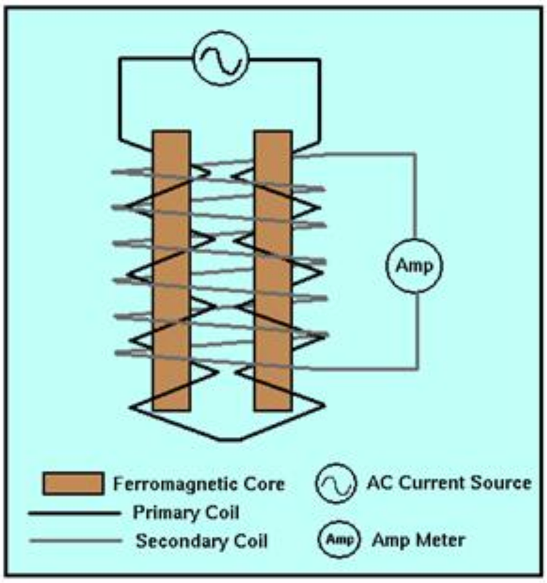

Figure 3.2 Fluxgate magnetometer mechanism. (Boyd, T., M., 1996)

3.2.2 The solar wind, electron, proton and alpha monitor, SWEPAM

SWEPAM is a 3-dimension electrostatic analyzer (ESA) to observe the interstellar medium, especially on the ion components of the solar wind. This ESA comprises of two experiments. A solar wind ion instrument (SWEPAM-I) provides the measurement of the wind protons and alpha particles and another is a solar wind electron instrument (SWEPAM-E) provides measurement of local electrons. The instruments are sensitive to any charge particles having energy between ~10 eV to several hundred MeV per nucleon. These ion measurements provide an effective studying in the context of various solar wind structures such as the low speed streamer belt flows, the high speed solar wind from corona hole, CMEs, the various and strength of IR, and the magnetic connection to the earth blow shock. The SWEPAM doesn't monitor the composition of this galaxy singly. It collaborates with SWOOP, another older ESA installed on the Ulysses, which orbits with an assisting of the Jupiter gravity.

An electrostatic analyzer mechanism needs employing an electric field to observe an element and isotopic composition. A stream of wind comes into the apparatus apertures, but then only charge particles are permitted to flow through the space between two opposite voltage curve plates. Because these plates set up an electric field, which act like a charge filter. Basically, an upper voltage plate attracts a dissimilarly incoming charge but repels similarly charge. The greater opposite charge (energy), the further it can travel as in the Figure 3-3. Its energy-per charge ratio, E/q effects, biases itself into its suitable channel electron multiplier (CEM) and be counted individually here. An ESA need knowing all velocities in three dimensions each a charge to characterize the bulk flow and the kinetic properties of the solar wind.

SWEPAM is programmed to provide a 64 s and 2.5° resolutions of full electron and ion distribution resulting from three factors, two angles and an ESA step level. Due to the direction of the fan-shaped aperture of SWEPAM sensor, two angles defined to point the direction in which a charge comes. The first one is the polar angle, θ, where 0° is parallel to Sun-pointing spin-axis direction of the ACE spacecraft, and another one is the azimuth angle, ϕ, which is in the plane perpendicular to the fan. Normally, the fan is pointed 18.75° in a polar angle and allows the instrument to measure ions arriving from 0° to 65 outward to the sun. Each ESA CEM steps 200 voltages from each others, both SWEPAM-I and SWEPAM-E.

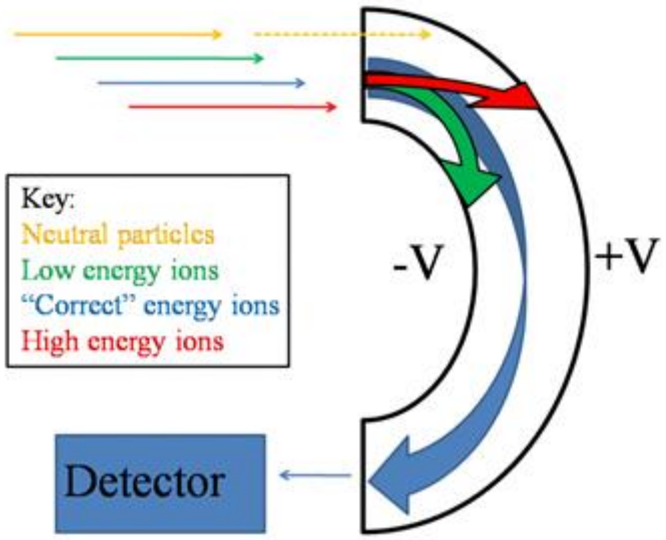

Figure 3.3 An electrostatic analyzer mechanism

(NASA website 2006)

SWEPAM-I sensor is negative high voltage and well-protected from any practical biases inside a spherical rib having apertures as Figure 3-4. An entrance aperture faces sunward direction at 3-4.5°, depended on the polar angle. Down inside the rectangle-shaped aperture, a gap width of 2.84 mm with radius of 100 mm is braced with a couple of curved plates having a 105° bending angle. The plates are made of aluminum alloy, coated with copper and darken to reduce UV scattering into the sensor. The blackened technique is Ebanol-C process. An inner plate is induced to be negative high voltage to introduce a particle into its own right channel of sixteen CEMs. The multiplier detectors are coated individually with 2 types of ceramic cards; the first one once more coated with a glass-coated thin film resister and one another is bear ceramic coupling capacitors. The 7 mm detector funnel has 5° of polar angle separation connected the gap as Figure 3-5. The CEMs are slightly positive to the exit end respectively.

A B

Figure 3.4 Drum-liked shapes of SWEPAM-I (A) and SWEPAM-E (B)

(NASA, 2006)

SWEPAM-I count is processed as Figure 3-6 and then calibrated. The SWEPAM counts particle at some given ESA voltages in any CEMs. CEMs have their own dedicated amplifier-discriminator and transmit a number of counts into their own miniature printed circuit board outside sensor, via a few centimeters of fully shielded signal line. The discriminator has 2 selectable levels; namely, $1x10^{6}$ and $2x10^{7}$ electrons per pulse. The lower level is to observe scientifically, whereas the higher level is use to calibrate a periodic CEM. After that cumulated pulses are processed in buffer/level-shifter modules, digitized into string, and calibrated finally. The SWEPAM-I calibration starts with forming 3D array of ESA voltage, azimuthal and polar angle of a given CEM and then approximates a count rate in gaussian profile with its geometric fitting, e.g., non-linear and trapezoid.

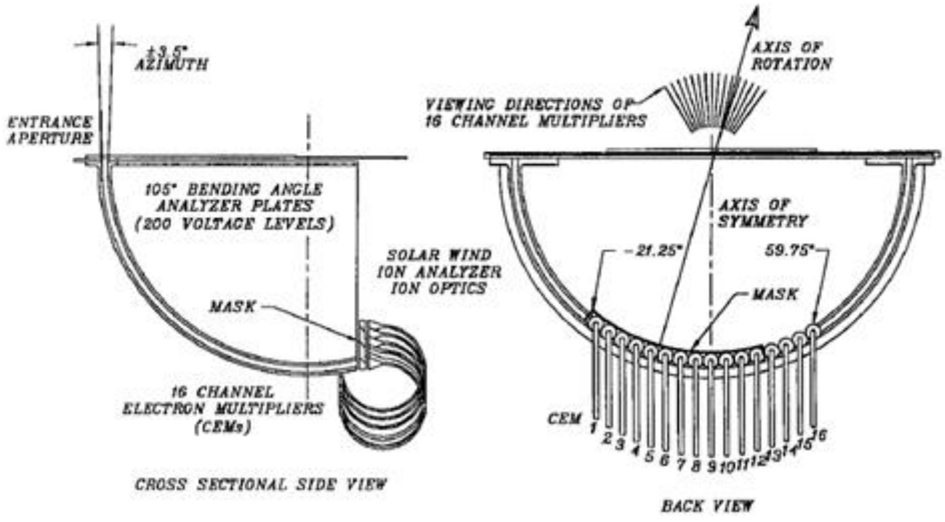

Figure 3.5 Inside the SWEPAM-I ESA and its CEMs arrangement

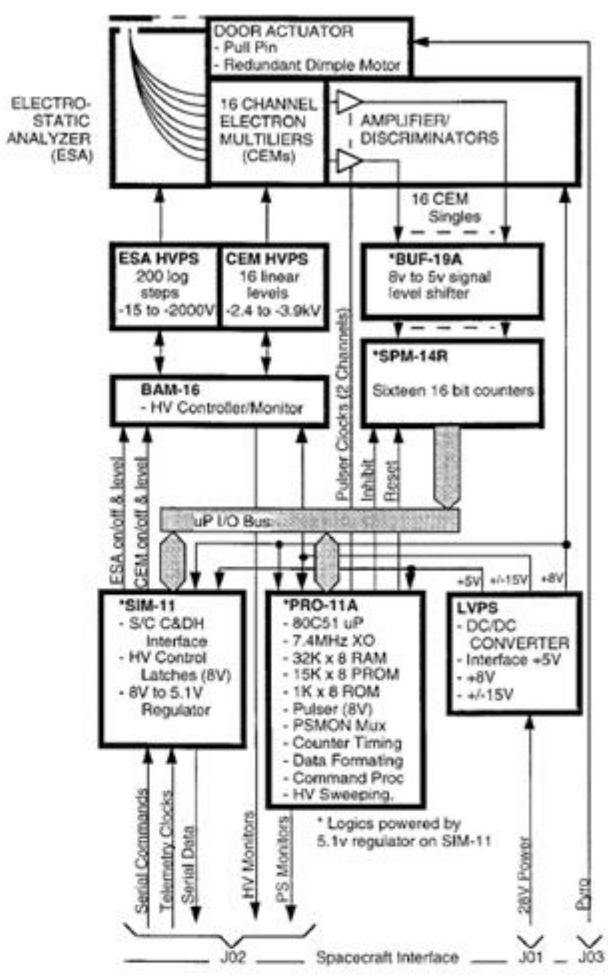

Figure 3.6 SWEPAM-I process.

SWEPAM-E body is quite similar to SWEPAM-I (see Figure 3-4). This instrument is based on around a spherical ESA. An entrance aperture of its points normally to the spacecraft spin axis. An inner gap width of 3.5 mm radiates average of 41.9 mm long. The 120 °bended ESA is positive high voltage inside and connects to seven funnels of CEMs as Figure 3-7. This ESA is also blackened to reduce background from UV scattering, photoelectron and secondary production in plate themselves. Because of sensitivity of low-energy electron to the spacecraft surface charge, The SWEPAM-E needs a special spacecraft blanket containing thermal characteristics of its spacecraft, coating apertures with silver/teflon film once more and covering spring-load dust for protecting contamination. 21° of polar angle separation of CEM funnels width of 11 mm diameter are along an exit, where covered with 92% transmission nickel mesh and been positive slightly. The CEMs count electrons having energies from 1.6 eV – 1.35 eV and transmit the signal through their own dedicated amplifier-discriminator into 20 contiguous energy bins as Figure 3-8.

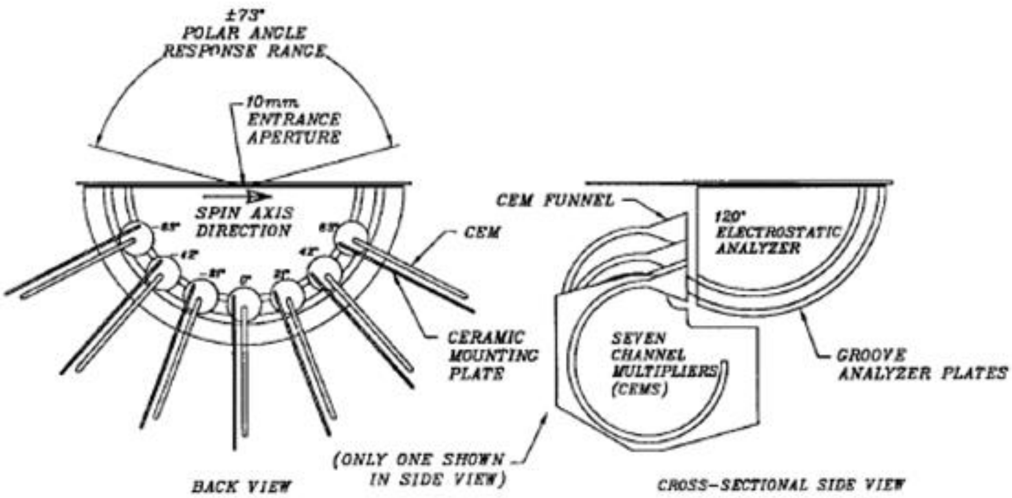

Figure 3.7 SWEPAM-E process.

The SWEPAM-E calibration is different from the SWEPAM-I, but both of their count rate adjustment is done similarly. There are 3 ways to calibrate SWEPAM-E; using a 1.05 keV proton beam, but simply much with using a negative high voltage or using ions with energies well above a few hundred volt post-acceleration bias on

CEM, the ions are far less effect by Earth's magnetic field than electrons. The count rate adjustment can be done with gaussian approximation and its geometric fitting.

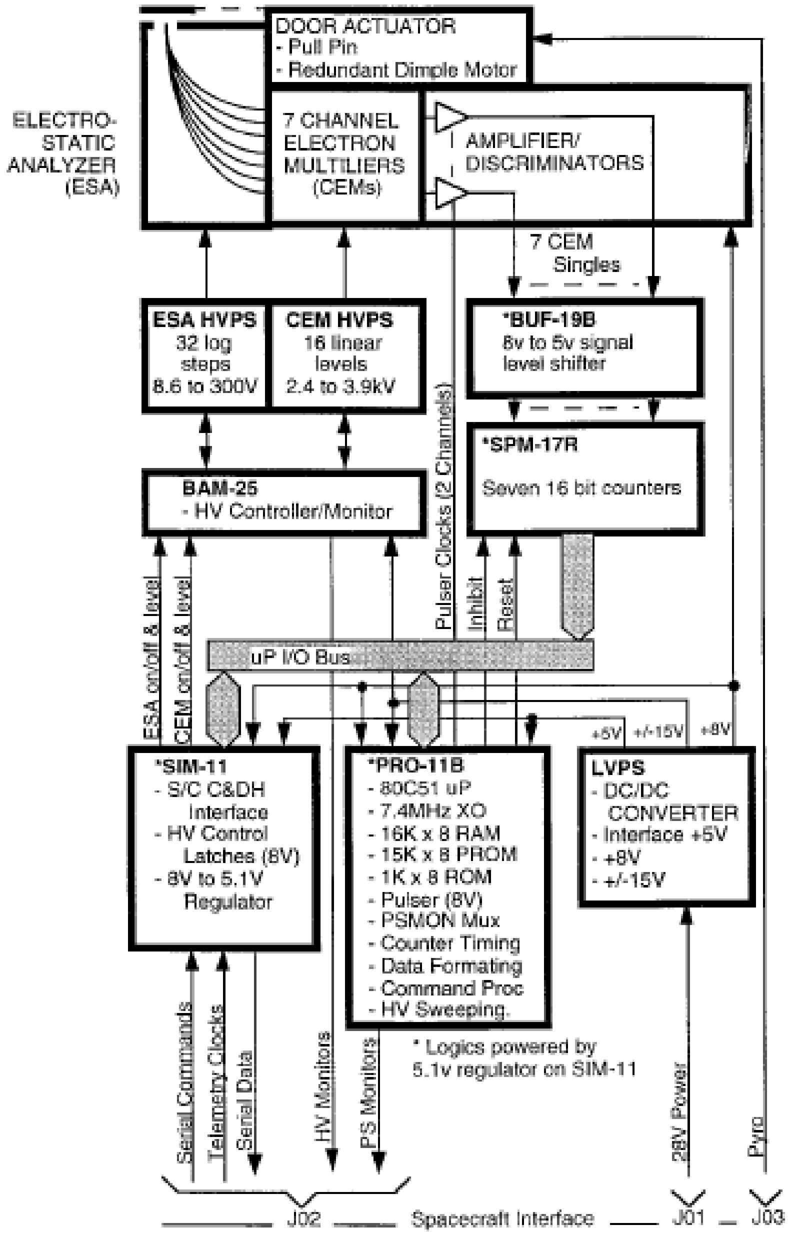

Figure 3.8 SWEPAM-E process

3.3 Ground-based measurement

There are 2 main ground-based instruments, a neutron monitor and GPS, used in this study. The monitors used in this recheck are mostly located over auroral zone (see Figure 1-1). They operated within the University of Delaware, Bartol research institute neutron monitor program. Another instrument is GPS data, which this investigation concentrates on the GPS stations in the North and South America continents, because, those places have the intensest station and have the most availability of data during 2005 – 2012. However, thai studies wouldn't able to reach the remote data without the global service sector as IGS.

3.3.1 Neutron monitor

A neutron monitor counts the secondary cosmic rays. The cosmic rays, ions and gamma ray, now known as a high energy particle consists of predominantly protons and helium nuclei from outer space. The ray from outer space is called primary cosmic ray. It encounters the earth and interacts with the atmosphere. The interaction produces more types of particles disintegration. The split molecule has high energy and be called the secondary cosmic ray, which is easier to detect and count than the primary cosmic ray, because it can be amplified after have collided with other molecules. The collision continues again and again as Figure 3-9. The process is called an atmospheric cascade. When a starting primary cosmic ray has energy above 500 MeV, the secondary cosmic ray can reach ground level, where neutron monitor can detect its byproducts, as neutrons.

Energy range of neutrons must more than 10 MeV. A neutron monitor counts the number of the incoming cosmic particles with four main components, as, a reflector, a producer, a moderator and a proportional counter. 10 MeV neutrons encounter the body of the monitor reflectors, in which made of a polyethylene. Other lower energy neutrons cannot penetrate the shell, because the polymer is proton-rich material. Neutrons get though the reflector and interact with an array of producer made of lead as Figure 3-10. The interaction produces a number of one-tenth energy neutrons of the previous neutron. These lower energy neutrons amplify the cosmic signal. The fast neutrons are slow down with a proton rich moderator, to confine, detect and count these neutrons within the reflector. Finally, disintegrate the proportional counter counts a number of neutrons via a 764 keV electrical signal produced by neutrons and helium reaction. The neutron monitor's invented first by Prof. John A Simpson in 1948.

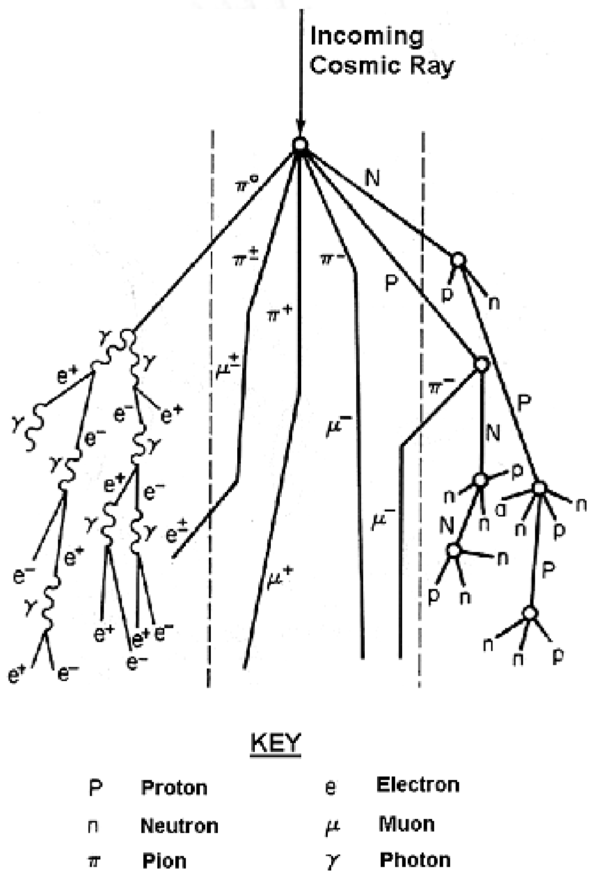

Figure 3.9 The atmospheric cascade starts in the deep upper atmosphere and interacts with air molecule and reaches the ground level.


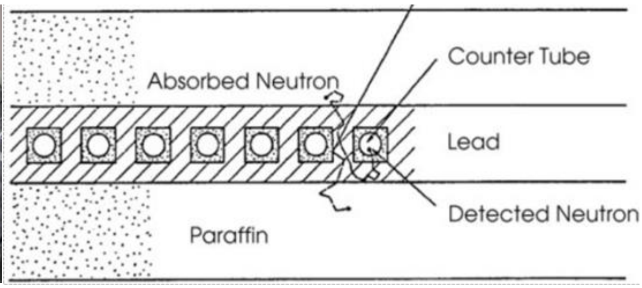

Figure 3.10 Inside a neutron monitor and its illustration respectively.

3.3.2 GPS

GPS project was first developed by the U.S. Department of Defense (DoD) in 1973. The department uses it in military affairs and allows civilians to some of the system also. The GPS is used widespread in business and also private individual nowadays because the system determines a one’s exact location and the precise time with the high accuracy. As a result, its application is famously used in various activities, such as, surveying, navigation in an airline business and shipping business, vehicle monitoring in the logistic business, determining the exact location of any places and holiday trekking. The system has little inaccuracy.

The accuracies of 2 determinations of GPS, an exact position and local time, are accepted satisfyingly. The determined position has an error less than a range of 20 m to approximately 1 mm. Another determining provides the time precision having an error less than 60 ns to approximately 5 ns. These values are determined by 3 the GPS main components, namely, satellites, theirs signals and their ground receivers.

The first twenty-eight GPS operated satellites were launched in 1978 and other satellites were later to 2013. Lately, there are sixty-four satellites operate and orbits the Earth in May 2013. The orbits are height of 20,180 km above the modeled surface. Satellites are located equal on six different orbital planes. The planes are inclined at 55° to the equator.

Each satellite has four atomic clocks, which being heart and known that their atom will lose a maximum of one second every 30,000 to 1,000,000 years. Satellites transmit their on board clock time and their position to ground receivers at

300,000 km/s as fast as the speed of light. Basically, a required time to reach the receiver, where located directly under the satellite, is approximately 67.3 ms.

At any determination, GPS requires four satellites to provide some exact positions. Measuring signal transmit time of a satellite derives a distance from a satellite to receiver as a radius of a sphere. Measuring signal transmit time of two satellites derives a position of receiver on the longitude (X) and latitude (Y) plane. Adding another one satellite in measurement provides the height (Z) of the receiver as Figure 3-11. These geographic coordinates seem to get enough to provide an exact location and a precise time, but these three coordinates are not enough. Another unknown variable need to be determined is time error (δt), so another satellite is needed to adjusted time error and distances in any works, however, there is another time error from receiver, which varies within approximately 5-10 m.

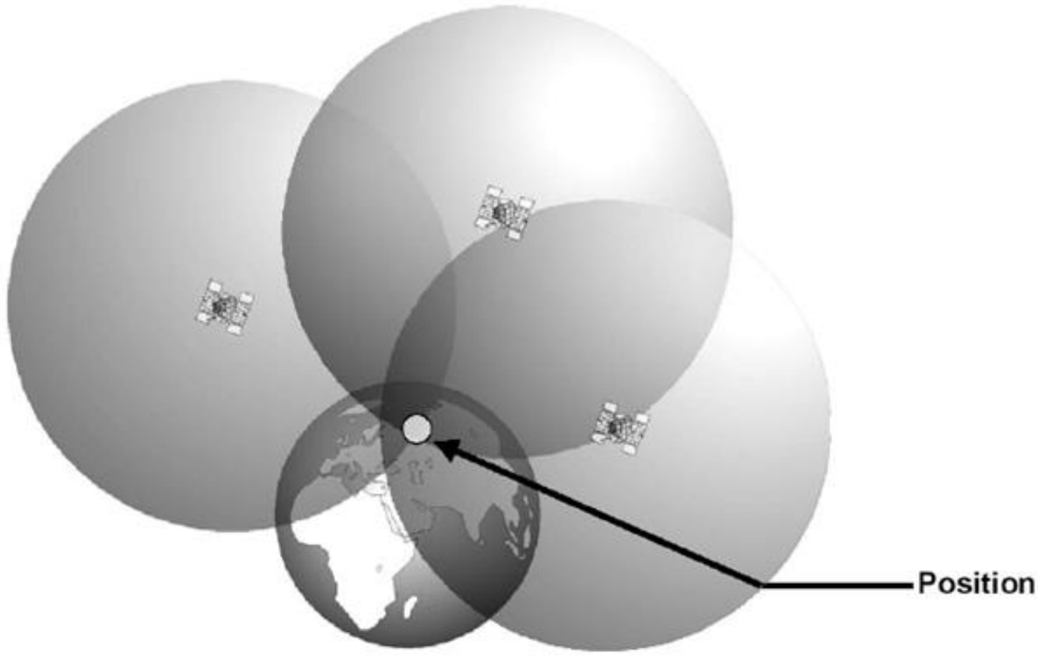

Figure 3.11 The position is determined at the point where all three spheres intersect.

A GPS signal contains an ephemeris data and an almanac, information about time and status of the entire satellite constellation, which allow user to determine the correct place and time. Both are coded in the Coarse/Acquisition (C/A) code and Precision (P) code, but the code that a public is allowed to use is C/A code, in which known as Pseudorandom Noise (PRN). The noise being a 1,023 bit deterministic sequence is transmitted repeatedly every millisecond or at 1.023 Mbit/s to receivers.

Receiver needs signals from at least four satellites to determine a correct three-dimensional position. At first, a receiver antenna evacuates weak signal, amplifies the transmitted 1575.42 MHz and converses the amplified signals into a lower intermediate frequency with the reference oscillator as a Figure 3-12. A means of a 2-bit ADC converts then an analogue intermediate frequency into a digital signal. After that, the digital signal has been undergone a correlating PRN pulse sequence to mix the satellite PRN sequence together and determines the signal transmit time from the satellites to the GPS receiver, before be transmitted to the signal processor. The signal processor controls the generated PRN sequence and uses it to calculate the correct position and save its in memory finally.

After receivers around the world generate raw orbit and tracking data, their products are transmitted to the Operational Data Centers (ODC) and the International GPS service (IGS) to format them according to a command standard. The data format named Receiver Independent Exchange (RINEX), which is commonly well-known.

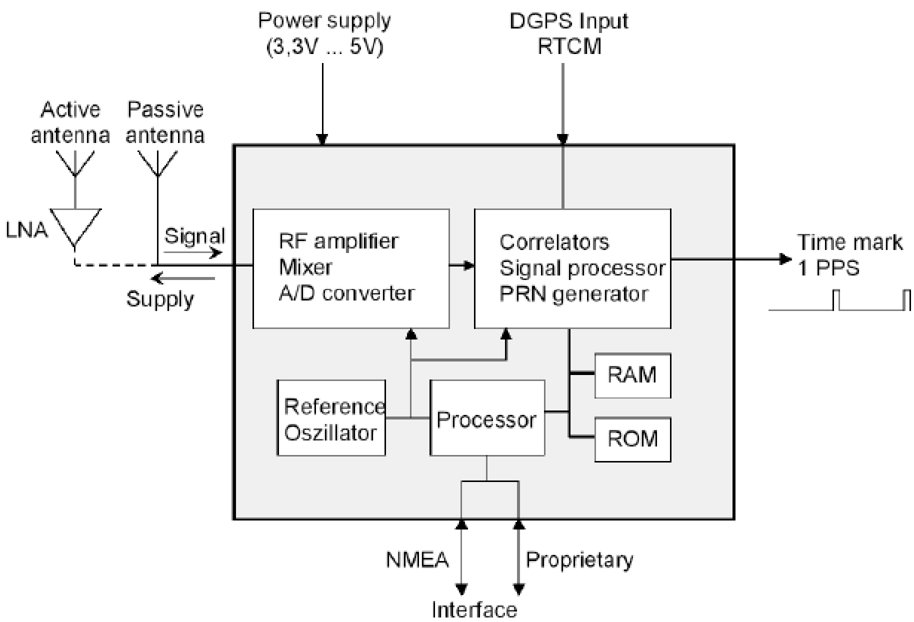

Figure 3.12 GPS module

3.3.3 International GPS service

A general public can reach GPS observation data sets of the IGS collection for free online easily at out the SOPAC website. Since 1994, the International Association of Geodesy (IAG) operated routinely to achieve and distribute data products such as, tracking data and GPS orbits data in support of geodetic and geophysical research. In particular, global navigation satellite system (GNSS) data, in support of Earth science research.

GPS data of IGS at any position around the world and for any purpose are almost available. The IGS took a part in many government sectors and association, such as, the service of the international Association of Geodesy since 1990, the Federation of Astronomical and Geophysical Data and Analysis Service (FAGS) since 1996 and the Scripps Orbit and Permanent Array Center (SOPAC) which collects and supports near real-time of their own at least 250 station data. Moreover, the SOPAC has many participants in various researches, such as, Plate Boundary Observatory (PBO), Sumatran GPS Array (SuGAr), NASA MEASUREs, Earth Systems Research Laboratory (ESRL) at NOAA, which locates many GPS sites for Meteorological studies around the world, so any individuals who interesting in the GPS data can reach approximately 800 continuous GPS data from more than 20 scientific networks around the world at IGS via SOPAC website.

Various IGS-GPS usages in various studies contribute many products and application available to IGS. The Service uses GPS data sets to generate following product: GPS satellite ephemerides, GLONASS satellite ephemerides, Earth rotation parameters, IGS tracking station coordinates and velocities, GPS satellite and IGS tracking station clock information, Zenith tropospheric path delay estimates and Global ionospheric maps. These can use as a applications in many purpose of studies, such as earthquake hazards, tectonic plate motion, plate boundary deformation, meteorological and upper atmospheric process, which is repeated in this study.

3.4 Data descriptions

All the data used in this study, is available on online databases. An interested person can reach them via their operator website. The level 2 IMF data are available on ACE level 2 data server on the Space Radiation Lab (SRL), under the California Institute of Technology (CALTECH) website. SWEPAM both need 64 s to spin-phase calibrate with spacecraft clock and other instrument, while MAG instrument required to only 16 s as fast as one spin to calibrate itself, so the 64 s and 16 s is the finest time resolution to use its. The observed neutron counts monitoring data adjusted with the reference pressure 563 mmHg at the princess Sirindhorn project are available on Thaispaceweather website. GPS data from stations are available in RINEX format, on the SOPAC website. These data is saved in difference pseudo-code as table 3-1.

Table 3.1 Parameters used in this study and their details.

No.	Parameters (Pseudo-code)	Time Resolution	Level in Used	Measurements	Instruments	Usage
1	the magnetic field magnitude in nT (Bmag)	16 s	2	Space-based	MAG instrument	- Identifying MCs, ISs IRs and HSS
2	the RTN latitude in degree (Delta)	16 s	2			- Classifying shock with its local angle
3	the RTN longitude in degree (Lambda)	16 s	2			- Classifying shock with its local angle
4	the x component of magnetic field vector in GSE coordinate system in nT (Bgse_x)	16 s	2			- MVA -correlating MCs to dTEC%
5	the y component of magnetic field vector in GSE coordinate system in nT (Bgse_y)	16 s	2			- MVA - correlation
6	the z component of magnetic field vector in GSE coordinate system in nT (Bgse_z)	16 s	2			- MVA - correlation - Classifying MCs
7	the x component of proton velocity vector in GSE coordinate system in km/s (Vgse_x)	64 s	2		SWEPAM-I	- lag time determination - correlation
8	the y component of proton velocity vector in GSE coordinate system in km/s (Vgse_y)	64 s	2			- lag time determination - correlation
9	the y component of proton velocity vector in GSE coordinate system in km/s (Vgse_y)	64 s	2			- lag time determination - correlation
7	proton speed in km/s (V_p)	64 s	2	Space-based	SWEPAM-I	- identifying IS and HSS

8	radial component of the proton temperature in °K ($T_{p,rr}$)	64 s	2			- identifying MCs
9	proton density in cm^{-3} (n_p)	64 s	2			- identifying MCs
10	the x component of the spacecraft position, in GSE, in km (pos_gse_x)	64 s	2		ACE spacecraft	- lag time determination
11	the y component of the spacecraft position, in GSE, in km (pos_gse_y)	64 s	2			-l time determination
12	the z component of the spacecraft position, in GSE, in km (pos_gse_z)	64 s	2			- lag time determination
13	the neutron monitor, corrected for pressure effect, in counts per hour (Corr)	1 h	Corrected with air pressure	Ground-based	neutron monitor	- rechecking arriving of the CME structures to the earth
14	GPS station latitude in degree (Lat)	6 m	Std		GPS	- lag time determination - generating dTEC% map
15	GPS tation longitude in degree (Lng)	6 m	Std			- lag time determination - generating dTEC% map
16	GPS station altitude in m (Al)	6 m	Std			- lag time determination - generating dTEC% map
17	mean TEC in TECU (VTEC)	6 m	Std			- deriving mTEC and dTEC%
18	average magnetic field of the planet in nT (A_p)	1 h	OMNI 2		magneto-meter	- identifying a quiet and a disturbed day

CHAPTER IV
METHODOLOGY

4.1 Introduction

Because lots of high-temporal-resolution datasets coming from the ground and space-based observations, are required in this study to confirm the CME, its ancillary structure and co-rotating region arrivals, a manual calculation is too drag. Programming is needed to carry these works out. The technical computing language used to execute provability in the study is MATLAB.

This chapter describes all processes, their concepts and their equations in the whole programs executing this study briefly. The content in chapter 4 starts from MCs and other phenomena identification with space instruments, investigation their arrivals with a ground instrument, coordination systems between GSE, GEO and GEI transformation, lag time from spacecraft to the GPS receivers calculation, time capture, change in TEC from quiet time determination and represents their deviation in maps generated with IDW interpolation.

4.2 Magnetic clouds identification

CMEs are observed with a photographic technique and those CMEs are identified once more specifically as MCs with their magnetic fields and particle measurement. Some driven ICMEs, pass through any spacecrafts. They may run into or away our earth. A few percent of ICMEs are MCs. Nonetheless, 72% of these MCs induce severe magnetic storms. Therefore, MCs identification in advance of reaching at the earth is well.

There are a lot of cloud criteria to identify. But, there are three processes to use typically. The earliest process is minimum variance analysis (MVA). The second one is an expected plasma temperature to the plasma temperature in measurement comparison. Another process is thermal pressure to the magnetic pressure ratio test. In my experience as a programmer I prefer to investigate two latter processes before MVA. Seeing that importing a lesser resolution file as small as the 64 second average SWEPAM data is much faster and easier than 16 second MAG data.

4.2.1 Minimum variance analysis

Generally, a space phenomenon reveals itself as a clustered data via a single or a multi-spacecraft based measurement. To confine the clustered physical configuration, MVA technique fits to border the magnetic boundary with its XYZ magnetic components. Base on its planar assumption, the MVA doesn't suit to all geometries. In particularly the multi-spacecraft case conflicts clearly with the assumption (Dunlop, M. N., Woodward, T. I. and Farrugia, C. J., 1994). Anyway, MVA is useful to estimate MC axis orientation (Echer, E., Gonzalez, W. D. and Alves, M. V., 2006). A unit normal vector $\hat{n}$, the eigenvectors (x_1,x_2,x_3) and the eigenvalues (λ_1,λ_2,λ_3) are three basically derivative values needed to generate a symmetric matrix $M^B_{\mu v}$ in MVA (Sonnerup, U. Ö. and Scheible, M., 1998). The complex procedures are directed as follows.

Brief MVA steps of the program 1 in the Appendix A are hereafter described. The earliest work is the $\hat{n}$ calculation from three distinct vector measurements given as B^1, B^2 and B^3 as equation (4.1).

$$\hat{n}= \pm\frac{(B^1\text{-}B^2)\times(B^2\text{-}B^3)}{(B^1\text{-}B^2)\times(B^3\text{-}B^3)} \tag{4.1}$$

The normal field component B_n computed left out the assumption $B \cdot \hat{n} =$ $B\cdot\hat{n}=0$ 0 allows calculation of its actual value, as equation (4.2).

$$B_n=B\cdot\hat{n}=\pm\frac{B^1\cdot(B^2\times B^3)}{|(B^1\text{-}B^2)\times(B^2\text{-}B^3)|} \quad B_n = B\cdot\hat{n} = \pm\frac{B^1\cdot\left(B^2\times B^3\right)}{\left|\left(B^1-B^2\right)\times\left(B^2-B^3\right)\right|}$$

(4.2)

Thenceforth, the result allows creation of an array B_n based on equation (4.3)

$$M^B_{\mu v} \equiv \langle B_\mu B_v\rangle - \langle B_\mu\rangle\langle B_v\rangle$$

$M^B_{\mu v}\equiv \langle B_\mu B_v\rangle\text{-}\langle B_\mu\rangle\langle B_v\rangle M^B_{\mu v}\equiv \langle B_\mu B_v\rangle\text{-}\langle B_\mu\rangle\langle B_v\rangle$

(4.3)

Where the subscripts μ and v are 1, 2 and 3 represent X, Y and Z in a Cartesian coordination system respectively.

An eigenvector of any square matrix is a non-zero vector in which multiplied by its matrix, yields the original vector multiplied by an eigenvalue specially. Owing to an eigenvector, the eigenvalue meant changing in a vector magnitude with keeping a same old direction under a given linear transformation. Consequently, an above matrix is usable to calculate the eigenvector and its eigenvalues with equation (4.4).

$$\sum_{v=1}^{3} M_{\mu v}^{B} n_v = \lambda n_v$$ $$\sum_{v=1}^{3} M_{\mu v}^{B} n_v = \lambda n_v \sum_{v=1}^{3} M_{\mu v}^{B} n_v = \lambda n_v$$ (4.4)

Siscoe and Suey suggested in 1980 that the λ_2 to λ_3 ratio in MCs must be or be higher than 2 because of its ellipsoid geometry. By the way, the equation 4.4 yields three λ, namely, λ_1, λ_2 and λ_3 which stand for eigenvalues of the maximum, medium and minimum variance direction.

4.2.2 An expected plasma temperature calculation

Ordinarily, velocities about 400 and faster than 600 km/s are used to assort solar stream blowing into a slow and fast wind respectively. But the velocity about 500 km per second is critical speed to select a formula allowing calculation of an expected proton temperature. Richardson and Cane found these empirical correlations in 1995.

An expected proton temperature is a proton temperature defined statistically from the solar wind speed V_P V_{sw} and the proton temperature V_P T_p at near-earth space. Two differentiate formulas are to use in the different wind speed as equation 4.5 and 4.6.

$$T_{exp} = 1000(0.031V_{sw} - 5.1)^2 \quad \text{for } V_{sw} < 500 km/s$$ $$T_{exp} = 1000(0.031V_{sw} - 5.1)^2 \quad for\ V_{sw} < 500 km/s$$

(4.5)

T_{exp} =510V_{sw}-142000 for V_{sw}≥500km/s$T_{exp} = 510V_{sw} - 142000 \quad for\, V_{sw} \geq 500km/s$ (4.6)

From a previous research, an actual MC temperature ought not to be higher a half of its expected temperature. Nowadays, many studies like holding the criteria and publish frequently.

4.2.3 The thermal pressure to the magnetic pressure ratio test

The thermal pressure to its magnetic pressure ratio β, is an effective index in MCs identification, since the ejected cloud contains more magnetizing compositions when compare it with a calm solar wind. Then, the magnetic field of the cloud has a greater effect on its motion than its dynamics. After all, the cloud has a higher pressure than the ambient medium, so the cloud ought to expand themselves to the surrounding medium and the proton temperature, , $T_p$is getting lower during the expansion. This anomaly makes MC different from wind and other ejecta. From Burlaga's result in his original study about the βin configurations of MC, in 1991, the empirical β was less than 1. The ACE observation allows us to determine β β with its 3 parameters, the proton density, N_p, the radial component of the proton temperature, T_p and the magnetic field magnitude, *B*, as an equation 4.7.

$$\beta = \frac{8\pi \cdot N_p \cdot k_B \cdot T_p}{B^2} \quad (4.7)$$

Where k_B kB devoting the Boltzmann constant, which equal 1.3806505 x 10^{-23} J/K.

4.3 An interplanetary shock (IS) identification and classification

Because there is no directly sound speed, Alfven speed, proton density and so on measurement, in addition working with IS must involve with many assumptions by reason of a limited of instruments. Assumptions are use to calculate many ratios concerned with the IS and describe the IS configurations. There are two famous ways to classify IS with its characteristic and this examining do also, one is an angle between the magnetic field direction and its shock normal θ_{Bn} and another is its speed classification.

4.3.1 Shock classification with the angle between the magnetic field direction and its shock normal

Colburn and Sonett stated the coplanarity theorem in 1966 that the shock normal $\mathbf{n}$ and the magnetic fields at two points, the upstream B_u and downstream B_d lie in a plane. After that θ_{Bn} can be calculated from three existing magnetic fields on ACE and their derived shock normal which are calculable with equation 4.8.

$$n = \frac{(B_u \times B_d) \times (B_u - B_d)}{|(B_u \times B_d) \times (B_u \times B_d)|} \quad (4.8)$$

The θ_{Bn} can hereafter compute with basic vector operation as equation 4.9

$$cos\theta_{Bn} = \frac{B_x \cdot n_x + B_y \cdot n_y + B_z \cdot n_z}{\sqrt{B_x^2 + B_y^2 + B_z^2} \cdot \sqrt{n_x^2 + n_y^2 + n_z^2}} \quad (4.9)$$

Then an angle is to classify IR into 3 major groups and 2 subgroups as follows:

- A perpendicular shock which propagates perpendicular to its magnetic field, $\theta_{Bn} = 90^\circ$.
- A parallel shock which propagates parallel to its magnetic fields, $\theta_{Bn} = 180^\circ$
- An oblique shock which propagate at any θ_{Bn} between 0° and 90°. This major class can subdivide more into 2 subgroups:
    - A quasi – parallel shock which propagate at $0^\circ < \theta_{Bn} < 45^\circ$ angle width.
    - A quasi – perpendicular shock which propagate at $45^\circ < \theta_{Bn} < 90^\circ$ angle width.

The θ_{Bn} does not only itself imply and takes a part in calculating the critical Mach number $\mathrm{M_c}$ also. So that, the angle is essential in IR classification with its speed.

4.3.2 Shock classification with its Mach number

The Mach number is object speed to the speed of its sound ratio. The ratio is widely used in describe how fast object might perform. Any object moving at 1 Mach means it can move 1,225 km per hour in other words is 761.2 miles per hour. Mach number divides objects into 4 groups as a subsonic, a transonic, a supersonic and a hypersonic which move slower than 1 Mach, equally 1 Mach, faster than 1 Mach and faster than 5 Mach respectively (Glenn research center, NASA website, 2010). The Mach number needs a sound speed to derive and ACE spacecraft, there is no direct measurement, so calculating sound speed is need as equation 4.10.

$$\text{Sonic Mach number} = \frac{V}{V_s} \tag{4.10}$$

Sound implies a disturbance and its speed implies how fast it moves. Sound and IS are a distinction with few difference. Hence, sound speed implies a small disturbance speed in IS. Basically, sound speed responses consistently to the temperature and the gamma, the ratio of specific heat of a given medium, because sound is a transmission resulting from the collision between disturbed randomly moving molecules in the medium. The speed of sound can be derived from equation 4.11 in the next page.

$$V_s = \sqrt{\text{gamma} * \left(\frac{\text{thermal pressure}}{\text{mass density}}\right)} \tag{4.11}$$

The operating missions as a Node on the internet (OMNI), NASA networking project details the derivation of several parameters including the finally derivation of the speed of sound, used in other spacecraft as equation 4.12.

$$V_s = 0.12 * \sqrt{T_p * \left(1.28 \times 10^5\right)} \tag{4.12}$$

In astrophysics, the solar wind is defined its characteristics as plasma. The plasma typically has a slow-frequency oscillation called Alfvén wave, a resulting from the inertia provided by the mass of its ions and the restoring force of the magnetic field tension. The Alfvén speed VA varies harmoniously to magnetic field magnitude and varies reverse a number of mass densities as equation 4.13.

$$VA = \frac{B}{\sqrt{4\pi * \text{mass density}}} \tag{4.13}$$

Practically, OMNI calculates Alfvén speed VA via derivation with equation 4.14.

$$VA = \frac{20B}{\sqrt{N_p}} \tag{4.14}$$

The critical Mach number is the ratio between difference in the speed of sound and its velocity at upstream to the Alfvén speed at a given θ_{Bn} angle as equation 4.15.

$$M_c = \frac{V_s - U_u}{VA\cos\theta_{Bn}} \tag{4.15}$$

This Mach number is to use as an indicator to classify shock into 3 groups:

- Slow group: a shock has $M_c < 1$.
- Intermediate group: a shock has $M_c = 1$.
- Fast group: a shock has $M_c > 1$.

4.4 Co-rotating interaction region identification

High Speed Streams (HSS) blows out of the poles of the sun, hits it's a former low speed wind and compresses itself together. Smith and Wolfe found and called them as a Co-Rotating interaction Region (CIR) since 1976. The CIR is mixed with high and slow wind and therefore an abrupt change appears as a noticeable peak in solar wind speed, density and magnetic field components graphs. Besides, these remarks are able to identify CIRs and the east-west deflection in velocity in y component also appear and been sometimes be noticed easily. Unfortunately, many times it seems the deflection doesn't clear. Hence, the other identifying CIR criteria are required to use.

Two characteristics of CIR are used to identify it. The first is fact that CIR is a vast structure of a magnetic continuity. Tsurutani and Smith regulated the TS criteria after their names in 1979, from their discovery. Studying at that time showed that the CIR was a sharp directional change in magnetic field, from seeing the experimentally differential magnetic field vector in any component being always greater than 26 and its one-half magnitude field magnitude also,as an inequality 4.16.

$$\Delta B > 0.5|B| \; ; \quad \Delta B > 26 \tag{4.16}$$

Another characteristic of CIR is resulting from its HSS. Its HSS comes from the coronal hole at any high latitude and contains a large-amplitude Alfvén wave, in which, its ΔB to $|B|$ ratio is typically around 1 and 2. Furthermore, the Alfvén wave exists in CIR, but doesn't exist in MCs. This fact is useful to bound and separate CIR and MC regions.

4.5 Investigating an arriving at the Earth of the MC and the others with a neutron monitor.

After the ACE spacecraft has caught a signal of ICMEs, A Forbush decrease, FD is use to detect an arrival of the ICMEs. FD was found and published by Scott E. Forbush in 1967. The FD is a temporal decrease in the number of the galactic cosmic ray reaching ground level of the earth following the CME and its ancillary structures. The decrease in the cosmic ray is detected with a neutron monitor.

The percentage FD can calculate from Kane formulation (Kane, R., P., 2011) which derived from Wada formulation (1957). The method used in this study can be tersely done as follows, declares *N* as an hourly counting rate which can determined with summarizing an average of counts per hour, $\hat{\mu}$, by adding its standard deviation,

$\sigma(\hat{\mu})\sigma(\hat{\mu})$ as an equation 4.17, where $\sigma(\hat{\mu})$ can be derived from equation 4.18. During the FD occurrence, N_i and N_j are the counting rate at the start of the FD and the counting rate at the end of the FD. After that the method need calculating the differential Wada value, *W*, between at the start (W_i) and the end (*W*j) with multiplying the reference pressure (*PO*), which is 563 mmHg at Doi Inthanon, with differential of counting rate at the start and the end as an equation 4.19.

$$N = \hat{\mu} \pm \sigma(\hat{\mu}) \quad (4.17)$$

$$\sigma(\hat{\mu}) = \sqrt{\frac{\hat{\mu}}{n}} \quad (4.18)$$

$$W_i - Wj = PO \times (\ln N_i - \ln N_j) \quad (4.19)$$

The last equation was derivated by Kane. The reference pressure is to use again as a factor as equation 4.20.

$$\text{Percentage FD} = (W_i - Wj)/PO \quad (4.20)$$

When there are two steps of decrease (more than 20%), the first drop is defined as the result of shock and the following drop is the result of CMEs.

4.6 TEC determination

After a neutron monitor confirms an arrival, The TEC datasets is used to describe their variation. TEC at the same time is declared as disturbed TEC and the TEC during an hourly averaged A-index called $A_p \leq 15$, in 13 days before and after event is declared as a quiet time TEC. With using both TECs, the percentage deviated TEC, dTEC%, is calculable.

Before TEC is derived and used in the study, a GPS RINEX file must have been batch processed with some programs. The program is used in this survey is

GOPI RINEX ⟶ TEC version 2.2, in which developed by Dr. Gopi Krishna Seemala and widely used in many publications.

4.6.1 Converting the differential delay into TEC in GOPI program and the acceptable temporal resolution in this study.

GOPI RINEX ⟶ TEC version 2.2 is able to execute data only on the internet. A RINEX file is an input file in GOPI process. GOPI reads 43 records in the file, such as its information about time, its station name and positions. The GOPI batch processes them, and afterwards the program needs the internet to download IGS navigation file to get satellite ephemeris from the IGS online database. After that, the processor processes cycle slips in phase data and read satellite biases from DCB IGS code. The program uses the bias to calculate the inter-channel bias for different satellite in the receiver and writes and ascii output files finally.

The accumulated effect by time and signal arrives at the GPS range observables is proportional to the integrated TEC from the receiver to satellite. GOPI integrates TEC from differential delay between f1 (1575.42 MHz) and f2 (1227.60 MHz) signals with summing the equation with 3 biases; receiver bias (B_{Rx}), receiver inter-channel bias (B_{Rich}) and satellite biases (B_{sat}) as written in equation (4.21).

$$\text{Desired slant TEC} = STEC + B_{Rx} + B_{Rich} + B_{sat} \quad (4.21)$$

The .CMN file-type output is processed again with the least – squared temporal difference method, which is described in the next topic. The .CMN file has 30s resolution. GOPI then writes the mean VTEC output, which is .std file type and has a much rougher time resolution which is 6 m. This study uses a 6 m data, since each an event is prolonged at least over a few days following the size of MCs and the others. Furthermore, this study studies trend of change in TEC, not its amplitude.

4.6.2 The average of TEC from different satellites calculation

At any given time, a GPS receiver detects signals from different PRNs, different satellite from a different ascension and declination. Consequently, there are many derivate TECs at any different celestial points. Sometimes, there are not any satellites on the zenith of the GPS station, so the vertical TEC is an imperfectly average value in the reinforcement learning.

The reinforcement learning is an approach to sequential decision made in an unknown environment by learning from past interactions with that environment and any TEC value derived from PRNs is a precision with the error. Any TEC computing programs have their own error and their own advantage. Gopi gives a short description about the tuple of his TEC, which is to use in this study as a "mean (2 sigma iterated) TEC". The description implies its derivation itself. A lower case δ δ is meant to the standard deviation (SD) of a population or probability distribution in statistics and iteration means repeatment. By the way of explanation, 2 sigma iteration TEC, is meant to a TEC computed from 2 SD value a 2 times loop program, in which developed for data analysis based on the least – squared temporal difference method (LSTD).

The LSTD is a data-efficient evaluation technique in a linear least square regression. It's controlled with linear value approximation. There are bugs in this algorithm. Possibly poor extrapolation properties and its sensitivity to the unusual data points being out over the long range of the straight line are the limitation of LSTD, so another technique is developed to remove these advantages. The least-squares policy iteration (LSPI) is an evaluation technique specifically after Markov decision process (MDPs). The process is directly proportional to five factors, a state $\mathbf{s}$, its action $\mathbf{a}$, its reward $\mathbf{r}$, the probability of reaching state $\mathbf{P}$ and a discount rate parameter γ.

State of TEC calculation depends on variable numbers of satellite at their inclination and declination. The furthest satellite with low declination is overestimated because of shear angle and the longer path it propagates. Conversely, the nearest zenith satellite is weighted most to set TEC on. Moreover, at any different given time, satellites move and stay different from a previous minute. Some satellites move and come closer, some satellites pass zenith and move down to horizon at the same time as Figure 4-1 and the condition in TEC calculation state changes. An action to calculate changes, a reward changes, so a discount rate of the incoming state changes finally. The following step is present and the next reward summation $\hat{b}$ calculation with equation (4.22). Finally, the last step is to reduce error with multiplication with an inversion of the difference between the probabilities of selecting action from states find weighted vector $\hat{A}$ (equation 4.23) which is a suitable TEC.

$$\hat{b}= \sum_t \phi(s_t,a_t)r_{t+1} \tag{4.22}$$

$$\hat{A}= \sum_t \phi(s_t,a_t)\left(\phi(s_t,a_t)-\gamma E_\pi[\phi(s_{t+1},a_{t+1})|s_{t+1}]\right)^T \tag{4.23}$$

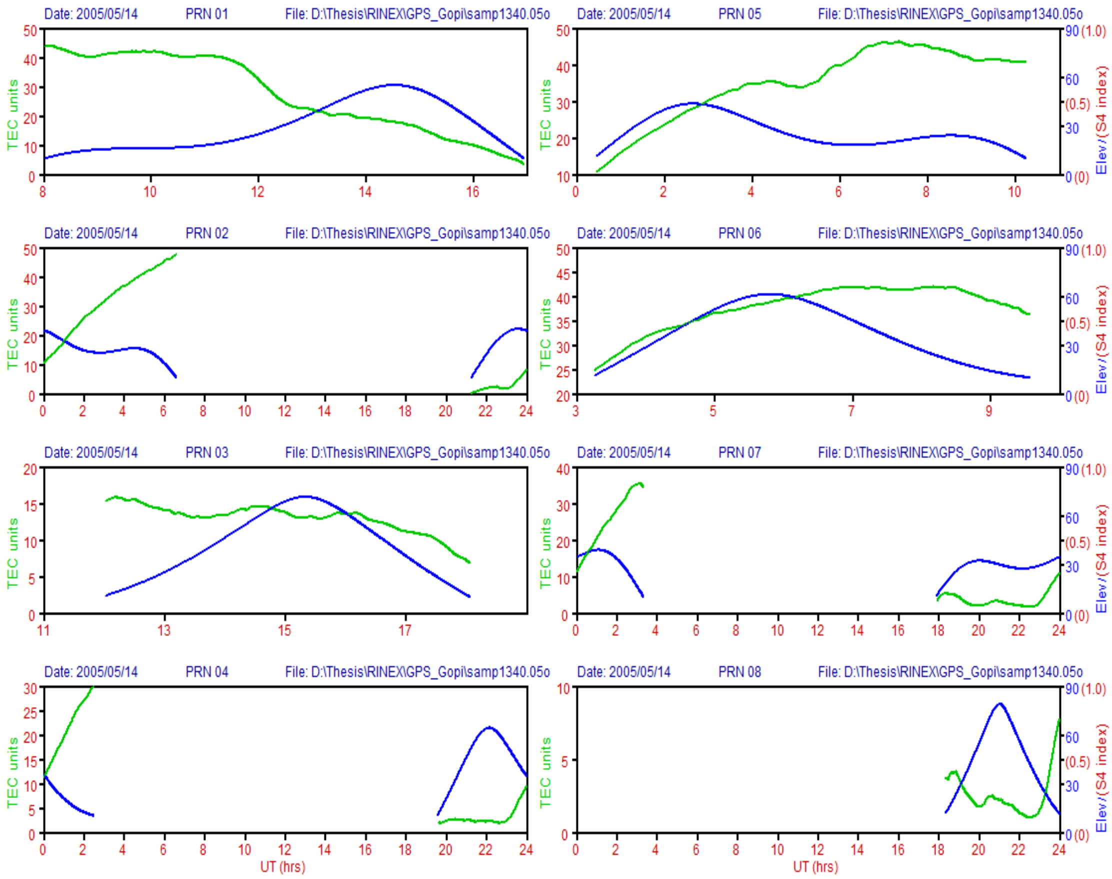

Figure 4.1 TEC plot from different elevation PRNs in GOPI observe type file.

One condition is to add in the GOPI's TEC calculation to remove error is a mask elevation filter. The mask elevation is a low angle filter which created to remove the atmospheric error. The error triggers from long path propagation in the irregularly noisy air. Basically, receivers detect signal form the angles above 15 degree from horizon as Figure and the program reward average TEC and its standard deviation from different PRN as Figure 4-2. In high accuracy TEC calculation, the program use signal from 20 degree above to calculate TEC again with another standard deviation as shown in a Figure 4-3. The finally TEC value is adjust third time with removing satellite and receiver biases.

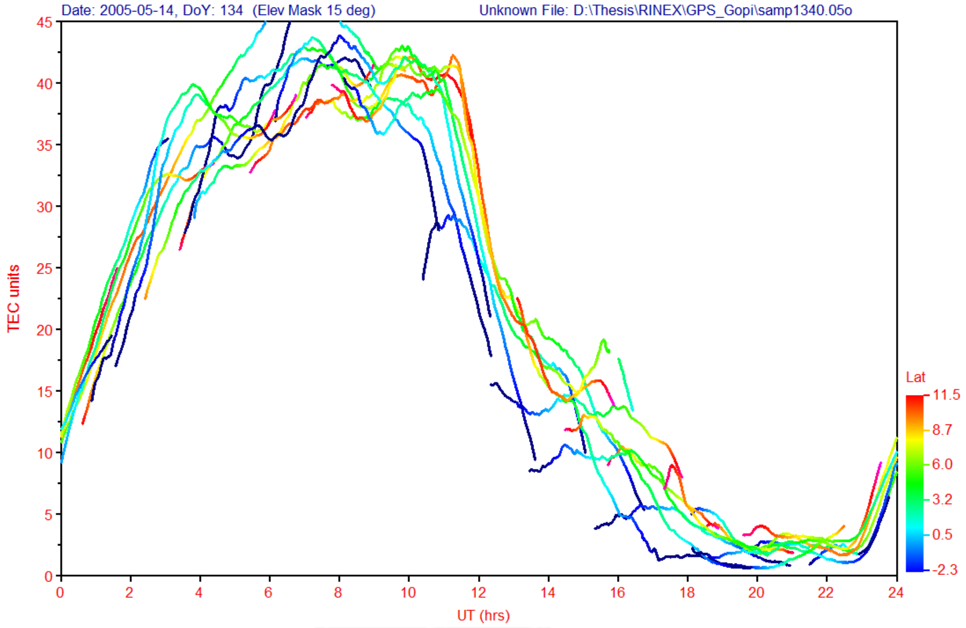

Figure 4.2 The adjusted TEC under elevation mask 15 degree filter.

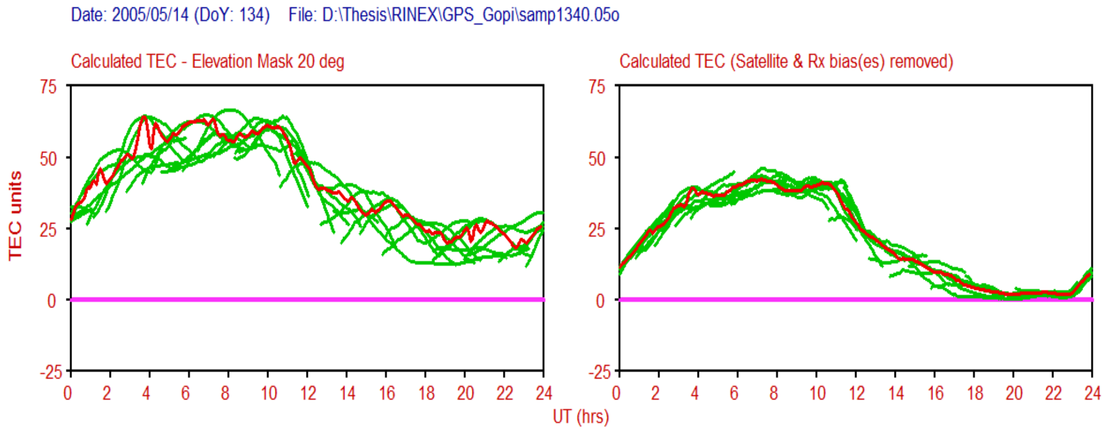

Figure 4.3 The once more adjusted TEC under elevation mask 20 degree filter.

4.7 Mean TEC and presenting a deviated TEC as its variation

A percentage relative deviation TEC $\mathrm{dTEC\%}$ was used originally and applied since 2006. The $\mathrm{dTEC\%}$ is the ratio of difference between TEC during disturbance and the quiet time to TEC in quiet time in percent as equation 4.24.

$$\mathrm{dTEC\%}=\left(\frac{\mathrm{TEC_{disturbed}}-\mathrm{TEC_{quiet}}}{\mathrm{TEC_{quiet}}}\right)\times 100 \tag{4.24}$$

The $TEC_{disturbed}$ is observed TEC at a given time. The TEC_{quiet} is an average of TEC during $A_p \leq 15$ in a window period, which is as long as one round of the solar rotation. It takes time 27 days. For example, if you would like to get TEC_{quiet} on the July 4th, you must average the TEC during $A_p \leq 15$ since June 20th to July 17th.

4.8 Clarify TEC variation with an inverse distance weighted (IDW) interpolation

A limitation of studying in the global scale is lacking of samples at any location and at any time. It can't help facing any lost samples in somewhere and sometimes. In these cases, an estimation of missing sample point is needed to be done before a changing in spatial and temporal interpretation and its presentation.

There are 3 main interpolation techniques in the Earth systemic science studies, namely, Kriging, Spline and IDW methods. Kriging technique suits to study a dense and clustered sample. Especially, some of which concerning a buffer zone. This technique was used in previous studying TEC variation resulting from geomagnetic storms by Akinori SAITO in 2006. Spline is a piecewise polynomial method. A calculation in the Spline is the most simplicity. It is widely used in biomedical imaging study and other common processing images. The calculation based on regression, but its doubt is that the coefficients in the technique are non-locally. A global smoothness decrease local fitting power between the nearest pair of tabulated points.

The IDW technique is used to interpolate the derived TEC in this study. The total electron content floating in the atmospheric body, in which has been studied continuously with the same method. There are two disadvantage of IDW. At first, it cannot make estimation below the minimum or above the maximum. Moreover, it removes trends rather to preserve and consider them. But its advantage is a more local power of closed measure data points to their center and it spreads the emphasis of the further points out. These two advantages satisfy this research, because the distance between each receiver is quite large and the observed value at the remote point doesn't been needed to use in an interpolation, such as, midnight value interpolation no need any value of midday to effect as an over estimation.

The Inverse distance weight, IDW, is able to interpolates an unknown TEC , Z, with randomizing 2 or more known TEC receivers and then averages them with weighted average method. The weight at the given known point increases when its distance, d, to an interpolated point decreases as a Figure 4-4. An equation (4.25) used in IDW is below.

$$Z_i = \frac{\Sigma_i \frac{Z_i}{d_{ij}^n}}{\Sigma_i \frac{1}{d_{ij}^n}} \tag{4.25}$$

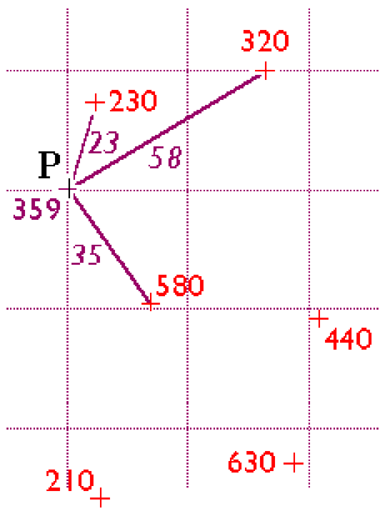

$$Z_P = \frac{\sum_{i=1}^{n} \left(\frac{z_i}{d_i}\right)}{\sum_{i=1}^{n} \left(\frac{1}{d_i}\right)} = \frac{\frac{230}{23} + \frac{320}{58} + \frac{580}{35}}{\frac{1}{23} + \frac{1}{58} + \frac{1}{35}}$$

Figure 4. 4 The inverse distance weighted interpolation procedure

From: Penn State's online geospatial education (2007)

4.9 Projecting the ACE spacecraft and the TEC information onto a same coordination system

ACE spacecraft is always in front of the earth and the earth orbits the sun, so the ACE spacecraft orbits the sun also. On the other hands, GPS receiver stations are on the fixed latitude and longitude. However, those fixed points still rotates and follows the earth's rotation. In addition, the earth axis does not direct to the geographic poles, but tilts at approximately 23.5° from the poles, so at a given time in different season in one year, a given-fixed locations of receiver don't at their own actually old position. The position might move to the upper and lower latitude when compare with the fixed solar ecliptic plane.

The space-based and ground-based measurements are collected and projected their location on the different coordination system. The ACE spacecraft parameters and its position change are kept in the Geocentric Solar Ecliptic system (GSE) while the ground instruments both a neutron monitor and GPS signals are kept in the Geographic coordinate system (GEO).

Any correlation studies between those places need transforming their coordinate system onto a same coordinate system, to be been able to calculate distance from one points to each other points. The Geocentric Equatorial Inertial system (GEI) is the most suitable to be a new coordination system of those three instruments. Because this system model adds the projection of the earth's equator onto the celestial sphere, so it is able to provide the most precise locations to operate them together.

The Figure 4-4 represents various coordinate systems, including, GEO with the most red, GEI with fuchsia and the GSE with lime green. Noticeably, GEI plane declines to the great circle at the vernal equinox at the same degree as the earth rotation.

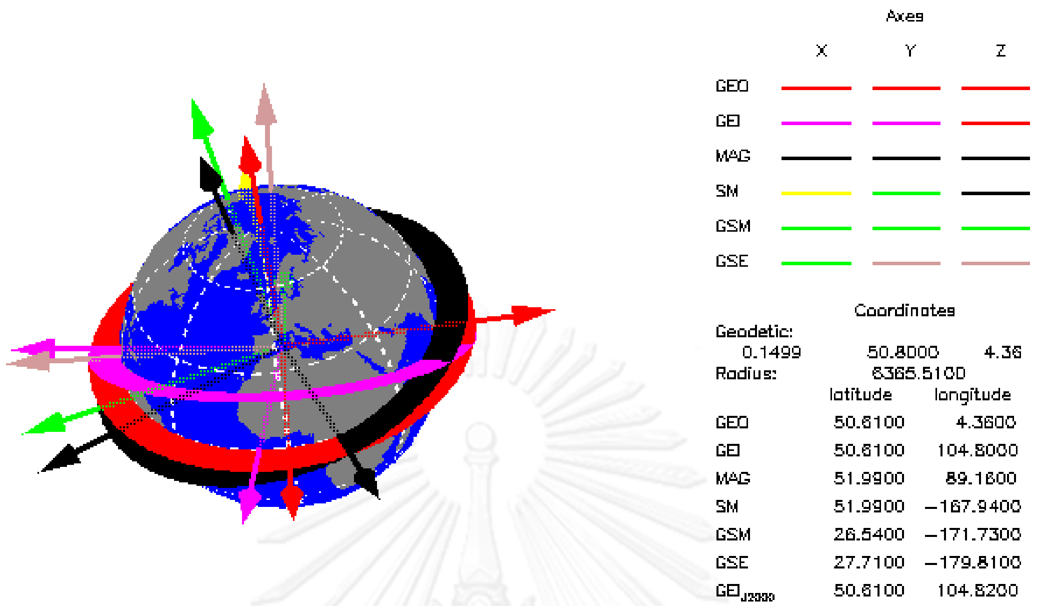

Figure 4.5 Coordinate transformations for Brussels

From: Belge (1950)

The ACE spacecraft does not stay exactly at the L1 point, but it moves in an ellipsoidal-shaped orbit around the L1 as Figure 4-6. The speed equation is applicable to the situation of CME events, speed and velocities on any components of CME are known expression. The position which contained in A/C code allows determining the distance between satellites, the neutron monitor at Doi Inthanon and GPS receivers located covering the North and the South America. When a velocity and distance are known expression, the lag time between those three instruments can be solved. However, transforming coordinate must be done at first.

Basically, the coordinate system transformation can be done with matrix operation. Every coordinate system in the solar-terrestrial relation studies has 3 axes perpendicular to each others. One of them fixes and the other two axes orient in the plane perpendicular to the first axe direction. Fortunately, anyone of latter two is always has a common direction with other coordination system. Hence, the transformation is done simply with transpose. Two features are need in transformation are rotation matrix, given as matrix *A* and its transformed vector V^a measured in system *a* to V^b measured in system *b*. Thus the matrix that transforms

V^b into V^a is A^t. We can describe these relations simply with writing equation (4.26) and its inversion as an equation (4.27).

$$A \cdot V^a = V^b \tag{4.26}$$

$$A^t \cdot V^b = V^a \tag{4.26}$$

When the transformation matrix A is needed to obtain, finding the directions of the three new coordinate axes in the old direction is the simplest way to do.

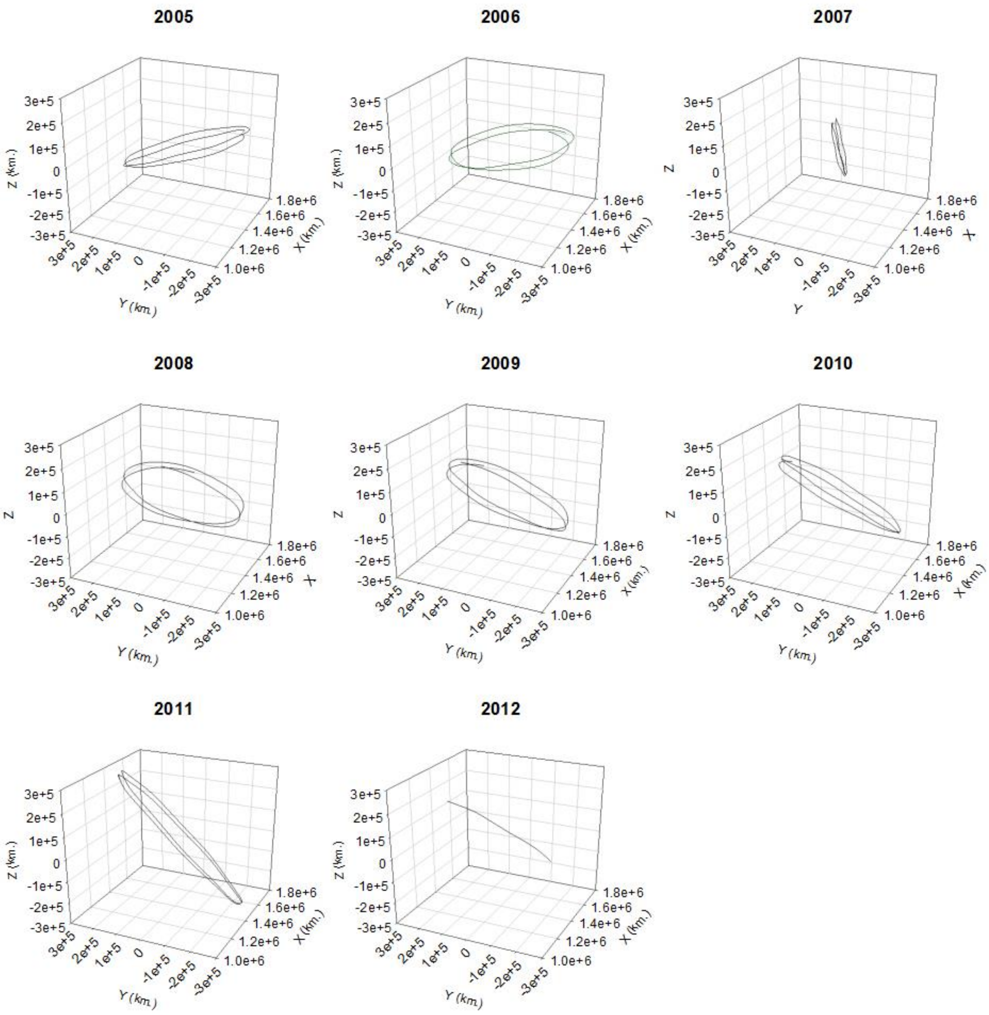

Figure 4.6 The ACE spacecraft positions during 2005 to February, 2012

Goldstein suggested in 1950 that “If the direction cosine of the new X-direction expressed in the old system are (X1, X2, X3), of the new Y-direction are (Y1, Y2, Y3) and the new Z-direction are (Z1, Z2, Z3), then the rotation matrix is formed by these three vectors as rows.” i.e.

$$\begin{bmatrix} X_1 & X_2 & X_3 \\ Y_1 & Y_2 & Y_3 \\ Z_1 & Z_2 & Z_3 \end{bmatrix} \begin{bmatrix} V_x^a \\ V_y^a \\ V_z^a \end{bmatrix} = \begin{bmatrix} V_x^b \\ V_y^b \\ V_z^b \end{bmatrix}$$

Conversely, the transformation from the system b to a is

$$\begin{bmatrix} X_1 & Y_1 & Z_1 \\ X_2 & Y_2 & Z_2 \\ X_3 & Y_3 & Z_3 \end{bmatrix} \begin{bmatrix} V_x^b \\ V_y^b \\ V_z^b \end{bmatrix} = \begin{bmatrix} V_x^a \\ V_y^a \\ V_z^a \end{bmatrix}$$

4.9.1 The transformation from the geocentric solar ecliptic system to the geocentric equatorial inertial system

GSE is commonly used in satellite trajectories like ACE and the solar wind observations. The X-axis in GSE points from the Earth toward to the Sun. The Y-axis is points toward dusk in the ecliptic plane and motives oppositely to the planetary motion. The direction (Z) of the ecliptic pole (0, -0.398, 0.917) locates constantly in the GEI system. The X-axis directs toward the sun is obtained in GEI system. The matrix T_2 is use to transform GEI to GSE, on the other hands, T_2^{-1} is matrix transforming GSE to GEI. Where the T2 can be calculated from two matrixes in equation (4.27)

$$T_2 = \langle \lambda_\Theta, Z\rangle * \langle \epsilon, X\rangle \qquad (4.29)$$

Where the first matrix responses to the rotation from the Earth’s equator to the plane of the ecliptic and the second matrix response to rotation in the plane of the ecliptic from the first point of Aries to the Earth-Sun direction.

The Sun's ecliptic longitude, λ_{Θ} is determined with equation 4.30 in the next page. Where the capital lambda (Λ) means to longitude (the capital lambda is calculable with equation 4.31), T_0 is the time in Julian centuries (36525 days) from 12:00 UT at epoch 2000.0 (January 1, 2000) to the previous midnight. The T_0 can be derived from equation 4.32 with the modified Julian date, MJD, which MATLAB has a function to find its. M is the Sun's mean anomaly in which is approximated from equation 4.33.

$$\lambda_{\Theta}= \Lambda+\left(1.915-0.0048\ T_0\right)\sin M +0.020\sin 2M \qquad (4.30)$$

$$\Lambda=280.46+36,000.772T_0 +0.04107UT \qquad (4.31)$$

$$T_0= \frac{MJD-51544.5}{36525.0} \qquad (4.32)$$

The obliquity of the ecliptic (ϵ) can be determined with equation 4.33 following the U.S. Naval observatory method in 1989 and *X* is the direction in GEO which can derived with its latitude and longitude.

$$\epsilon=23.439-0.013T_0 \qquad (4.33)$$

4.9.2 The transformation from the geographic coordinate system to the geocentric equatorial inertial system

Z-direction of GEO commonly used in astronomy and GEI commonly used in ground observation are in common, but the two other directions is difference from each others. The Z-direction in both systems is parallel to the earth rotation axis. Conversely, the X-axis of the GEO is in the Earth's equatorial plane while the X-axis of the GEI is pointed from the Earth's center toward to the first point of Aries, where is the position of the Sun at the vernal equinox. Consequence of the difference in their X-axis, their perpendicular Y-directions are difference from each others also.

The first point of Aries is the intersection of the Earth's equatorial plane and the ecliptic plane. The angle between the first point of Aries (GEI) and the Greenwich meridian (GEO) measured eastward from the first point of Aries in the Earth's equator is 0, then we can express the first point of Aries as ($cos\theta - sin\theta\ 0$) in the GEO, so the transformation to find position (*P*) from GEO to GEI is equation (4.34)

$$\begin{bmatrix} \cos\theta & -\sin\theta & 0 \\ \sin\theta & \cos\theta & 0 \\ 0 & 0 & 1 \end{bmatrix} \begin{bmatrix} P_x \\ P_y \\ P_z \end{bmatrix}_{GEO} = \begin{bmatrix} P_x \\ P_y \\ P_z \end{bmatrix}_{GEI} \quad (4.34)$$

The angle θ is the Greenwich Mean Sidereal Time, in which MATLAB has function JD2GMST to convert the Julian date to the Greenwich Mean Sidereal Time.

4.10 The ACE Spacecraft and TEC observation point lag time calculation

The geographic coordinate points need in transformation to GEI, are X, Y and Z, not the latitude θ and longitude φ or the height at 350 km above the Earth's surface. In latitude and longitude to X-Y conversion needs the earth radius (*r*) to derive, but the study doesn't concentrate on the ground level, so the R_E at 350 km is compensated.

The R_E at 350 km height, R_{350} are derived from its longitude, θ, the equatorial radius, *a*, which is 6,378.1370 km and polar radius, *b*, which is 6,356.7523 km as the equation 4.35.

$$R_E \text{ at 350 km height} = R_{350} = \sqrt{\frac{\left(a^2\cos(\theta)\right)^2 + \left(b^2\sin(\theta)\right)^2}{\left(a\cos(\theta)\right)^2 + \left(b\sin(\theta)\right)^2}} + 350 \quad (4.35)$$

Then, X and Y in Cartesian components can be derived with equation 4.36 – 4.37.

$$x = R_{350}\sin\theta\cos\varphi \quad (4.36)$$

$$y = R_{350}\sin\theta\sin\varphi \quad (4.37)$$

After we get *X*, *Y* and R_{350} as *Z* in GEO, the equation 4.34 is to transform them onto GEI. We now have got ACE and 350km above the receiver location in common GEI, we can calculate the distance between ACE and 350 km above receivers, $S_{ACE-GPS}$, with equation 4.38. In addition the SWEPAM on the ACE provide the solar wind speed, V_w, so the lag time , $\tau_{ACE-GPS}$, from spacecraft to the 350 km height above receiver is been able to calculate via their distance with equation 4.39.

$$S_{ACE\text{-}GPS} = \sqrt{(P_x^{ACE} - P_x^{GPS})^2 + (P_y^{ACE} - P_y^{GPS})^2 + (P_z^{ACE} - P_z^{GPS})^2} \quad (4.38)$$

$$\tau\_(ACE\text{-}GPS) = S\_(ACE\text{-}GPS)/V_w \quad (4.39)$$

Finally, the study will get lag time to capture to time period of MCs and the other phenomena and separates them off to interpret them.

CHAPTER V

RESULTS

5.1 Programming

This study worked with lots of different temporal-spatial resolution data, to use, determine other derivatives and analysis measurements. In addition, those of data came from remote location and were positioned in different coordination system. Therefore, the computer programs were construct to manage and solving these problems with different algorithms accordingly to specific purpose.

Four most important programs were developed on MATLAB, program A and B needed inputting ACE measurements to identify MCs and classify IS with procedures in section 4.2 and section 4.3 respectively. The module of program A and B are shown in Figure A-1 and Figure A-2 in Appendix A. Two other programs are to convert positions of ACE and GPS into GEI coordinate system. GSE-GEI coordinate transformation program (program C in Appendix A) and GEO-GEI coordinate transformation program (program D in Appendix A), both needed importing T_0, but program C needed Sun's properties, while program D needed importing the Earth radius at given latitude, to transform their positions into GEI coordination system (see Figure A-3 and Figure A-4 in Appendix A).

Applications process data and provided these outputs. Program A provides MC boundary to confine and divide samples to test with statistical methods. MVA analysis need 16-second solution magnetic measurements from MAG, but other two criteria need measurements from SPEWAM, so the time resolution of program A and B are 64-second resolutions. Program C and D allow to determine ACE and GPS position in GEI, both need another descended extraordinary program to calculate travelling time, which developed on MS EXCEL. Resulting from acceptable time solution of TEC measurement, a space of lag time shorter than 6 minute appears.

5.2 Results

During 2005 and 2012 was the duration got the deep declination of solar maximum of the solar cycle 23, a through (solar minimum) was in 2009, and then the number of Sunspot had risen since 2010. That meant this study was in once most quiet period of the solar activity, so the MC and phenomena gotten were quite light.

Availabilities in ACE and GPS data limited periods and magnitudes each events in study. The ACE data was often unavailable when the spacecraft encountered an intense ejection and also bad weather. One key parameter always having an inacceptable error is proton density. Speed and temperature of proton were then sequential parameters resulting from proton undetectability.

All of selected GPS station was not valid along years of this study and even each event. Vacuums in GPS track were able to be found when satellites stayed at too low declinations and the atmospheres did not permit. In addition to these the SWEPAM was getting badly worse since 2009. Finally, 7 proper events in Table 5.1 were selected to study.

Table 5.1 Period of Events in study

Event	Year	Start time (DOY)	End time (DOY)
I	2005	08 January (008)	10 January (010)
II	2005	15 May (135)	17 May (137)
III	2006	13 April (103)	15 April (105)
IV		14 December (348)	16 December (350)
V	2007	19 November (323)	21 November (325)
VI	2008	08 March (068)	10 March (070)
VII	2009	21 July (202)	23 July (204)

5.2.1 Event I

Event I began from 7 to 10 January, 2005. TEC within those three days could be defined into 4 circumstances as follows: TEC under HSS circumstance (A), TEC under FFS embedded in HSS circumstance (B), TEC under HSS after FFS passage circumstance (C) and TEC under quiet SW circumstance (D) (see Figure 5.1)

Phenomena traveled from the L1 point to the study area within an hour (as seen in Figure 5.2-3). Neutron monitor detected Forbush decrease (δF) with magnitude larger than -2% as Figure 5.4. (see more plot of δF at stations in Appendix B) Percent deviation of TEC in $Q_{\parallel}$ FFS circumstance (more details about its time at ACE and its class in Table 5.5 and 5.6) is higher than other phenomena notably (as seen Figure 5.5b). FFS hit the ionosphere in a midnight section and the HSS ended within a dawn section.

Table 5.2 Periods of 5 ISs in this study.

code	event	year	start time		end time	
			date (DOY)	time (UT)	date (DOY)	Time (UT)
1	I	2005	08 Jan (008)	0.02	08 Jan (008)	0.29
2	II		15 May (135)	1.56	15 May (135)	2.33
3	IV	2006	14 Dec (348)	13.32	14 Dec (348)	14.20
4			16 Dec (350)	17.24	16 Dec (350)	17.39
5	V	2007	19 Nov (323)	17.09	19 Nov (323)	17.33

Table 5.3 Classes of 5 ISs

code	event	year	Angle between B direction		M_C classification
			local angle (degree)	class	
1	I	2005	29.5°	$Q_{\parallel}$	FF
2	II		56.2°	$Q_{\perp}$	FF
3	IV	2006	59.0°	$Q_{\perp}$	FF
4			10.9°	$Q_{\parallel}$	SF
5	V	2007	06.9°	$Q_{\parallel}$	FF

Fishers Least Significant different (LSD) test showed that global deviations in TECU didn't respond clearly to the HSS, on the opposite of FFS that disturbed TEC throughout all latitudes. The FFS generated extraordinary TEC, especially at northern high latitudes. All latitude TEC is able to back into day-to-day balance in spite of still was being in the HSS. Finally, LSD showed that there was no HSS or FFS affect left in the quiet SW after ejection passages.

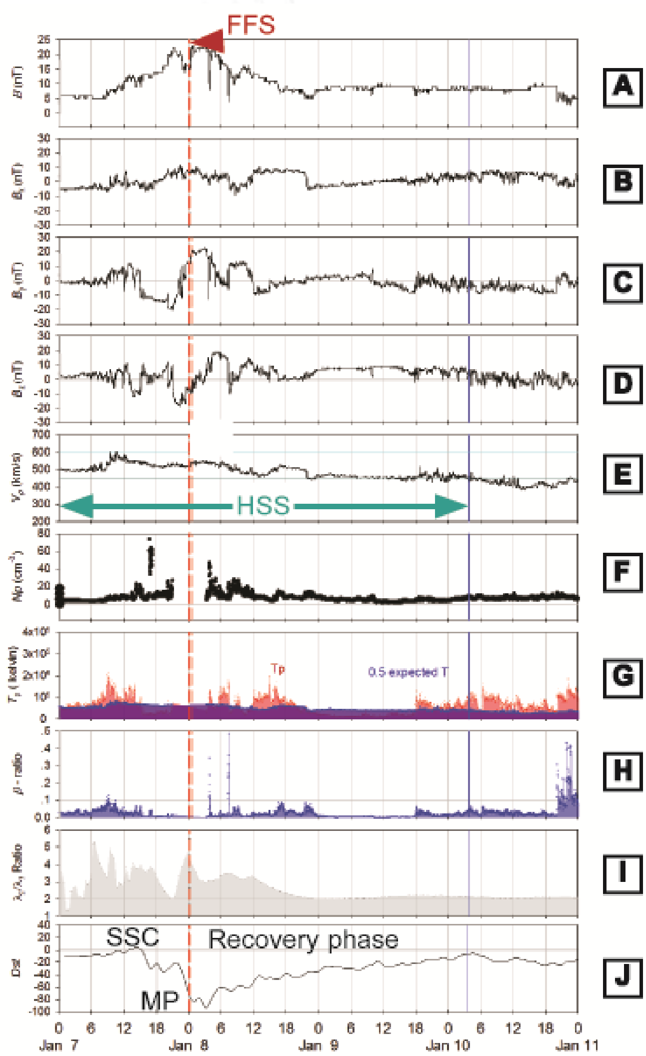

(A-G) Observations by the the ACE spacecraft (G-I), results from programs and (H) geomagnetic activity (*Dst*) from OMNI between 7-10 January 2005. From top to bottom are (A) plottedinterplanetary magnetic field (*B*), (B) Sun-Earth component of the IMF (*Bx*), (C) east-westcomponent of the IMF (*By*), (D) north-south component of the IMF (*Bz*), (E) proton speed (*Vp*),(F) proton density (*Np*), (G) proton temperature (*Tp*), (H) plasma beta (β), (I) eigenvalues forthe medium and minimum variance directions, (J) *Dst*.

Figure 5.1 Solar wind measurements, MC signatures at L1 and D_{st} at the Earth observed between 7-10 January 2005

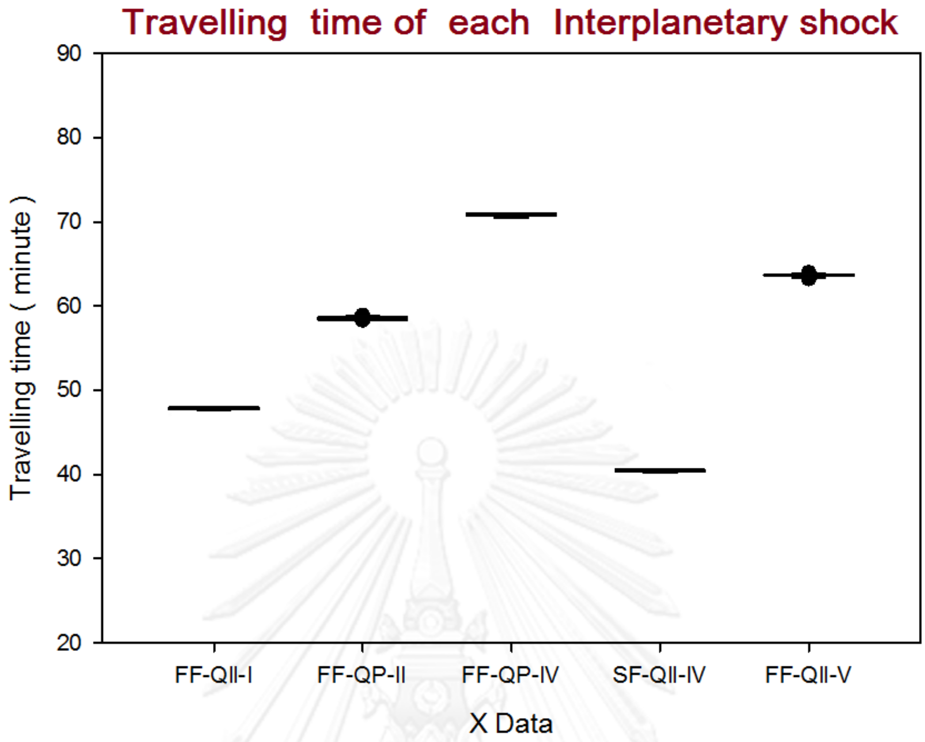

Figure 5.2 Travelling time of each interplanetary shock code

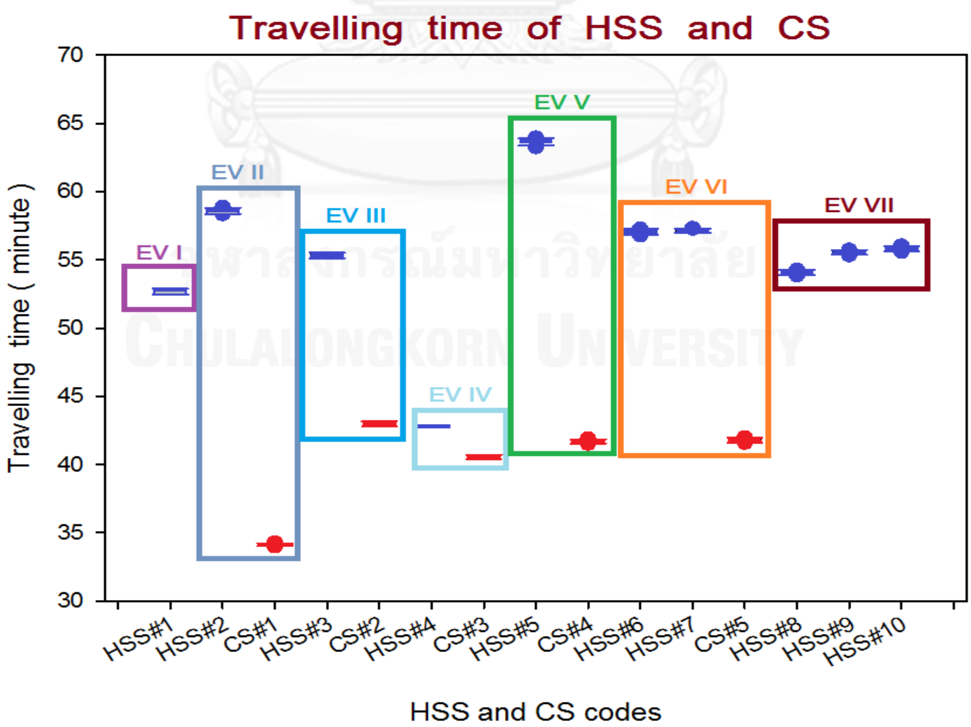

Figure 5.3 Travelling time of HSS and CS

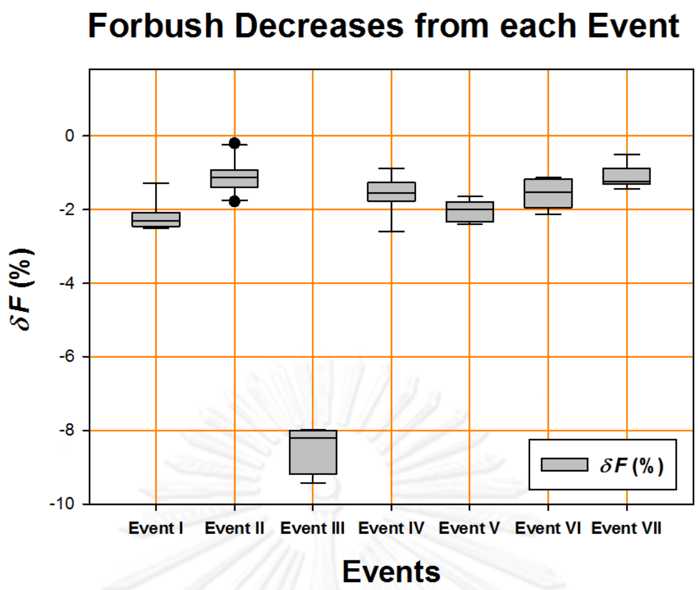

Figure 5.4 Forbush decreases from each event

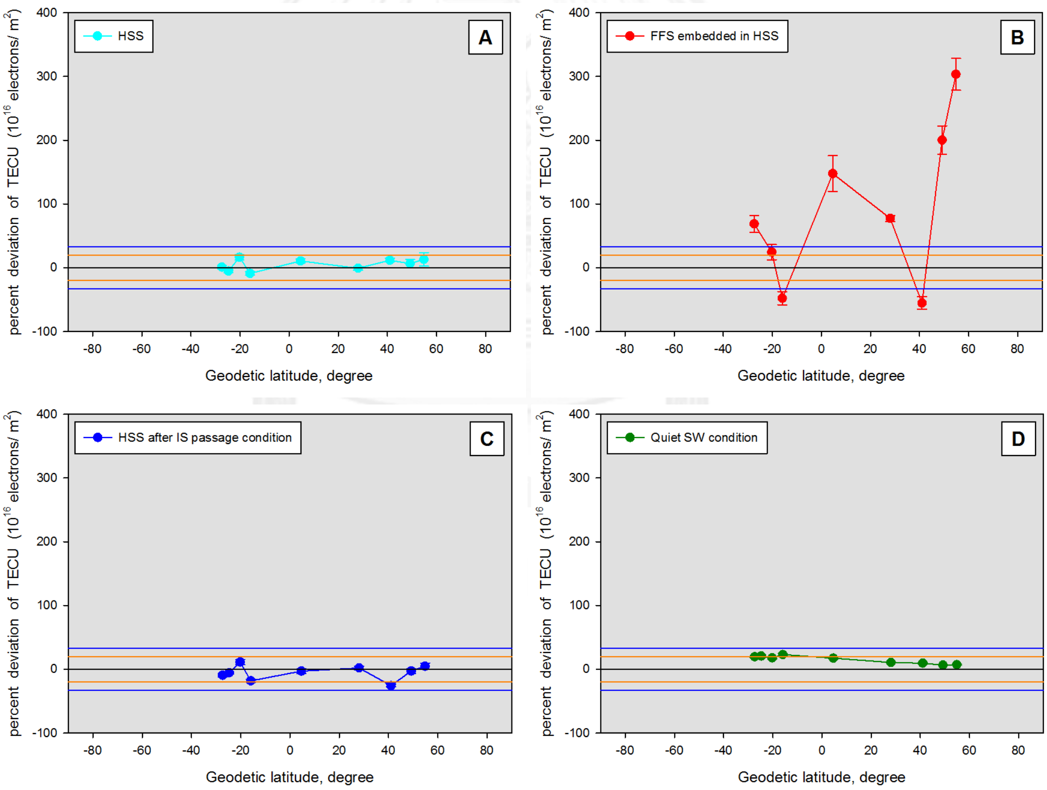

Figure 5.5 Mean percentage deviation of TECU on 7-10 January 2005

(DOY 07-10)

by geodetic latitude; categorized by phenomena

5.2.2 Event II

Event II began from 15 to 17 May, 2005. TEC within those three days could be defined into 8 circumstances (see Figure 5.7) as follows: TEC under quiet SW circumstance (A), TEC under HSS circumstance (B), TEC under FFS circumstance (C), TEC under sheath circumstance (D), TEC under sheath with CS circumstance (E), TEC under MC circumstance (F), TEC under CS with post MC passage (G), and TEC under SW circumstance with post ejection passage (H). See period of identification and the properties of MC in Table 5.2 and Table 5.3.

MC, which has size 0.39 AU, took 29 minutes (see Figure 5.6) from the L1 to the study area which stayed in midnight side and made the HSS took the longest time to the study area in the evening zone (see Appendix C).

The LSD test showed that global deviations of TECU within HSS and FFS passages were significantly indifferent to the quiet time being. Then the sheath region following an HSS and FFS effected on TEC as a significantly positive deviation at the northern equatorial (4°N) and high latitude (54°N). The percentage deviations at both latitudes were larger than their ordinary day-to-day deviations. The sheath didn't cause any significant deviation in TECU between 20°N-49°N and 41°S -49°S in that way (see Appendix D).

Table 5.4 Period of Events in study.

code	event	year	start time		end time	
			date (DOY)	time (UT)	date (DOY)	Time (UT)
1	II	2005	15 May (135)	05.42	15 May (135)	22.18
2	III	2006	13 Apr (103)	14.48	13 Apr (103)	20.48
3			13 Apr (103)	20.36	14 Apr (104)	09.54
4	IV		14 Dec (348)	22.48	15 Dec (349)	19.48
5	V	2007	19 Nov (323)	23.24	19 Nov (324)	12.54
6	VII	2009	21 Jul (202)	03.54	21 Jul (202)	17.06

Table 5.5 MC types and their configurations.

code	event	year	start time		end time		Properties							
			date (DOY)	(UT)	date (DOY)	(UT)	ΔT^{a}	$\phi\ A^{b}$	$\theta\ A^{b}$	V^{c}	$2R_0^{d}$	H^{e}	type	B_0^{f}
1	II	2005	15 May (135)	05.42	15 May (135)	22.18	16:36	94	67	843	0.39	L	SN	56
2	III	2006	13 Apr (103)	14.48	13 Apr (103)	20.48	06:00	244	77	517	0.096	L	SN	17
3	III		13 Apr (103)	20.36	14 Apr (104)	09.54	13:24	262	-13	517	0.225	L	NS	20
4	IV		14 Dec (348)	22.48	15 Dec (349)	19.48	21:00	85	27	725	0.724	L	SN	18
5	V	2007	19 Nov (323)	23.24	19 Nov (324)	12.54	13:50	272	-4	470	0.132	L	NS	20
6	VII	2009	21 Jul (202)	03.54	21 Jul (202)	17.06	13:05	117	-17	320	0.182	R	NS	8

a ΔT is a duration of the MC encounter (HH:MM) *b* ϕA and θA are estimated longitude and latitude in GSE

c V is an average solar wind speed (in km/s) *d* $2R_0$ is an estimated diameter (in AU)

e H is a handedness (right and left-handed) *f* B_0 is an estimated axial field magnitude (in nT)

The sheath behind the HSS and FFS was caught with a CS and influenced on TEC in the study area differently from previous region in sheath. The content of TEC at 49°N was still being larger than a normal day-to-day deviation and the TEC at 4°N and 54°N were exceeding its normal deviations as well. The TEC at 20°S decreased significantly from its quiet time deviation, yet TEC in sheath with CS was not different to the TEC in front of the sheath. There also was a TEC increment at 41°N especially. However, TEC didn’t exceed its normal day-to-day variations.

A SW-NE MC passed the ionosphere above the section of America and made δF . The feature enriched the TEC into abnormal contents at 04°N, 45°N, 53°S, 20°N and 28°N notably. Nevertheless, only two first latitudes had an exceeded day-to-day TEC. A result proved that the deviation in TEC caused by this MC and inhomogeneity in each hemisphere.

Here was another CS after the MC passage. Nearly all of diverse latitudes had significantly distinctive to TEC in a previous CS-passed condition, but 45°N and 41°N. Anyway, all of them were not far from their day-to-day variations. TEC at around 20°S in both hemispheres (20°N, 28°N and 20°N) were larger and other regions were lower than TEC within the previous CS passage.

Speed of the SW was dropped and there was no ejection passage. The SW backed into a quiet time condition. TEC at high latitude (49°N and 54°N) and above 20°S backed to their deviation while a quiet time TEC also was no ejection passage.

At 20°S, Northern equatorial latitude (4°N) and around 20°N, the TEC deviations were different from before. 20°S TEC dropped while the TEC at other 20°N were still accreting. They deviated less than their day-to-day deviation, but the TEC at 4°N which increased greater than the TEC during the pre-ejection passage (see Figure 5.8).

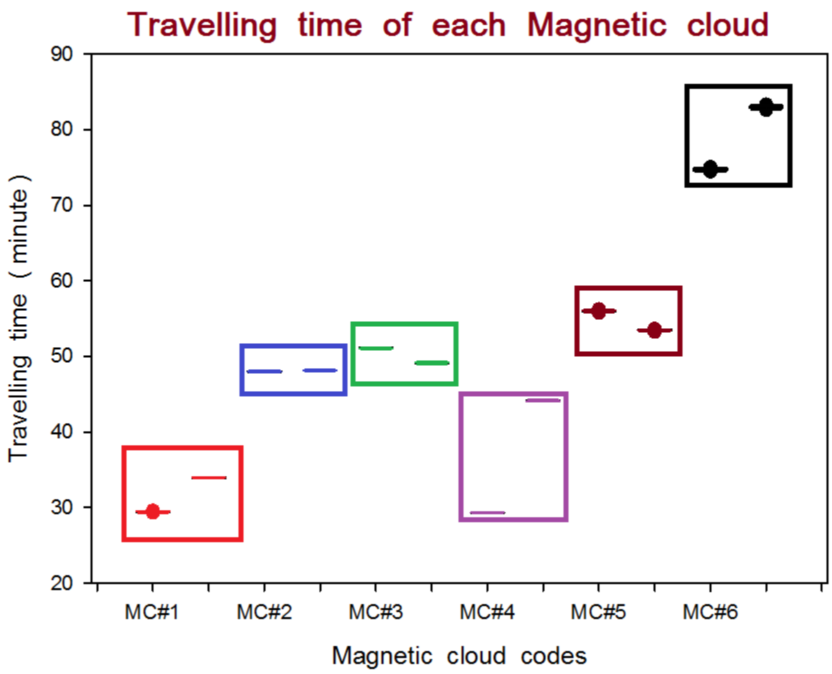

Figure 5.6 Travelling time of MCs.

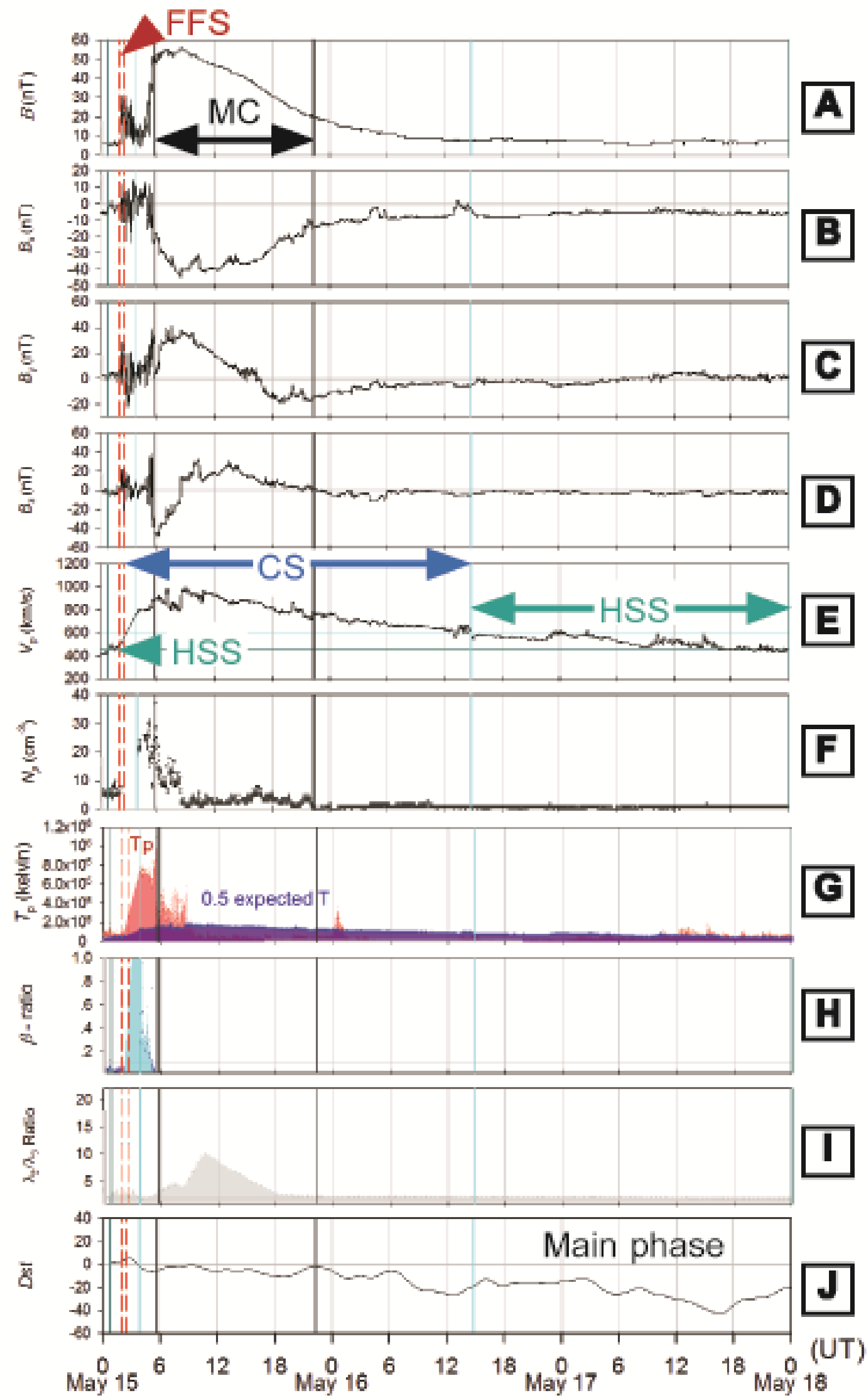

(A-G) Observations by the the ACE spacecraft (G-I), results from programs and (H) geomagnetic activity (*Dst*) from OMNI between 15-17 May 2005. From top to bottom are (A) plottedinterplanetary magnetic field (*B*), (B) Sun-Earth component of the IMF (*Bx*), (C) east-westcomponent of the IMF (*By*), (D) north-south component of the IMF (*Bz*), (E) proton speed (*Vp*),(F) proton density (*Np*), (G) proton temperature (*Tp*), (H) plasma beta (β), (I) eigenvalues forthe medium and minimum variance directions, (J) *Dst*.

Figure 5.7 Solar wind measurements, MC signatures at L1 and D_{st} at the Earth observed between 15-17 May 2005

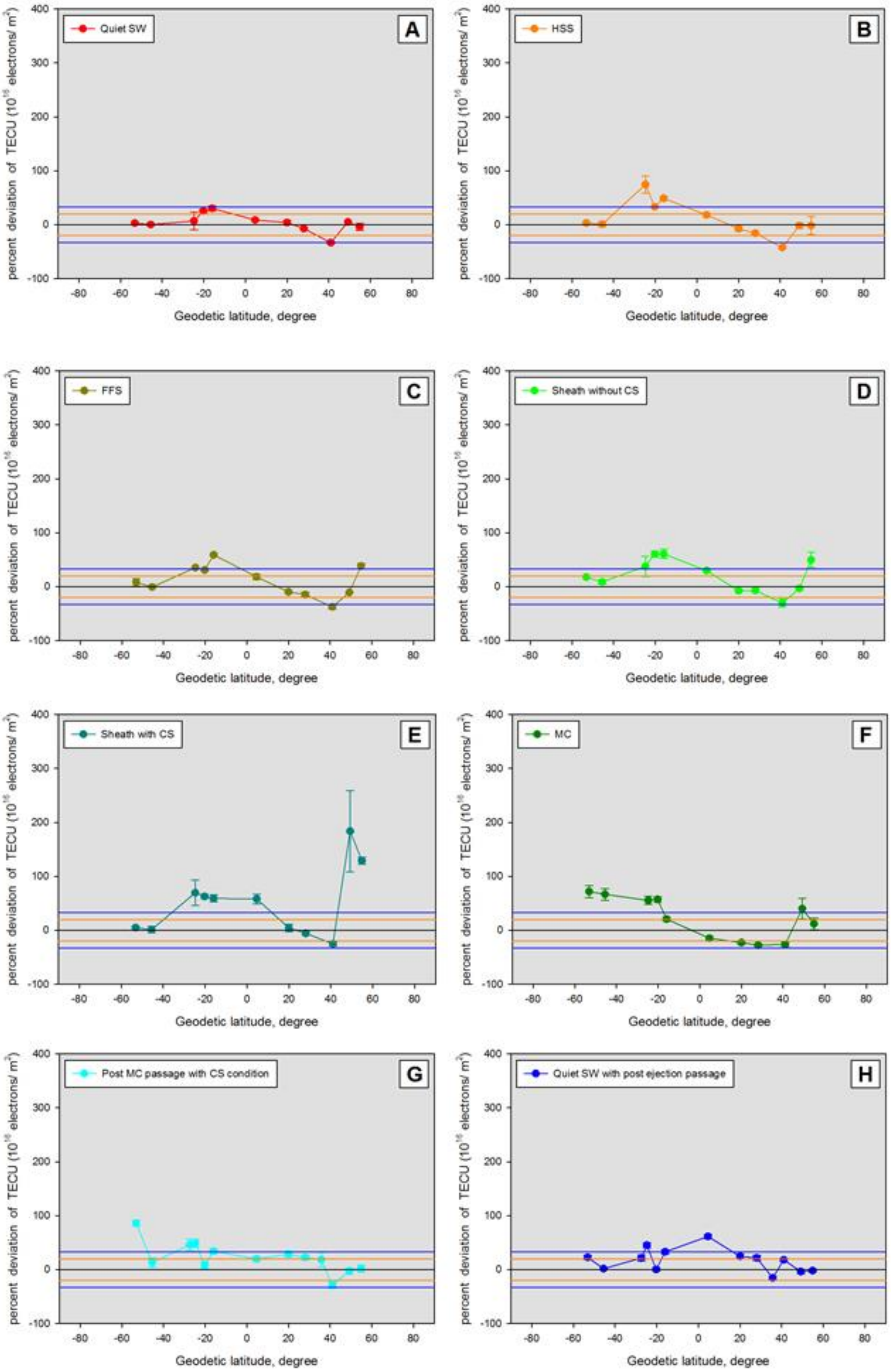

Figure 5.8 Mean plot of percent deviation in TECU on 15-17 May 2005 (DOY 135-137) by geodetic latitude; categorized by phenomena

5.2.3 Event III

Event III began from 13 to 15 April, 2006. TEC within those three days could be defined into 7 circumstances (see Figure 5.9) as follows: TEC under quiet SW circumstance (A), TEC under HSS circumstance (B), TEC under the first MC circumstance (C), TEC under IR circumstance (D), TEC under the second MC circumstance (E), TEC under CS with post MC passage (F), and TEC under quiet SW with post ejection passage circumstance (G).

The HSS, the first MC and also IR between the first and the second MC passage didn't effect on any TEC in the study area. However, the second MC induced an overproducing in TEC at latitudes between 24°S and 20°N. There no abnormal TEC degeneration found at any region.

The second MC affect was left over 49°N after it passed, while other latitudes recovered into their normal TEC balances. Finally, CS disturbed TEC at 4°N and 24°S.

5.2.4 Event IV

Event IV was from 14 to 16 December, 2006. TEC within those three days could be defined into 7 circumstances (see Figure 5.11) as follows: TEC under CS circumstance (A), TEC under FFS circumstance (B), TEC under sheath circumstance (C), TEC under MC circumstance (D), TEC under CS with post MC passage (E), TEC under FFS passage (F), and TEC under quiet SW with post ejection passage circumstance (G).

All latitude except 27°S and 15°S responded to sheath following the FFS. The higher latitude TEC got the higher overproduction. MC triggered the largest δF and made a lower overproduction at 15°S, 4°N, 49°N and 54°N than the sheath did (see Figure 5.12c-Figure 5.12e). The below day-to-day deviation was also found at 33°N when the MC passed.

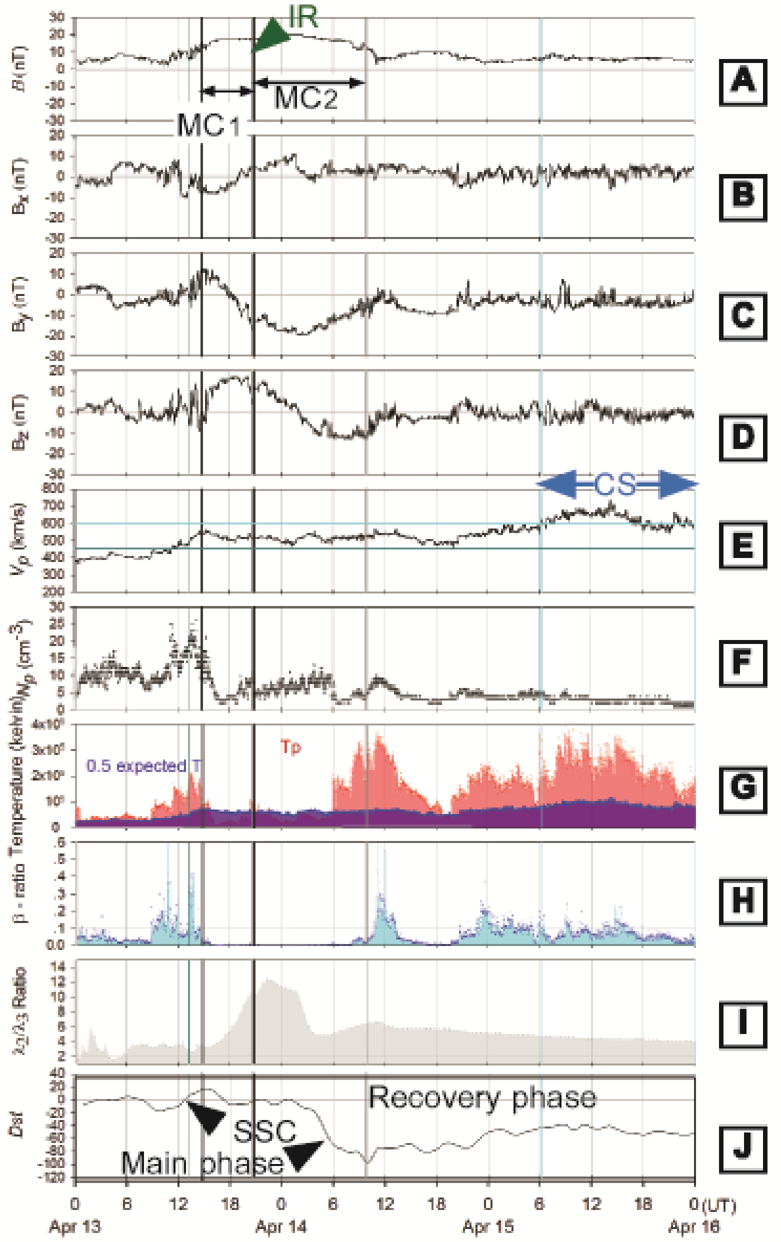

(A-G) Observations by the the ACE spacecraft (G-I), results from programs and (H) geomagnetic activity (*Dst*) from OMNI between 13-15 April 2006. From top to bottom are (A) plottedinterplanetary magnetic field (*B*), (B) Sun-Earth component of the IMF (*Bx*), (C) east-westcomponent of the IMF (*By*), (D) north-south component of the IMF (*Bz*), (E) proton speed (*Vp*),(F) proton density (*Np*), (G) proton temperature (*Tp*), (H) plasma beta (β), (I) eigenvalues forthe medium and minimum variance directions, (J) *Dst*.

Figure 5.9 Solar wind measurements, MC signatures at L1 and the *D*st observed between 13-15 April 2006

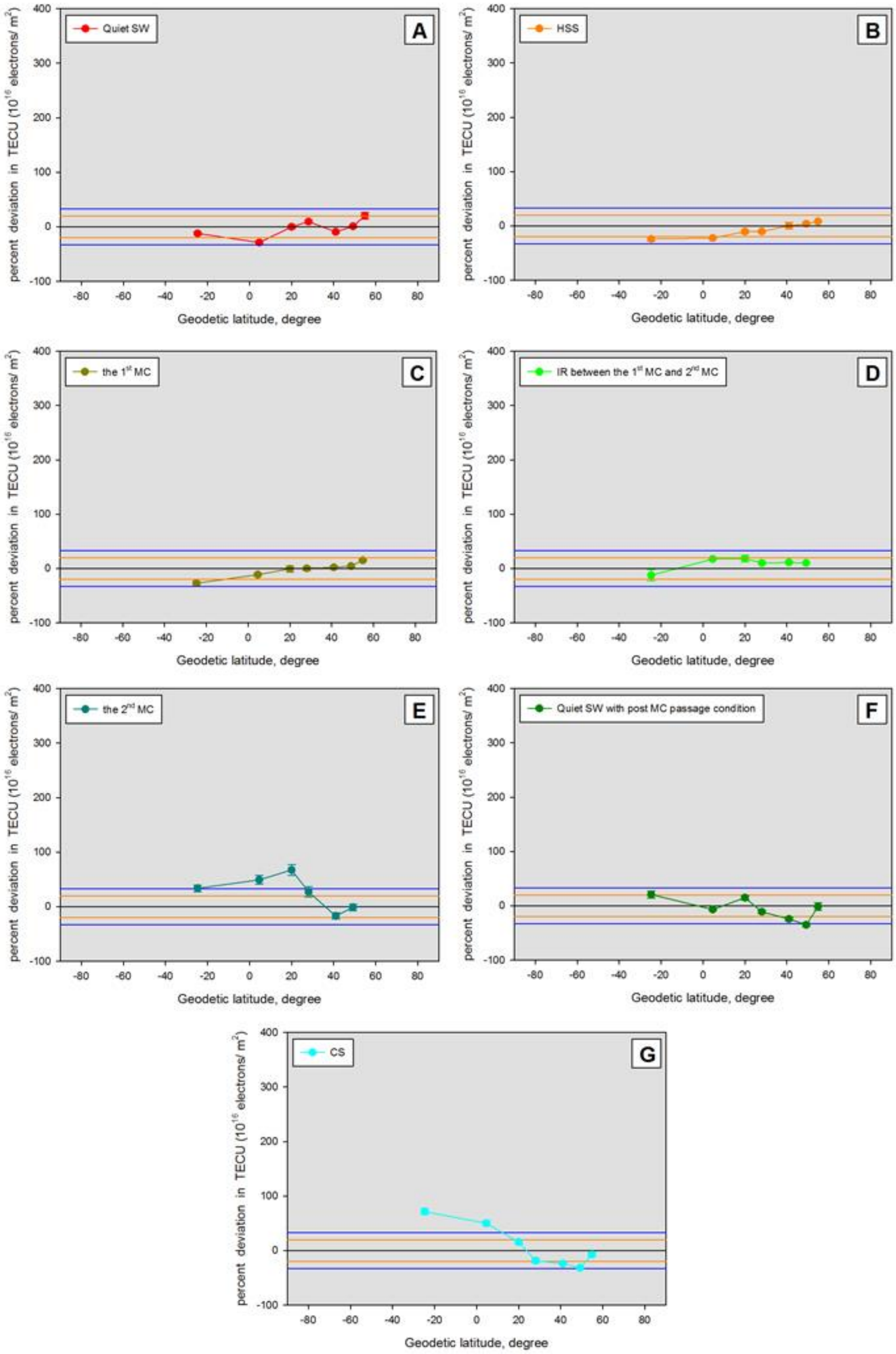

Figure 5.10 Mean plot of percentage deviation of TECU on 13-15 April 2006 (DOY 103-105) by geodetic latitude; categorized by phenomena

After the MC had gone, there were still had CS. For latitudes 28°N and 35°N TEC was degenerated deeply. Extraordinary contents at 15°S and 43°N gradually eased, but they were larger than normal deviations. TEC at 4°S was still rising continually. At 33°N, TEC didn't overproduce during the MC cover the ionosphere.

After CS was declined, then the space weather got claim and no TEC deviated larger than normal oscillations. There was second FFS travelling through the Earth, but only 35°N and 54°N responded to the FFS as a losing TEC deeper abnormally. The quiet time SW behind the shock disturbed TEC at only 49°N and 35°N as enrichment and decreasing respectively.

5.2.5 Event V

Event V began from 19 to 21 November, 2007. TEC within those three days could be defined into 7 circumstances (see Figure 5.13) as follows: TEC under quiet SW circumstance (A), TEC under FFS circumstance (B), TEC under sheath circumstance (C), TEC under MC circumstance (D), TEC under the IR circumstance (E), TEC under CS with post MC passage (F) and TEC under quiet SW with post MC and CS passage circumstance (G).

TEC at 8°S and 41°N in front of FFS were more than normal contents. TEC was decreased in corresponding latitude in northern hemisphere but TEC was increased in corresponding latitude in southern hemisphere at FSS (see Figure 5.14a-Figure5.14b). Both variations were within normal day-to-day deviations.

TEC at 4°S and 45°S were only significantly sheath-responded. TEC at 45°S was overproduced and TEC at 4°S decreased extraordinarily. TEC at 20°S and 1°S had never got affects from FSS and its sheath. There was no bimodal tend between two hemispheres during the sheath passage. Only TEC at 33°N overproduced extraordinarily when the MC passed.

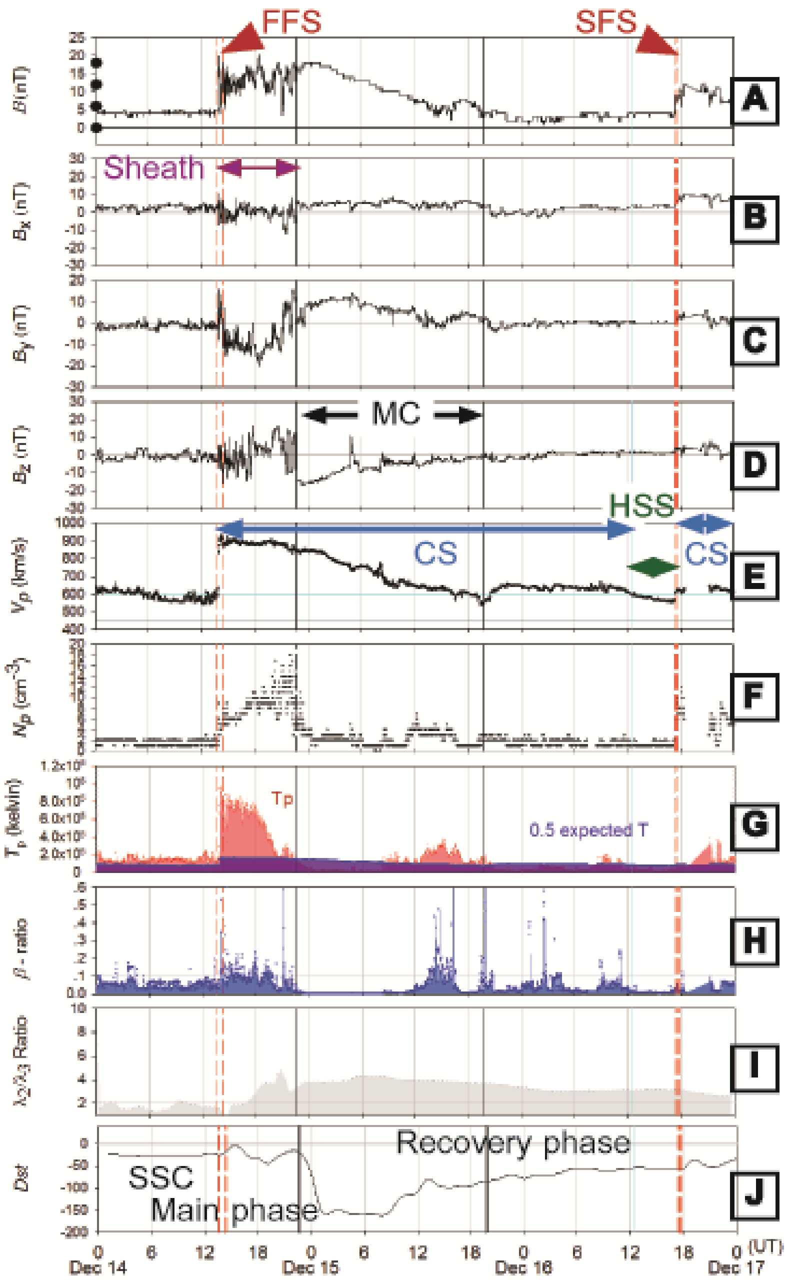

(A-G) Observations by the the ACE spacecraft (G-I), results from programs and (H) geomagnetic activity (*Dst*) from OMNI between 14-16 December 2006. From top to bottom are (A) plottedinterplanetary magnetic field (*B*), (B) Sun-Earth component of the IMF (*Bx*), (C) east-westcomponent of the IMF (*By*), (D) north-south component of the IMF (*Bz*), (E) proton speed (*V*p),(F) proton density (*N*p), (G) proton temperature (*T*p), (H) plasma beta (β), (I) eigenvalues forthe medium and minimum variance directions, (J) *Dst*.

Figure 5.11 Solar wind measurements, MC signatures at L1 and *D*st observed on 14-16 December 2006

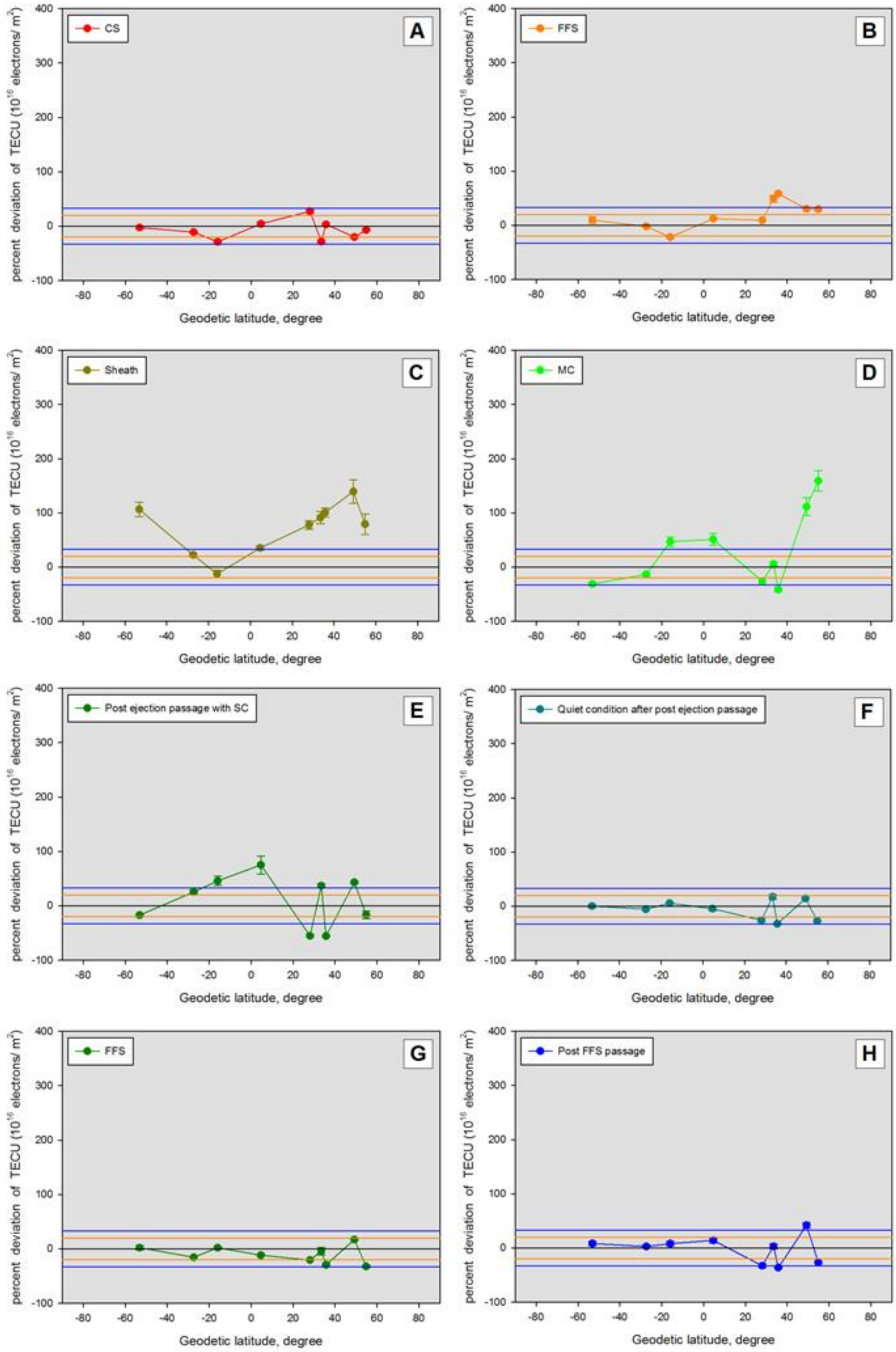

Figure 5.12 Mean plot of percentage deviation of TECU on 14-16 December 2006 (DOY 348-350) by geodetic latitude; categorized by phenomena

CS had followed that MC and arrived at the Earth about 12 hours after the passage of MC. There was only abnormally CS-responded TEC at 4°N. The IR between MC and the following CS triggered extraordinary deviations few north equator to few south equator and 20°S in the southern hemisphere.

After the passage of CS, TEC at 4°S and 33°N degenerated lower than a quiet-time TEC. TEC at 41°N overproduced.

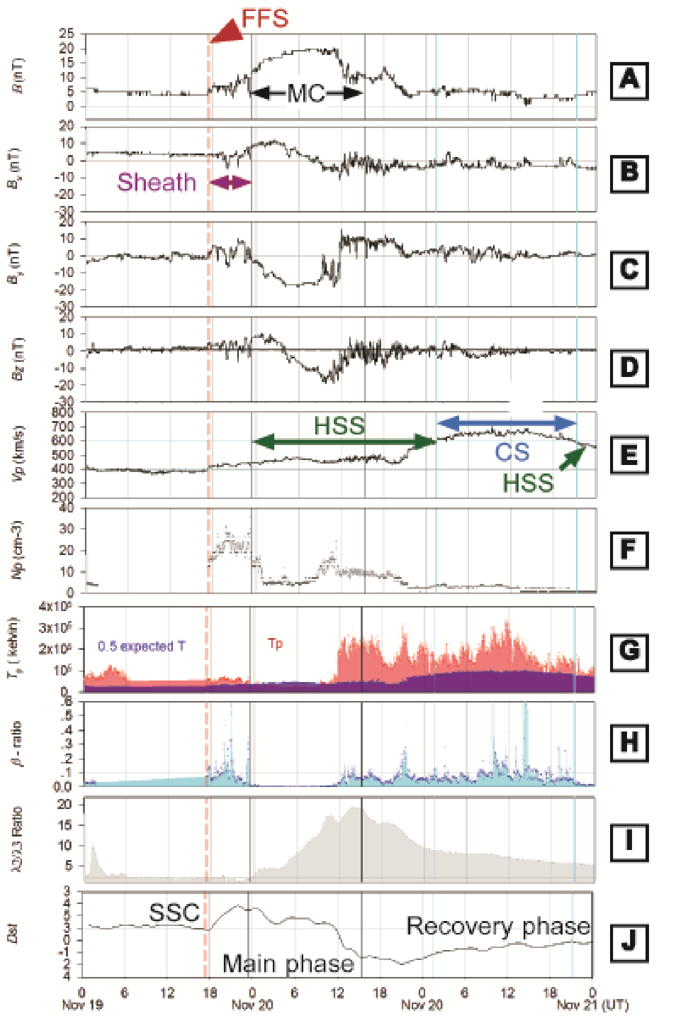

(A-G) Observations by the the ACE spacecraft (G-I), results from programs and (H) geomagnetic activity (*Dst*) from OMNI between 19-20 November 2007. From top to bottom are (A) plottedinterplanetary magnetic field (*B*), (B) Sun-Earth component of the IMF (*Bx*), (C) east-westcomponent of the IMF (*By*), (D) north-south component of the IMF (*Bz*), (E) proton speed (*Vp*),(F) proton density (*Np*), (G) proton temperature (*Tp*), (H) plasma beta (β), (I) eigenvalues forthe medium and minimum variance directions, (J) *Dst*.

Figure 5.13 Solar wind measurements, MC signatures at L1 and *D*st observed on 19-21 November 2007

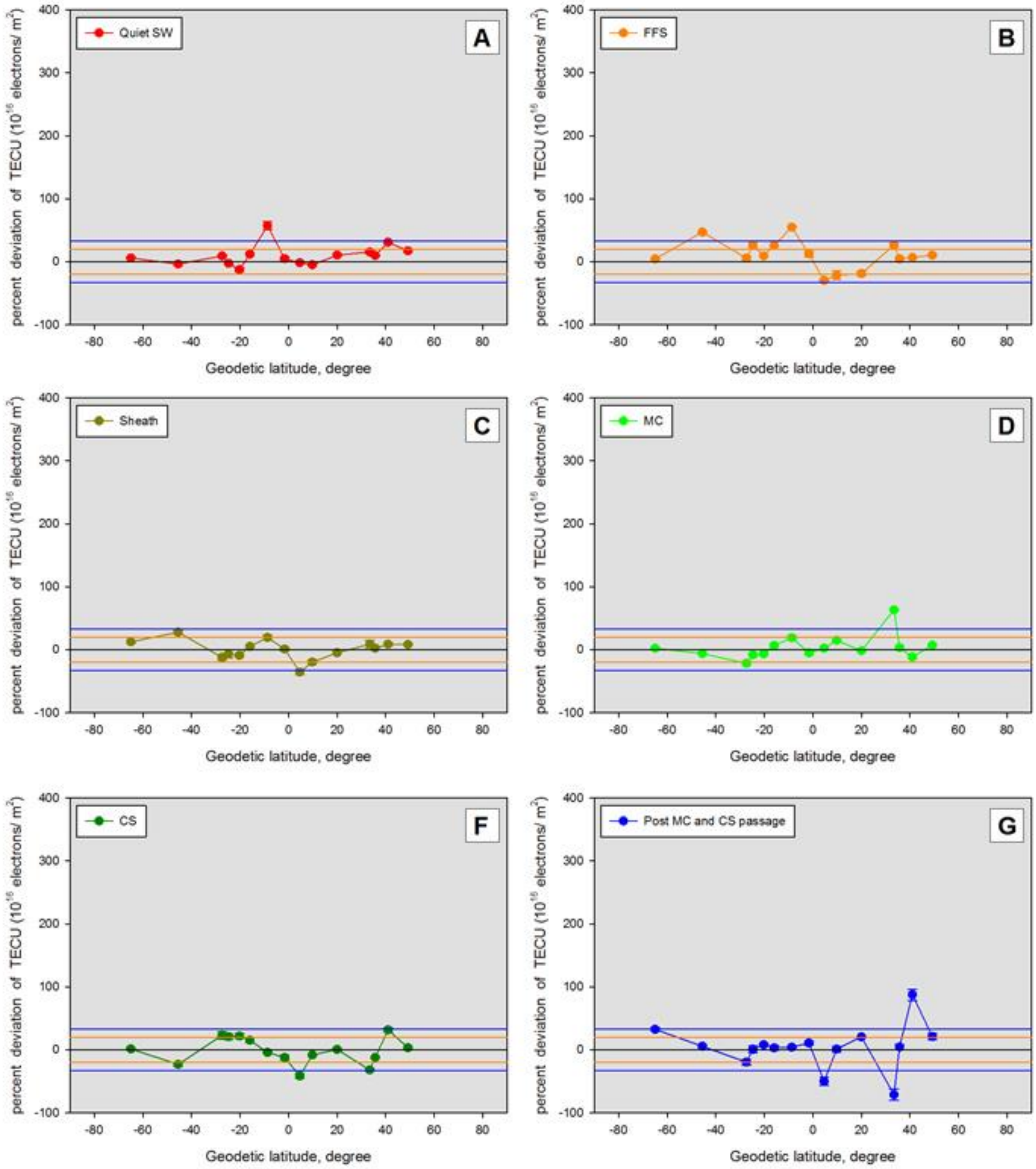

Figure 5.14 Mean plot of percent deviation in TECU on 19-21 November 2007 (DOY 348-350) by geodetic latitude; categorized by phenomena.

5.2.6 Event VI

Event VI began from 8 to 10 March, 2008. TEC within those three days could be defined into 5 circumstances (see Figure 5.15) as follows: TEC under quiet SW circumstance (A), TEC under the HSS#1 circumstance (B), TEC under quiet SW with post HSS#1 passage circumstance (C), TEC under the HSS#2 circumstance (D), TEC under quiet SW with post HSS#2 passage circumstance (E), and TEC under CS circumstance (F).

The first stream had driven irregularities to the 49°N and 15°S TEC as abnormal increasing and decreasing accordingly before it blew above the Earth's ionosphere. During the stream was emanating the Earth: TEC at 49°N rose continually larger than normal deviation.

TEC at 15°S also extremely dropped larger than normal deviation. Other two latitudes just got an extreme HSS affect, were 35°N and 49°S. The TEC decreased abnormally at first latitude and increased abnormally at another. TEC rose with a normal day-to-day deviation at 20°S in the Northern hemisphere and the southern equator. The TEC at another hemisphere did oppositely during the HSS passage.

The first HSS affect still was left over the ionosphere as an abnormal decrease in TEC at the 49°N and overproducing TEC at the southern equator (4°S).

Statistically, there was no significantly abnormal deviation in TEC at any latitude during the second HSS passed through the Earth. At 54°N is only latitude significantly presented overproducing TEC along the passage of the CS.

5.2.7 Event VII

Event VII began from 21 to 23 July, 2009. TEC within those three days could be defined into 8 circumstances (see Figure 5.17) as follows: (A) TEC under quiet SW circumstance, (B) MC circumstance, (C) TEC under quiet SW with post MC passage circumstance, (D) TEC under HSS#1 circumstance, (E) TEC under quiet SW with post HSS#1 passage circumstance, (F) TEC under HSS#2 circumstance, (G) TEC under quiet SW with post HSS#2 passage circumstance and (H) TEC under HSS#3 circumstance.

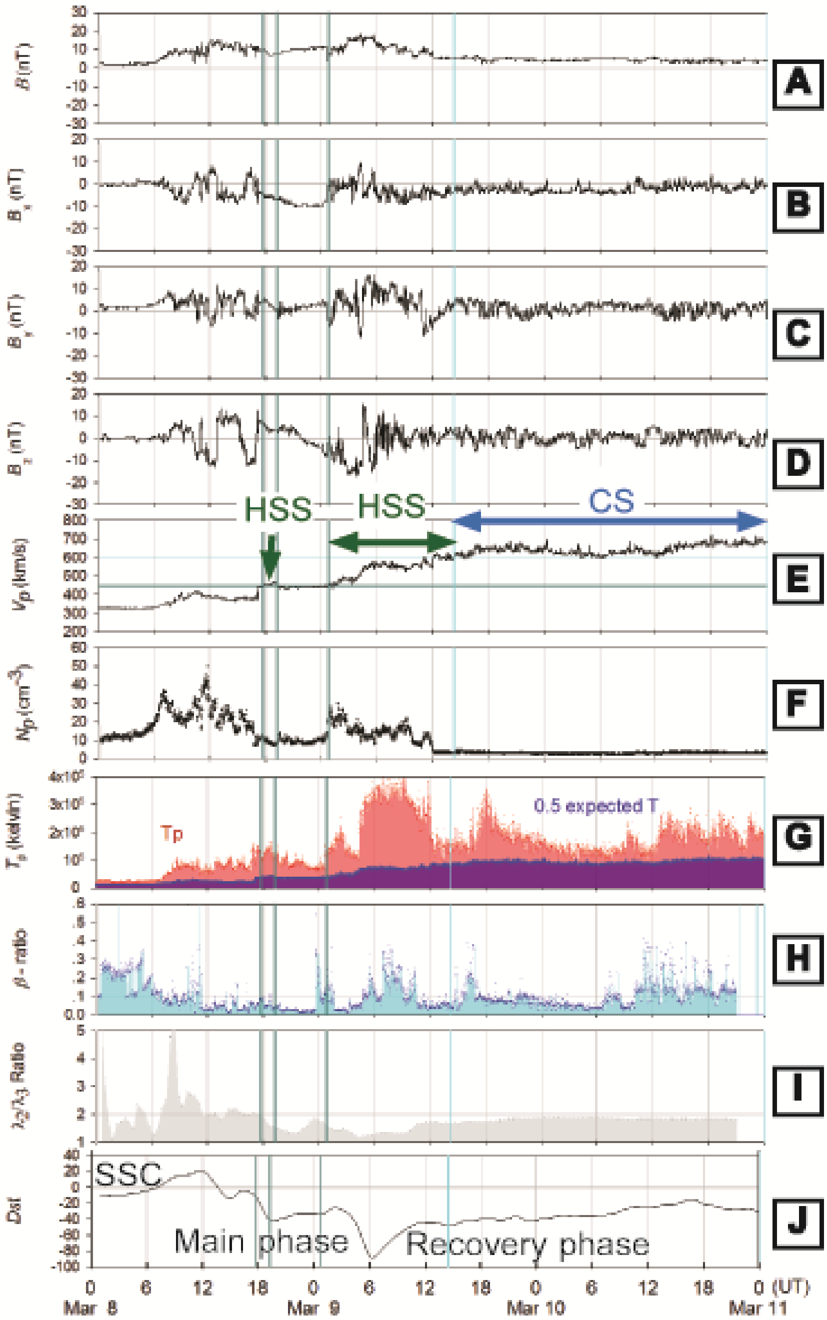

(A-G) Observations by the the ACE spacecraft (G-I), results from programs and (H) geomagnetic activity (*Dst*) from OMNI between 8-10 March 2008. From top to bottom are (A) plottedinterplanetary magnetic field (*B*), (B) Sun-Earth component of the IMF (*Bx*), (C) east-westcomponent of the IMF (*By*), (D) north-south component of the IMF (*Bz*), (E) proton speed (*Vp*),(F) proton density (*Np*), (G) proton temperature (*Tp*), (H) plasma beta (β), (I) eigenvalues forthe medium and minimum variance directions, (J) *Dst*.

Figure 5.15 Solar wind measurements, MC signatures at L1 and *Dst* observed on 8-10 March 2008.

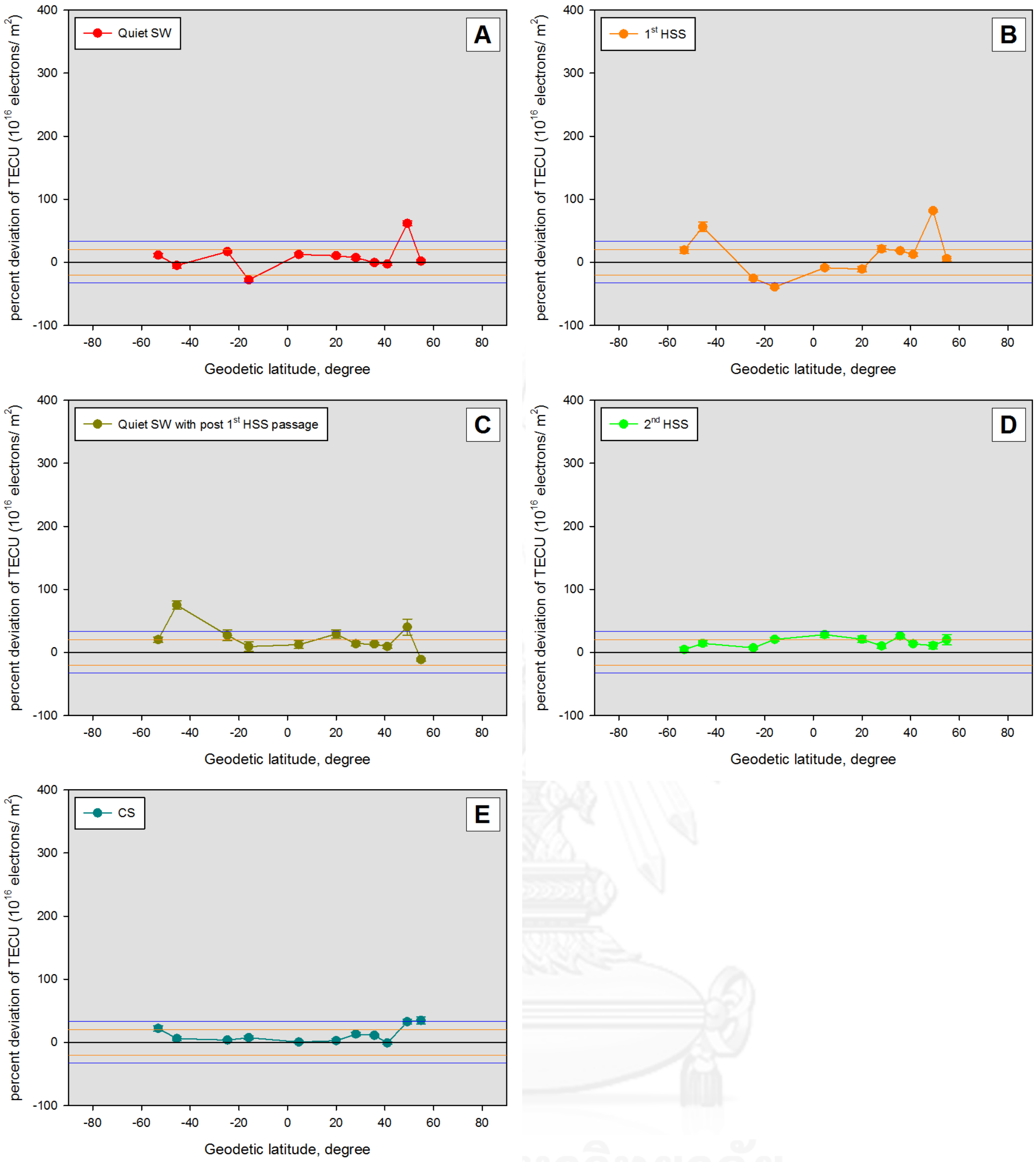

Figure 5. 16 Mean plot of percent deviation of TECU on 8-10 March 2008 (DOY 68-70) by geodetic latitude; categorized by phenomena.

This dawn MC passage triggers an abnormal decreasing in TEC, particularly in the southern hemisphere. TEC in the ionosphere at only 27°S and 45°S got disturbance before the MC enshrouded the ionosphere at those latitudes. The irregularity had reduced TEC at 27°S, but generated extraordinary TEC at 45°S abnormally since quiet time before the MC passage to the MC-passed duration. While the MC-passed duration, northern mid and high latitudes TEC (33°N and 54°N) and 20°S TEC increased at a normal oscillation. TEC at 8°S and 33°S degenerated at a normal oscillation as well.

After the MC passed, TEC at 45°S lessened into a normal TEC but the TEC at 27°S rose continually from abnormal decrease onto abnormal content. Electron at 20°N and 54°N rose but the TEC at over the 33°N declined within normal oscillation. TEC at the higher than 8°S gradually had decreased with a normal oscillation after the MC passed. This detection generally found in the Southern hemisphere but 1°S showed decreasing in TEC significantly in comparison with pre-MC passed TEC. High equatorial and above high-mid latitudes detection in the Northern hemisphere presented that TEC at those regions were generated more than an arrival of the MC.

There were three high speed streams blew the Earth between July, 22-24. The first stream generated TEC disturbance most. The third stream triggered disturbance more than the second one. The bimodal variations happened most clearly during the first stream: extraordinary increase in TEC in the southern hemisphere and did oppositely in the northern hemisphere. TEC at the 27°S and the 45°S always responded to HSSs. The first stream generated extraordinary TEC and the two left streams had abnormally degenerated TEC at both latitudes.

TEC after HSSs had gone always recovered into a normal content. In detail, all eased latitudinal ionosphere needed decreasing in TEC to balance the first stream affect. Oppositely, all eased latitudinal ionosphere needed generating TEC to recover the TEC balance from the second stream affect (see Figure 5.18).

$$Y_i = \alpha + \beta_{\mathrm{i}} X_{\mathrm{i}} + \varepsilon \qquad (5.1)$$

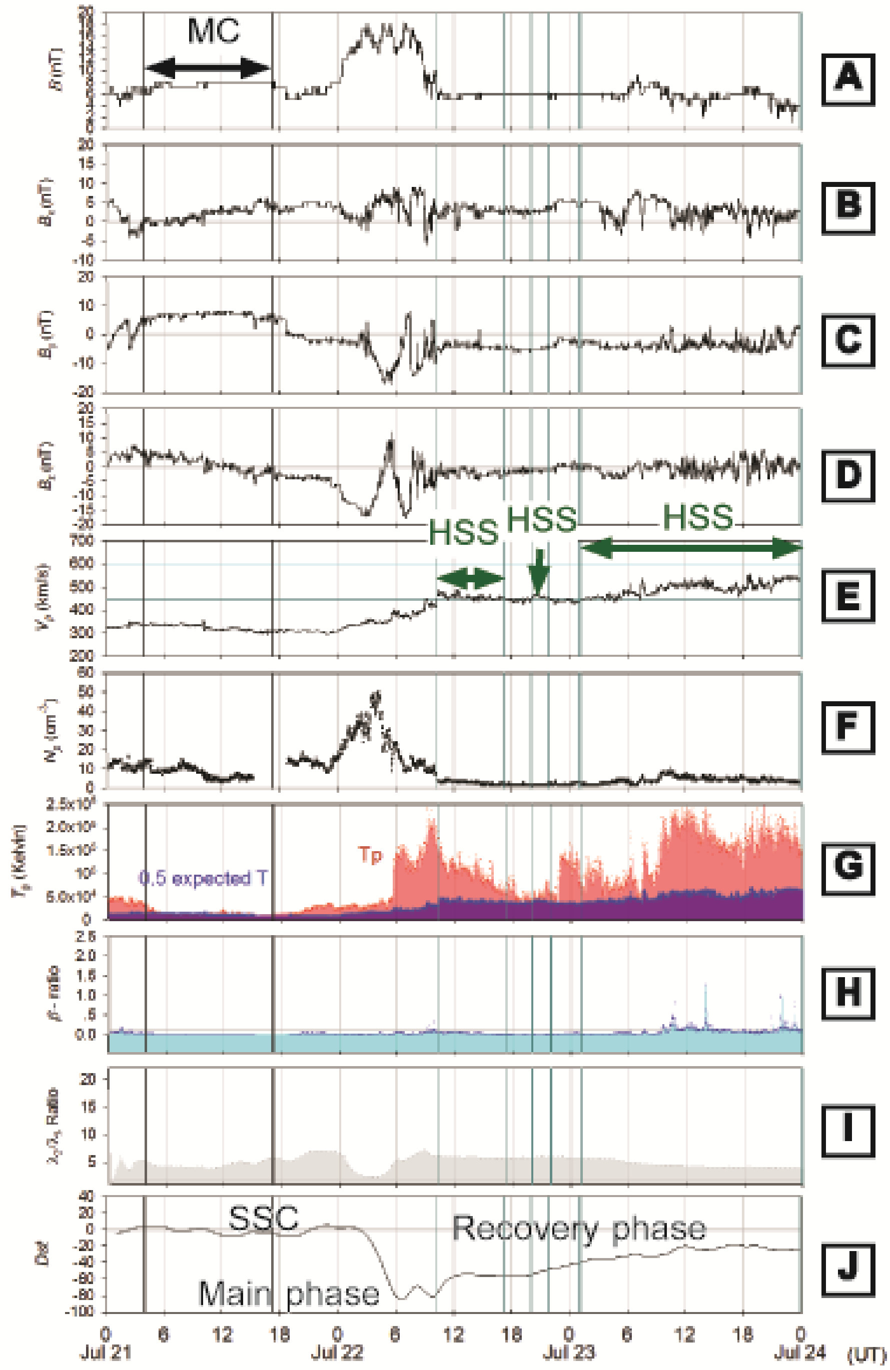

(A-G) Observations by the the ACE spacecraft (G-I), results from programs and (H) geomagnetic activity (*Dst*) from OMNI between 21-22 July 2009. From top to bottom are (A) plottedinterplanetary magnetic field (*B*), (B) Sun-Earth component of the IMF (*Bx*), (C) east-westcomponent of the IMF (*By*), (D) north-south component of the IMF (*Bz*), (E) proton speed (*Vp*),(F) proton density (*Np*), (G) proton temperature (*Tp*), (H) plasma beta (β), (I) eigenvalues forthe medium and minimum variance directions, (J) *Dst*.

Figure 5. 17 Solar wind measurements, MC signatures at L1 and Dst observed on 21-23 July 2008.

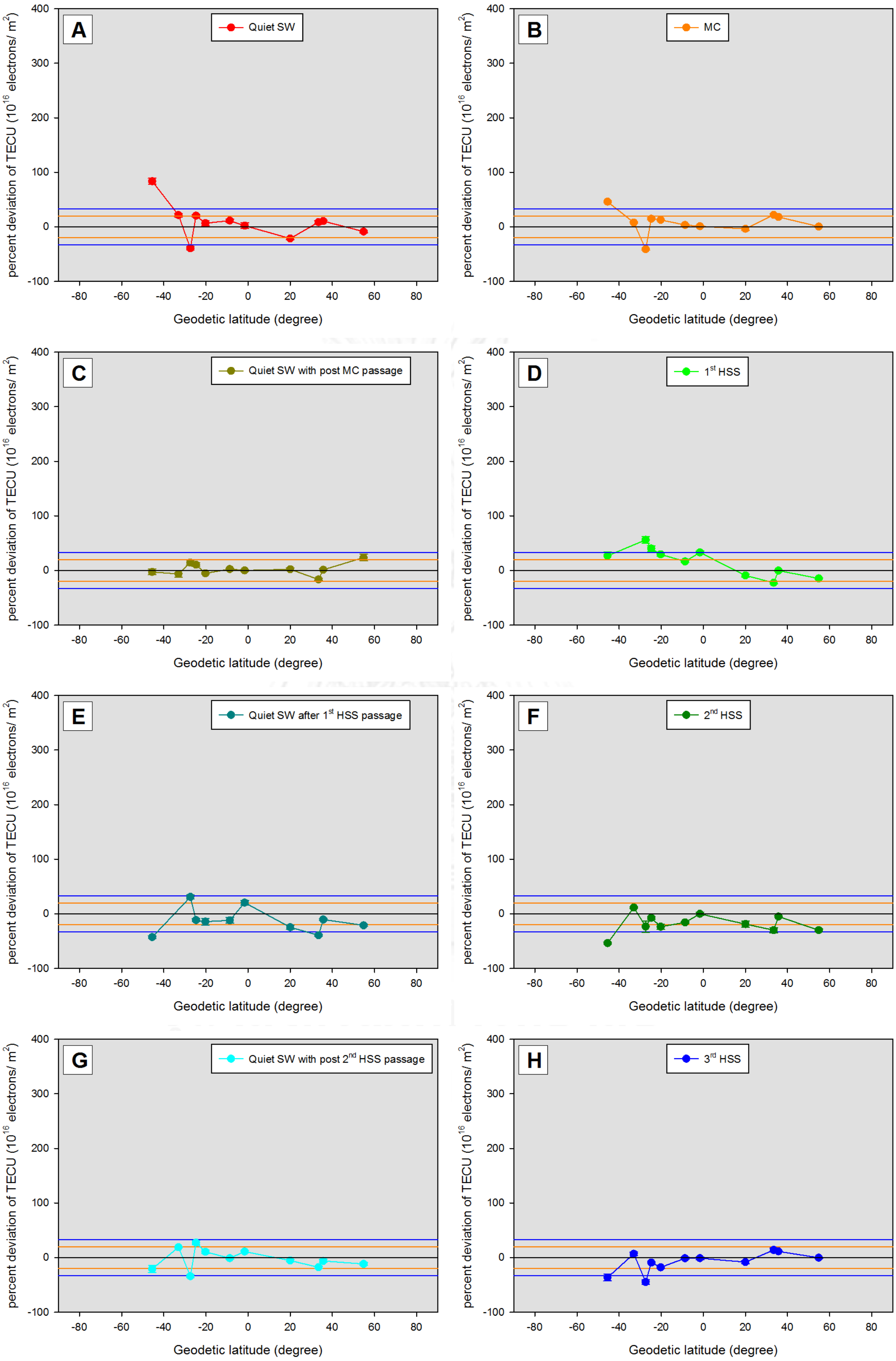

Figure 5. 18 Mean plot of percent deviation on TECU on 21-23 July 2008 (DOY 202-204) by geodetic latitude; categorized by phenomena.

Summary

The TEC variation was asymmetry in global scale (see Figure 5.19). The TEC variation always found was as the TEC increment. Interpretation from all of event which selected from different period of a year reveal as follows:

- TEC increments were able to occur before and the after the passage of MC and phenomena, and TEC under post passage had more increase than the TEC increment before the passage.
- TID occurrences were often found at low to mid-latitude *F* region, before the EIA occurrence (sometimes the EIA disappeared). The TID liked moving to the higher latitude and the poles finally. TID occurrence in the southern hemisphere in January, March, May and July. TID occurs in the northern in April, November and December.
- EIA occurrence with various sizes. Smaller EIA found with TEC under IS and the larger EIA found with TEC under the passage of sheathes, CSs, MCs and also in the TEC under quiet space circumstance after the passage of those motions. The EIA were always found in the northern hemisphere in January, March and May. The EIA were found in the southern hemisphere in November and December.

5.3 Relation between dTEC and MC and phenomenal parameters

The multiple regression model assumes that a dependence (Y_i) response to four variables, namely, predictors (X_i), their effects (regression coefficient, β_i), the predictors' noise (ε) and sometimes constant (α) is the intercept, needed to fix the estimated dependence closer by adjusting Y_i to X_i at zero value (see equation (5.1)). Multiple regressions assume that Y_i and X_i have linearly related.

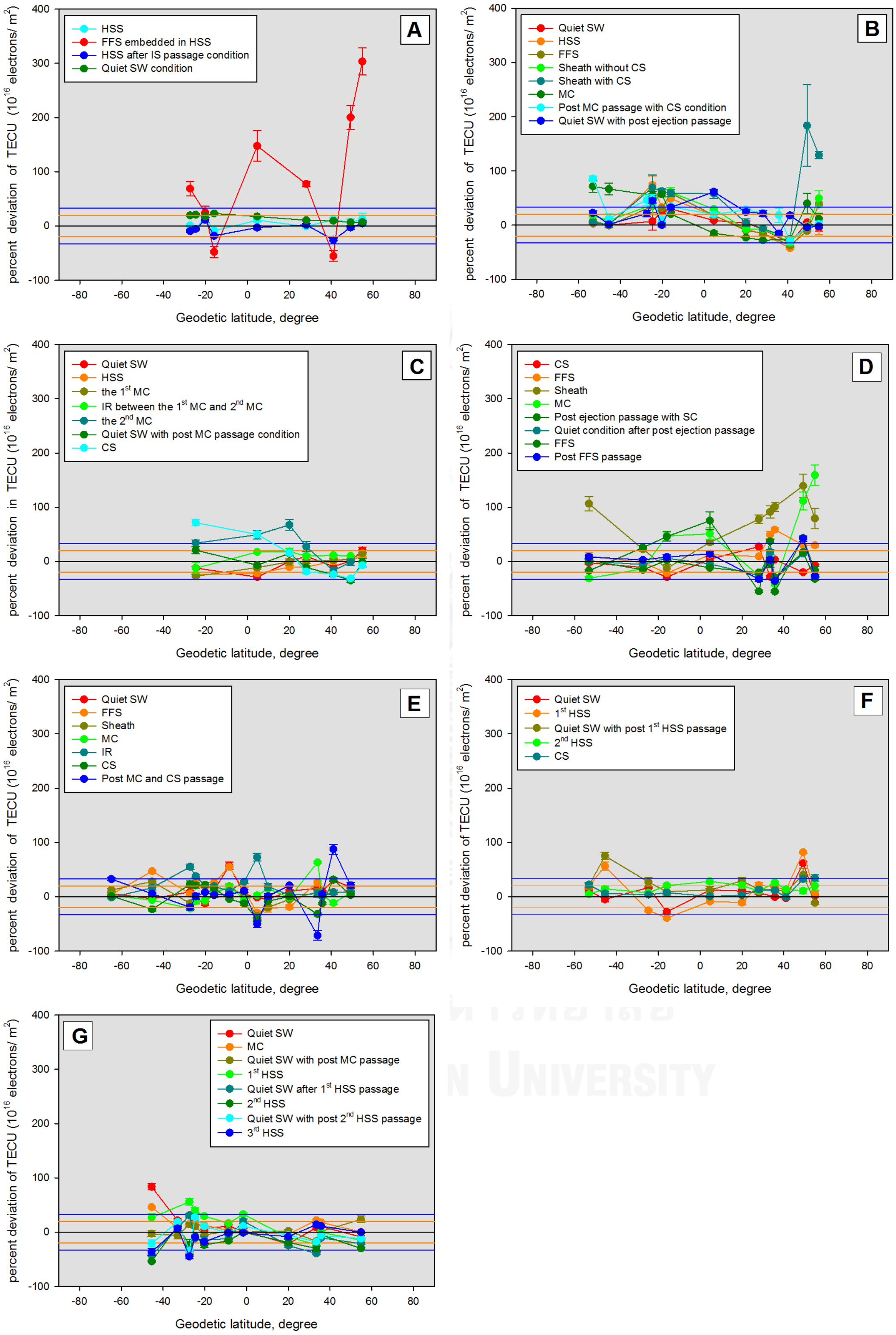

Figure 5. 19 Mean plot of percent deviation on TECU of each Event by geodetic latitude; categorized by phenomena.

With this study, ionosphere is a co-product of change in properties of the solar-terrestrial environment. The ionosphere is the complex system produced with geospace, hence, the simplest multiple linear regressions is needed to answer the relations between TEC variation and the extraterrestrial weather which are measurable at L1.

Parameter used in statistical analysis

The majority of valuables emphasized in this study were observed interplanetary magnetic field and its components because they are key parameters of MC. Solar wind properties were also to analyze their relation to TEC. Another good point of this statistical method is final equation to estimate TEC at specific event.

Six joining derivatives are needed to success the method. R^2 is the coefficient of determination, the first derivative from the model, which was larger than 0.5 when any predictors relate to TEC variation. The regression doesn't need to do next when R^2 is smaller than 0.05. The second derivative is the regression coefficient, R to confirm the accuracy of the model in percent. Then, the significant of the coefficients via ANOVA is to confirm that one of all parameters relates to TEC, the next process doesn't need when this value is greater than 0.05. After that, the significance of coefficients, which are smaller than 0.05 is a derivative, to confirm a relation of specific parameters and TEC. Then, a larger absolute slope parameter value (β) implied more priority of effect it takes. The last derivative is the change in percent deviation of TECU for each one increment change in any parameter.

Final product of joining derivates is estimated TEC equation with accuracy. This study used SSPP program to analyze. All of results each event are shown in Appendix E accordingly to the number of event. Only model which have accuracy larger than 0.70 is to show in next section.

Model relation between dTEC and parameters

5.3.1 Results of Event I

Seven observatories from thirteen available GPS stations didn't response to any MC and phenomenal parameter and a geomagnetic activity. However, other six observations had strong relations with variables. The models in event I at given latitudes were follows:

$$dTEC\%_{SCH2}^{0.89} = 5.88N_P - 2.42\,B_z - 0.44\,Dst$$
$$dTEC\%_{GOGA}^{0.87} = 4.27B_y + 3.86B_M + 2.33B_z + 8.95E - 5\,T_P - 2.18B_x$$
$$dTEC\%_{UNSA}^{0.76} = 185.55 - 0.37\,V_P - 2.25\,B_x - 1.11B_z$$
$$dTEC\%_{SG05}^{0.76} = 3.9\,B_M - 1.87\,B_x - 1.44\,B_y - 14.60\beta$$
$$dTEC\%_{COPO}^{0.72} = 180.14 + 5.25\,B_M - 1.47\,V_P + 1.76B_y + 0.5\,Dst - 1.92\,B_x - 1.47B_z$$

5.3.2 Results of Event II

Six observatories from seven available GPS stations were response to some of MC and phenomenal parameter and a geomagnetic activity. However, these six observations had strong relations with variables. The models in event II at given latitudes are follows:

$$dTEC\%_{BAIE}^{0.92} = 13.14\,N_P - 42.06\beta - 3.17B_z + 2.17B_y$$
$$dTEC\%_{SCH2}^{0.83} = 12.49N_P + 4.33\,B_x - 0.66\,Dst + 1.48\,B_y$$
$$dTEC\%_{PARC}^{0.75} = -142.24 - 6.14\,B_M + 0.34\,V_P - 1.79\,B_y$$
$$dTEC\%_{IQQE}^{0.73} = 4.36\,B_M + 0.64\,Dst - 2.1\,B_y$$
$$dTEC\%_{BOGT}^{0.72} = -35.05\beta + 2.28\,B_y$$
$$dTEC\%_{COYQ}^{0.71} = -2.8\,B_y$$

5.3.3 Results of Event III

Three observatories from nine available GPS stations didn't response to any MC and phenomenal parameter and a geomagnetic activity. However, other six observations have strong relations with variables. The event-III models at given latitudes are follows:

$$dTEC\%_{GOGA}^{0.87} = 4.27B_y + 3.86B_M + 2.33B_z + 8.95E-5\,T_P - 2.18B_x$$

$$dTEC\%_{SG05}^{0.81} = -2.19\,B_y$$

$$dTEC\%_{SCUB}^{0.80} = -103.186 - 4.3\,B_y + 0.22\,V_P$$

$$dTEC\%_{LAMT}^{0.78} = -143.24 - 6.14\,B_M + 0.34\,V_P - 1.79\,B_y$$

$$dTEC\%_{BOGT}^{0.73} = -107.45 + 3.77\,B_z + 2.26\,V_P$$

$$dTEC\%_{UNSA}^{0.73} = 0.22\,V_P - 2.5\,B_z + 4.25\,B_x$$

5.3.4 Results of Event IV

Nearly half of observatories from fifteen available GPS stations didn't response to any MC and phenomenal parameter and a geomagnetic activity. However, other seven observations had strong relations with variables. The event-IV models at given latitudes were follows:

$$dTEC\%_{BAIE}^{0.87} = -359.02 + 22.68\,B_M + 0.00T_P + 0.48V_P - 12.03\,N_P + 41.47\beta + 4.84\,B_z - 8.07\,B_x$$

$$dTEC\%_{SCH2}^{0.88} = 10.56\,B_M - 0.84\,D\mathrm{st} - 7.08B_z - -11.82B_x + 5.75\,B_y$$

$$dTEC\%_{P\ddot{A}\ddot{A}R}^{0.87} = 6.36B_M - 5.34B_y + 3.56B_z - 5.01E-5T_P + 0.30D\mathrm{st} + 3.01N_P$$

$$dTEC\%_{CONO}^{0.81} = +7.00B_M + 0.63D\mathrm{st} + 4.40N_P - 2.90B_y$$

$$dTEC\%_{GOGA}^{0.77} = 0.39V_P + 0.00T_P + 0.51B_z - 4.42B_y - 0.38D\mathrm{st} + 13.53\beta$$

$$dTEC\%_{SG05}^{0.70} = 10.79B_M - 3.37B_z + 1.07D\mathrm{st}$$

$$dTEC\%_{BRAZ}^{0.53} = -10.07B_M + 3.93B_z + 1.90Dst + 6.70B_y$$

5.3.5 Results of Event V

Nearly half of observatories from fifteen available GPS stations didn't response to any MC and phenomenal parameter and a geomagnetic activity. However, other seven observations had strong relations with variables. The event-IV models at given latitudes were follows:

$$dTEC\%_{GOGA}^{0.92} = 51.17 - 0.19\,V_P + 2.48B_x + 1.3\,N_P$$

$$dTEC\%_{BOGT}^{0.81} = 111.54 - 2.01\,D\mathrm{st} - 2.30V_P + 4.96B_M$$

$$dTEC\%_{COPO}^{0.80} = -1.94D\mathrm{st} + 6.5\,B_x - 4.2\,B_z$$

$$dTEC\%_{POVE}^{0.78} = 139.96 - 0.19\,V_P - 3.34\,B_M - 7.49\beta$$

$$dTEC\%_{COYQ}^{0.55} = 4.37B_M - 5.40B_x - 0.18\,V_P + 2.44B_y + 2.60B_z$$

$$dTEC\%_{UNSA}^{0.53} = 0.00T_P - +0.28D\text{st}$$

$$dTEC\%_{LAMT}^{0.52} = -5.00B_M - 10.50\beta$$

5.3.6 Results of Event VI

There was only one observatory from eleven available GPS stations response to any MC and phenomenal parameter and a geomagnetic activity. An only event-VI model at given latitude was follow:

$$dTEC\%_{COYQ}^{0.78} = 153.21 - 0.22\,V_{\text{P}} - 6.21\beta - 1.89N_{\text{P}}$$

5.3.7 Results of Event VII

Five observatories from eleven available GPS stations didn’t response to any MC and phenomenal parameter and a geomagnetic activity. However, other six observations had strong relations with variables. The event-IV models at given latitudes were follows:

$$dTEC\%_{GOGA}^{0.87} = 4.27B_y + 3.86B_M + 2.33B_z + 8.95E - 5\,T_{\text{P}} - 2.18B_x$$

$$dTEC\%_{SCH2}^{0.86} = -86.97 + 6.51B_M + 8.42\beta + 1.80B_y - 2.38B_x$$

$$dTEC\%_{COPO}^{0.81} = -1.04D\text{st} - 3.29B_y - 3.7B_z$$

$$dTEC\%_{COYQ}^{0.78} = 2.33.35 - 0.46\,V_{\text{P}} - 8.8B_x$$

$$dTEC\%_{VALP}^{0.73} = -3.68\,N_{\text{P}}$$

$$dTEC\%_{CONO}^{0.73} = 1.6B_y$$

Summary

The first effective priority of predictors in TEC estimation at high latitude were always solar wind parameter (N_P and V_P). The depended-magnetic field models related with $B_{M,y\,\text{and}\,z}$.

Regression coefficients of all events didn’t depend on geodetic latitudes, but the Event VI, which had only streams (see R^2 in Figure 5.20).

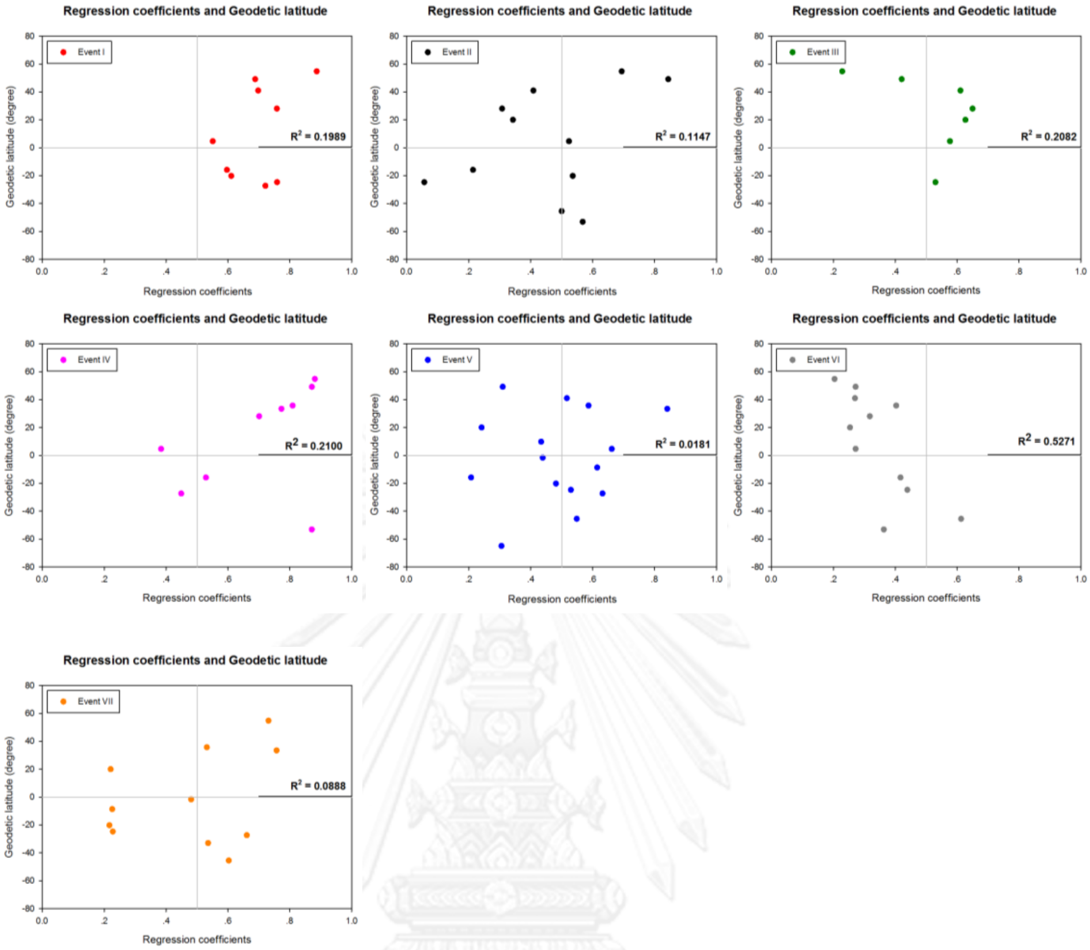

Figure 5.20 Plots of regression coefficients and geodetic latitude in each event.

CHAPTER VI
DISCUSSIONS AND CONCLUSIONS

6.1 Discussions

6.1.1 Results

Abnormal increment and decrement of TEC before the passage of MC found this time coincided to the events reported by Liu *et al*., 2008 that they appear near nightside EIA crest. Oppositely, TEC decrement at the equator after the storm found at event V contrasted to TEC increment in 2000-2002 (reported by Kutiev *et al.*, 2006) although they was in a same evening side section.

TEC variations resulting from HSS and CS in this study sometimes were not different from the TEC variation under the slower SW significantly. The residual variation could also back into normal variation within CS condition. The result confirms that although the large increases in solar wind speed happened, but they was a small responsible to magnetosphere-ionosphere-thermosphere environment as Solomon *et al* s' Model (2012).

TEC increased after the 4 of 5 IS events, which can't be explained why another didn't increase, because it was a FFS and its magnetic fields and directions same as others. TEC clearly and steeply after the IS passage, however it was not always rise exceed normal variation.

TID in this study were found in both hemispheres at higher than 20° stations. TID started in the lower latitude and moved the higher latitude. It was opposite to Otsuka *et al*.'s TID study over Europe in 2013. That Result implied the TID move south-westward. Hocke and Schegel suggested in 1996 that mid-latitude TID was wave-like structure and Otsuka *et al*. speculated that the daytime TID generated by gravity wave and frequently triggered most in winter, coincide to this study.

6.1.2 Relation between dTEC and MC and phenomenal parameters

MC often induced asymmetric TEC variation in hemisphere scale. MC had the largest B_M triggered abnormal increment and decrement in TEC broadly in northern hemisphere, TEC in the smallest B_M MC condition was enriched more than TEC before the MC passed. It seem the larger B_M brought the larger percent deviation of TEC but the SN-MC with axial B_M equaled 17 nT (as medium B_M found in this study) didn't bring any clear deviation of TEC.

Disappearance of abnormal TEC variation caused by medium-B_M MC in the study confirmed that the B_M is not a main factor to vary TEC. Oppositely, B_z is still a key. Because, the irregular TEC variation dues to the penetration of the electric fields and the electric fields came into the ionosphere during the Southward and Northward IMF turnings.

Recently, we used the nearest 16-second measurement from ACE to test the coefficient with the closest GPS data. The coefficient was poor (R^2<0.3), but hourly average of spacecraft measurement give a better coefficients. Percent deviation of TEC has a good relationship with the IMF and SW (R^2>0.7) properties all of those events.

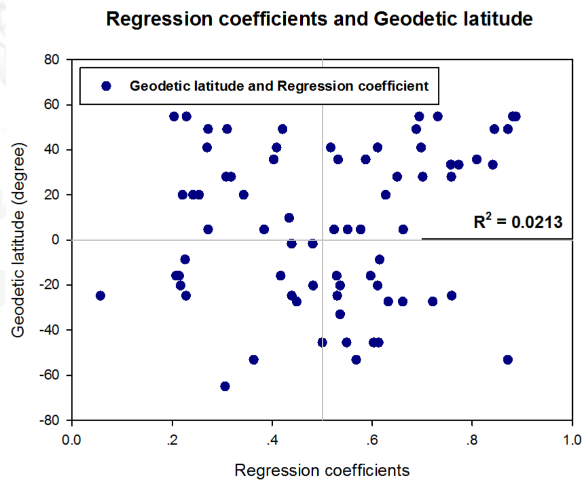

Figure 6.1 Plots of regression coefficients and geodetic latitude.

The largest and the smallest squared multiple correlations in the study are at event IV and event VI respectively. Solomon *et al* s' Model (2012) is still able to explain these differences, because there were only HSSs and CS at event VI.

From short-term relationship of TEC with geomagnetic activity in equatorial regions (Wang *et al*., 2008), the critical frequency (f_0F_2) which is able to be TEC representative had the most significant coefficient with Dst in a local noon.

6.2 Conclusions

This thesis emphasizes the study of percent deviation of TEC resulting from MCs various phenomena and also describes their relationships. The solar wind measurement is used to identify and then classify different structure with computer program specifically constructed. Neutron monitors are to confirm arrival of CME and the phenomena as δF recheck. GPS data are to derive TEC, 27 days average and percent deviation of TECU. ACE and TEC measurements are converted to the same coordinate system. Travelling times are calculated to divide TEC into each condition.

TID occurrences were often found at low to mid-latitude *F* region, before the EIA occurrence (sometimes the EIA disappeared). The TID liked moving to the higher latitude and the poles finally. TID occurrence in the Southern hemisphere in summer solstice. TID occurs in the Northern in winter solstice.

EIA occurs in various sizes. Smaller EIA found with TEC under IS and the larger EIA found with TEC under the passage of sheathes, CSs, MCs and also in the TEC under quiet space circumstance after the passage of those motions. The EIA were always found in the Northern hemisphere in summer solstice. The EIA were found in the Southern hemisphere in winter solstice.

REFERENCES

Akasofu, S. I. (1964). "The development of the auroral substorm." Planetary and Space Science **12**(4): 273-282.

Badruddin and Y. P. Singh (2009). "Geoeffectiveness of magnetic cloud, shock/sheath, interaction region, high-speed stream and their combined occurrence." Planetary and Space Science **57**(3): 318-331.

Belehaki, A. and I. Tsagouri (2002). "On the occurrence of storm-induced nighttime ionization enhancements at ionospheric middle latitudes." Journal of Geophysical Research: Space Physics **107**(A8): SIA 23-21-SIA 23-19.

Beloff, N., et al. (2004). "Storm time changes in total electron content in ionosphere measured by low orbiting topside sounder." Ann. Geophys. **22**(8): 2741-2746.

Blelly, P. L. and D. Alcayde (2007). Handbook of the Solar-Terrestrial Environment. Berlin, Springer.

Burlaga, L. F. (1991). "Intermittent turbulence in the solar wind." Journal of Geophysical Research: Space Physics **96**(A4): 5847-5851.

Burlaga, L. F., et al. (1981). "The coronal and interplanetary current sheet in early 1976." Journal of Geophysical Research: Space Physics **86**(A11): 8893-8898.

Cai, C. (2007). "Monitoring seasonal variations of ionospheric TEC using GPS measurements." Geo-spatial Information Science **10**(2): 96-99.

Cargill, P. J. and L. K. Harra (2007). Handbook of the Solar-Terrestrial Environment. Berlin, Springer.

Chian, A. C.-L. and Y. Kamide (2007). Handbook of the Solar-Terrestrial Environment. Berlin, Springer.

Gopalswamy, N., et al. (2007). "Geoeffectiveness of halo coronal mass ejections." Journal of Geophysical Research: Space Physics **112**(A6): A06112.

Huang, X. and B. W. Reinisch (2001). "Vertical electron content from ionograms in real time." Radio Science **36**(2): 335-342.

Hundhausen, A. J. (1993). "Sizes and locations of coronal mass ejections: SMM observations from 1980 and 1984-1989." Journal of Geophysical Research: Space Physics **98**(A8): 13177-13200.

Kahler, S. W. and A. Vourlidas (2005). "Fast coronal mass ejection environments and the production of solar energetic particle events." Journal of Geophysical Research: Space Physics **110**(A12): A12S01.

Klein, L. W. and L. F. Burlaga (1982). "Interplanetary magnetic clouds At 1 AU." Journal of Geophysical Research: Space Physics **87**(A2): 613-624.

Kumar, S. and A. Raizada (2010). "Geoeffectiveness of magnetic clouds occurred during solar cycle 23." Planetary and Space Science **58**(5): 741-748.

Kunow, H., et al. (2006). "Foreword." Space Science Reviews **123**(1-3): 1-2.

Lepping, R. P., et al. (1990). "Magnetic field structure of interplanetary magnetic clouds at 1 AU." Journal of Geophysical Research: Space Physics **95**(A8): 11957-11965.

Nsumei, P. A., et al. (2008). "Polar cap electron density distribution from IMAGE radio plasma imager measurements: Empirical model with the effects of solar illumination and geomagnetic activity." Journal of Geophysical Research: Space Physics **113**(A1): A01217.

Rostoker, G., et al. (1980). "Magnetospheric substorms—definition and signatures." Journal of Geophysical Research: Space Physics **85**(A4): 1663-1668.

Sastri, J. H., et al. (1993). "Penetration of polar electric fields to the nightside dip equator at times of geomagnetic sudden commencements." Journal of Geophysical Research: Space Physics **98**(A10): 17517-17523.

St. Cyr, O. C., et al. (2000). "Properties of coronal mass ejections: SOHO LASCO observations from January 1996 to June 1998." Journal of Geophysical Research: Space Physics **105**(A8): 18169-18185.

Yashiro, S., et al. (2004). "A catalog of white light coronal mass ejections observed by the SOHO spacecraft." Journal of Geophysical Research: Space Physics **109**(A7): A07105.

APPENDIX

APPENDIX A

PROGRAMS

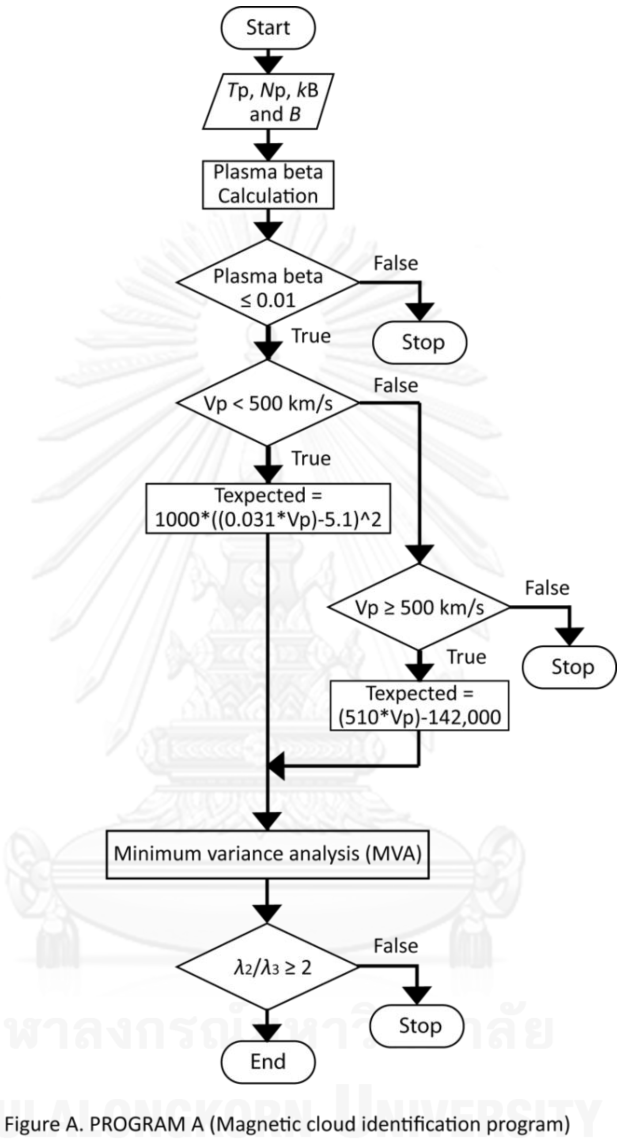

Figure A-1 Program A

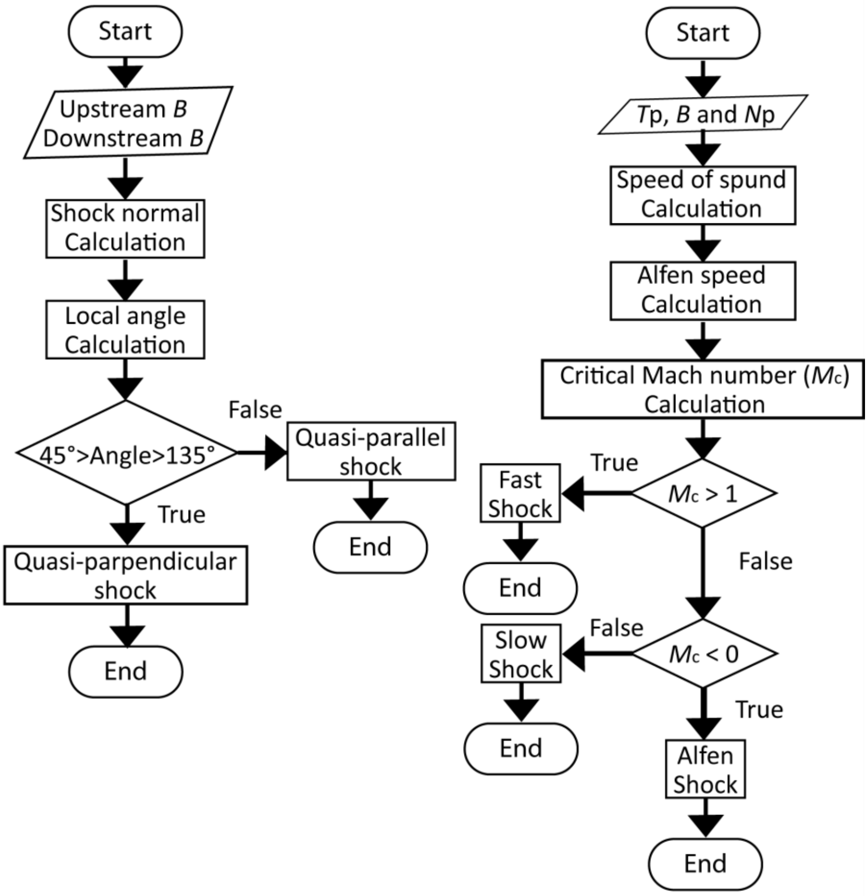

Figure B. PROGRAM B (Interplanetary shock classification program)

Figure A-2 Program B

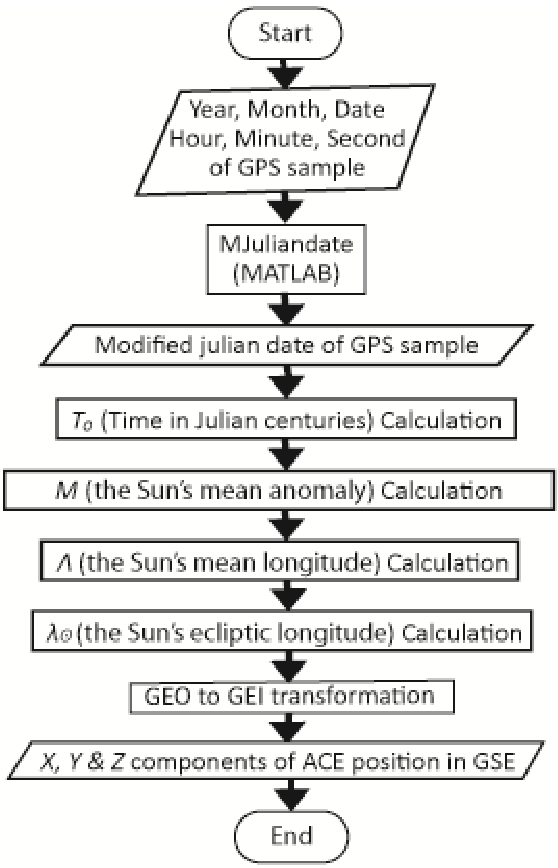

Figure C. PROGRAM D (GSE-GEI transformation program)

Figure A-3 Program C

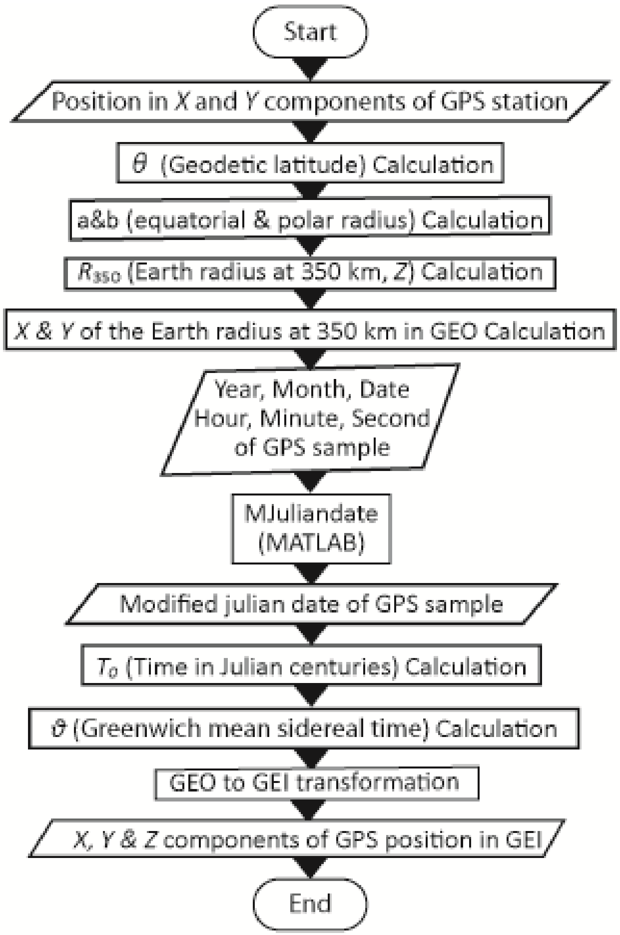

Figure D. PROGRAM D (GEO-GEI transformation program)

Figure A-4 Program D

APPENDIX B

FORSH DEREASE PLOT FROM SECTION

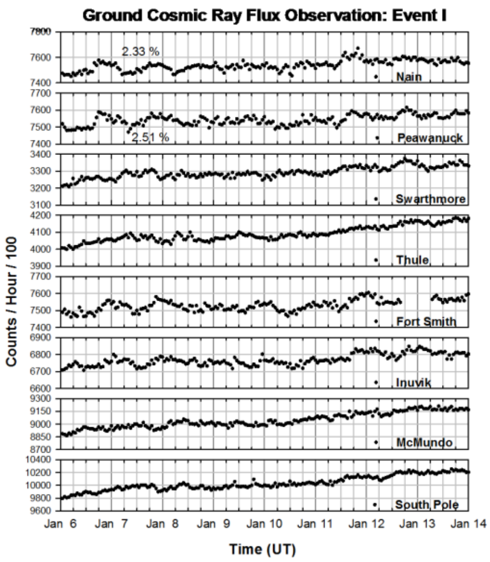

Figure B-1 Forbush decrease on 2005 January 7 (DOY-07)

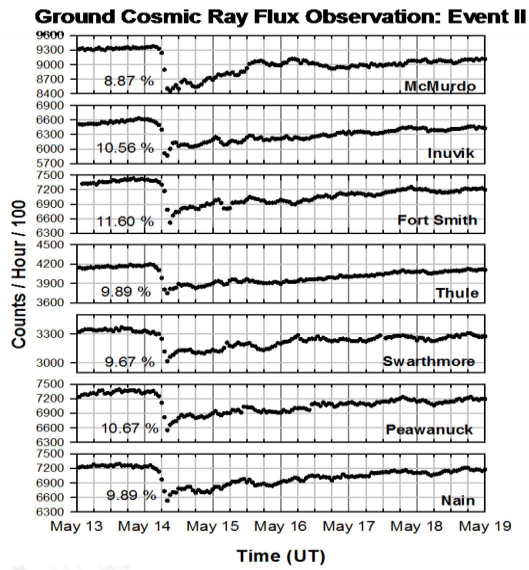

Figure B-2 Forbush decrease on 2005 May 14 (DOY-134)

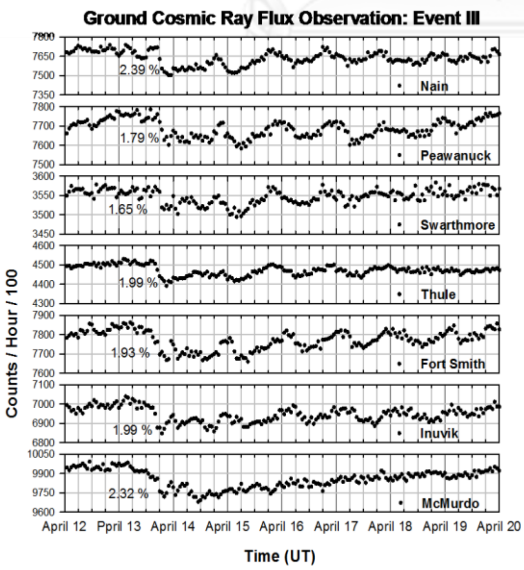

Figure B-3 Forbush decrease on 2006 April 13 (DOY-103)

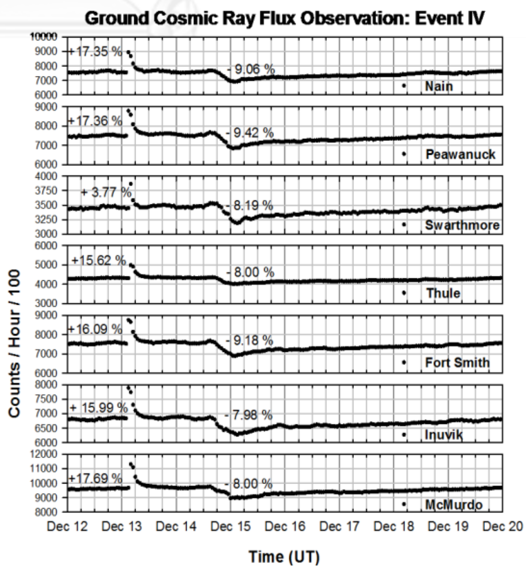

Figure B-4 Forbush decrease on 2006 December 15 (DOY-149)

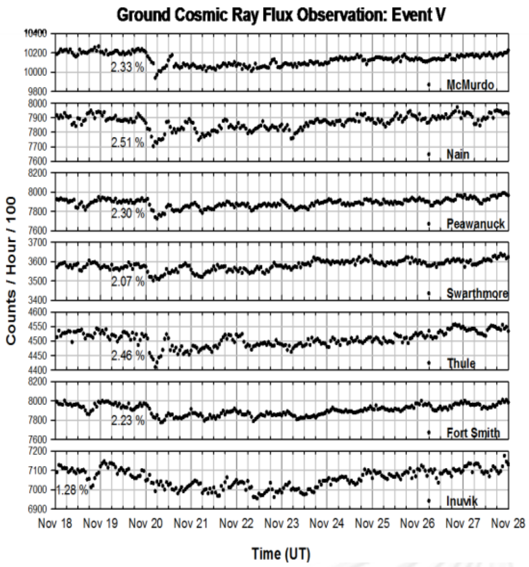

Figure B-5 Forbush decrease on 2007 November 20 (DOY-324)

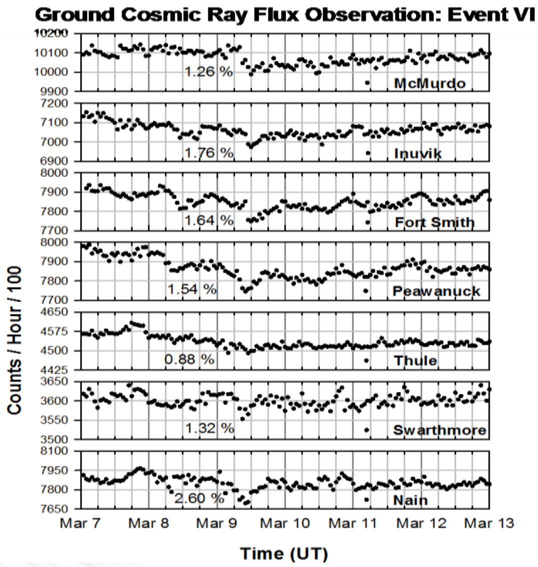

Figure B-6 Forbush decrease on 2008 March 9 (DOY-069)

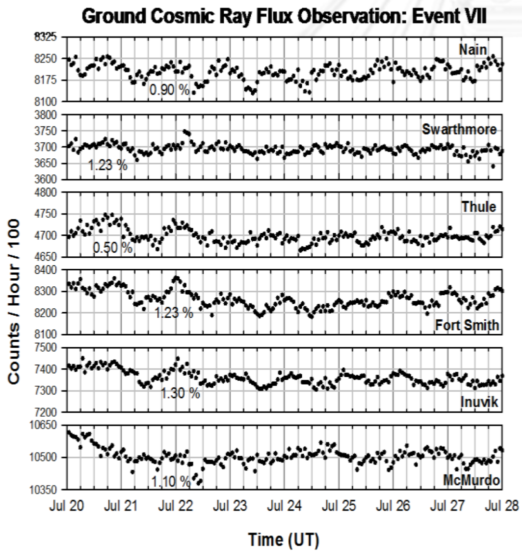

Figure B-7 Forbush decrease on 2009 July 21 (DOY-202)

APPENDIX C

FULL FISHER's LSD MULTIPLE COMPARISONS RESULTS FROM SECTION 5.2

Event I

Table C-1 Mean percentage deviation of TECU for each phenomena of Event I from IGS stations.

Station	Latitude/ longitude	A	B	C	D
SCH2	63°45'23"N/ 68°30'36"W	13.12±5.33 (n=250)	303.56±12.50 (n=5)	4.62±2.54 (n=512)	7.09±0.38 (n=193)
BAIE	49°11'12"N/ 68°15'46"W	6.45±3.15 (n=250)	200.41±11.11 (n=5)	-2.81±1.84 (n=512)	6.48±0.29 (n=193)
LAMT	42°00'16"N/ 73°54'31"W	11.76±1.47 (n=250)	-55.47±5.02 (n=5)	-25.82±0.89 (n=512)	9.50±0.45 (n=193)
SG05	28°03'54"N/ 80°37'21"W	-0.79±1.44 (n=250)	77.26±2.21 (n=5)	1.99±1.37 (n=512)	10.61±0.35 (n=193)
BOGT	04°38'23"N/ 74°04'48"W	10.60±1.54 (n=250)	147.80±1.88 (n=5)	-2.97±1.88 (n=512)	17.39±0.65 (n=189)
BRAZ	15°56'50"S/ 47°52'48"W	-8.95±1.42 (n=231)	-47.95±5.10 (n=5)	-18.23±1.13 (n=499)	22.92±0.83 (n=928)
IQQE	20°16'24"S/ 70°07'54"W	16.46±2.07 (n=250)	24.49±5.96 (n=5)	11.28±2.03 (n=389)	17.82±0.77 (n=193)
UNSA	24°43'40"S/ 65°53'46"W	-5.24±1.35 (n=239)	N/D	-5.60±0.87 (n=287)	20.62±0.79 (n=181)
COPO	27°23'04"S/ 70°20'16"W	0.88±1.33 (n=250)	68.77±6.60 (n=5)	-9.44±1.42 (n=512)	19.48±0.66 (n=193)

Table C-2 BAIE

Dependent Variable	(I) LFeat	(J) LFeat	Mean Difference (I-J)	Std. Error	Sig.	95% Confidence Interval	
						Lower Bound	Upper Bound
dTEC	1.00	2.00	-193.96247*	17.93	0.00	-229.16	-158.77
		3.00	9.26135*	3.06	0.00	3.25	15.27
		4.00	-0.03	3.80	0.99	-7.50	7.44
	2.00	1.00	193.96247*	17.93	0.00	158.77	229.16
		3.00	203.22382*	17.84	0.00	168.20	238.24
		4.00	193.93300*	17.99	0.00	158.64	229.23
	3.00	1.00	-9.26135*	3.06	0.00	-15.27	-3.25
		2.00	-203.22382*	17.84	0.00	-238.24	-168.20
		4.00	-9.29082*	3.35	0.01	-15.87	-2.71
	4.00	1.00	0.03	3.80	0.99	-7.44	7.50
		2.00	-193.93300*	17.99	0.00	-229.23	-158.64
		3.00	9.29082*	3.35	0.01	2.71	15.87

Table C-3 BOGT

Dependent Variable	(I) LFeat	(J) LFeat	Mean Difference (I-J)	Std. Error	Sig.	95% Confidence Interval	
						Lower Bound	Upper Bound
dTEC	1.00	2.00	-137.20624*	15.30	0.00	-167.23	-107.18
		3.00	13.56335*	2.61	0.00	8.43	18.69
		4.00	-6.79095*	3.26	0.04	-13.20	-0.38
	2.00	1.00	137.20624*	15.30	0.00	107.18	167.23
		3.00	150.76959*	15.22	0.00	120.90	180.64
		4.00	130.41529*	15.35	0.00	100.30	160.53
	3.00	1.00	-13.56335*	2.61	0.00	-18.69	-8.43
		2.00	-150.76959*	15.22	0.00	-180.64	-120.90
		4.00	-20.35430*	2.88	0.00	-26.01	-14.70
	4.00	1.00	6.79095*	3.26	0.04	0.38	13.20
		2.00	-130.41529*	15.35	0.00	-160.53	-100.30
		3.00	20.35430*	2.88	0.00	14.70	26.01

Table C-4 BRAZ

Dependent Variable	(I) LFeat	(J) LFeat	Mean Difference (I-J)	Std. Error	Sig.	95% Confidence Interval	
						Lower Bound	Upper Bound
dTEC	1.00	2.00	38.99375*	10.01	0.00	19.34	58.65
		3.00	9.28326*	1.76	0.00	5.82	12.74
		4.00	-31.87570*	2.16	0.00	-36.12	-27.64
	2.00	1.00	-38.99375*	10.01	0.00	-58.65	-19.34
		3.00	-29.71049*	9.96	0.00	-49.25	-10.17
		4.00	-70.86945*	10.03	0.00	-90.56	-51.18
	3.00	1.00	-9.28326*	1.76	0.00	-12.74	-5.82
		2.00	29.71049*	9.96	0.00	10.17	49.25
		4.00	-41.15895*	1.88	0.00	-44.84	-37.47
	4.00	1.00	31.87570*	2.16	0.00	27.64	36.12
		2.00	70.86945*	10.03	0.00	51.18	90.56
		3.00	41.15895*	1.88	0.00	37.47	44.84

Table C-5 COPO

Dependent Variable	(I) LFeat	(J) LFeat	Mean Difference (I-J)	Std. Error	Sig.	95% Confidence Interval	
						Lower Bound	Upper Bound
dTEC	1.00	2.00	-67.89077*	11.83	0.00	-91.12	-44.67
		3.00	10.32346*	2.02	0.00	6.36	14.29
		4.00	-18.59747*	2.51	0.00	-23.52	-13.67
	2.00	1.00	67.89077*	11.83	0.00	44.67	91.12
		3.00	78.21424*	11.78	0.00	55.11	101.32
		4.00	49.29330*	11.87	0.00	26.00	72.59
	3.00	1.00	-10.32346*	2.02	0.00	-14.29	-6.36
		2.00	-78.21424*	11.78	0.00	-101.32	-55.11
		4.00	-28.92093*	2.21	0.00	-33.26	-24.58
	4.00	1.00	18.59747*	2.51	0.00	13.67	23.52
		2.00	-49.29330*	11.87	0.00	-72.59	-26.00
		3.00	28.92093*	2.21	0.00	24.58	33.26

Table C-6 IQQE

Dependent Variable	(I) LFeat	(J) LFeat	Mean Difference (I-J)	Std. Error	Sig.	95% Confidence Interval	
						Lower Bound	Upper Bound
dTEC	1.00	2.00	-8.03	14.91	0.59	-37.30	21.23
		3.00	5.18	2.68	0.05	-0.08	10.43
		4.00	-1.37	3.16	0.67	-7.58	4.84
	2.00	1.00	8.03	14.91	0.59	-21.23	37.30
		3.00	13.21	14.86	0.37	-15.96	42.37
		4.00	6.67	14.95	0.66	-22.69	36.02
	3.00	1.00	-5.18	2.68	0.05	-10.43	0.08
		2.00	-13.21	14.86	0.37	-42.37	15.96
		4.00	-6.54232*	2.91	0.02	-12.25	-0.84
	4.00	1.00	1.37	3.16	0.67	-4.84	7.58
		2.00	-6.67	14.95	0.66	-36.02	22.69
		3.00	6.54232*	2.91	0.02	0.84	12.25

Table C-7 LAMT

Dependent Variable	(I) LFeat	(J) LFeat	Mean Difference (I-J)	Std. Error	Sig.	95% Confidence Interval	
						Lower Bound	Upper Bound
dTEC	1.00	2.00	67.23093*	8.63	0.00	50.30	84.16
		3.00	37.58131*	1.47	0.00	34.69	40.47
		4.00	2.26	1.83	0.22	-1.33	5.85
	2.00	1.00	-67.23093*	8.63	0.00	-84.16	-50.30
		3.00	-29.64962*	8.58	0.00	-46.49	-12.81
		4.00	-64.97119*	8.65	0.00	-81.95	-47.99
	3.00	1.00	-37.58131*	1.47	0.00	-40.47	-34.69
		2.00	29.64962*	8.58	0.00	12.81	46.49
		4.00	-35.32157*	1.61	0.00	-38.49	-32.16
	4.00	1.00	-2.26	1.83	0.22	-5.85	1.33
		2.00	64.97119*	8.65	0.00	47.99	81.95
		3.00	35.32157*	1.61	0.00	32.16	38.49

Table C- 8 SCH2

Dependent Variable	(I) LFeat	(J) LFeat	Mean Difference (I-J)	Std. Error	Sig.	95% Confidence Interval	
						Lower Bound	Upper Bound
dTEC	1.00	2.00	-290.43896*	27.18	0.00	-343.77	-237.11
		3.00	8.49	4.64	0.07	-0.62	17.60
		4.00	6.02	5.77	0.30	-5.29	17.34
	2.00	1.00	290.43896*	27.18	0.00	237.11	343.77
		3.00	298.93255*	27.04	0.00	245.87	352.00
		4.00	296.46268*	27.25	0.00	242.98	349.95
	3.00	1.00	-8.49	4.64	0.07	-17.60	0.62
		2.00	-298.93255*	27.04	0.00	-352.00	-245.87
		4.00	-2.47	5.08	0.63	-12.44	7.50
	4.00	1.00	-6.02	5.77	0.30	-17.34	5.29
		2.00	-296.46268*	27.25	0.00	-349.95	-242.98
		3.00	2.47	5.08	0.63	-7.50	12.44

Table C- 9 SG05

Dependent Variable	(I) LFeat	(J) LFeat	Mean Difference (I-J)	Std. Error	Sig.	95% Confidence Interval	
						Lower Bound	Upper Bound
dTEC	1.00	2.00	-78.04975*	11.54	0.00	-100.70	-55.39
		3.00	-2.78	1.97	0.16	-6.66	1.09
		4.00	-11.40065*	2.45	0.00	-16.21	-6.59
	2.00	1.00	78.04975*	11.54	0.00	55.39	100.70
		3.00	75.26476*	11.49	0.00	52.72	97.81
		4.00	66.64910*	11.58	0.00	43.93	89.37
	3.00	1.00	2.78	1.97	0.16	-1.09	6.66
		2.00	-75.26476*	11.49	0.00	-97.81	-52.72
		4.00	-8.61566*	2.16	0.00	-12.85	-4.38
	4.00	1.00	11.40065*	2.45	0.00	6.59	16.21
		2.00	-66.64910*	11.58	0.00	-89.37	-43.93
		3.00	8.61566*	2.16	0.00	4.38	12.85

Table C-10 UNSA

Dependent Variable	(I) LFeat	(J) LFeat	Mean Difference (I-J)	Std. Error	Sig.	95% Confidence Interval	
						Lower Bound	Upper Bound
dTEC	1.00	3.00	0.36	1.43	0.80	-2.45	3.16
		4.00	-25.86889*	1.61	0.00	-29.02	-22.71
	3.00	1.00	-0.36	1.43	0.80	-3.16	2.45
		4.00	-26.22584*	1.55	0.00	-29.26	-23.19
	4.00	1.00	25.86889*	1.61	0.00	22.71	29.02
		3.00	26.22584*	1.55	0.00	23.19	29.26

Event II Mean percentage deviation of TECU for each phenomena of Event II from IGS stations.

Table C-11 BAIE

Dependent Variable	(I) LFeat	(J) LFeat	Mean Difference (I-J)	Std. Error	Sig.	95% Confidence Interval	
						Lower Bound	Upper Bound
dTEC	1	2	6.86519	26.25836	.794	-44.6879	58.4183
		3	15.96447	38.12741	.676	-58.8911	90.8201
		4	8.47186	24.94633	.734	-40.5053	57.4490
		5	-178.45240*	23.13823	.000	-223.8797	-133.0251
		6	-34.70251*	16.78037	.039	-67.6474	-1.7576
		7	8.26358	16.77527	.622	-24.6713	41.1985
		8	9.07783	16.36403	.579	-23.0497	41.2054
	2	1	-6.86519	26.25836	.794	-58.4183	44.6879
		3	9.09927	40.46686	.822	-70.3494	88.5479
		4	1.60667	28.39342	.955	-54.1382	57.3515
		5	-185.31759*	26.81874	.000	-237.9709	-132.6643
		6	-41.56770	21.57424	.054	-83.9244	.7890
		7	1.39838	21.57028	.948	-40.9506	43.7473
		8	2.21263	21.25203	.917	-39.5115	43.9368
	3	1	-15.96447	38.12741	.676	-90.8201	58.8911
		2	-9.09927	40.46686	.822	-88.5479	70.3494
		4	-7.49261	39.62807	.850	-85.2945	70.3092
		5	-194.41687*	38.51548	.000	-270.0344	-118.7994
		6	-50.66698	35.06630	.149	-119.5127	18.1787
		7	-7.70089	35.06386	.826	-76.5418	61.1400
		8	-6.88664	34.86899	.843	-75.3450	61.5717
	4	1	-8.47186	24.94633	.734	-57.4490	40.5053
		2	-1.60667	28.39342	.955	-57.3515	54.1382
		3	7.49261	39.62807	.850	-70.3092	85.2945
		5	-186.92426*	25.53552	.000	-237.0582	-136.7903
		6	-43.17437*	19.95660	.031	-82.3552	-3.9936
		7	-.20828	19.95231	.992	-39.3807	38.9641
		8	.60597	19.60782	.975	-37.8901	39.1020
	5	1	178.45240*	23.13823	.000	133.0251	223.8797
		2	185.31759*	26.81874	.000	132.6643	237.9709
		3	194.41687*	38.51548	.000	118.7994	270.0344
		4	186.92426*	25.53552	.000	136.7903	237.0582
		6	143.74989*	17.64438	.000	109.1087	178.3911
		7	186.71598*	17.63953	.000	152.0843	221.3477
		8	187.53022*	17.24891	.000	153.6654	221.3950
	6	1	34.70251*	16.78037	.039	1.7576	67.6474
		2	41.56770	21.57424	.054	-.7890	83.9244
		3	50.66698	35.06630	.149	-18.1787	119.5127
		4	43.17437*	19.95660	.031	3.9936	82.3552
		5	-143.74989*	17.64438	.000	-178.3911	-109.1087
		7	42.96608*	7.57338	.000	28.0973	57.8349
		8	43.78033*	6.61271	.000	30.7976	56.7631
	7	1	-8.26358	16.77527	.622	-41.1985	24.6713
		2	-1.39838	21.57028	.948	-43.7473	40.9506
		3	7.70089	35.06386	.826	-61.1400	76.5418
		4	.20828	19.95231	.992	-38.9641	39.3807
		5	-186.71598*	17.63953	.000	-221.3477	-152.0843
		6	-42.96608*	7.57338	.000	-57.8349	-28.0973
		8	.81425	6.59975	.902	-12.1430	13.7715
	8	1	-9.07783	16.36403	.579	-41.2054	23.0497
		2	-2.21263	21.25203	.917	-43.9368	39.5115
		3	6.88664	34.86899	.843	-61.5717	75.3450
		4	-.60597	19.60782	.975	-39.1020	37.8901
		5	-187.53022*	17.24891	.000	-221.3950	-153.6654
		6	-43.78033*	6.61271	.000	-56.7631	-30.7976
		7	-.81425	6.59975	.902	-13.7715	12.1430

Table C-12 BOGE

Dependent Variable	(I) LFeat	(J) LFeat	Mean Difference (I-J)	Std. Error	Sig.	95% Confidence Interval	
						Lower Bound	Upper Bound
dTEC	1	2	-9.26764	11.16122	.407	-31.1805	12.6452
		3	-9.46364	16.20620	.559	-41.2813	22.3540
		4	-0.97401*	10.60353	.048	-41.7919	-.1561
		5	-49.15990*	9.83499	.000	-68.4690	-29.8508
		6	23.68525*	7.13256	.001	9.6819	37.6886
		7	-10.99351	7.13039	.124	-24.9926	3.0056
		8	-52.56972*	6.95559	.000	-66.2256	-38.9138
	2	1	9.26764	11.16122	.407	-12.6452	31.1805
		3	-.19600	17.20059	.991	-33.9659	33.5739
		4	-11.70638	12.06873	.332	-35.4009	11.9882
		5	-39.89226*	11.39941	.000	-62.2727	-17.5118
		6	32.95289*	9.17021	.000	14.9490	50.9568
		7	-1.72588	9.16853	.851	-19.7265	16.2747
		8	-43.30208*	9.03325	.000	-61.0371	-25.5671
	3	1	9.46364	16.20620	.559	-22.3540	41.2813
		2	.19600	17.20059	.991	-33.5739	33.9659
		4	-11.51037	16.84406	.495	-44.5803	21.5596
		5	-39.69626*	16.37115	.016	-71.8378	-7.5548
		6	33.14889*	14.90506	.026	3.8858	62.4120
		7	-1.52987	14.90403	.918	-30.7910	27.7312
		8	-43.10608*	14.82119	.004	-72.2045	-14.0076
	4	1	20.97401*	10.60353	.048	.1561	41.7919
		2	11.70638	12.06873	.332	-11.9882	35.4009
		3	11.51037	16.84406	.495	-21.5596	44.5803
		5	-28.18589*	10.85397	.010	-49.4955	-6.8763
		6	44.65926*	8.48263	.000	28.0053	61.3132
		7	9.98050	8.48080	.240	-6.6699	26.6309
		8	-31.59571*	8.33438	.000	-47.9586	-15.2328
	5	1	49.15990*	9.83499	.000	29.8508	68.4690
		2	39.89226*	11.39941	.000	17.5118	62.2727
		3	39.69626*	16.37115	.016	7.5548	71.8378
		4	28.18589*	10.85397	.010	6.8763	49.4955
		6	72.84515*	7.49981	.000	58.1208	87.5695
		7	38.16639*	7.49775	.000	23.4460	52.8867
		8	-3.40982	7.33171	.642	-17.8042	10.9845
	6	1	-23.68525*	7.13256	.001	-37.6886	-9.6819
		2	-32.95289*	9.17021	.000	-50.9568	-14.9490
		3	-33.14889*	14.90506	.026	-62.4120	-3.8858
		4	-44.65926*	8.48263	.000	-61.3132	-28.0053
		5	-72.84515*	7.49981	.000	-87.5695	-58.1208
		7	-34.67876*	3.21909	.000	-40.9988	-28.3587
		8	-76.25497*	2.81076	.000	-81.7733	-70.7366
	7	1	10.99351	7.13039	.124	-3.0056	24.9926
		2	1.72588	9.16853	.851	-16.2747	19.7265
		3	1.52987	14.90403	.918	-27.7312	30.7910
		4	-9.98050	8.48080	.240	-26.6309	6.6699
		5	-38.16639*	7.49775	.000	-52.8867	-23.4460
		6	34.67876*	3.21909	.000	28.3587	40.9988
		8	-41.57620*	2.80525	.000	-47.0838	-36.0687
	8	1	52.56972*	6.95559	.000	38.9138	66.2256
		2	43.30208*	9.03325	.000	25.5671	61.0371
		3	43.10608*	14.82119	.004	14.0076	72.2045
		4	31.59571*	8.33438	.000	15.2328	47.9586
		5	3.40982	7.33171	.642	-10.9845	17.8042
		6	76.25497*	2.81076	.000	70.7366	81.7733
		7	41.57620*	2.80525	.000	36.0687	47.0838

Table C-13 BRAZ

Dependent Variable	(I) LFeat	(J) LFeat	Mean Difference (I-J)	Std. Error	Sig.	95% Confidence Interval	
						Lower Bound	Upper Bound
dTEC	1	2	-18.59113	10.91680	.089	-40.0243	2.8420
		3	-28.72131	15.85131	.070	-59.8424	2.3998
		4	-30.47152*	10.37133	.003	-50.8337	-10.1093
		5	-28.94242*	9.61962	.003	-47.8288	-10.0561
		6	9.60233	6.97637	.169	-4.0945	23.2991
		7	-3.72794	6.97425	.593	-17.4206	9.9647
		8	-2.63466	6.80507	.699	-15.9952	10.7258
	2	1	18.59113	10.91680	.089	-2.8420	40.0243
		3	-10.13018	16.82392	.547	-43.1608	22.9005
		4	-11.88039	11.80445	.315	-35.0562	11.2955
		5	-10.35129	11.14978	.354	-32.2418	11.5392
		6	28.19346*	8.96940	.002	10.5837	45.8032
		7	14.86319	8.96775	.098	-2.7433	32.4697
		8	15.95647	8.83682	.071	-1.3930	33.3059
	3	1	28.72131	15.85131	.070	-2.3998	59.8424
		2	10.13018	16.82392	.547	-22.9005	43.1608
		4	-1.75021	16.47520	.915	-34.0962	30.5958
		5	-.22112	16.01265	.989	-31.6590	31.2168
		6	38.32364*	14.57867	.009	9.7011	66.9462
		7	24.99337	14.57765	.087	-3.6272	53.6139
		8	26.08665	14.49747	.072	-2.3765	54.5498
	4	1	30.47152*	10.37133	.003	10.1093	50.8337
		2	11.88039	11.80445	.315	-11.2955	35.0562
		3	1.75021	16.47520	.915	-30.5958	34.0962
		5	1.52909	10.61628	.886	-19.3140	22.3722
		6	40.07385*	8.29687	.000	23.7845	56.3632
		7	26.74358*	8.29509	.001	10.4577	43.0295
		8	27.83686*	8.15336	.001	11.8292	43.8445
	5	1	28.94242*	9.61962	.003	10.0561	47.8288
		2	10.35129	11.14978	.354	-11.5392	32.2418
		3	.22112	16.01265	.989	-31.2168	31.6590
		4	-1.52909	10.61628	.886	-22.3722	19.3140
		6	38.54475*	7.33558	.000	24.1427	52.9468
		7	25.21448*	7.33356	.001	10.8164	39.6126
		8	26.30777*	7.17286	.000	12.2252	40.3904
	6	1	-9.60233	6.97637	.169	-23.2991	4.0945
		2	-28.19346*	8.96940	.002	-45.8032	-10.5837
		3	-38.32364*	14.57867	.009	-66.9462	-9.7011
		4	-40.07385*	8.29687	.000	-56.3632	-23.7845
		5	-38.54475*	7.33558	.000	-52.9468	-24.1427
		7	-13.33027*	3.14860	.000	-19.5120	-7.1486
		8	-12.23699*	2.75364	.000	-17.6432	-6.8307
	7	1	3.72794	6.97425	.593	-9.9647	17.4206
		2	-14.86319	8.96775	.098	-32.4697	2.7433
		3	-24.99337	14.57765	.087	-53.6139	3.6272
		4	-26.74358*	8.29509	.001	-43.0295	-10.4577
		5	-25.21448*	7.33356	.001	-39.6126	-10.8164
		6	13.33027*	3.14860	.000	7.1486	19.5120
		8	1.09328	2.74826	.691	-4.3024	6.4890
	8	1	2.63466	6.80507	.699	-10.7258	15.9952
		2	-15.95647	8.83682	.071	-33.3059	1.3930
		3	-26.08665	14.49747	.072	-54.5498	2.3765
		4	-27.83686*	8.15336	.001	-43.8445	-11.8292
		5	-26.30777*	7.17286	.000	-40.3904	-12.2252
		6	12.23699*	2.75364	.000	6.8307	17.6432
		7	-1.09328	2.74826	.691	-6.4890	4.3024

Table C-14 COYQ

Dependent Variable	(I) LFeat	(J) LFeat	Mean Difference (I-J)	Std. Error	Sig.	95% Confidence Interval	
						Lower Bound	Upper Bound
dTEC	1	2	-.57752	16.78325	.973	-33.5281	32.3731
		3	1.06051	24.36945	.965	-46.7841	48.9051
		4	-8.42200	15.94465	.598	-39.7262	22.8822
		5	-.76037	14.78899	.959	-29.7956	28.2749
		6	-66.29252*	10.72531	.000	-87.3496	-45.2355
		7	-12.62783	10.72531	.239	-33.6849	8.4292
		8	-1.37761	10.45830	.895	-21.9104	19.1552
	2	1	.57752	16.78325	.973	-32.3731	33.5281
		3	1.63802	25.86473	.950	-49.1422	52.4183
		4	-7.84449	18.14789	.666	-43.4743	27.7853
		5	-.18286	17.14142	.991	-33.8366	33.4709
		6	-65.71501*	13.78936	.000	-92.7877	-38.6423
		7	-12.05031	13.78936	.382	-39.1230	15.0224
		8	-.80009	13.58271	.953	-27.4670	25.8669
	3	1	-1.06051	24.36945	.965	-48.9051	46.7841
		2	-1.63802	25.86473	.950	-52.4183	49.1422
		4	-9.48251	25.32861	.708	-59.2102	40.2452
		5	-1.82088	24.61749	.941	-50.1524	46.5107
		6	-67.35303*	22.41292	.003	-111.3563	-23.3497
		7	-13.68834	22.41292	.542	-57.6917	30.3150
		8	-2.43812	22.28638	.913	-46.1930	41.3168
	4	1	8.42200	15.94465	.598	-22.8822	39.7262
		2	7.84449	18.14789	.666	-27.7853	43.4743
		3	9.48251	25.32861	.708	-40.2452	59.2102
		5	7.66163	16.32124	.639	-24.3819	39.7051
		6	-57.87052*	12.75543	.000	-82.9133	-32.8278
		7	-4.20583	12.75543	.742	-29.2486	20.8369
		8	7.04439	12.53174	.574	-17.5592	31.6480
	5	1	.76037	14.78899	.959	-28.2749	29.7956
		2	.18286	17.14142	.991	-33.4709	33.8366
		3	1.82088	24.61749	.941	-46.5107	50.1524
		4	-7.66163	16.32124	.639	-39.7051	24.3819
		6	-65.53215*	11.27755	.000	-87.6734	-43.3909
		7	-11.86746	11.27755	.293	-34.0087	10.2738
		8	-.61724	11.02392	.955	-22.2605	21.0260
	6	1	66.29252*	10.72531	.000	45.2355	87.3496
		2	65.71501*	13.78936	.000	38.6423	92.7877
		3	67.35303*	22.41292	.003	23.3497	111.3563
		4	57.87052*	12.75543	.000	32.8278	82.9133
		5	65.53215*	11.27755	.000	43.3909	87.6734
		7	53.66469*	4.84781	.000	44.1470	63.1824
		8	64.91491*	4.22432	.000	56.6213	73.2085
	7	1	12.62783	10.72531	.239	-8.4292	33.6849
		2	12.05031	13.78936	.382	-15.0224	39.1230
		3	13.68834	22.41292	.542	-30.3150	57.6917
		4	4.20583	12.75543	.742	-20.8369	29.2486
		5	11.86746	11.27755	.293	-10.2738	34.0087
		6	-53.66469*	4.84781	.000	-63.1824	-44.1470
		8	11.25022*	4.22432	.008	2.9566	19.5438
	8	1	1.37761	10.45830	.895	-19.1552	21.9104
		2	.80009	13.58271	.953	-25.8669	27.4670
		3	2.43812	22.28638	.913	-41.3168	46.1930
		4	-7.04439	12.53174	.574	-31.6480	17.5592
		5	.61724	11.02392	.955	-21.0260	22.2605
		6	-64.91491*	4.22432	.000	-73.2085	-56.6213
		7	-11.25022*	4.22432	.008	-19.5438	-2.9566

Table C-15 IQQE

Dependent Variable	(I) LFeat	(J) LFeat	Mean Difference (I-J)	Std. Error	Sig.	95% Confidence Interval	
						Lower Bound	Upper Bound
dTEC	1	2	-7.76507	12.93843	.549	-33.1671	17.6370
		3	-5.51362	18.78673	.769	-42.3976	31.3704
		4	-35.03779*	12.29194	.004	-59.1706	-10.9050
		5	-37.33324*	11.40103	.001	-59.7169	-14.9496
		6	-31.78476*	8.26828	.000	-48.0179	-15.5516
		7	16.76453*	8.26577	.043	.5363	32.9927
		8	25.15546*	8.06314	.002	9.3251	40.9858
	2	1	7.76507	12.93843	.549	-17.6370	33.1671
		3	2.25146	19.93945	.910	-36.8957	41.3986
		4	-27.27272	13.99045	.052	-54.7402	.1947
		5	-29.56817*	13.21454	.026	-55.5123	-3.6240
		6	-24.01968*	10.63039	.024	-44.8904	-3.1490
		7	24.52960*	10.62844	.021	3.6628	45.3964
		8	32.92054*	10.47163	.002	12.3616	53.4795
	3	1	5.51362	18.78673	.769	-31.3704	42.3976
		2	-2.25146	19.93945	.910	-41.3986	36.8957
		4	-29.52417	19.52616	.131	-67.8599	8.8116
		5	-31.81962	18.97794	.094	-69.0790	5.4398
		6	-26.27114	17.27841	.129	-60.1939	7.6516
		7	22.27814	17.27721	.198	-11.6422	56.1985
		8	30.66908	17.18119	.075	-3.0628	64.4009
	4	1	35.03779*	12.29194	.004	10.9050	59.1706
		2	27.27272	13.99045	.052	-.1947	54.7402
		3	29.52417	19.52616	.131	-8.8116	67.8599
		5	-2.29545	12.58225	.855	-26.9982	22.4073
		6	3.25303	9.83332	.741	-16.0527	22.5588
		7	51.80232*	9.83121	.000	32.5007	71.1039
		8	60.19325*	9.66147	.000	41.2249	79.1616
	5	1	37.33324*	11.40103	.001	14.9496	59.7169
		2	29.56817*	13.21454	.026	3.6240	55.5123
		3	31.81962	18.97794	.094	-5.4398	69.0790
		4	2.29545	12.58225	.855	-22.4073	26.9982
		6	5.54849	8.69401	.524	-11.5205	22.6175
		7	54.09777*	8.69162	.000	37.0335	71.1620
		8	62.48871*	8.49915	.000	45.8023	79.1751
	6	1	31.78476*	8.26828	.000	15.5516	48.0179
		2	24.01968*	10.63039	.024	3.1490	44.8904
		3	26.27114	17.27841	.129	-7.6516	60.1939
		4	-3.25303	9.83332	.741	-22.5588	16.0527
		5	-5.54849	8.69401	.524	-22.6175	11.5205
		7	48.54928*	3.73167	.000	41.2229	55.8757
		8	56.94022*	3.25832	.000	50.5432	63.3373
	7	1	-16.76453*	8.26577	.043	-32.9927	-.5363
		2	-24.52960*	10.62844	.021	-45.3964	-3.6628
		3	-22.27814	17.27721	.198	-56.1985	11.6422
		4	-51.80232*	9.83121	.000	-71.1039	-32.5007
		5	-54.09777*	8.69162	.000	-71.1620	-37.0335
		6	-48.54928*	3.73167	.000	-55.8757	-41.2229
		8	8.39094*	3.25193	.010	2.0064	14.7755
	8	1	-25.15546*	8.06314	.002	-40.9858	-9.3251
		2	-32.92054*	10.47163	.002	-53.4795	-12.3616
		3	-30.66908	17.18119	.075	-64.4009	3.0628
		4	-60.19325*	9.66147	.000	-79.1616	-41.2249
		5	-62.48871*	8.49915	.000	-79.1751	-45.8023
		6	-56.94022*	3.25832	.000	-63.3373	-50.5432
		7	-8.39094*	3.25193	.010	-14.7755	-2.0064

Table C-16 LAMT

Dependent Variable	(I) LFeat	(J) LFeat	Mean Difference (I-J)	Std. Error	Sig.	95% Confidence Interval	
						Lower Bound	Upper Bound
dTEC	1	2	9.02963	10.70057	.399	-11.9788	30.0381
		3	4.34232	15.53734	.780	-26.1622	34.8468
		4	-2.75873	10.16591	.786	-22.7175	17.2000
		5	-8.20102	9.42908	.385	-26.7132	10.3111
		6	-7.15092	6.83819	.296	-20.5763	6.2745
		7	-4.34409	6.83611	.525	-17.7654	9.0773
		8	-51.31996*	6.66852	.000	-64.4123	-38.2276
	2	1	-9.02963	10.70057	.399	-30.0381	11.9788
		3	-4.68731	16.49069	.776	-37.0635	27.6889
		4	-11.78836	11.57063	.309	-34.5050	10.9283
		5	-17.23065	10.92893	.115	-38.6874	4.2261
		6	-16.18055	8.79174	.066	-33.4414	1.0803
		7	-13.37372	8.79013	.129	-30.6314	3.8839
		8	-60.34959*	8.66044	.000	-77.3526	-43.3465
	3	1	-4.34232	15.53734	.780	-34.8468	26.1622
		2	4.68731	16.49069	.776	-27.6889	37.0635
		4	-7.10105	16.14888	.660	-38.8062	24.6041
		5	-12.54334	15.69548	.424	-43.3583	18.2716
		6	-11.49324	14.28991	.421	-39.5486	16.5622
		7	-8.68641	14.28891	.543	-36.7398	19.3670
		8	-55.66228*	14.20950	.000	-83.5598	-27.7648
	4	1	2.75873	10.16591	.786	-17.2000	22.7175
		2	11.78836	11.57063	.309	-10.9283	34.5050
		3	7.10105	16.14888	.660	-24.6041	38.8062
		5	-5.44229	10.40600	.601	-25.8724	14.9878
		6	-4.39219	8.13253	.589	-20.3588	11.5744
		7	-1.58536	8.13079	.845	-17.5485	14.3778
		8	-48.56123*	7.99040	.000	-64.2488	-32.8737
	5	1	8.20102	9.42908	.385	-10.3111	26.7132
		2	17.23065	10.92893	.115	-4.2261	38.6874
		3	12.54334	15.69548	.424	-18.2716	43.3583
		4	5.44229	10.40600	.601	-14.9878	25.8724
		6	1.05010	7.19028	.884	-13.0666	15.1668
		7	3.85693	7.18830	.592	-10.2559	17.9697
		8	-43.11894*	7.02912	.000	-56.9192	-29.3187
	6	1	7.15092	6.83819	.296	-6.2745	20.5763
		2	16.18055	8.79174	.066	-1.0803	33.4414
		3	11.49324	14.28991	.421	-16.5622	39.5486
		4	4.39219	8.13253	.589	-11.5744	20.3588
		5	-1.05010	7.19028	.884	-15.1668	13.0666
		7	2.80683	3.08624	.363	-3.2524	8.8660
		8	-44.16904*	2.69475	.000	-49.4596	-38.8784
	7	1	4.34409	6.83611	.525	-9.0773	17.7654
		2	13.37372	8.79013	.129	-3.8839	30.6314
		3	8.68641	14.28891	.543	-19.3670	36.7398
		4	1.58536	8.13079	.845	-14.3778	17.5485
		5	-3.85693	7.18830	.592	-17.9697	10.2559
		6	-2.80683	3.08624	.363	-8.8660	3.2524
		8	-46.97587*	2.68947	.000	-52.2561	-41.6956
	8	1	51.31996*	6.66852	.000	38.2276	64.4123
		2	60.34959*	8.66044	.000	43.3465	77.3526
		3	55.66228*	14.20950	.000	27.7648	83.5598
		4	48.56123*	7.99040	.000	32.8737	64.2488
		5	43.11894*	7.02912	.000	29.3187	56.9192
		6	44.16904*	2.69475	.000	38.8784	49.4596
		7	46.97587*	2.68947	.000	41.6956	52.2561

Table C-17 PARC

Dependent Variable	(I) LFeat	(J) LFeat	Mean Difference (I-J)	Std. Error	Sig.	95% Confidence Interval	
						Lower Bound	Upper Bound
dTEC	1	2	-.21545	17.07389	.990	-33.7366	33.3057
		3	-5.16364	24.79146	.835	-53.8367	43.5095
		4	-14.64747	16.22077	.367	-46.4937	17.1988
		5	-1.87097	15.04510	.901	-31.4090	27.6671
		6	-68.77667*	10.91105	.000	-90.1983	-47.3550
		7	-82.83977*	10.90773	.000	-104.2549	-61.4246
		8	-19.66195	10.64033	.065	-40.5521	1.2282
	2	1	.21545	17.07389	.990	-33.3057	33.7366
		3	-4.94819	26.31263	.851	-56.6078	46.7114
		4	-14.43202	18.46216	.435	-50.6788	21.8148
		5	-1.65551	17.43826	.924	-35.8921	32.5811
		6	-68.56122*	14.02815	.000	-96.1027	-41.0197
		7	-82.62432*	14.02557	.000	-110.1607	-55.0879
		8	-19.44650	13.81864	.160	-46.5766	7.6836
	3	1	5.16364	24.79146	.835	-43.5095	53.8367
		2	4.94819	26.31263	.851	-46.7114	56.6078
		4	-9.48383	25.76723	.713	-60.0727	41.1050
		5	3.29268	25.04380	.895	-45.8758	52.4612
		6	-63.61303*	22.80105	.005	-108.3784	-18.8477
		7	-77.67613*	22.79946	.001	-122.4383	-32.9139
		8	-14.49831	22.67275	.523	-59.0117	30.0151
	4	1	14.64747	16.22077	.367	-17.1988	46.4937
		2	14.43202	18.46216	.435	-21.8148	50.6788
		3	9.48383	25.76723	.713	-41.1050	60.0727
		5	12.77651	16.60388	.442	-19.8219	45.3749
		6	-54.12920*	12.97631	.000	-79.6056	-28.6528
		7	-68.19230*	12.97352	.000	-93.6632	-42.7214
		8	-5.01448	12.74953	.694	-30.0456	20.0167
	5	1	1.87097	15.04510	.901	-27.6671	31.4090
		2	1.65551	17.43826	.924	-32.5811	35.8921
		3	-3.29268	25.04380	.895	-52.4612	45.8758
		4	-12.77651	16.60388	.442	-45.3749	19.8219
		6	-66.90570*	11.47285	.000	-89.4304	-44.3810
		7	-80.96880*	11.46969	.000	-103.4873	-58.4503
		8	-17.79099	11.21570	.113	-39.8108	4.2288
	6	1	68.77667*	10.91105	.000	47.3550	90.1983
		2	68.56122*	14.02815	.000	41.0197	96.1027
		3	63.61303*	22.80105	.005	18.8477	108.3784
		4	54.12920*	12.97631	.000	28.6528	79.6056
		5	66.90570*	11.47285	.000	44.3810	89.4304
		7	-14.06310*	4.92441	.004	-23.7312	-4.3950
		8	49.11472*	4.29976	.000	40.6730	57.5564
	7	1	82.83977*	10.90773	.000	61.4246	104.2549
		2	82.62432*	14.02557	.000	55.0879	110.1607
		3	77.67613*	22.79946	.001	32.9139	122.4383
		4	68.19230*	12.97352	.000	42.7214	93.6632
		5	80.96880*	11.46969	.000	58.4503	103.4873
		6	14.06310*	4.92441	.004	4.3950	23.7312
		8	63.17782*	4.29133	.000	54.7526	71.6030
	8	1	19.66195	10.64033	.065	-1.2282	40.5521
		2	19.44650	13.81864	.160	-7.6836	46.5766
		3	14.49831	22.67275	.523	-30.0151	59.0117
		4	5.01448	12.74953	.694	-20.0167	30.0456
		5	17.79099	11.21570	.113	-4.2288	39.8108
		6	-49.11472*	4.29976	.000	-57.5564	-40.6730
		7	-63.17782*	4.29133	.000	-71.6030	-54.7526

Table C-18 SCH2

Dependent Variable	(I) LFeat	(J) LFeat	Mean Difference (I-J)	Std. Error	Sig.	95% Confidence Interval	
						Lower Bound	Upper Bound
dTEC	1	2	-2.65178	16.32958	.871	-34.7117	29.4081
		3	-42.35295	23.71071	.074	-88.9042	4.1983
		4	-53.83927*	15.51365	.001	-84.2972	-23.3813
		5	-133.61838*	14.38923	.000	-161.8688	-105.3680
		6	-15.99110	10.43540	.126	-36.4789	4.4967
		7	-6.26253	10.43222	.548	-26.7441	14.2191
		8	-2.31785	10.17648	.820	-22.2973	17.6617
	2	1	2.65178	16.32958	.871	-29.4081	34.7117
		3	-39.70118	25.16557	.115	-89.1088	9.7064
		4	-51.18750*	17.65733	.004	-85.8542	-16.5208
		5	-130.96660*	16.67807	.000	-163.7107	-98.2225
		6	-13.33932	13.41661	.320	-39.6802	13.0015
		7	-3.61075	13.41415	.788	-29.9468	22.7253
		8	.33393	13.21623	.980	-25.6135	26.2814
	3	1	42.35295	23.71071	.074	-4.1983	88.9042
		2	39.70118	25.16557	.115	-9.7064	89.1088
		4	-11.48632	24.64395	.641	-59.8698	36.8972
		5	-91.26542*	23.95205	.000	-138.2905	-44.2403
		6	26.36185	21.80707	.227	-16.4520	69.1757
		7	36.09042	21.80555	.098	-6.7204	78.9013
		8	40.03511	21.68436	.065	-2.5378	82.6080
	4	1	53.83927*	15.51365	.001	23.3813	84.2972
		2	51.18750*	17.65733	.004	16.5208	85.8542
		3	11.48632	24.64395	.641	-36.8972	59.8698
		5	-79.77910*	15.88006	.000	-110.9564	-48.6018
		6	37.84817*	12.41063	.002	13.4824	62.2140
		7	47.57674*	12.40796	.000	23.2162	71.9373
		8	51.52143*	12.19373	.000	27.5815	75.4614
	5	1	133.61838*	14.38923	.000	105.3680	161.8688
		2	130.96660*	16.67807	.000	98.2225	163.7107
		3	91.26542*	23.95205	.000	44.2403	138.2905
		4	79.77910*	15.88006	.000	48.6018	110.9564
		6	117.62728*	10.97271	.000	96.0845	139.1700
		7	127.35585*	10.96969	.000	105.8190	148.8927
		8	131.30053*	10.72677	.000	110.2407	152.3604
	6	1	15.99110	10.43540	.126	-4.4967	36.4789
		2	13.33932	13.41661	.320	-13.0015	39.6802
		3	-26.36185	21.80707	.227	-69.1757	16.4520
		4	-37.84817*	12.41063	.002	-62.2140	-13.4824
		5	-117.62728*	10.97271	.000	-139.1700	-96.0845
		7	9.72857*	4.70974	.039	.4819	18.9752
		8	13.67325*	4.11232	.001	5.5995	21.7470
	7	1	6.26253	10.43222	.548	-14.2191	26.7441
		2	3.61075	13.41415	.788	-22.7253	29.9468
		3	-36.09042	21.80555	.098	-78.9013	6.7204
		4	-47.57674*	12.40796	.000	-71.9373	-23.2162
		5	-127.35585*	10.96969	.000	-148.8927	-105.8190
		6	-9.72857*	4.70974	.039	-18.9752	-.4819
		8	3.94468	4.10426	.337	-4.1132	12.0026
	8	1	2.31785	10.17648	.820	-17.6617	22.2973
		2	-.33393	13.21623	.980	-26.2814	25.6135
		3	-40.03511	21.68436	.065	-82.6080	2.5378
		4	-51.52143*	12.19373	.000	-75.4614	-27.5815
		5	-131.30053*	10.72677	.000	-152.3604	-110.2407
		6	-13.67325*	4.11232	.001	-21.7470	-5.5995
		7	-3.94468	4.10426	.337	-12.0026	4.1132

Table C-19 SCUB

Dependent Variable	(I) LFeat	(J) LFeat	Mean Difference (I-J)	Std. Error	Sig.	95% Confidence Interval	
						Lower Bound	Upper Bound
dTEC	1	2	11.38969	12.25035	.353	-12.6628	35.4422
		3	13.64195	17.78763	.443	-21.2825	48.5664
		4	11.50654	11.63824	.323	-11.3441	34.3572
		5	-.33424	10.79471	.975	-21.5287	20.8602
		6	26.86002*	7.82857	.001	11.4893	42.2307
		7	-24.71000*	7.82619	.002	-40.0760	-9.3440
		8	-20.55360*	7.65078	.007	-35.5752	-5.5320
	2	1	-11.38969	12.25035	.353	-35.4422	12.6628
		3	2.25226	18.87905	.905	-34.8151	39.3196
		4	.11685	13.24642	.993	-25.8913	26.1250
		5	-11.72393	12.51178	.349	-36.2897	12.8419
		6	15.47034	10.06506	.125	-4.2915	35.2322
		7	-36.09969*	10.06321	.000	-55.8579	-16.3415
		8	-31.94329*	9.92740	.001	-51.4349	-12.4517
	3	1	-13.64195	17.78763	.443	-48.5664	21.2825
		2	-2.25226	18.87905	.905	-39.3196	34.8151
		4	-2.13541	18.48773	.908	-38.4345	34.1637
		5	-13.97619	17.96868	.437	-49.2561	21.3037
		6	13.21808	16.35953	.419	-18.9024	45.3386
		7	-38.35195*	16.35839	.019	-70.4702	-6.2337
		8	-34.19555*	16.27520	.036	-66.1505	-2.2406
	4	1	-11.50654	11.63824	.323	-34.3572	11.3441
		2	-.11685	13.24642	.993	-26.1250	25.8913
		3	2.13541	18.48773	.908	-34.1637	38.4345
		5	-11.84078	11.91312	.321	-35.2311	11.5496
		6	15.35348	9.31038	.100	-2.9266	33.6336
		7	-36.21655*	9.30838	.000	-54.4927	-17.9404
		8	-32.06014*	9.16139	.000	-50.0477	-14.0726
	5	1	.33424	10.79471	.975	-20.8602	21.5287
		2	11.72393	12.51178	.349	-12.8419	36.2897
		3	13.97619	17.96868	.437	-21.3037	49.2561
		4	11.84078	11.91312	.321	-11.5496	35.2311
		6	27.19426*	8.23165	.001	11.0321	43.3564
		7	-24.37577*	8.22939	.003	-40.5335	-8.2181
		8	-20.21936*	8.06276	.012	-36.0499	-4.3888
	6	1	-26.86002*	7.82857	.001	-42.2307	-11.4893
		2	-15.47034	10.06506	.125	-35.2322	4.2915
		3	-13.21808	16.35953	.419	-45.3386	18.9024
		4	-15.35348	9.31038	.100	-33.6336	2.9266
		5	-27.19426*	8.23165	.001	-43.3564	-11.0321
		7	-51.57003*	3.53322	.000	-58.5072	-44.6329
		8	-47.41362*	3.12551	.000	-53.5503	-41.2770
	7	1	24.71000*	7.82619	.002	9.3440	40.0760
		2	36.09969*	10.06321	.000	16.3415	55.8579
		3	38.35195*	16.35839	.019	6.2337	70.4702
		4	36.21655*	9.30838	.000	17.9404	54.4927
		5	24.37577*	8.22939	.003	8.2181	40.5335
		6	51.57003*	3.53322	.000	44.6329	58.5072
		8	4.15640	3.11954	.183	-1.9685	10.2814
	8	1	20.55360*	7.65078	.007	5.5320	35.5752
		2	31.94329*	9.92740	.001	12.4517	51.4349
		3	34.19555*	16.27520	.036	2.2406	66.1505
		4	32.06014*	9.16139	.000	14.0726	50.0477
		5	20.21936*	8.06276	.012	4.3888	36.0499
		6	47.41362*	3.12551	.000	41.2770	53.5503
		7	-4.15640	3.11954	.183	-10.2814	1.9685

Table C-20 SG05

Dependent ariable	(I) LFeat	(J) LFeat	Mean Difference (I-J)	Std. Error	Sig.	95% Confidence Interval	
						Lower Bound	Upper Bound
dTEC	1	2	8.56433	13.15840	.515	-17.2696	34.3982
		3	7.55189	19.10613	.693	-29.9592	45.0630
		4	-.06125	12.50093	.996	-24.6043	24.4818
		5	-1.20323	11.59486	.917	-23.9674	21.5610
		6	20.62253*	8.40886	.014	4.1134	37.1316
		7	-29.60106*	8.40630	.000	-46.1052	-13.0970
		8	-28.76775*	8.20023	.000	-44.8673	-12.6682
	2	1	-8.56433	13.15840	.515	-34.3982	17.2696
		3	-1.01243	20.27846	.960	-40.8252	38.8003
		4	-8.62557	14.22831	.545	-36.5600	19.3089
		5	-9.76756	13.43921	.468	-36.1528	16.6177
		6	12.05820	10.81113	.265	-9.1673	33.2837
		7	-38.16539*	10.80914	.000	-59.3870	-16.9438
		8	-37.33208*	10.64966	.000	-58.2406	-16.4236
	3	1	-7.55189	19.10613	.693	-45.0630	29.9592
		2	1.01243	20.27846	.960	-38.8003	40.8252
		4	-7.61314	19.85813	.702	-46.6006	31.3744
		5	-8.75512	19.30060	.650	-46.6480	29.1378
		6	13.07063	17.57217	.457	-21.4288	47.5701
		7	-37.15295*	17.57095	.035	-71.6500	-2.6559
		8	-36.31965*	17.47330	.038	-70.6250	-2.0143
	4	1	.06125	12.50093	.996	-24.4818	24.6043
		2	8.62557	14.22831	.545	-19.3089	36.5600
		3	7.61314	19.85813	.702	-31.3744	46.6006
		5	-1.14198	12.79617	.929	-26.2647	23.9808
		6	20.68377*	10.00051	.039	1.0498	40.3178
		7	-29.53981*	9.99836	.003	-49.1696	-9.9100
		8	-28.70651*	9.82573	.004	-47.9974	-9.4156
	5	1	1.20323	11.59486	.917	-21.5610	23.9674
		2	9.76756	13.43921	.468	-16.6177	36.1528
		3	8.75512	19.30060	.650	-29.1378	46.6480
		4	1.14198	12.79617	.929	-23.9808	26.2647
		6	21.82575*	8.84182	.014	4.4666	39.1849
		7	-28.39783*	8.83939	.001	-45.7522	-11.0434
		8	-27.56452*	8.64365	.001	-44.5346	-10.5944
	6	1	-20.62253*	8.40886	.014	-37.1316	-4.1134
		2	-12.05820	10.81113	.265	-33.2837	9.1673
		3	-13.07063	17.57217	.457	-47.5701	21.4288
		4	-20.68377*	10.00051	.039	-40.3178	-1.0498
		5	-21.82575*	8.84182	.014	-39.1849	-4.4666
		7	-50.22358*	3.79512	.000	-57.6745	-42.7726
		8	-49.39028*	3.31371	.000	-55.8961	-42.8845
	7	1	29.60106*	8.40630	.000	13.0970	46.1052
		2	38.16539*	10.80914	.000	16.9438	59.3870
		3	37.15295*	17.57095	.035	2.6559	71.6500
		4	29.53981*	9.99836	.003	9.9100	49.1696
		5	28.39783*	8.83939	.001	11.0434	45.7522
		6	50.22358*	3.79512	.000	42.7726	57.6745
		8	.83331	3.30722	.801	-5.6598	7.3264
	8	1	28.76775*	8.20023	.000	12.6682	44.8673
		2	37.33208*	10.64966	.000	16.4236	58.2406
		3	36.31965*	17.47330	.038	2.0143	70.6250
		4	28.70651*	9.82573	.004	9.4156	47.9974
		5	27.56452*	8.64365	.001	10.5944	44.5346
		6	49.39028*	3.31371	.000	42.8845	55.8961
		7	-.83331	3.30722	.801	-7.3264	5.6598

CONO and UNSA station Lack of data

Event III Mean percentage deviation of TECU for each phenomena of Event I from IGS stations.

Table C-21 BAIE

Dependent Variable	(I) LFeat	(J) LFeat	Mean Difference (I-J)	Std. Error	Sig.	95% Confidence Interval	
						Lower Bound	Upper Bound
dTEC	1	2	-3.09340	6.01359	.607	-14.8999	8.7131
		3	-3.55558	3.44933	.303	-10.3276	3.2165
		4	-9.11961	12.92607	.481	-34.4973	16.2581
		5	2.09725	2.67972	.434	-3.1638	7.3583
		6	35.91209*	2.42150	.000	31.1580	40.6662
		7	32.43470*	2.52102	.000	27.4852	37.3842
	2	1	3.09340	6.01359	.607	-8.7131	14.8999
		3	-.46218	6.41831	.943	-13.0632	12.1389
		4	-6.02621	14.01356	.667	-33.5390	21.4866
		5	5.19065	6.03968	.390	-6.6670	17.0483
		6	39.00549*	5.92962	.000	27.3639	50.6471
		7	35.52810*	5.97096	.000	23.8053	47.2509
	3	1	3.55558	3.44933	.303	-3.2165	10.3276
		2	.46218	6.41831	.943	-12.1389	13.0632
		4	-5.56402	13.11925	.672	-31.3210	20.1929
		5	5.65283	3.49462	.106	-1.2081	12.5138
		6	39.46767*	3.30077	.000	32.9873	45.9481
		7	35.99028*	3.37446	.000	29.3652	42.6153
	4	1	9.11961	12.92607	.481	-16.2581	34.4973
		2	6.02621	14.01356	.667	-21.4866	33.5390
		3	5.56402	13.11925	.672	-20.1929	31.3210
		5	11.21686	12.93822	.386	-14.1847	36.6184
		6	45.03170*	12.88722	.001	19.7303	70.3331
		7	41.55431*	12.90629	.001	16.2154	66.8932
	5	1	-2.09725	2.67972	.434	-7.3583	3.1638
		2	-5.19065	6.03968	.390	-17.0483	6.6670
		3	-5.65283	3.49462	.106	-12.5138	1.2081
		4	-11.21686	12.93822	.386	-36.6184	14.1847
		6	33.81484*	2.48559	.000	28.9349	38.6948
		7	30.33745*	2.58264	.000	25.2670	35.4079
	6	1	-35.91209*	2.42150	.000	-40.6662	-31.1580
		2	-39.00549*	5.92962	.000	-50.6471	-27.3639
		3	-39.46767*	3.30077	.000	-45.9481	-32.9873
		4	-45.03170*	12.88722	.001	-70.3331	-19.7303
		5	-33.81484*	2.48559	.000	-38.6948	-28.9349
		7	-3.47739	2.31360	.133	-8.0197	1.0649
	7	1	-32.43470*	2.52102	.000	-37.3842	-27.4852
		2	-35.52810*	5.97096	.000	-47.2509	-23.8053
		3	-35.99028*	3.37446	.000	-42.6153	-29.3652
		4	-41.55431*	12.90629	.001	-66.8932	-16.2154
		5	-30.33745*	2.58264	.000	-35.4079	-25.2670
		6	3.47739	2.31360	.133	-1.0649	8.0197

Table C-22 BOGT

Dependent Variable	(I) LFeat	(J) LFeat	Mean Difference (I-J)	Std. Error	Sig.	95% Confidence Interval	
						Lower Bound	Upper Bound
dTEC	1	2	-6.44627	7.24450	.374	-20.6694	7.7768
		3	-17.47623*	4.15537	.000	-25.6344	-9.3180
		4	-46.33765*	15.57188	.003	-76.9099	-15.7654
		5	-78.03776*	3.22823	.000	-84.3757	-71.6998
		6	-21.93062*	2.91715	.000	-27.6579	-16.2034
		7	-78.79373*	3.03704	.000	-84.7563	-72.8311
	2	1	6.44627	7.24450	.374	-7.7768	20.6694
		3	-11.02996	7.73206	.154	-26.2103	4.1504
		4	-39.89138*	16.88198	.018	-73.0357	-6.7471
		5	-71.59149*	7.27593	.000	-85.8763	-57.3067
		6	-15.48435*	7.14335	.031	-29.5089	-1.4598
		7	-72.34746*	7.19314	.000	-86.4697	-58.2252
	3	1	17.47623*	4.15537	.000	9.3180	25.6344
		2	11.02996	7.73206	.154	-4.1504	26.2103
		4	-28.86142	15.80460	.068	-59.8906	2.1677
		5	-60.56153*	4.20993	.000	-68.8269	-52.2962
		6	-4.45440	3.97640	.263	-12.2613	3.3525
		7	-61.31750*	4.06517	.000	-69.2986	-53.3364
	4	1	46.33765*	15.57188	.003	15.7654	76.9099
		2	39.89138*	16.88198	.018	6.7471	73.0357
		3	28.86142	15.80460	.068	-2.1677	59.8906
		5	-31.70011*	15.58653	.042	-62.3011	-1.0991
		6	24.40703	15.52508	.116	-6.0733	54.8874
		7	-32.45608*	15.54806	.037	-62.9815	-1.9306
	5	1	78.03776*	3.22823	.000	71.6998	84.3757
		2	71.59149*	7.27593	.000	57.3067	85.8763
		3	60.56153*	4.20993	.000	52.2962	68.8269
		4	31.70011*	15.58653	.042	1.0991	62.3011
		6	56.10713*	2.99436	.000	50.2283	61.9860
		7	-.75597	3.11128	.808	-6.8643	5.3524
	6	1	21.93062*	2.91715	.000	16.2034	27.6579
		2	15.48435*	7.14335	.031	1.4598	29.5089
		3	4.45440	3.97640	.263	-3.3525	12.2613
		4	-24.40703	15.52508	.116	-54.8874	6.0733
		5	-56.10713*	2.99436	.000	-61.9860	-50.2283
		7	-56.86311*	2.78717	.000	-62.3352	-51.3911
	7	1	78.79373*	3.03704	.000	72.8311	84.7563
		2	72.34746*	7.19314	.000	58.2252	86.4697
		3	61.31750*	4.06517	.000	53.3364	69.2986
		4	32.45608*	15.54806	.037	1.9306	62.9815
		5	.75597	3.11128	.808	-5.3524	6.8643
		6	56.86311*	2.78717	.000	51.3911	62.3352

Table C-23 LAMT

Dependent Variable	(I) LFeat	(J) LFeat	Mean Difference (I-J)	Std. Error	Sig.	95% Confidence Interval	
						Lower Bound	Upper Bound
dTEC	1	2	-9.72143	5.20765	.062	-19.9456	.5027
		3	-11.42445*	2.98705	.000	-17.2889	-5.5600
		4	-20.53585	11.19372	.067	-42.5125	1.4407
		5	7.74555*	2.32059	.001	3.1895	12.3016
		6	14.99294*	2.09697	.000	10.8760	19.1099
		7	14.66126*	2.18315	.000	10.3751	18.9474
	2	1	9.72143	5.20765	.062	-.5027	19.9456
		3	-1.70302	5.55813	.759	-12.6153	9.2092
		4	-10.81443	12.13547	.373	-34.6400	13.0111
		5	17.46697*	5.23024	.001	7.1985	27.7355
		6	24.71437*	5.13494	.000	14.6330	34.7958
		7	24.38269*	5.17073	.000	14.2310	34.5344
	3	1	11.42445*	2.98705	.000	5.5600	17.2889
		2	1.70302	5.55813	.759	-9.2092	12.6153
		4	-9.11141	11.36101	.423	-31.4164	13.1936
		5	19.17000*	3.02627	.000	13.2285	25.1115
		6	26.41739*	2.85840	.000	20.8055	32.0293
		7	26.08571*	2.92222	.000	20.3485	31.8229
	4	1	20.53585	11.19372	.067	-1.4407	42.5125
		2	10.81443	12.13547	.373	-13.0111	34.6400
		3	9.11141	11.36101	.423	-13.1936	31.4164
		5	28.28140*	11.20425	.012	6.2841	50.2787
		6	35.52880*	11.16008	.002	13.6182	57.4393
		7	35.19712*	11.17660	.002	13.2541	57.1401
	5	1	-7.74555*	2.32059	.001	-12.3016	-3.1895
		2	-17.46697*	5.23024	.001	-27.7355	-7.1985
		3	-19.17000*	3.02627	.000	-25.1115	-13.2285
		4	-28.28140*	11.20425	.012	-50.2787	-6.2841
		6	7.24740*	2.15247	.001	3.0215	11.4733
		7	6.91572*	2.23652	.002	2.5248	11.3067
	6	1	-14.99294*	2.09697	.000	-19.1099	-10.8760
		2	-24.71437*	5.13494	.000	-34.7958	-14.6330
		3	-26.41739*	2.85840	.000	-32.0293	-20.8055
		4	-35.52880*	11.16008	.002	-57.4393	-13.6182
		5	-7.24740*	2.15247	.001	-11.4733	-3.0215
		7	-.33168	2.00354	.869	-4.2652	3.6019
	7	1	-14.66126*	2.18315	.000	-18.9474	-10.3751
		2	-24.38269*	5.17073	.000	-34.5344	-14.2310
		3	-26.08571*	2.92222	.000	-31.8229	-20.3485
		4	-35.19712*	11.17660	.002	-57.1401	-13.2541
		5	-6.91572*	2.23652	.002	-11.3067	-2.5248
		6	.33168	2.00354	.869	-3.6019	4.2652

Table C-24 SCH2

Dependent Variable	(I) LFeat	(J) LFeat	Mean Difference (I-J)	Std. Error	Sig.	95% Confidence Interval	
						Lower Bound	Upper Bound
dTEC	1	2	11.93514	8.74433	.173	-5.2483	29.1186
		3	5.24411	7.23825	.469	-8.9798	19.4680
		6	21.86902*	3.99780	.000	14.0129	29.7251
		7	27.47753*	3.66580	.000	20.2739	34.6812
	2	1	-11.93514	8.74433	.173	-29.1186	5.2483
		3	-6.69103	10.69286	.532	-27.7036	14.3215
		6	9.93388	8.82764	.261	-7.4133	27.2811
		7	15.54239	8.68234	.074	-1.5193	32.6041
	3	1	-5.24411	7.23825	.469	-19.4680	8.9798
		2	6.69103	10.69286	.532	-14.3215	27.7036
		6	16.62491*	7.33869	.024	2.2037	31.0462
		7	22.23342*	7.16324	.002	8.1569	36.3099
	6	1	-21.86902*	3.99780	.000	-29.7251	-14.0129
		2	-9.93388	8.82764	.261	-27.2811	7.4133
		3	-16.62491*	7.33869	.024	-31.0462	-2.2037
		7	5.60851	3.86033	.147	-1.9774	13.1944
	7	1	-27.47753*	3.66580	.000	-34.6812	-20.2739
		2	-15.54239	8.68234	.074	-32.6041	1.5193
		3	-22.23342*	7.16324	.002	-36.3099	-8.1569
		6	-5.60851	3.86033	.147	-13.1944	1.9774

Table C-25 SCUB

Dependent Variable	(I) LFeat	(J) LFeat	Mean Difference (I-J)	Std. Error	Sig.	95% Confidence Interval	
						Lower Bound	Upper Bound
dTEC	1	2	10.34498	8.59836	.229	-6.5362	27.2261
		3	.57981	4.93193	.906	-9.1030	10.2627
		4	-18.40766	18.48199	.320	-54.6933	17.8780
		5	-67.41951*	3.83153	.000	-74.9419	-59.8971
		6	-14.97081*	3.46232	.000	-21.7684	-8.1733
		7	-15.79840*	3.60461	.000	-22.8753	-8.7215
	2	1	-10.34498	8.59836	.229	-27.2261	6.5362
		3	-9.76517	9.17704	.288	-27.7824	8.2521
		4	-28.75264	20.03692	.152	-68.0911	10.5858
		5	-77.76449*	8.63567	.000	-94.7189	-60.8101
		6	-25.31579*	8.47831	.003	-41.9612	-8.6703
		7	-26.14338*	8.53741	.002	-42.9049	-9.3819
	3	1	-.57981	4.93193	.906	-10.2627	9.1030
		2	9.76517	9.17704	.288	-8.2521	27.7824
		4	-18.98747	18.75820	.312	-55.8154	17.8404
		5	-67.99933*	4.99669	.000	-77.8093	-58.1893
		6	-15.55062*	4.71952	.001	-24.8164	-6.2848
		7	-16.37821*	4.82488	.001	-25.8509	-6.9055
	4	1	18.40766	18.48199	.320	-17.8780	54.6933
		2	28.75264	20.03692	.152	-10.5858	68.0911
		3	18.98747	18.75820	.312	-17.8404	55.8154
		5	-49.01185*	18.49938	.008	-85.3316	-12.6921
		6	3.43685	18.42645	.852	-32.7397	39.6134
		7	2.60926	18.45371	.888	-33.6209	38.8394
	5	1	67.41951*	3.83153	.000	59.8971	74.9419
		2	77.76449*	8.63567	.000	60.8101	94.7189
		3	67.99933*	4.99669	.000	58.1893	77.8093
		4	49.01185*	18.49938	.008	12.6921	85.3316
		6	52.44870*	3.55395	.000	45.4712	59.4262
		7	51.62111*	3.69272	.000	44.3712	58.8710
	6	1	14.97081*	3.46232	.000	8.1733	21.7684
		2	25.31579*	8.47831	.003	8.6703	41.9612
		3	15.55062*	4.71952	.001	6.2848	24.8164
		4	-3.43685	18.42645	.852	-39.6134	32.7397
		5	-52.44870*	3.55395	.000	-59.4262	-45.4712
		7	-.82759	3.30805	.803	-7.3223	5.6671
	7	1	15.79840*	3.60461	.000	8.7215	22.8753
		2	26.14338*	8.53741	.002	9.3819	42.9049
		3	16.37821*	4.82488	.001	6.9055	25.8509
		4	-2.60926	18.45371	.888	-38.8394	33.6209
		5	-51.62111*	3.69272	.000	-58.8710	-44.3712
		6	.82759	3.30805	.803	-5.6671	7.3223

Table C-26 SG05

Dependent Variable	(I) LFeat	(J) LFeat	Mean Difference (I-J)	Std. Error	Sig.	95% Confidence Interval	
						Lower Bound	Upper Bound
dTEC	1	2	19.79142*	8.15839	.016	3.7741	35.8088
		3	9.18799*	4.67957	.050	.0006	18.3754
		4	-.34415	17.53627	.984	-34.7731	34.0848
		5	-17.71818*	3.63548	.000	-24.8557	-10.5807
		6	20.68497*	3.28515	.000	14.2352	27.1347
		7	28.26183*	3.42017	.000	21.5470	34.9766
	2	1	-19.79142*	8.15839	.016	-35.8088	-3.7741
		3	-10.60343	8.70746	.224	-27.6988	6.4919
		4	-20.13557	19.01164	.290	-57.4611	17.1899
		5	-37.50960*	8.19379	.000	-53.5964	-21.4228
		6	.89355	8.04448	.912	-14.9002	16.6873
		7	8.47041	8.10056	.296	-7.4334	24.3742
	3	1	-9.18799*	4.67957	.050	-18.3754	-.0006
		2	10.60343	8.70746	.224	-6.4919	27.6988
		4	-9.53214	17.79835	.592	-44.4756	25.4113
		5	-26.90617*	4.74101	.000	-36.2142	-17.5982
		6	11.49698*	4.47803	.010	2.7053	20.2887
		7	19.07384*	4.57799	.000	10.0859	28.0618
	4	1	.34415	17.53627	.984	-34.0848	34.7731
		2	20.13557	19.01164	.290	-17.1899	57.4611
		3	9.53214	17.79835	.592	-25.4113	44.4756
		5	-17.37403	17.55277	.323	-51.8353	17.0873
		6	21.02913	17.48357	.229	-13.2963	55.3546
		7	28.60598	17.50944	.103	-5.7703	62.9822
	5	1	17.71818*	3.63548	.000	10.5807	24.8557
		2	37.50960*	8.19379	.000	21.4228	53.5964
		3	26.90617*	4.74101	.000	17.5982	36.2142
		4	17.37403	17.55277	.323	-17.0873	51.8353
		6	38.40315*	3.37210	.000	31.7827	45.0236
		7	45.98001*	3.50376	.000	39.1011	52.8589
	6	1	-20.68497*	3.28515	.000	-27.1347	-14.2352
		2	-.89355	8.04448	.912	-16.6873	14.9002
		3	-11.49698*	4.47803	.010	-20.2887	-2.7053
		4	-21.02913	17.48357	.229	-55.3546	13.2963
		5	-38.40315*	3.37210	.000	-45.0236	-31.7827
		7	7.57685*	3.13877	.016	1.4145	13.7392
	7	1	-28.26183*	3.42017	.000	-34.9766	-21.5470
		2	-8.47041	8.10056	.296	-24.3742	7.4334
		3	-19.07384*	4.57799	.000	-28.0618	-10.0859
		4	-28.60598	17.50944	.103	-62.9822	5.7703
		5	-45.98001*	3.50376	.000	-52.8589	-39.1011
		6	-7.57685*	3.13877	.016	-13.7392	-1.4145

Table C-27 UNSA

Dependent Variable	(I) LFeat	(J) LFeat	Mean Difference (I-J)	Std. Error	Sig.	95% Confidence Interval	
						Lower Bound	Upper Bound
dTEC	1	2	11.95338	9.33696	.201	-6.3786	30.2854
		3	15.09940*	5.35923	.005	4.5772	25.6216
		4	.31608	20.06432	.987	-39.0778	39.7099
		5	-45.89673*	4.16626	.000	-54.0767	-37.7168
		6	-32.93444*	3.76621	.000	-40.3289	-25.5399
		7	-83.63998*	4.01377	.000	-91.5205	-75.7594
	2	1	-11.95338	9.33696	.201	-30.2854	6.3786
		3	3.14602	9.96201	.752	-16.4132	22.7052
		4	-11.63730	21.75080	.593	-54.3424	31.0677
		5	-57.85011*	9.37433	.000	-76.2555	-39.4447
		6	-44.88783*	9.20352	.000	-62.9578	-26.8178
		7	-95.59336*	9.30756	.000	-113.8676	-77.3191
	3	1	-15.09940*	5.35923	.005	-25.6216	-4.5772
		2	-3.14602	9.96201	.752	-22.7052	16.4132
		4	-14.78332	20.36271	.468	-54.7630	25.1964
		5	-60.99613*	5.42409	.000	-71.6457	-50.3466
		6	-48.03384*	5.12321	.000	-58.0926	-37.9750
		7	-98.73938*	5.30786	.000	-109.1607	-88.3181
	4	1	-.31608	20.06432	.987	-39.7099	39.0778
		2	11.63730	21.75080	.593	-31.0677	54.3424
		3	14.78332	20.36271	.468	-25.1964	54.7630
		5	-46.21281*	20.08174	.022	-85.6409	-6.7848
		6	-33.25052	20.00257	.097	-72.5231	6.0221
		7	-83.95606*	20.05066	.000	-123.3231	-44.5890
	5	1	45.89673*	4.16626	.000	37.7168	54.0767
		2	57.85011*	9.37433	.000	39.4447	76.2555
		3	60.99613*	5.42409	.000	50.3466	71.6457
		4	46.21281*	20.08174	.022	6.7848	85.6409
		6	12.96229*	3.85795	.001	5.3877	20.5369
		7	-37.74325*	4.09997	.000	-45.7930	-29.6935
	6	1	32.93444*	3.76621	.000	25.5399	40.3289
		2	44.88783*	9.20352	.000	26.8178	62.9578
		3	48.03384*	5.12321	.000	37.9750	58.0926
		4	33.25052	20.00257	.097	-6.0221	72.5231
		5	-12.96229*	3.85795	.001	-20.5369	-5.3877
		7	-50.70554*	3.69275	.000	-57.9558	-43.4553
	7	1	83.63998*	4.01377	.000	75.7594	91.5205
		2	95.59336*	9.30756	.000	77.3191	113.8676
		3	98.73938*	5.30786	.000	88.3181	109.1607
		4	83.95606*	20.05066	.000	44.5890	123.3231
		5	37.74325*	4.09997	.000	29.6935	45.7930
		6	50.70554*	3.69275	.000	43.4553	57.9558

Event IV Mean percentage deviation of TECU for each phenomena of Event I from IGS stations.

Table C- 28 BAIE

Dependent Variable	(I) LFeat	(J) LFeat	Mean Difference (I-J)	Std. Error	Sig.	95% Confidence Interval	
						Lower Bound	Upper Bound
dTEC	1	2	-50.33465	53.94644	.351	-156.2478	55.5785
		3	-159.51961*	10.34017	.000	-179.8205	-139.2187
		4	-131.39617*	8.09382	.000	-147.2868	-115.5056
		5	-63.14179*	8.56470	.000	-79.9569	-46.3267
		6	-34.33214*	12.57772	.006	-59.0260	-9.6383
		7	-37.08460	34.45598	.282	-104.7321	30.5629
		8	-61.93242*	12.03761	.000	-85.5659	-38.2990
	2	1	50.33465	53.94644	.351	-55.5785	156.2478
		3	-109.18495*	54.22219	.044	-215.6394	-2.7305
		4	-81.06152	53.83899	.133	-186.7637	24.6406
		5	-12.80713	53.91178	.812	-118.6522	93.0379
		6	16.00252	54.69301	.770	-91.3763	123.3814
		7	13.25006	63.40616	.835	-111.2353	137.7355
		8	-11.59777	54.57133	.832	-118.7377	95.5422
	3	1	159.51961*	10.34017	.000	139.2187	179.8205
		2	109.18495*	54.22219	.044	2.7305	215.6394
		4	28.12343*	9.76408	.004	8.9536	47.2933
		5	96.37782*	10.15782	.000	76.4350	116.3207
		6	125.18747*	13.71226	.000	98.2662	152.1088
		7	122.43501*	34.88613	.000	53.9430	190.9270
		8	97.58718*	13.21860	.000	71.6351	123.5393
	4	1	131.39617*	8.09382	.000	115.5056	147.2868
		2	81.06152	53.83899	.133	-24.6406	186.7637
		3	-28.12343*	9.76408	.004	-47.2933	-8.9536
		5	68.25439*	7.85953	.000	52.8238	83.6850
		6	97.06404*	12.10855	.000	73.2913	120.8368
		7	94.31158*	34.28750	.006	26.9949	161.6283
		8	69.46375*	11.54653	.000	46.7944	92.1331
	5	1	63.14179*	8.56470	.000	46.3267	79.9569
		2	12.80713	53.91178	.812	-93.0379	118.6522
		3	-96.37782*	10.15782	.000	-116.3207	-76.4350
		4	-68.25439*	7.85953	.000	-83.6850	-52.8238
		6	28.80965*	12.42824	.021	4.4093	53.2100
		7	26.05719	34.40170	.449	-41.4837	93.5981
		8	1.20936	11.88135	.919	-22.1173	24.5360
	6	1	34.33214*	12.57772	.006	9.6383	59.0260
		2	-16.00252	54.69301	.770	-123.3814	91.3763
		3	-125.18747*	13.71226	.000	-152.1088	-98.2662
		4	-97.06404*	12.10855	.000	-120.8368	-73.2913
		5	-28.80965*	12.42824	.021	-53.2100	-4.4093
		7	-2.75246	35.61351	.938	-72.6725	67.1676
		8	-27.60028	15.03367	.067	-57.1159	1.9153
	7	1	37.08460	34.45598	.282	-30.5629	104.7321
		2	-13.25006	63.40616	.835	-137.7355	111.2353
		3	-122.43501*	34.88613	.000	-190.9270	-53.9430
		4	-94.31158*	34.28750	.006	-161.6283	-26.9949
		5	-26.05719	34.40170	.449	-93.5981	41.4837
		6	2.75246	35.61351	.938	-67.1676	72.6725
		8	-24.84782	35.42636	.483	-94.4005	44.7048
	8	1	61.93242*	12.03761	.000	38.2990	85.5659
		2	11.59777	54.57133	.832	-95.5422	118.7377
		3	-97.58718*	13.21860	.000	-123.5393	-71.6351
		4	-69.46375*	11.54653	.000	-92.1331	-46.7944
		5	-1.20936	11.88135	.919	-24.5360	22.1173
		6	27.60028	15.03367	.067	-1.9153	57.1159
		7	24.84782	35.42636	.483	-44.7048	94.4005

Table C-29 BOGT

Dependent Variable	(I) LFeat	(J) LFeat	Mean Difference (I-J)	Std. Error	Sig.	95% Confidence Interval	
						Lower Bound	Upper Bound
dTEC	1	2	-8.04682	47.56107	.866	-101.4267	85.3331
		3	-30.90683*	9.08190	.001	-48.7379	-13.0757
		4	-46.72793*	7.23063	.000	-60.9243	-32.5316
		5	-70.86873*	7.57289	.000	-85.7371	-56.0004
		6	8.78603	11.08896	.428	-12.9857	30.5577
		7	15.95605	30.37760	.600	-43.6864	75.5985
		8	-9.79494	10.61278	.356	-30.6317	11.0419
	2	1	8.04682	47.56107	.866	-85.3331	101.4267
		3	-22.86001	47.79764	.633	-116.7044	70.9844
		4	-38.68111	47.48068	.416	-131.9032	54.5410
		5	-62.82191	47.53401	.187	-156.1487	30.5049
		6	16.83285	48.21927	.727	-77.8394	111.5050
		7	24.00287	55.90109	.668	-85.7516	133.7573
		8	-1.74812	48.11200	.971	-96.2097	92.7135
	3	1	30.90683*	9.08190	.001	13.0757	48.7379
		2	22.86001	47.79764	.633	-70.9844	116.7044
		4	-15.82110	8.65106	.068	-32.8063	1.1641
		5	-39.96190*	8.93910	.000	-57.5126	-22.4112
		6	39.69286*	12.06332	.001	16.0081	63.3776
		7	46.86288	30.74667	.128	-13.5042	107.2299
		8	21.11190	11.62712	.070	-1.7164	43.9402
	4	1	46.72793*	7.23063	.000	32.5316	60.9243
		2	38.68111	47.48068	.416	-54.5410	131.9032
		3	15.82110	8.65106	.068	-1.1641	32.8063
		5	-24.14080*	7.05043	.001	-37.9834	-10.2982
		6	55.51396*	10.73894	.000	34.4295	76.5985
		7	62.68398*	30.25159	.039	3.2890	122.0790
		8	36.93300*	10.24652	.000	16.8153	57.0507
	5	1	70.86873*	7.57289	.000	56.0004	85.7371
		2	62.82191	47.53401	.187	-30.5049	156.1487
		3	39.96190*	8.93910	.000	22.4112	57.5126
		4	24.14080*	7.05043	.001	10.2982	37.9834
		6	79.65476*	10.97231	.000	58.1121	101.1974
		7	86.82478*	30.33522	.004	27.2656	146.3840
		8	61.07380*	10.49084	.000	40.4764	81.6712
	6	1	-8.78603	11.08896	.428	-30.5577	12.9857
		2	-16.83285	48.21927	.727	-111.5050	77.8394
		3	-39.69286*	12.06332	.001	-63.3776	-16.0081
		4	-55.51396*	10.73894	.000	-76.5985	-34.4295
		5	-79.65476*	10.97231	.000	-101.1974	-58.1121
		7	7.17002	31.39812	.819	-54.4760	68.8161
		8	-18.58096	13.25421	.161	-44.6039	7.4419
	7	1	-15.95605	30.37760	.600	-75.5985	43.6864
		2	-24.00287	55.90109	.668	-133.7573	85.7516
		3	-46.86288	30.74667	.128	-107.2299	13.5042
		4	-62.68398*	30.25159	.039	-122.0790	-3.2890
		5	-86.82478*	30.33522	.004	-146.3840	-27.2656
		6	-7.17002	31.39812	.819	-68.8161	54.4760
		8	-25.75098	31.23312	.410	-87.0731	35.5711
	8	1	9.79494	10.61278	.356	-11.0419	30.6317
		2	1.74812	48.11200	.971	-92.7135	96.2097
		3	-21.11190	11.62712	.070	-43.9402	1.7164
		4	-36.93300*	10.24652	.000	-57.0507	-16.8153
		5	-61.07380*	10.49084	.000	-81.6712	-40.4764
		6	18.58096	13.25421	.161	-7.4419	44.6039
		7	25.75098	31.23312	.410	-35.5711	87.0731

Table C-30 BRAZ

Dependent Variable	(I) LFeat	(J) LFeat	Mean Difference (I-J)	Std. Error	Sig.	95% Confidence Interval Lower Bound	95% Confidence Interval Upper Bound
dTEC	1	2	-6.91283	32.93878	.834	-71.5817	57.7561
		3	-15.88827*	6.31353	.012	-28.2837	-3.4929
		4	-75.65311*	4.94675	.000	-85.3651	-65.9411
		5	-74.49697*	5.22946	.000	-84.7640	-64.2299
		6	-34.44621*	7.67974	.000	-49.5239	-19.3685
		7	-30.72908	21.03824	.145	-72.0336	10.5754
		8	-36.88712*	7.34996	.000	-51.3173	-22.4569
	2	1	6.91283	32.93878	.834	-57.7561	71.5817
		3	-8.97544	33.10714	.786	-73.9749	56.0240
		4	-68.74029*	32.87389	.037	-133.2818	-4.1988
		5	-67.58414*	32.91762	.040	-132.2115	-2.9568
		6	-27.53339	33.39462	.410	-93.0972	38.0305
		7	-23.81626	38.71472	.539	-99.8251	52.1926
		8	-29.97429	33.32033	.369	-95.3923	35.4437
	3	1	15.88827*	6.31353	.012	3.4929	28.2837
		2	8.97544	33.10714	.786	-56.0240	73.9749
		4	-59.76484*	5.96575	.000	-71.4774	-48.0522
		5	-58.60870*	6.20219	.000	-70.7855	-46.4319
		6	-18.55795*	8.37247	.027	-34.9957	-2.1202
		7	-14.84081	21.30088	.486	-56.6610	26.9793
		8	-20.99885*	8.07105	.009	-36.8448	-5.1529
	4	1	75.65311*	4.94675	.000	65.9411	85.3651
		2	68.74029*	32.87389	.037	4.1988	133.2818
		3	59.76484*	5.96575	.000	48.0522	71.4774
		5	1.15614	4.80383	.810	-8.2753	10.5875
		6	41.20690*	7.39648	.000	26.6853	55.7285
		7	44.92403*	20.93650	.032	3.8193	86.0288
		8	38.76599*	7.05347	.000	24.9179	52.6141
	5	1	74.49697*	5.22946	.000	64.2299	84.7640
		2	67.58414*	32.91762	.040	2.9568	132.2115
		3	58.60870*	6.20219	.000	46.4319	70.7855
		4	-1.15614	4.80383	.810	-10.5875	8.2753
		6	40.05075*	7.58847	.000	25.1523	54.9492
		7	43.76789*	21.00509	.038	2.5285	85.0073
		8	37.60985*	7.25455	.000	23.3670	51.8527
	6	1	34.44621*	7.67974	.000	19.3685	49.5239
		2	27.53339	33.39462	.410	-38.0305	93.0972
		3	18.55795*	8.37247	.027	2.1202	34.9957
		4	-41.20690*	7.39648	.000	-55.7285	-26.6853
		5	-40.05075*	7.58847	.000	-54.9492	-25.1523
		7	3.71713	21.74500	.864	-38.9750	46.4092
		8	-2.44090	9.17930	.790	-20.4627	15.5809
	7	1	30.72908	21.03824	.145	-10.5754	72.0336
		2	23.81626	38.71472	.539	-52.1926	99.8251
		3	14.84081	21.30088	.486	-26.9793	56.6610
		4	-44.92403*	20.93650	.032	-86.0288	-3.8193
		5	-43.76789*	21.00509	.038	-85.0073	-2.5285
		6	-3.71713	21.74500	.864	-46.4092	38.9750
		8	-6.15804	21.63073	.776	-48.6258	36.3097
	8	1	36.88712*	7.34996	.000	22.4569	51.3173
		2	29.97429	33.32033	.369	-35.4437	95.3923
		3	20.99885*	8.07105	.009	5.1529	36.8448
		4	-38.76599*	7.05347	.000	-52.6141	-24.9179
		5	-37.60985*	7.25455	.000	-51.8527	-23.3670
		6	2.44090	9.17930	.790	-15.5809	20.4627
		7	6.15804	21.63073	.776	-36.3097	48.6258

Table C-31 CONO

Dependent Variable	(I) LFeat	(J) LFeat	Mean Difference (I-J)	Std. Error	Sig.	95% Confidence Interval	
						Lower Bound	Upper Bound
dTEC	1	2	-55.14206*	13.86384	.000	-82.3609	-27.9232
		3	-97.41718*	2.86081	.000	-103.0338	-91.8006
		4	44.97949*	2.00790	.000	41.0374	48.9216
		5	58.92147*	2.13320	.000	54.7334	63.1096
		6	35.74028*	3.18794	.000	29.4814	41.9992
		7	32.69334*	8.84484	.000	15.3283	50.0584
		8	39.59663*	3.04688	.000	33.6147	45.5786
	2	1	55.14206*	13.86384	.000	27.9232	82.3609
		3	-42.27512*	13.99622	.003	-69.7539	-14.7963
		4	100.12154*	13.84708	.000	72.9356	127.3075
		5	114.06353*	13.86580	.000	86.8408	141.2863
		6	90.88234*	14.06673	.000	63.2651	118.4996
		7	87.83540*	16.30770	.000	55.8185	119.8523
		8	94.73869*	14.03543	.000	67.1829	122.2945
	3	1	97.41718*	2.86081	.000	91.8006	103.0338
		2	42.27512*	13.99622	.003	14.7963	69.7539
		4	142.39667*	2.77846	.000	136.9417	147.8516
		5	156.33865*	2.87031	.000	150.7034	161.9739
		6	133.15747*	3.72171	.000	125.8506	140.4643
		7	130.11052*	9.05093	.000	112.3408	147.8802
		8	137.01381*	3.60162	.000	129.9427	144.0849
	4	1	-44.97949*	2.00790	.000	-48.9216	-41.0374
		2	-100.12154*	13.84708	.000	-127.3075	-72.9356
		3	-142.39667*	2.77846	.000	-147.8516	-136.9417
		5	13.94198*	2.02143	.000	9.9733	17.9107
		6	-9.23920*	3.11425	.003	-15.3534	-3.1250
		7	-12.28614	8.81855	.164	-29.5996	5.0273
		8	-5.38286	2.96970	.070	-11.2133	.4476
	5	1	-58.92147*	2.13320	.000	-63.1096	-54.7334
		2	-114.06353*	13.86580	.000	-141.2863	-86.8408
		3	-156.33865*	2.87031	.000	-161.9739	-150.7034
		4	-13.94198*	2.02143	.000	-17.9107	-9.9733
		6	-23.18118*	3.19647	.000	-29.4568	-16.9055
		7	-26.22813*	8.84792	.003	-43.5993	-8.8570
		8	-19.32484*	3.05581	.000	-25.3243	-13.3254
	6	1	-35.74028*	3.18794	.000	-41.9992	-29.4814
		2	-90.88234*	14.06673	.000	-118.4996	-63.2651
		3	-133.15747*	3.72171	.000	-140.4643	-125.8506
		4	9.23920*	3.11425	.003	3.1250	15.3534
		5	23.18118*	3.19647	.000	16.9055	29.4568
		7	-3.04694	9.15959	.739	-21.0300	14.9361
		8	3.85634	3.86657	.319	-3.7349	11.4476
	7	1	-32.69334*	8.84484	.000	-50.0584	-15.3283
		2	-87.83540*	16.30770	.000	-119.8523	-55.8185
		3	-130.11052*	9.05093	.000	-147.8802	-112.3408
		4	12.28614	8.81855	.164	-5.0273	29.5996
		5	26.22813*	8.84792	.003	8.8570	43.5993
		6	3.04694	9.15959	.739	-14.9361	21.0300
		8	6.90329	9.11146	.449	-10.9852	24.7918
	8	1	-39.59663*	3.04688	.000	-45.5786	-33.6147
		2	-94.73869*	14.03543	.000	-122.2945	-67.1829
		3	-137.01381*	3.60162	.000	-144.0849	-129.9427
		4	5.38286	2.96970	.070	-.4476	11.2133
		5	19.32484*	3.05581	.000	13.3254	25.3243
		6	-3.85634	3.86657	.319	-11.4476	3.7349
		7	-6.90329	9.11146	.449	-24.7918	10.9852

Table C-32 COPO

Dependent Variable	(I) LFeat	(J) LFeat	Mean Difference (I-J)	Std. Error	Sig.	95% Confidence Interval	
						Lower Bound	Upper Bound
dTEC	1	2	-9.00578	13.40837	.502	-35.3305	17.3189
		3	-33.60521*	2.57005	.000	-38.6510	-28.5594
		4	2.41658	2.01172	.230	-1.5330	6.3662
		5	-36.44753*	2.12875	.000	-40.6269	-32.2681
		6	-5.35301	3.12619	.087	-11.4907	.7846
		7	4.55311	8.56403	.595	-12.2607	21.3669
		8	-13.69804*	2.99195	.000	-19.5721	-7.8239
	2	1	9.00578	13.40837	.502	-17.3189	35.3305
		3	-24.59943	13.47691	.068	-51.0587	1.8598
		4	11.42236	13.38167	.394	-14.8499	37.6946
		5	-27.44176*	13.39976	.041	-53.7495	-1.1340
		6	3.65277	13.59393	.788	-23.0362	30.3418
		7	13.55888	15.75958	.390	-17.3819	44.4997
		8	-4.69226	13.56369	.729	-31.3219	21.9374
	3	1	33.60521*	2.57005	.000	28.5594	38.6510
		2	24.59943	13.47691	.068	-1.8598	51.0587
		4	36.02179*	2.42686	.000	31.2571	40.7864
		5	-2.84232	2.52472	.261	-7.7991	2.1145
		6	28.25220*	3.40818	.000	21.5609	34.9435
		7	38.15831*	8.67094	.000	21.1346	55.1820
		8	19.90717*	3.28548	.000	13.4568	26.3576
	4	1	-2.41658	2.01172	.230	-6.3662	1.5330
		2	-11.42236	13.38167	.394	-37.6946	14.8499
		3	-36.02179*	2.42686	.000	-40.7864	-31.2571
		5	-38.86411*	1.95348	.000	-42.6994	-35.0288
		6	-7.76959*	3.00958	.010	-13.6783	-1.8609
		7	2.13652	8.52215	.802	-14.5950	18.8681
		8	-16.11462*	2.86989	.000	-21.7491	-10.4802
	5	1	36.44753*	2.12875	.000	32.2681	40.6269
		2	27.44176*	13.39976	.041	1.1340	53.7495
		3	2.84232	2.52472	.261	-2.1145	7.7991
		4	38.86411*	1.95348	.000	35.0288	42.6994
		6	31.09453*	3.08904	.000	25.0298	37.1592
		7	41.00064*	8.55053	.000	24.2134	57.7879
		8	22.74950*	2.95311	.000	16.9517	28.5473
	6	1	5.35301	3.12619	.087	-.7846	11.4907
		2	-3.65277	13.59393	.788	-30.3418	23.0362
		3	-28.25220*	3.40818	.000	-34.9435	-21.5609
		4	7.76959*	3.00958	.010	1.8609	13.6783
		5	-31.09453*	3.08904	.000	-37.1592	-25.0298
		7	9.90611	8.85173	.263	-7.4725	27.2847
		8	-8.34503*	3.73661	.026	-15.6811	-1.0089
	7	1	-4.55311	8.56403	.595	-21.3669	12.2607
		2	-13.55888	15.75958	.390	-44.4997	17.3819
		3	-38.15831*	8.67094	.000	-55.1820	-21.1346
		4	-2.13652	8.52215	.802	-18.8681	14.5950
		5	-41.00064*	8.55053	.000	-57.7879	-24.2134
		6	-9.90611	8.85173	.263	-27.2847	7.4725
		8	-18.25114*	8.80521	.039	-35.5384	-.9639
	8	1	13.69804*	2.99195	.000	7.8239	19.5721
		2	4.69226	13.56369	.729	-21.9374	31.3219
		3	-19.90717*	3.28548	.000	-26.3576	-13.4568
		4	16.11462*	2.86989	.000	10.4802	21.7491
		5	-22.74950*	2.95311	.000	-28.5473	-16.9517
		6	8.34503*	3.73661	.026	1.0089	15.6811
		7	18.25114*	8.80521	.039	.9639	35.5384

Table C-33 GOGA

Dependent Variable	(I) LFeat	(J) LFeat	Mean Difference (I-J)	Std. Error	Sig.	95% Confidence Interval	
						Lower Bound	Upper Bound
dTEC	1	2	-77.46309*	18.12565	.000	-113.0492	-41.8770
		3	-119.45688*	3.74023	.000	-126.8001	-112.1137
		4	-34.04166*	2.62514	.000	-39.1956	-28.8877
		5	-65.22171*	2.78896	.000	-70.6973	-59.7461
		6	-45.68185*	4.16792	.000	-53.8647	-37.4990
		7	-24.12864*	11.56379	.037	-46.8318	-1.4254
		8	-31.43815*	3.98351	.000	-39.2590	-23.6173
	2	1	77.46309*	18.12565	.000	41.8770	113.0492
		3	-41.99379*	18.29872	.022	-77.9197	-6.0679
		4	43.42144*	18.10374	.017	7.8783	78.9645
		5	12.24138	18.12821	.500	-23.3498	47.8325
		6	31.78124	18.39091	.084	-4.3257	67.8881
		7	53.33446*	21.32077	.013	11.4754	95.1935
		8	46.02495*	18.34999	.012	9.9984	82.0515
	3	1	119.45688*	3.74023	.000	112.1137	126.8001
		2	41.99379*	18.29872	.022	6.0679	77.9197
		4	85.41523*	3.63257	.000	78.2834	92.5471
		5	54.23517*	3.75266	.000	46.8676	61.6028
		6	73.77503*	4.86578	.000	64.2220	83.3280
		7	95.32824*	11.83323	.000	72.0960	118.5604
		8	88.01873*	4.70877	.000	78.7740	97.2635
	4	1	34.04166*	2.62514	.000	28.8877	39.1956
		2	-43.42144*	18.10374	.017	-78.9645	-7.8783
		3	-85.41523*	3.63257	.000	-92.5471	-78.2834
		5	-31.18005*	2.64282	.000	-36.3687	-25.9914
		6	-11.64020*	4.07159	.004	-19.6339	-3.6464
		7	9.91302	11.52941	.390	-12.7227	32.5487
		8	2.60351	3.88260	.503	-5.0192	10.2262
	5	1	65.22171*	2.78896	.000	59.7461	70.6973
		2	-12.24138	18.12821	.500	-47.8325	23.3498
		3	-54.23517*	3.75266	.000	-61.6028	-46.8676
		4	31.18005*	2.64282	.000	25.9914	36.3687
		6	19.53986*	4.17908	.000	11.3351	27.7447
		7	41.09307*	11.56781	.000	18.3820	63.8042
		8	33.78356*	3.99519	.000	25.9398	41.6273
	6	1	45.68185*	4.16792	.000	37.4990	53.8647
		2	-31.78124	18.39091	.084	-67.8881	4.3257
		3	-73.77503*	4.86578	.000	-83.3280	-64.2220
		4	11.64020*	4.07159	.004	3.6464	19.6339
		5	-19.53986*	4.17908	.000	-27.7447	-11.3351
		7	21.55322	11.97529	.072	-1.9579	45.0643
		8	14.24371*	5.05518	.005	4.3189	24.1685
	7	1	24.12864*	11.56379	.037	1.4254	46.8318
		2	-53.33446*	21.32077	.013	-95.1935	-11.4754
		3	-95.32824*	11.83323	.000	-118.5604	-72.0960
		4	-9.91302	11.52941	.390	-32.5487	12.7227
		5	-41.09307*	11.56781	.000	-63.8042	-18.3820
		6	-21.55322	11.97529	.072	-45.0643	1.9579
		8	-7.30951	11.91236	.540	-30.6971	16.0780
	8	1	31.43815*	3.98351	.000	23.6173	39.2590
		2	-46.02495*	18.34999	.012	-82.0515	-9.9984
		3	-88.01873*	4.70877	.000	-97.2635	-78.7740
		4	-2.60351	3.88260	.503	-10.2262	5.0192
		5	-33.78356*	3.99519	.000	-41.6273	-25.9398
		6	-14.24371*	5.05518	.005	-24.1685	-4.3189
		7	7.30951	11.91236	.540	-16.0780	30.6971

Table C-34 PARC

Dependent Variable	(I) LFeat	(J) LFeat	Mean Difference (I-J)	Std. Error	Sig.	95% Confidence Interval	
						Lower Bound	Upper Bound
dTEC	1	2	-12.11127	18.98076	.524	-49.3762	25.1537
		3	-109.06680*	3.63813	.000	-116.2096	-101.9241
		4	28.66985*	2.84777	.000	23.0788	34.2609
		5	14.55431*	3.01344	.000	8.6380	20.4706
		6	-2.83958	4.42540	.521	-11.5280	5.8488
		7	-4.65404	12.12315	.701	-28.4554	19.1474
		8	-10.84990*	4.23537	.011	-19.1652	-2.5346
	2	1	12.11127	18.98076	.524	-25.1537	49.3762
		3	-96.95554*	19.07778	.000	-134.4110	-59.5001
		4	40.78112*	18.94295	.032	3.5904	77.9718
		5	26.66558	18.96856	.160	-10.5754	63.9066
		6	9.27168	19.24343	.630	-28.5090	47.0523
		7	7.45722	22.30911	.738	-36.3423	51.2567
		8	1.26136	19.20062	.948	-36.4352	38.9580
	3	1	109.06680*	3.63813	.000	101.9241	116.2096
		2	96.95554*	19.07778	.000	59.5001	134.4110
		4	137.73666*	3.43544	.000	130.9919	144.4815
		5	123.62111*	3.57397	.000	116.6043	130.6379
		6	106.22722*	4.82458	.000	96.7551	115.6993
		7	104.41276*	12.27449	.000	80.3142	128.5113
		8	98.21690*	4.65089	.000	89.0858	107.3480
	4	1	-28.66985*	2.84777	.000	-34.2609	-23.0788
		2	-40.78112*	18.94295	.032	-77.9718	-3.5904
		3	-137.73666*	3.43544	.000	-144.4815	-130.9919
		5	-14.11554*	2.76533	.000	-19.5447	-8.6864
		6	-31.50944*	4.26033	.000	-39.8737	-23.1451
		7	-33.32389*	12.06387	.006	-57.0089	-9.6389
		8	-39.51975*	4.06258	.000	-47.4958	-31.5437
	5	1	-14.55431*	3.01344	.000	-20.4706	-8.6380
		2	-26.66558	18.96856	.160	-63.9066	10.5754
		3	-123.62111*	3.57397	.000	-130.6379	-116.6043
		4	14.11554*	2.76533	.000	8.6864	19.5447
		6	-17.39389*	4.37281	.000	-25.9790	-8.8088
		7	-19.20835	12.10405	.113	-42.9722	4.5555
		8	-25.40421*	4.18039	.000	-33.6116	-17.1969
	6	1	2.83958	4.42540	.521	-5.8488	11.5280
		2	-9.27168	19.24343	.630	-47.0523	28.5090
		3	-106.22722*	4.82458	.000	-115.6993	-96.7551
		4	31.50944*	4.26033	.000	23.1451	39.8737
		5	17.39389*	4.37281	.000	8.8088	25.9790
		7	-1.81446	12.53042	.885	-26.4154	22.7865
		8	-8.01032	5.28951	.130	-18.3952	2.3746
	7	1	4.65404	12.12315	.701	-19.1474	28.4554
		2	-7.45722	22.30911	.738	-51.2567	36.3423
		3	-104.41276*	12.27449	.000	-128.5113	-80.3142
		4	33.32389*	12.06387	.006	9.6389	57.0089
		5	19.20835	12.10405	.113	-4.5555	42.9722
		6	1.81446	12.53042	.885	-22.7865	26.4154
		8	-6.19586	12.46457	.619	-30.6676	18.2758
	8	1	10.84990*	4.23537	.011	2.5346	19.1652
		2	-1.26136	19.20062	.948	-38.9580	36.4352
		3	-98.21690*	4.65089	.000	-107.3480	-89.0858
		4	39.51975*	4.06258	.000	31.5437	47.4958
		5	25.40421*	4.18039	.000	17.1969	33.6116
		6	8.01032	5.28951	.130	-2.3746	18.3952
		7	6.19586	12.46457	.619	-18.2758	30.6676

Table C-35 SCH2

Dependent Variable	(I) LFeat	(J) LFeat	Mean Difference (I-J)	Std. Error	Sig.	95% Confidence Interval	
						Lower Bound	Upper Bound
dTEC	1	2	-36.82578	59.49134	.536	-153.6252	79.9737
		3	-86.23835*	11.40299	.000	-108.6258	-63.8509
		4	-166.25781*	8.92575	.000	-183.7818	-148.7339
		5	9.44900	9.44503	.317	-9.0944	27.9924
		6	20.07451	13.87052	.148	-7.1575	47.3065
		7	25.25051	37.99755	.507	-49.3501	99.8512
		8	19.69502	13.27490	.138	-6.3676	45.7577
	2	1	36.82578	59.49134	.536	-79.9737	153.6252
		3	-49.41257	59.79543	.409	-166.8090	67.9839
		4	-129.43204*	59.37284	.030	-245.9988	-12.8653
		5	46.27477	59.45312	.437	-70.4496	162.9992
		6	56.90029	60.31465	.346	-61.5155	175.3161
		7	62.07628	69.92338	.375	-75.2044	199.3570
		8	56.52080	60.18047	.348	-61.6316	174.6732
	3	1	86.23835*	11.40299	.000	63.8509	108.6258
		2	49.41257	59.79543	.409	-67.9839	166.8090
		4	-80.01946*	10.76768	.000	-101.1597	-58.8793
		5	95.68735*	11.20189	.000	73.6947	117.6800
		6	106.31286*	15.12168	.000	76.6244	136.0013
		7	111.48886*	38.47191	.004	35.9569	187.0208
		8	105.93337*	14.57728	.000	77.3138	134.5530
	4	1	166.25781*	8.92575	.000	148.7339	183.7818
		2	129.43204*	59.37284	.030	12.8653	245.9988
		3	80.01946*	10.76768	.000	58.8793	101.1597
		5	175.70681*	8.66737	.000	158.6901	192.7235
		6	186.33232*	13.35314	.000	160.1161	212.5486
		7	191.50832*	37.81176	.000	117.2724	265.7442
		8	185.95284*	12.73334	.000	160.9535	210.9522
	5	1	-9.44900	9.44503	.317	-27.9924	9.0944
		2	-46.27477	59.45312	.437	-162.9992	70.4496
		3	-95.68735*	11.20189	.000	-117.6800	-73.6947
		4	-175.70681*	8.66737	.000	-192.7235	-158.6901
		6	10.62551	13.70568	.438	-16.2829	37.5339
		7	15.80151	37.93769	.677	-58.6816	90.2846
		8	10.24603	13.10257	.434	-15.4783	35.9703
	6	1	-20.07451	13.87052	.148	-47.3065	7.1575
		2	-56.90029	60.31465	.346	-175.3161	61.5155
		3	-106.31286*	15.12168	.000	-136.0013	-76.6244
		4	-186.33232*	13.35314	.000	-212.5486	-160.1161
		5	-10.62551	13.70568	.438	-37.5339	16.2829
		7	5.17600	39.27405	.895	-71.9308	82.2828
		8	-.37949	16.57891	.982	-32.9289	32.1699
	7	1	-25.25051	37.99755	.507	-99.8512	49.3501
		2	-62.07628	69.92338	.375	-199.3570	75.2044
		3	-111.48886*	38.47191	.004	-187.0208	-35.9569
		4	-191.50832*	37.81176	.000	-265.7442	-117.2724
		5	-15.80151	37.93769	.677	-90.2846	58.6816
		6	-5.17600	39.27405	.895	-82.2828	71.9308
		8	-5.55548	39.06767	.887	-82.2571	71.1461
	8	1	-19.69502	13.27490	.138	-45.7577	6.3676
		2	-56.52080	60.18047	.348	-174.6732	61.6316
		3	-105.93337*	14.57728	.000	-134.5530	-77.3138
		4	-185.95284*	12.73334	.000	-210.9522	-160.9535
		5	-10.24603	13.10257	.434	-35.9703	15.4783
		6	.37949	16.57891	.982	-32.1699	32.9289
		7	5.55548	39.06767	.887	-71.1461	82.2571

Table C-36 SG05

Dependent Variable	(I) LFeat	(J) LFeat	Mean Difference (I-J)	Std. Error	Sig.	95% Confidence Interval	
						Lower Bound	Upper Bound
dTEC	1	2	18.07591	22.07605	.413	-25.2692	61.4210
		3	-50.42893*	4.23142	.000	-58.7371	-42.1208
		4	53.60130*	3.31217	.000	47.0980	60.1046
		5	82.63801*	3.67791	.000	75.4166	89.8594
		6	53.30537*	5.14707	.000	43.1994	63.4114
		7	47.84354*	14.10013	.001	20.1587	75.5284
		8	59.99036*	4.92605	.000	50.3183	69.6624
	2	1	-18.07591	22.07605	.413	-61.4210	25.2692
		3	-68.50485*	22.18889	.002	-112.0715	-24.9382
		4	35.52539	22.03208	.107	-7.7334	78.7841
		5	64.56210*	22.09002	.004	21.1896	107.9346
		6	35.22946	22.38156	.116	-8.7155	79.1744
		7	29.76763	25.94717	.252	-21.1782	80.7134
		8	41.91444	22.33177	.061	-1.9327	85.7616
	3	1	50.42893*	4.23142	.000	42.1208	58.7371
		2	68.50485*	22.18889	.002	24.9382	112.0715
		4	104.03023*	3.99567	.000	96.1850	111.8755
		5	133.06694*	4.30371	.000	124.6168	141.5170
		6	103.73430*	5.61135	.000	92.7167	114.7519
		7	98.27248*	14.27616	.000	70.2420	126.3029
		8	110.41929*	5.40934	.000	99.7984	121.0402
	4	1	-53.60130*	3.31217	.000	-60.1046	-47.0980
		2	-35.52539	22.03208	.107	-78.7841	7.7334
		3	-104.03023*	3.99567	.000	-111.8755	-96.1850
		5	29.03671*	3.40404	.000	22.3531	35.7203
		6	-.29593	4.95508	.952	-10.0250	9.4331
		7	-5.75776	14.03119	.682	-33.3072	21.7917
		8	6.38906	4.72509	.177	-2.8884	15.6665
	5	1	-82.63801*	3.67791	.000	-89.8594	-75.4166
		2	-64.56210*	22.09002	.004	-107.9346	-21.1896
		3	-133.06694*	4.30371	.000	-141.5170	-124.6168
		4	-29.03671*	3.40404	.000	-35.7203	-22.3531
		6	-29.33264*	5.20667	.000	-39.5556	-19.1096
		7	-34.79447*	14.12200	.014	-62.5222	-7.0667
		8	-22.64765*	4.98829	.000	-32.4419	-12.8534
	6	1	-53.30537*	5.14707	.000	-63.4114	-43.1994
		2	-35.22946	22.38156	.116	-79.1744	8.7155
		3	-103.73430*	5.61135	.000	-114.7519	-92.7167
		4	.29593	4.95508	.952	-9.4331	10.0250
		5	29.33264*	5.20667	.000	19.1096	39.5556
		7	-5.46183	14.57382	.708	-34.0767	23.1530
		8	6.68499	6.15210	.278	-5.3943	18.7643
	7	1	-47.84354*	14.10013	.001	-75.5284	-20.1587
		2	-29.76763	25.94717	.252	-80.7134	21.1782
		3	-98.27248*	14.27616	.000	-126.3029	-70.2420
		4	5.75776	14.03119	.682	-21.7917	33.3072
		5	34.79447*	14.12200	.014	7.0667	62.5222
		6	5.46183	14.57382	.708	-23.1530	34.0767
		8	12.14681	14.49723	.402	-16.3177	40.6113
	8	1	-59.99036*	4.92605	.000	-69.6624	-50.3183
		2	-41.91444	22.33177	.061	-85.7616	1.9327
		3	-110.41929*	5.40934	.000	-121.0402	-99.7984
		4	-6.38906	4.72509	.177	-15.6665	2.8884
		5	22.64765*	4.98829	.000	12.8534	32.4419
		6	-6.68499	6.15210	.278	-18.7643	5.3943
		7	-12.14681	14.49723	.402	-40.6113	16.3177

Event V Mean percentage deviation of TECU for each phenomena of Event I from IGS stations.

Table C-37 BAIE

Dependent Variable	(I) LFeat	(J) LFeat	Mean Difference (I-J)	Std. Error	Sig.	95% Confidence Interval	
						Lower Bound	Upper Bound
dTEC	1	2	6.84463	7.65067	.371	-8.1759	21.8652
		3	9.02941*	1.96782	.000	5.1660	12.8928
		4	9.93116*	1.48809	.000	7.0096	12.8527
		5	8.34977*	1.52519	.000	5.3554	11.3442
		6	14.00349*	1.35112	.000	11.3508	16.6561
		7	-3.78682	3.24687	.244	-10.1614	2.5878
	2	1	-6.84463	7.65067	.371	-21.8652	8.1759
		3	2.18478	7.77926	.779	-13.0882	17.4578
		4	3.08653	7.67196	.688	-11.9758	18.1489
		5	1.50514	7.67925	.845	-13.5715	16.5818
		6	7.15886	7.64658	.349	-7.8536	22.1714
		7	-10.63145	8.19676	.195	-26.7241	5.4612
	3	1	-9.02941*	1.96782	.000	-12.8928	-5.1660
		2	-2.18478	7.77926	.779	-17.4578	13.0882
		4	.90175	2.04904	.660	-3.1211	4.9246
		5	-.67963	2.07614	.743	-4.7557	3.3965
		6	4.97408*	1.95184	.011	1.1420	8.8061
		7	-12.81623*	3.53926	.000	-19.7648	-5.8676
	4	1	-9.93116*	1.48809	.000	-12.8527	-7.0096
		2	-3.08653	7.67196	.688	-18.1489	11.9758
		3	-.90175	2.04904	.660	-4.9246	3.1211
		5	-1.58138	1.62864	.332	-4.7789	1.6161
		6	4.07233*	1.46690	.006	1.1924	6.9523
		7	-13.71798*	3.29673	.000	-20.1904	-7.2455
	5	1	-8.34977*	1.52519	.000	-11.3442	-5.3554
		2	-1.50514	7.67925	.845	-16.5818	13.5715
		3	.67963	2.07614	.743	-3.3965	4.7557
		4	1.58138	1.62864	.332	-1.6161	4.7789
		6	5.65371*	1.50452	.000	2.6999	8.6075
		7	-12.13659*	3.31365	.000	-18.6423	-5.6309
	6	1	-14.00349*	1.35112	.000	-16.6561	-11.3508
		2	-7.15886	7.64658	.349	-22.1714	7.8536
		3	-4.97408*	1.95184	.011	-8.8061	-1.1420
		4	-4.07233*	1.46690	.006	-6.9523	-1.1924
		5	-5.65371*	1.50452	.000	-8.6075	-2.6999
		7	-17.79031*	3.23722	.000	-24.1459	-11.4347
	7	1	3.78682	3.24687	.244	-2.5878	10.1614
		2	10.63145	8.19676	.195	-5.4612	26.7241
		3	12.81623*	3.53926	.000	5.8676	19.7648
		4	13.71798*	3.29673	.000	7.2455	20.1904
		5	12.13659*	3.31365	.000	5.6309	18.6423
		6	17.79031*	3.23722	.000	11.4347	24.1459

Table C-38 BOGT

Dependent Variable	(I) LFeat	(J) LFeat	Mean Difference (I-J)	Std. Error	Sig.	95% Confidence Interval Lower Bound	95% Confidence Interval Upper Bound
dTEC	1	2	28.00399*	13.75027	.042	1.0081	54.9999
		3	33.90368*	3.53669	.000	26.9601	40.8473
		4	-4.12092	2.67449	.124	-9.3717	1.1299
		5	-74.32149*	2.74117	.000	-79.7032	-68.9398
		6	40.04458*	2.42833	.000	35.2771	44.8121
		7	48.46434*	5.83549	.000	37.0075	59.9211
	2	1	-28.00399*	13.75027	.042	-54.9999	-1.0081
		3	5.89969	13.98139	.673	-21.5499	33.3493
		4	-32.12491*	13.78854	.020	-59.1959	-5.0539
		5	-102.32548*	13.80163	.000	-129.4222	-75.2288
		6	12.04059	13.74292	.381	-14.9408	39.0220
		7	20.46035	14.73173	.165	-8.4624	49.3831
	3	1	-33.90368*	3.53669	.000	-40.8473	-26.9601
		2	-5.89969	13.98139	.673	-33.3493	21.5499
		4	-38.02460*	3.68267	.000	-45.2548	-30.7944
		5	-108.22518*	3.73138	.000	-115.5510	-100.8994
		6	6.14089	3.50798	.080	-.7463	13.0281
		7	14.56065*	6.36098	.022	2.0722	27.0491
	4	1	4.12092	2.67449	.124	-1.1299	9.3717
		2	32.12491*	13.78854	.020	5.0539	59.1959
		3	38.02460*	3.68267	.000	30.7944	45.2548
		5	-70.20057*	2.92709	.000	-75.9473	-64.4538
		6	44.16550*	2.63641	.000	38.9894	49.3415
		7	52.58526*	5.92510	.000	40.9525	64.2180
	5	1	74.32149*	2.74117	.000	68.9398	79.7032
		2	102.32548*	13.80163	.000	75.2288	129.4222
		3	108.22518*	3.73138	.000	100.8994	115.5510
		4	70.20057*	2.92709	.000	64.4538	75.9473
		6	114.36607*	2.70402	.000	109.0573	119.6749
		7	122.78583*	5.95549	.000	111.0934	134.4782
	6	1	-40.04458*	2.42833	.000	-44.8121	-35.2771
		2	-12.04059	13.74292	.381	-39.0220	14.9408
		3	-6.14089	3.50798	.080	-13.0281	.7463
		4	-44.16550*	2.63641	.000	-49.3415	-38.9894
		5	-114.36607*	2.70402	.000	-119.6749	-109.0573
		7	8.41976	5.81813	.148	-3.0030	19.8425
	7	1	-48.46434*	5.83549	.000	-59.9211	-37.0075
		2	-20.46035	14.73173	.165	-49.3831	8.4624
		3	-14.56065*	6.36098	.022	-27.0491	-2.0722
		4	-52.58526*	5.92510	.000	-64.2180	-40.9525
		5	-122.78583*	5.95549	.000	-134.4782	-111.0934
		6	-8.41976	5.81813	.148	-19.8425	3.0030

Table C-39 BRA2

Dependent Variable	(I) LFeat	(J) LFeat	Mean Difference (I-J)	Std. Error	Sig.	95% Confidence Interval Lower Bound	95% Confidence Interval Upper Bound
dTEC	1	2	-14.11467	11.44248	.218	-36.5796	8.3503
		3	6.58008*	2.94311	.026	.8019	12.3583
		4	5.10192*	2.22562	.022	.7324	9.4715
		5	-7.44191*	2.28110	.001	-11.9204	-2.9634
		6	-3.30188	2.02076	.103	-7.2692	.6655
		7	8.79755	4.85608	.070	-.7364	18.3315
	2	1	14.11467	11.44248	.218	-8.3503	36.5796
		3	20.69475	11.63480	.076	-2.1478	43.5373
		4	19.21659	11.47432	.094	-3.3109	41.7441
		5	6.67276	11.48521	.561	-15.8761	29.2216
		6	10.81279	11.43636	.345	-11.6402	33.2657
		7	22.91222	12.25921	.062	-1.1562	46.9807
	3	1	-6.58008*	2.94311	.026	-12.3583	-.8019
		2	-20.69475	11.63480	.076	-43.5373	2.1478
		4	-1.47815	3.06458	.630	-7.4948	4.5385
		5	-14.02199*	3.10511	.000	-20.1182	-7.9257
		6	-9.88196*	2.91921	.001	-15.6132	-4.1507
		7	2.21748	5.29338	.675	-8.1750	12.6099
	4	1	-5.10192*	2.22562	.022	-9.4715	-.7324
		2	-19.21659	11.47432	.094	-41.7441	3.3109
		3	1.47815	3.06458	.630	-4.5385	7.4948
		5	-12.54383*	2.43582	.000	-17.3261	-7.7616
		6	-8.40381*	2.19392	.000	-12.7111	-4.0965
		7	3.69563	4.93065	.454	-5.9847	13.3760
	5	1	7.44191*	2.28110	.001	2.9634	11.9204
		2	-6.67276	11.48521	.561	-29.2216	15.8761
		3	14.02199*	3.10511	.000	7.9257	20.1182
		4	12.54383*	2.43582	.000	7.7616	17.3261
		6	4.14002	2.25019	.066	-.2778	8.5578
		7	16.23946*	4.95595	.001	6.5095	25.9695
	6	1	3.30188	2.02076	.103	-.6655	7.2692
		2	-10.81279	11.43636	.345	-33.2657	11.6402
		3	9.88196*	2.91921	.001	4.1507	15.6132
		4	8.40381*	2.19392	.000	4.0965	12.7111
		5	-4.14002	2.25019	.066	-8.5578	.2778
		7	12.09944*	4.84164	.013	2.5939	21.6050
	7	1	-8.79755	4.85608	.070	-18.3315	.7364
		2	-22.91222	12.25921	.062	-46.9807	1.1562
		3	-2.21748	5.29338	.675	-12.6099	8.1750
		4	-3.69563	4.93065	.454	-13.3760	5.9847
		5	-16.23946*	4.95595	.001	-25.9695	-6.5095
		6	-12.09944*	4.84164	.013	-21.6050	-2.5939

Table C-40 CONO

Dependent Variable	(I) LFeat	(J) LFeat	Mean Difference (I-J)	Std. Error	Sig.	95% Confidence Interval	
						Lower Bound	Upper Bound
dTEC	1	2	5.32651	7.23105	.462	-8.8702	19.5232
		3	7.37272*	1.85989	.000	3.7212	11.0242
		4	6.37820*	1.40647	.000	3.6169	9.1395
		5	9.77264*	1.43813	.000	6.9492	12.5961
		6	22.04368*	1.27860	.000	19.5334	24.5539
		7	5.40044	3.06879	.079	-.6245	11.4254
	2	1	-5.32651	7.23105	.462	-19.5232	8.8702
		3	2.04621	7.35259	.781	-12.3891	16.4815
		4	1.05169	7.25118	.885	-13.1845	15.2879
		5	4.44613	7.25738	.540	-9.8023	18.6945
		6	16.71717*	7.22746	.021	2.5275	30.9068
		7	.07393	7.74718	.992	-15.1361	15.2840
	3	1	-7.37272*	1.85989	.000	-11.0242	-3.7212
		2	-2.04621	7.35259	.781	-16.4815	12.3891
		4	-.99452	1.93666	.608	-4.7968	2.8077
		5	2.39992	1.95977	.221	-1.4477	6.2475
		6	14.67096*	1.84589	.000	11.0469	18.2950
		7	-1.97228	3.34514	.556	-8.5398	4.5952
	4	1	-6.37820*	1.40647	.000	-9.1395	-3.6169
		2	-1.05169	7.25118	.885	-15.2879	13.1845
		3	.99452	1.93666	.608	-2.8077	4.7968
		5	3.39444*	1.53613	.027	.3786	6.4103
		6	15.66548*	1.38790	.000	12.9406	18.3903
		7	-.97776	3.11592	.754	-7.0952	5.1397
	5	1	-9.77264*	1.43813	.000	-12.5961	-6.9492
		2	-4.44613	7.25738	.540	-18.6945	9.8023
		3	-2.39992	1.95977	.221	-6.2475	1.4477
		4	-3.39444*	1.53613	.027	-6.4103	-.3786
		6	12.27104*	1.41998	.000	9.4832	15.0589
		7	-4.37220	3.13034	.163	-10.5180	1.7736
	6	1	-22.04368*	1.27860	.000	-24.5539	-19.5334
		2	-16.71717*	7.22746	.021	-30.9068	-2.5275
		3	-14.67096*	1.84589	.000	-18.2950	-11.0469
		4	-15.66548*	1.38790	.000	-18.3903	-12.9406
		5	-12.27104*	1.41998	.000	-15.0589	-9.4832
		7	-16.64324*	3.06032	.000	-22.6516	-10.6349
	7	1	-5.40044	3.06879	.079	-11.4254	.6245
		2	-.07393	7.74718	.992	-15.2840	15.1361
		3	1.97228	3.34514	.556	-4.5952	8.5398
		4	.97776	3.11592	.754	-5.1397	7.0952
		5	4.37220	3.13034	.163	-1.7736	10.5180
		6	16.64324*	3.06032	.000	10.6349	22.6516

Table C-41 COPO

Dependent Variable	(I) LFeat	(J) LFeat	Mean Difference (I-J)	Std. Error	Sig.	95% Confidence Interval	
						Lower Bound	Upper Bound
dTEC	1	2	3.52705	16.31243	.829	-28.4991	35.5532
		3	21.40970*	4.19570	.000	13.1723	29.6471
		4	30.84807*	3.17284	.000	24.6188	37.0773
		5	-45.83320*	3.25195	.000	-52.2177	-39.4487
		6	-14.01585*	2.88081	.000	-19.6717	-8.3600
		7	28.86450*	6.92285	.000	15.2729	42.4561
	2	1	-3.52705	16.31243	.829	-35.5532	28.4991
		3	17.88265	16.58661	.281	-14.6818	50.4471
		4	27.32101	16.35783	.095	-4.7943	59.4363
		5	-49.36025*	16.37336	.003	-81.5060	-17.2145
		6	-17.54290	16.30370	.282	-49.5519	14.4661
		7	25.33745	17.47677	.148	-8.9746	59.6495
	3	1	-21.40970*	4.19570	.000	-29.6471	-13.1723
		2	-17.88265	16.58661	.281	-50.4471	14.6818
		4	9.43836*	4.36888	.031	.8610	18.0158
		5	-67.24291*	4.42666	.000	-75.9338	-58.5521
		6	-35.42555*	4.16164	.000	-43.5961	-27.2550
		7	7.45479	7.54626	.324	-7.3607	22.2703
	4	1	-30.84807*	3.17284	.000	-37.0773	-24.6188
		2	-27.32101	16.35783	.095	-59.4363	4.7943
		3	-9.43836*	4.36888	.031	-18.0158	-.8610
		5	-76.68127*	3.47252	.000	-83.4988	-69.8637
		6	-44.86391*	3.12766	.000	-51.0044	-38.7234
		7	-1.98357	7.02915	.778	-15.7839	11.8167
	5	1	45.83320*	3.25195	.000	39.4487	52.2177
		2	49.36025*	16.37336	.003	17.2145	81.5060
		3	67.24291*	4.42666	.000	58.5521	75.9338
		4	76.68127*	3.47252	.000	69.8637	83.4988
		6	31.81736*	3.20788	.000	25.5193	38.1154
		7	74.69770*	7.06521	.000	60.8266	88.5688
	6	1	14.01585*	2.88081	.000	8.3600	19.6717
		2	17.54290	16.30370	.282	-14.4661	49.5519
		3	35.42555*	4.16164	.000	27.2550	43.5961
		4	44.86391*	3.12766	.000	38.7234	51.0044
		5	-31.81736*	3.20788	.000	-38.1154	-25.5193
		7	42.88035*	6.90225	.000	29.3292	56.4315
	7	1	-28.86450*	6.92285	.000	-42.4561	-15.2729
		2	-25.33745	17.47677	.148	-59.6495	8.9746
		3	-7.45479	7.54626	.324	-22.2703	7.3607
		4	1.98357	7.02915	.778	-11.8167	15.7839
		5	-74.69770*	7.06521	.000	-88.5688	-60.8266
		6	-42.88035*	6.90225	.000	-56.4315	-29.3292

Table C-42 COYQ

Dependent Variable	(I) LFeat	(J) LFeat	Mean Difference (I-J)	Std. Error	Sig.	95% Confidence Interval	
						Lower Bound	Upper Bound
dTEC	1	2	-50.84132*	11.90903	.000	-74.2223	-27.4604
		3	-31.66233*	3.06311	.000	-37.6761	-25.6485
		4	2.28765	2.54433	.369	-2.7076	7.2829
		5	-20.32399*	2.21079	.000	-24.6644	-15.9836
		6	19.40463*	2.10316	.000	15.2755	23.5338
		7	-9.29170	5.05408	.066	-19.2144	.6310
	2	1	50.84132*	11.90903	.000	27.4604	74.2223
		3	19.17899	12.10920	.114	-4.5950	42.9529
		4	53.12897*	11.98848	.000	29.5920	76.6659
		5	30.51733*	11.92215	.011	7.1106	53.9240
		6	70.24594*	11.90266	.000	46.8775	93.6144
		7	41.54962*	12.75907	.001	16.4998	66.5995
	3	1	31.66233*	3.06311	.000	25.6485	37.6761
		2	-19.17899	12.10920	.114	-42.9529	4.5950
		4	33.94998*	3.35876	.000	27.3557	40.5442
		5	11.33834*	3.11371	.000	5.2252	17.4515
		6	51.06696*	3.03824	.000	45.1020	57.0319
		7	22.37063*	5.50921	.000	11.5544	33.1868
	4	1	-2.28765	2.54433	.369	-7.2829	2.7076
		2	-53.12897*	11.98848	.000	-76.6659	-29.5920
		3	-33.94998*	3.35876	.000	-40.5442	-27.3557
		5	-22.61164*	2.60503	.000	-27.7261	-17.4972
		6	17.11698*	2.51434	.000	12.1806	22.0534
		7	-11.57935*	5.23855	.027	-21.8642	-1.2945
	5	1	20.32399*	2.21079	.000	15.9836	24.6644
		2	-30.51733*	11.92215	.011	-53.9240	-7.1106
		3	-11.33834*	3.11371	.000	-17.4515	-5.2252
		4	22.61164*	2.60503	.000	17.4972	27.7261
		6	39.72861*	2.17620	.000	35.4561	44.0011
		7	11.03229*	5.08491	.030	1.0491	21.0155
	6	1	-19.40463*	2.10316	.000	-23.5338	-15.2755
		2	-70.24594*	11.90266	.000	-93.6144	-46.8775
		3	-51.06696*	3.03824	.000	-57.0319	-45.1020
		4	-17.11698*	2.51434	.000	-22.0534	-12.1806
		5	-39.72861*	2.17620	.000	-44.0011	-35.4561
		7	-28.69633*	5.03905	.000	-38.5895	-18.8032
	7	1	9.29170	5.05408	.066	-.6310	19.2144
		2	-41.54962*	12.75907	.001	-66.5995	-16.4998
		3	-22.37063*	5.50921	.000	-33.1868	-11.5544
		4	11.57935*	5.23855	.027	1.2945	21.8642
		5	-11.03229*	5.08491	.030	-21.0155	-1.0491
		6	28.69633*	5.03905	.000	18.8032	38.5895

Table C-43 GOGA

Dependent Variable	(I) LFeat	(J) LFeat	Mean Difference (I-J)	Std. Error	Sig.	95% Confidence Interval	
						Lower Bound	Upper Bound
dTEC	1	2	-11.06151	11.59976	.341	-33.8353	11.7123
		3	6.56927*	2.98356	.028	.7117	12.4269
		4	-47.91407*	2.25621	.000	-52.3437	-43.4845
		5	9.78119*	2.31246	.000	5.2412	14.3212
		6	47.38484*	2.04854	.000	43.3629	51.4067
		7	86.79296*	4.92283	.000	77.1280	96.4579
	2	1	11.06151	11.59976	.341	-11.7123	33.8353
		3	17.63078	11.79473	.135	-5.5258	40.7873
		4	-36.85256*	11.63205	.002	-59.6897	-14.0154
		5	20.84270	11.64309	.074	-2.0161	43.7015
		6	58.44635*	11.59356	.000	35.6848	81.2079
		7	97.85447*	12.42772	.000	73.4552	122.2538
	3	1	-6.56927*	2.98356	.028	-12.4269	-.7117
		2	-17.63078	11.79473	.135	-40.7873	5.5258
		4	-54.48334*	3.10671	.000	-60.5827	-48.3839
		5	3.21192	3.14780	.308	-2.9681	9.3920
		6	40.81557*	2.95934	.000	35.0055	46.6256
		7	80.22369*	5.36614	.000	69.6884	90.7590
	4	1	47.91407*	2.25621	.000	43.4845	52.3437
		2	36.85256*	11.63205	.002	14.0154	59.6897
		3	54.48334*	3.10671	.000	48.3839	60.5827
		5	57.69527*	2.46930	.000	52.8473	62.5432
		6	95.29891*	2.22408	.000	90.9324	99.6654
		7	134.70704*	4.99843	.000	124.8936	144.5204
	5	1	-9.78119*	2.31246	.000	-14.3212	-5.2412
		2	-20.84270	11.64309	.074	-43.7015	2.0161
		3	-3.21192	3.14780	.308	-9.3920	2.9681
		4	-57.69527*	2.46930	.000	-62.5432	-52.8473
		6	37.60365*	2.28112	.000	33.1251	42.0822
		7	77.01177*	5.02407	.000	67.1480	86.8755
	6	1	-47.38484*	2.04854	.000	-51.4067	-43.3629
		2	-58.44635*	11.59356	.000	-81.2079	-35.6848
		3	-40.81557*	2.95934	.000	-46.6256	-35.0055
		4	-95.29891*	2.22408	.000	-99.6654	-90.9324
		5	-37.60365*	2.28112	.000	-42.0822	-33.1251
		7	39.40812*	4.90819	.000	29.7719	49.0444
	7	1	-86.79296*	4.92283	.000	-96.4579	-77.1280
		2	-97.85447*	12.42772	.000	-122.2538	-73.4552
		3	-80.22369*	5.36614	.000	-90.7590	-69.6884
		4	-134.70704*	4.99843	.000	-144.5204	-124.8936
		5	-77.01177*	5.02407	.000	-86.8755	-67.1480
		6	-39.40812*	4.90819	.000	-49.0444	-29.7719

Table C-44 HUGO

Dependent Variable	(I) LFeat	(J) LFeat	Mean Difference (I-J)	Std. Error	Sig.	95% Confidence Interval	
						Lower Bound	Upper Bound
dTEC	1	2	1.57276	6.48453	.808	-11.1583	14.3038
		3	-6.42722*	1.66788	.000	-9.7018	-3.1527
		4	3.59415*	1.26127	.005	1.1179	6.0704
		5	7.56146*	1.29272	.000	5.0235	10.0994
		6	4.51589*	1.14518	.000	2.2676	6.7642
		7	-26.51643*	2.75197	.000	-31.9194	-21.1135
	2	1	-1.57276	6.48453	.808	-14.3038	11.1583
		3	-7.99998	6.59352	.225	-20.9450	4.9450
		4	2.02139	6.50257	.756	-10.7451	14.7879
		5	5.98870	6.50875	.358	-6.7899	18.7673
		6	2.94313	6.48106	.650	-9.7811	15.6674
		7	-28.08919*	6.94738	.000	-41.7290	-14.4494
	3	1	6.42722*	1.66788	.000	3.1527	9.7018
		2	7.99998	6.59352	.225	-4.9450	20.9450
		4	10.02137*	1.73672	.000	6.6117	13.4311
		5	13.98868*	1.75969	.000	10.5339	17.4435
		6	10.94311*	1.65434	.000	7.6952	14.1911
		7	-20.08921*	2.99979	.000	-25.9787	-14.1997
	4	1	-3.59415*	1.26127	.005	-6.0704	-1.1179
		2	-2.02139	6.50257	.756	-14.7879	10.7451
		3	-10.02137*	1.73672	.000	-13.4311	-6.6117
		5	3.96732*	1.38040	.004	1.2572	6.6774
		6	.92174	1.24331	.459	-1.5192	3.3627
		7	-30.11058*	2.79423	.000	-35.5965	-24.6247
	5	1	-7.56146*	1.29272	.000	-10.0994	-5.0235
		2	-5.98870	6.50875	.358	-18.7673	6.7899
		3	-13.98868*	1.75969	.000	-17.4435	-10.5339
		4	-3.96732*	1.38040	.004	-6.6774	-1.2572
		6	-3.04557*	1.27520	.017	-5.5492	-.5420
		7	-34.07789*	2.80857	.000	-39.5919	-28.5638
	6	1	-4.51589*	1.14518	.000	-6.7642	-2.2676
		2	-2.94313	6.48106	.650	-15.6674	9.7811
		3	-10.94311*	1.65434	.000	-14.1911	-7.6952
		4	-.92174	1.24331	.459	-3.3627	1.5192
		5	3.04557*	1.27520	.017	.5420	5.5492
		7	-31.03232*	2.74379	.000	-36.4192	-25.6454
	7	1	26.51643*	2.75197	.000	21.1135	31.9194
		2	28.08919*	6.94738	.000	14.4494	41.7290
		3	20.08921*	2.99979	.000	14.1997	25.9787
		4	30.11058*	2.79423	.000	24.6247	35.5965
		5	34.07789*	2.80857	.000	28.5638	39.5919
		6	31.03232*	2.74379	.000	25.6454	36.4192

Table C-45 IQQE

Dependent Variable	(I) LFeat	(J) LFeat	Mean Difference (I-J)	Std. Error	Sig.	95% Confidence Interval	
						Lower Bound	Upper Bound
dTEC	1	2	-21.85485	11.71387	.062	-44.8527	1.1430
		3	-3.50347	3.01291	.245	-9.4187	2.4118
		4	-5.97939*	2.50264	.017	-10.8928	-1.0660
		5	-33.38057*	2.17456	.000	-37.6499	-29.1113
		6	-34.40772*	2.06869	.000	-38.4692	-30.3463
		7	-20.71964*	4.97126	.000	-30.4797	-10.9596
	2	1	21.85485	11.71387	.062	-1.1430	44.8527
		3	18.35138	11.91076	.124	-5.0330	41.7357
		4	15.87546	11.79202	.179	-7.2758	39.0267
		5	-11.52571	11.72677	.326	-34.5489	11.4974
		6	-12.55287	11.70761	.284	-35.5384	10.4326
		7	1.13521	12.54998	.928	-23.5041	25.7745
	3	1	3.50347	3.01291	.245	-2.4118	9.4187
		2	-18.35138	11.91076	.124	-41.7357	5.0330
		4	-2.47592	3.30372	.454	-8.9621	4.0103
		5	-29.87709*	3.06269	.000	-35.8901	-23.8641
		6	-30.90425*	2.98845	.000	-36.7715	-25.0370
		7	-17.21617*	5.41893	.002	-27.8551	-6.5772
	4	1	5.97939*	2.50264	.017	1.0660	10.8928
		2	-15.87546	11.79202	.179	-39.0267	7.2758
		3	2.47592	3.30372	.454	-4.0103	8.9621
		5	-27.40117*	2.56234	.000	-32.4318	-22.3705
		6	-28.42833*	2.47314	.000	-33.2838	-23.5728
		7	-14.74025*	5.15270	.004	-24.8565	-4.6240
	5	1	33.38057*	2.17456	.000	29.1113	37.6499
		2	11.52571	11.72677	.326	-11.4974	34.5489
		3	29.87709*	3.06269	.000	23.8641	35.8901
		4	27.40117*	2.56234	.000	22.3705	32.4318
		6	-1.02716	2.14054	.631	-5.2297	3.1754
		7	12.66093*	5.00158	.012	2.8413	22.4805
	6	1	34.40772*	2.06869	.000	30.3463	38.4692
		2	12.55287	11.70761	.284	-10.4326	35.5384
		3	30.90425*	2.98845	.000	25.0370	36.7715
		4	28.42833*	2.47314	.000	23.5728	33.2838
		5	1.02716	2.14054	.631	-3.1754	5.2297
		7	13.68809*	4.95647	.006	3.9571	23.4191
	7	1	20.71964*	4.97126	.000	10.9596	30.4797
		2	-1.13521	12.54998	.928	-25.7745	23.5041
		3	17.21617*	5.41893	.002	6.5772	27.8551
		4	14.74025*	5.15270	.004	4.6240	24.8565
		5	-12.66093*	5.00158	.012	-22.4805	-2.8413
		6	-13.68809*	4.95647	.006	-23.4191	-3.9571

Table C-46 LAFE

Dependent Variable	(I) LFeat	(J) LFeat	Mean Difference (I-J)	Std. Error	Sig.	95% Confidence Interval	
						Lower Bound	Upper Bound
dTEC	1	2	16.45578	10.60896	.121	-4.3729	37.2845
		3	14.72085*	2.74645	.000	9.3287	20.1130
		4	-19.79442*	2.06349	.000	-23.8457	-15.7431
		5	-23.60540*	2.12000	.000	-27.7676	-19.4432
		6	3.37070	1.87356	.072	-.3077	7.0491
		7	-5.90378	4.62133	.202	-14.9769	3.1693
	2	1	-16.45578	10.60896	.121	-37.2845	4.3729
		3	-1.73493	10.79177	.872	-22.9225	19.4527
		4	-36.25020*	10.63848	.001	-57.1369	-15.3636
		5	-40.06118*	10.64959	.000	-60.9696	-19.1527
		6	-13.08508	10.60328	.218	-33.9026	7.7325
		7	-22.35956	11.41385	.051	-44.7685	.0494
	3	1	-14.72085*	2.74645	.000	-20.1130	-9.3287
		2	1.73493	10.79177	.872	-19.4527	22.9225
		4	-34.51527*	2.85838	.000	-40.1272	-28.9034
		5	-38.32625*	2.89943	.000	-44.0187	-32.6338
		6	-11.35015*	2.72444	.000	-16.6991	-6.0012
		7	-20.62463*	5.02683	.000	-30.4939	-10.7554
	4	1	19.79442*	2.06349	.000	15.7431	23.8457
		2	36.25020*	10.63848	.001	15.3636	57.1369
		3	34.51527*	2.85838	.000	28.9034	40.1272
		5	-3.81098	2.26313	.093	-8.2542	.6322
		6	23.16512*	2.03411	.000	19.1715	27.1587
		7	13.89064*	4.68872	.003	4.6852	23.0961
	5	1	23.60540*	2.12000	.000	19.4432	27.7676
		2	40.06118*	10.64959	.000	19.1527	60.9696
		3	38.32625*	2.89943	.000	32.6338	44.0187
		4	3.81098	2.26313	.093	-.6322	8.2542
		6	26.97610*	2.09141	.000	22.8700	31.0822
		7	17.70162*	4.71386	.000	8.4468	26.9564
	6	1	-3.37070	1.87356	.072	-7.0491	.3077
		2	13.08508	10.60328	.218	-7.7325	33.9026
		3	11.35015*	2.72444	.000	6.0012	16.6991
		4	-23.16512*	2.03411	.000	-27.1587	-19.1715
		5	-26.97610*	2.09141	.000	-31.0822	-22.8700
		7	-9.27448*	4.60829	.045	-18.3220	-.2270
	7	1	5.90378	4.62133	.202	-3.1693	14.9769
		2	22.35956	11.41385	.051	-.0494	44.7685
		3	20.62463*	5.02683	.000	10.7554	30.4939
		4	-13.89064*	4.68872	.003	-23.0961	-4.6852
		5	-17.70162*	4.71386	.000	-26.9564	-8.4468
		6	9.27448*	4.60829	.045	.2270	18.3220

Table C-47 LAMT

Dependent Variable	(I) LFeat	(J) LFeat	Mean Difference (I-J)	Std. Error	Sig.	95% Confidence Interval	
						Lower Bound	Upper Bound
dTEC	1	2	24.14928*	11.38103	.034	1.8049	46.4936
		3	22.06446*	2.92730	.000	16.3173	27.8116
		4	42.45987*	2.21366	.000	38.1138	46.8059
		5	23.03301*	2.26885	.000	18.5786	27.4874
		6	-.66497	2.00991	.741	-4.6110	3.2811
		7	-56.56192*	4.83000	.000	-66.0446	-47.0792
	2	1	-24.14928*	11.38103	.034	-46.4936	-1.8049
		3	-2.08482	11.57232	.857	-24.8047	20.6351
		4	18.31059	11.41271	.109	-4.0959	40.7171
		5	-1.11627	11.42354	.922	-23.5441	21.3115
		6	-24.81425*	11.37494	.029	-47.1466	-2.4819
		7	-80.71120*	12.19338	.000	-104.6504	-56.7720
	3	1	-22.06446*	2.92730	.000	-27.8116	-16.3173
		2	2.08482	11.57232	.857	-20.6351	24.8047
		4	20.39541*	3.04813	.000	14.4110	26.3798
		5	.96855	3.08844	.754	-5.0950	7.0321
		6	-22.72943*	2.90354	.000	-28.4299	-17.0289
		7	-78.62638*	5.26495	.000	-88.9630	-68.2897
	4	1	-42.45987*	2.21366	.000	-46.8059	-38.1138
		2	-18.31059	11.41271	.109	-40.7171	4.0959
		3	-20.39541*	3.04813	.000	-26.3798	-14.4110
		5	-19.42686*	2.42274	.000	-24.1834	-14.6703
		6	-43.12484*	2.18214	.000	-47.4090	-38.8407
		7	-99.02179*	4.90417	.000	-108.6501	-89.3934
	5	1	-23.03301*	2.26885	.000	-27.4874	-18.5786
		2	1.11627	11.42354	.922	-21.3115	23.5441
		3	-.96855	3.08844	.754	-7.0321	5.0950
		4	19.42686*	2.42274	.000	14.6703	24.1834
		6	-23.69798*	2.23811	.000	-28.0920	-19.3039
		7	-79.59492*	4.92933	.000	-89.2727	-69.9172
	6	1	.66497	2.00991	.741	-3.2811	4.6110
		2	24.81425*	11.37494	.029	2.4819	47.1466
		3	22.72943*	2.90354	.000	17.0289	28.4299
		4	43.12484*	2.18214	.000	38.8407	47.4090
		5	23.69798*	2.23811	.000	19.3039	28.0920
		7	-55.89695*	4.81564	.000	-65.3515	-46.4424
	7	1	56.56192*	4.83000	.000	47.0792	66.0446
		2	80.71120*	12.19338	.000	56.7720	104.6504
		3	78.62638*	5.26495	.000	68.2897	88.9630
		4	99.02179*	4.90417	.000	89.3934	108.6501
		5	79.59492*	4.92933	.000	69.9172	89.2727
		6	55.89695*	4.81564	.000	46.4424	65.3515

Table C-48 POYE

Dependent Variable	(I) LFeat	(J) LFeat	Mean Difference (I-J)	Std. Error	Sig.	95% Confidence Interval	
						Lower Bound	Upper Bound
dTEC	1	2	2.06373	14.62633	.888	-26.6521	30.7795
		3	37.63841*	3.76202	.000	30.2524	45.0244
		4	37.99580*	2.85093	.000	32.3986	43.5930
		5	46.81374*	2.90893	.000	41.1026	52.5248
		6	61.15578*	2.58304	.000	56.0845	66.2270
		7	52.89209*	6.20728	.000	40.7054	65.0788
	2	1	-2.06373	14.62633	.888	-30.7795	26.6521
		3	35.57468*	14.87217	.017	6.3762	64.7732
		4	35.93207*	14.66821	.015	7.1340	64.7301
		5	44.75001*	14.67959	.002	15.9296	73.5704
		6	59.09205*	14.61850	.000	30.3916	87.7925
		7	50.82836*	15.67032	.001	20.0629	81.5938
	3	1	-37.63841*	3.76202	.000	-45.0244	-30.2524
		2	-35.57468*	14.87217	.017	-64.7732	-6.3762
		4	.35739	3.92169	.927	-7.3420	8.0568
		5	9.17533*	3.96405	.021	1.3927	16.9579
		6	23.51737*	3.73148	.000	16.1914	30.8434
		7	15.25368*	6.76625	.024	1.9695	28.5378
	4	1	-37.99580*	2.85093	.000	-43.5930	-32.3986
		2	-35.93207*	14.66821	.015	-64.7301	-7.1340
		3	-.35739	3.92169	.927	-8.0568	7.3420
		5	8.81794*	3.11267	.005	2.7068	14.9290
		6	23.15998*	2.81050	.000	17.6421	28.6778
		7	14.89629*	6.30533	.018	2.5171	27.2755
	5	1	-46.81374*	2.90893	.000	-52.5248	-41.1026
		2	-44.75001*	14.67959	.002	-73.5704	-15.9296
		3	-9.17533*	3.96405	.021	-16.9579	-1.3927
		4	-8.81794*	3.11267	.005	-14.9290	-2.7068
		6	14.34204*	2.86932	.000	8.7087	19.9754
		7	6.07835	6.33176	.337	-6.3528	18.5095
	6	1	-61.15578*	2.58304	.000	-66.2270	-56.0845
		2	-59.09205*	14.61850	.000	-87.7925	-30.3916
		3	-23.51737*	3.73148	.000	-30.8434	-16.1914
		4	-23.15998*	2.81050	.000	-28.6778	-17.6421
		5	-14.34204*	2.86932	.000	-19.9754	-8.7087
		7	-8.26369	6.18882	.182	-20.4142	3.8868
	7	1	-52.89209*	6.20728	.000	-65.0788	-40.7054
		2	-50.82836*	15.67032	.001	-81.5938	-20.0629
		3	-15.25368*	6.76625	.024	-28.5378	-1.9695
		4	-14.89629*	6.30533	.018	-27.2755	-2.5171
		5	-6.07835	6.33176	.337	-18.5095	6.3528
		6	8.26369	6.18882	.182	-3.8868	20.4142

Table C-49 RIOP

Dependent Variable	(I) LFeat	(J) LFeat	Mean Difference (I-J)	Std. Error	Sig.	95% Confidence Interval	
						Lower Bound	Upper Bound
dTEC	1	2	-7.38241	11.99779	.539	-30.9376	16.1728
		3	3.81787	3.08594	.216	-2.2407	9.8765
		4	9.97813*	2.33363	.000	5.3965	14.5597
		5	-22.70330*	2.39181	.000	-27.3991	-18.0075
		6	17.07335*	2.11883	.000	12.9134	21.2332
		7	-5.94522	5.09175	.243	-15.9418	4.0514
	2	1	7.38241	11.99779	.539	-16.1728	30.9376
		3	11.20028	12.19945	.359	-12.7509	35.1514
		4	17.36054	12.03118	.149	-6.2602	40.9813
		5	-15.32089	12.04260	.204	-38.9641	8.3223
		6	24.45576*	11.99137	.042	.9131	47.9984
		7	1.43719	12.85416	.911	-23.7993	26.6737
	3	1	-3.81787	3.08594	.216	-9.8765	2.2407
		2	-11.20028	12.19945	.359	-35.1514	12.7509
		4	6.16026	3.21331	.056	-.1484	12.4689
		5	-26.52117*	3.25581	.000	-32.9133	-20.1290
		6	13.25548*	3.06089	.000	7.2461	19.2649
		7	-9.76309	5.55027	.079	-20.6599	1.1337
	4	1	-9.97813*	2.33363	.000	-14.5597	-5.3965
		2	-17.36054	12.03118	.149	-40.9813	6.2602
		3	-6.16026	3.21331	.056	-12.4689	.1484
		5	-32.68143*	2.55403	.000	-37.6958	-27.6671
		6	7.09522*	2.30040	.002	2.5789	11.6116
		7	-15.92335*	5.16994	.002	-26.0735	-5.7732
	5	1	22.70330*	2.39181	.000	18.0075	27.3991
		2	15.32089	12.04260	.204	-8.3223	38.9641
		3	26.52117*	3.25581	.000	20.1290	32.9133
		4	32.68143*	2.55403	.000	27.6671	37.6958
		6	39.77665*	2.35939	.000	35.1445	44.4088
		7	16.75808*	5.19646	.001	6.5559	26.9603
	6	1	-17.07335*	2.11883	.000	-21.2332	-12.9134
		2	-24.45576*	11.99137	.042	-47.9984	-.9131
		3	-13.25548*	3.06089	.000	-19.2649	-7.2461
		4	-7.09522*	2.30040	.002	-11.6116	-2.5789
		5	-39.77665*	2.35939	.000	-44.4088	-35.1445
		7	-23.01856*	5.07661	.000	-32.9855	-13.0517
	7	1	5.94522	5.09175	.243	-4.0514	15.9418
		2	-1.43719	12.85416	.911	-26.6737	23.7993
		3	9.76309	5.55027	.079	-1.1337	20.6599
		4	15.92335*	5.16994	.002	5.7732	26.0735
		5	-16.75808*	5.19646	.001	-26.9603	-6.5559
		6	23.01856*	5.07661	.000	13.0517	32.9855

Table C-50 SCUB

Dependent Variable	(I) LFeat	(J) LFeat	Mean Difference (I-J)	Std. Error	Sig.	95% Confidence Interval	
						Lower Bound	Upper Bound
dTEC	1	2	29.37210*	7.75673	.000	14.1433	44.6009
		3	15.36519*	1.99510	.000	11.4482	19.2822
		4	12.12134*	1.50872	.000	9.1593	15.0834
		5	7.52677*	1.54633	.000	4.4909	10.5627
		6	9.90485*	1.36985	.000	7.2154	12.5943
		7	-10.09231*	3.29188	.002	-16.5553	-3.6294
	2	1	-29.37210*	7.75673	.000	-44.6009	-14.1433
		3	-14.00691	7.88710	.076	-29.4916	1.4778
		4	-17.25077*	7.77832	.027	-32.5219	-1.9796
		5	-21.84534*	7.78570	.005	-37.1310	-6.5597
		6	-19.46726*	7.75258	.012	-34.6879	-4.2466
		7	-39.46442*	8.31038	.000	-55.7802	-23.1487
	3	1	-15.36519*	1.99510	.000	-19.2822	-11.4482
		2	14.00691	7.88710	.076	-1.4778	29.4916
		4	-3.24385	2.07745	.119	-7.3225	.8348
		5	-7.83842*	2.10492	.000	-11.9710	-3.7058
		6	-5.46034*	1.97890	.006	-9.3455	-1.5752
		7	-25.45750*	3.58832	.000	-32.5024	-18.4126
	4	1	-12.12134*	1.50872	.000	-15.0834	-9.1593
		2	17.25077*	7.77832	.027	1.9796	32.5219
		3	3.24385	2.07745	.119	-.8348	7.3225
		5	-4.59457*	1.65122	.006	-7.8364	-1.3527
		6	-2.21649	1.48724	.137	-5.1364	.7034
		7	-22.21365*	3.34243	.000	-28.7758	-15.6515
	5	1	-7.52677*	1.54633	.000	-10.5627	-4.4909
		2	21.84534*	7.78570	.005	6.5597	37.1310
		3	7.83842*	2.10492	.000	3.7058	11.9710
		4	4.59457*	1.65122	.006	1.3527	7.8364
		6	2.37808	1.52538	.119	-.6167	5.3729
		7	-17.61908*	3.35958	.000	-24.2149	-11.0232
	6	1	-9.90485*	1.36985	.000	-12.5943	-7.2154
		2	19.46726*	7.75258	.012	4.2466	34.6879
		3	5.46034*	1.97890	.006	1.5752	9.3455
		4	2.21649	1.48724	.137	-.7034	5.1364
		5	-2.37808	1.52538	.119	-5.3729	.6167
		7	-19.99716*	3.28209	.000	-26.4409	-13.5534
	7	1	10.09231*	3.29188	.002	3.6294	16.5553
		2	39.46442*	8.31038	.000	23.1487	55.7802
		3	25.45750*	3.58832	.000	18.4126	32.5024
		4	22.21365*	3.34243	.000	15.6515	28.7758
		5	17.61908*	3.35958	.000	11.0232	24.2149
		6	19.99716*	3.28209	.000	13.5534	26.4409

Table C-51 UNSA

Dependent Variable	(I) LFeat	(J) LFeat	Mean Difference (I-J)	Std. Error	Sig.	95% Confidence Interval	
						Lower Bound	Upper Bound
dTEC	1	2	-28.75918*	13.23991	.030	-54.7543	-2.7641
		3	4.39002	3.85486	.255	-3.1786	11.9586
		4	5.70063*	2.57522	.027	.6445	10.7568
		5	-40.34871*	2.65214	.000	-45.5559	-35.1415
		6	-23.30221*	2.33819	.000	-27.8930	-18.7114
		7	-3.28454	5.76739	.569	-14.6082	8.0391
	2	1	28.75918*	13.23991	.030	2.7641	54.7543
		3	33.14920*	13.58309	.015	6.4803	59.8181
		4	34.45982*	13.27675	.010	8.3924	60.5272
		5	-11.58953	13.29189	.384	-37.6867	14.5076
		6	5.45698	13.23282	.680	-20.5242	31.4381
		7	25.47464	14.24441	.074	-2.4927	53.4420
	3	1	-4.39002	3.85486	.255	-11.9586	3.1786
		2	-33.14920*	13.58309	.015	-59.8181	-6.4803
		4	1.31062	3.97958	.742	-6.5028	9.1241
		5	-44.73873*	4.02978	.000	-52.6508	-36.8267
		6	-27.69222*	3.83046	.000	-35.2129	-20.1715
		7	-7.67456	6.51676	.239	-20.4695	5.1204
	4	1	-5.70063*	2.57522	.027	-10.7568	-.6445
		2	-34.45982*	13.27675	.010	-60.5272	-8.3924
		3	-1.31062	3.97958	.742	-9.1241	6.5028
		5	-46.04935*	2.83037	.000	-51.6065	-40.4922
		6	-29.00284*	2.53855	.000	-33.9870	-24.0187
		7	-8.98517	5.85149	.125	-20.4739	2.5036
	5	1	40.34871*	2.65214	.000	35.1415	45.5559
		2	11.58953	13.29189	.384	-14.5076	37.6867
		3	44.73873*	4.02978	.000	36.8267	52.6508
		4	46.04935*	2.83037	.000	40.4922	51.6065
		6	17.04651*	2.61655	.000	11.9092	22.1838
		7	37.06417*	5.88575	.000	25.5082	48.6202
	6	1	23.30221*	2.33819	.000	18.7114	27.8930
		2	-5.45698	13.23282	.680	-31.4381	20.5242
		3	27.69222*	3.83046	.000	20.1715	35.2129
		4	29.00284*	2.53855	.000	24.0187	33.9870
		5	-17.04651*	2.61655	.000	-22.1838	-11.9092
		7	20.01766*	5.75111	.001	8.7260	31.3093
	7	1	3.28454	5.76739	.569	-8.0391	14.6082
		2	-25.47464	14.24441	.074	-53.4420	2.4927
		3	7.67456	6.51676	.239	-5.1204	20.4695
		4	8.98517	5.85149	.125	-2.5036	20.4739
		5	-37.06417*	5.88575	.000	-48.6202	-25.5082
		6	-20.01766*	5.75111	.001	-31.3093	-8.7260

Event VI Mean percentage deviation of TECU for each phenomena of Event I from IGS stations.

Table C-52 BAIE

Dependent Variable	(I) LFeat	(J) LFeat	Mean Difference (I-J)	Std. Error	Sig.	95% Confidence Interval	
						Lower Bound	Upper Bound
dTEC	1	2	-20.10090*	8.45233	.018	-36.6953	-3.5065
		3	21.40543*	5.00917	.000	11.5710	31.2399
		4	50.97333*	3.65033	.000	43.8067	58.1400
		5	28.94303*	2.96961	.000	23.1128	34.7732
	2	1	20.10090*	8.45233	.018	3.5065	36.6953
		3	41.50632*	9.24023	.000	23.3651	59.6475
		4	71.07423*	8.57991	.000	54.2294	87.9191
		5	49.04392*	8.31316	.000	32.7228	65.3650
	3	1	-21.40543*	5.00917	.000	-31.2399	-11.5710
		2	-41.50632*	9.24023	.000	-59.6475	-23.3651
		4	29.56790*	5.22157	.000	19.3165	39.8193
		5	7.53760	4.77058	.115	-1.8284	16.9036
	4	1	-50.97333*	3.65033	.000	-58.1400	-43.8067
		2	-71.07423*	8.57991	.000	-87.9191	-54.2294
		3	-29.56790*	5.22157	.000	-39.8193	-19.3165
		5	-22.03030*	3.31535	.000	-28.5393	-15.5213
	5	1	-28.94303*	2.96961	.000	-34.7732	-23.1128
		2	-49.04392*	8.31316	.000	-65.3650	-32.7228
		3	-7.53760	4.77058	.115	-16.9036	1.8284
		4	22.03030*	3.31535	.000	15.5213	28.5393

Table C- 53 BOGT

Dependent Variable	(I) LFeat	(J) LFeat	Mean Difference (I-J)	Std. Error	Sig.	95% Confidence Interval	
						Lower Bound	Upper Bound
dTEC	1	2	21.00126*	5.17944	.000	10.8325	31.1701
		3	-.03561	3.06953	.991	-6.0620	5.9908
		4	-15.97890*	2.24167	.000	-20.3800	-11.5778
		5	11.75088*	1.82180	.000	8.1741	15.3276
	2	1	-21.00126*	5.17944	.000	-31.1701	-10.8325
		3	-21.03686*	5.66225	.000	-32.1536	-9.9202
		4	-36.98015*	5.25967	.000	-47.3065	-26.6538
		5	-9.25038	5.09490	.070	-19.2532	.7524
	3	1	.03561	3.06953	.991	-5.9908	6.0620
		2	21.03686*	5.66225	.000	9.9202	32.1536
		4	-15.94329*	3.20305	.000	-22.2318	-9.6547
		5	11.78649*	2.92462	.000	6.0446	17.5284
	4	1	15.97890*	2.24167	.000	11.5778	20.3800
		2	36.98015*	5.25967	.000	26.6538	47.3065
		3	15.94329*	3.20305	.000	9.6547	22.2318
		5	27.72978*	2.03874	.000	23.7271	31.7324
	5	1	-11.75088*	1.82180	.000	-15.3276	-8.1741
		2	9.25038	5.09490	.070	-.7524	19.2532
		3	-11.78649*	2.92462	.000	-17.5284	-6.0446
		4	-27.72978*	2.03874	.000	-31.7324	-23.7271

Table C-54 BRAZ

Dependent Variable	(I) LFeat	(J) LFeat	Mean Difference (I-J)	Std. Error	Sig.	95% Confidence Interval	
						Lower Bound	Upper Bound
dTEC	1	2	11.18721	5.83612	.056	-.2708	22.6452
		3	-37.09937*	3.45871	.000	-43.8898	-30.3089
		4	-48.39089*	2.52588	.000	-53.3499	-43.4319
		5	-35.37470*	2.04928	.000	-39.3980	-31.3514
	2	1	-11.18721	5.83612	.056	-22.6452	.2708
		3	-48.28657*	6.38014	.000	-60.8126	-35.7605
		4	-59.57810*	5.92652	.000	-71.2136	-47.9426
		5	-46.56191*	5.73961	.000	-57.8304	-35.2934
	3	1	37.09937*	3.45871	.000	30.3089	43.8898
		2	48.28657*	6.38014	.000	35.7605	60.8126
		4	-11.29152*	3.60915	.002	-18.3773	-4.2057
		5	1.72466	3.29325	.601	-4.7409	8.1903
	4	1	48.39089*	2.52588	.000	43.4319	53.3499
		2	59.57810*	5.92652	.000	47.9426	71.2136
		3	11.29152*	3.60915	.002	4.2057	18.3773
		5	13.01619*	2.29410	.000	8.5122	17.5202
	5	1	35.37470*	2.04928	.000	31.3514	39.3980
		2	46.56191*	5.73961	.000	35.2934	57.8304
		3	-1.72466	3.29325	.601	-8.1903	4.7409
		4	-13.01619*	2.29410	.000	-17.5202	-8.5122

Table C- 55 CONO

Dependent Variable	(I) LFeat	(J) LFeat	Mean Difference (I-J)	Std. Error	Sig.	95% Confidence Interval	
						Lower Bound	Upper Bound
dTEC	1	2	-18.84387*	4.09856	.000	-26.8905	-10.7972
		3	-13.91489*	2.42896	.000	-18.6836	-9.1461
		4	-26.68927*	1.77386	.000	-30.1719	-23.2067
		5	-11.59890*	1.43916	.000	-14.4244	-8.7734
	2	1	18.84387*	4.09856	.000	10.7972	26.8905
		3	4.92897	4.48062	.272	-3.8678	13.7257
		4	-7.84540	4.16205	.060	-16.0167	.3259
		5	7.24497	4.03079	.073	-.6686	15.1586
	3	1	13.91489*	2.42896	.000	9.1461	18.6836
		2	-4.92897	4.48062	.272	-13.7257	3.8678
		4	-12.77438*	2.53462	.000	-17.7506	-7.7982
		5	2.31599	2.31277	.317	-2.2246	6.8566
	4	1	26.68927*	1.77386	.000	23.2067	30.1719
		2	7.84540	4.16205	.060	-.3259	16.0167
		3	12.77438*	2.53462	.000	7.7982	17.7506
		5	15.09037*	1.61109	.000	11.9273	18.2534
	5	1	11.59890*	1.43916	.000	8.7734	14.4244
		2	-7.24497	4.03079	.073	-15.1586	.6686
		3	-2.31599	2.31277	.317	-6.8566	2.2246
		4	-15.09037*	1.61109	.000	-18.2534	-11.9273

Table C-56 COYQ

Dependent Variable	(I) LFeat	(J) LFeat	Mean Difference (I-J)	Std. Error	Sig.	95% Confidence Interval	
						Lower Bound	Upper Bound
dTEC	1	2	-61.06136*	7.92697	.000	-76.6243	-45.4984
		3	-80.01390*	4.69782	.000	-89.2371	-70.7907
		4	-19.37372*	3.43081	.000	-26.1094	-12.6381
		5	-11.04014*	2.78346	.000	-16.5049	-5.5754
	2	1	61.06136*	7.92697	.000	45.4984	76.6243
		3	-18.95254*	8.66590	.029	-35.9662	-1.9389
		4	41.68764*	8.04976	.000	25.8836	57.4916
		5	50.02122*	7.79589	.000	34.7156	65.3268
	3	1	80.01390*	4.69782	.000	70.7907	89.2371
		2	18.95254*	8.66590	.029	1.9389	35.9662
		4	60.64018*	4.90217	.000	51.0158	70.2646
		5	68.97376*	4.47309	.000	60.1918	77.7557
	4	1	19.37372*	3.43081	.000	12.6381	26.1094
		2	-41.68764*	8.04976	.000	-57.4916	-25.8836
		3	-60.64018*	4.90217	.000	-70.2646	-51.0158
		5	8.33358*	3.11599	.008	2.2160	14.4512
	5	1	11.04014*	2.78346	.000	5.5754	16.5049
		2	-50.02122*	7.79589	.000	-65.3268	-34.7156
		3	-68.97376*	4.47309	.000	-77.7557	-60.1918
		4	-8.33358*	3.11599	.008	-14.4512	-2.2160

Table C-57 LAMT

Dependent Variable	(I) LFeat	(J) LFeat	Mean Difference (I-J)	Std. Error	Sig.	95% Confidence Interval	
						Lower Bound	Upper Bound
dTEC	1	2	-15.12499*	3.28226	.000	-21.5691	-8.6809
		3	-12.14252*	1.94519	.000	-15.9616	-8.3235
		4	-16.50647*	1.42057	.000	-19.2955	-13.7174
		5	-1.81227	1.15716	.118	-4.0841	.4596
	2	1	15.12499*	3.28226	.000	8.6809	21.5691
		3	2.98247	3.58822	.406	-4.0624	10.0273
		4	-1.38148	3.33311	.679	-7.9254	5.1625
		5	13.31272*	3.22964	.000	6.9719	19.6535
	3	1	12.14252*	1.94519	.000	8.3235	15.9616
		2	-2.98247	3.58822	.406	-10.0273	4.0624
		4	-4.36394*	2.02981	.032	-8.3491	-.3788
		5	10.33025*	1.85502	.000	6.6882	13.9723
	4	1	16.50647*	1.42057	.000	13.7174	19.2955
		2	1.38148	3.33311	.679	-5.1625	7.9254
		3	4.36394*	2.02981	.032	.3788	8.3491
		5	14.69419*	1.29435	.000	12.1530	17.2354
	5	1	1.81227	1.15716	.118	-.4596	4.0841
		2	-13.31272*	3.22964	.000	-19.6535	-6.9719
		3	-10.33025*	1.85502	.000	-13.9723	-6.6882
		4	-14.69419*	1.29435	.000	-17.2354	-12.1530

Table C-58 PARC

Dependent Variable	(I) LFeat	(J) LFeat	Mean Difference (I-J)	Std. Error	Sig.	95% Confidence Interval	
						Lower Bound	Upper Bound
dTEC	1	2	-7.99540	7.75048	.303	-23.2118	7.2210
		3	-9.00619	4.59323	.050	-18.0240	.0116
		4	6.72216*	3.35442	.045	.1365	13.3079
		5	-10.81144*	2.72149	.000	-16.1545	-5.4684
	2	1	7.99540	7.75048	.303	-7.2210	23.2118
		3	-1.01078	8.47296	.905	-17.6456	15.6241
		4	14.71756	7.87054	.062	-.7346	30.1697
		5	-2.81604	7.62232	.712	-17.7808	12.1488
	3	1	9.00619	4.59323	.050	-.0116	18.0240
		2	1.01078	8.47296	.905	-15.6241	17.6456
		4	15.72835*	4.79303	.001	6.3183	25.1384
		5	-1.80526	4.37350	.680	-10.3917	6.7812
	4	1	-6.72216*	3.35442	.045	-13.3079	-.1365
		2	-14.71756	7.87054	.062	-30.1697	.7346
		3	-15.72835*	4.79303	.001	-25.1384	-6.3183
		5	-17.53360*	3.04661	.000	-23.5150	-11.5522
	5	1	10.81144*	2.72149	.000	5.4684	16.1545
		2	2.81604	7.62232	.712	-12.1488	17.7808
		3	1.80526	4.37350	.680	-6.7812	10.3917
		4	17.53360*	3.04661	.000	11.5522	23.5150

Table C-59 SCH2

Dependent Variable	(I) LFeat	(J) LFeat	Mean Difference (I-J)	Std. Error	Sig.	95% Confidence Interval	
						Lower Bound	Upper Bound
dTEC	1	2	-3.90533	10.87144	.720	-25.2491	17.4384
		3	13.08287*	6.44283	.043	.4338	25.7320
		4	-18.22668*	4.70518	.000	-27.4643	-8.9891
		5	-32.99422*	3.81738	.000	-40.4888	-25.4996
	2	1	3.90533	10.87144	.720	-17.4384	25.2491
		3	16.98820	11.88484	.153	-6.3452	40.3216
		4	-14.32135	11.03984	.195	-35.9957	7.3530
		5	-29.08890*	10.69167	.007	-50.0797	-8.0981
	3	1	-13.08287*	6.44283	.043	-25.7320	-.4338
		2	-16.98820	11.88484	.153	-40.3216	6.3452
		4	-31.30955*	6.72308	.000	-44.5089	-18.1102
		5	-46.07710*	6.13461	.000	-58.1211	-34.0331
	4	1	18.22668*	4.70518	.000	8.9891	27.4643
		2	14.32135	11.03984	.195	-7.3530	35.9957
		3	31.30955*	6.72308	.000	18.1102	44.5089
		5	-14.76754*	4.27342	.001	-23.1575	-6.3776
	5	1	32.99422*	3.81738	.000	25.4996	40.4888
		2	29.08890*	10.69167	.007	8.0981	50.0797
		3	46.07710*	6.13461	.000	34.0331	58.1211
		4	14.76754*	4.27342	.001	6.3776	23.1575

Table C-60 SCUB

Dependent Variable	(I) LFeat	(J) LFeat	Mean Difference (I-J)	Std. Error	Sig.	95% Confidence Interval Lower Bound	95% Confidence Interval Upper Bound
dTEC	1	2	21.17394*	6.42558	.001	8.5587	33.7892
		3	-18.76051*	3.80804	.000	-26.2368	-11.2842
		4	-10.41574*	2.78100	.000	-15.8756	-4.9558
		5	7.73243*	2.25627	.001	3.3027	12.1621
	2	1	-21.17394*	6.42558	.001	-33.7892	-8.5587
		3	-39.93444*	7.02455	.000	-53.7257	-26.1432
		4	-31.58967*	6.52511	.000	-44.4003	-18.7790
		5	-13.44151*	6.31933	.034	-25.8482	-1.0349
	3	1	18.76051*	3.80804	.000	11.2842	26.2368
		2	39.93444*	7.02455	.000	26.1432	53.7257
		4	8.34477*	3.97369	.036	.5433	16.1463
		5	26.49294*	3.62587	.000	19.3743	33.6116
	4	1	10.41574*	2.78100	.000	4.9558	15.8756
		2	31.58967*	6.52511	.000	18.7790	44.4003
		3	-8.34477*	3.97369	.036	-16.1463	-.5433
		5	18.14817*	2.52581	.000	13.1893	23.1071
	5	1	-7.73243*	2.25627	.001	-12.1621	-3.3027
		2	13.44151*	6.31933	.034	1.0349	25.8482
		3	-26.49294*	3.62587	.000	-33.6116	-19.3743
		4	-18.14817*	2.52581	.000	-23.1071	-13.1893

Table C-61 SG05

Dependent Variable	(I) LFeat	(J) LFeat	Mean Difference (I-J)	Std. Error	Sig.	95% Confidence Interval Lower Bound	95% Confidence Interval Upper Bound
dTEC	1	2	-13.99509*	5.78204	.016	-25.3476	-2.6426
		3	-6.30060	3.57400	.078	-13.3178	.7166
		4	-2.88465	2.52840	.254	-7.8489	2.0796
		5	-5.85469*	2.07616	.005	-9.9310	-1.7783
	2	1	13.99509*	5.78204	.016	2.6426	25.3476
		3	7.69449	6.37894	.228	-4.8300	20.2190
		4	11.11044	5.85749	.058	-.3902	22.6111
		5	8.14040	5.67695	.152	-3.0058	19.2866
	3	1	6.30060	3.57400	.078	-.7166	13.3178
		2	-7.69449	6.37894	.228	-20.2190	4.8300
		4	3.41595	3.69482	.356	-3.8385	10.6704
		5	.44591	3.40138	.896	-6.2324	7.1242
	4	1	2.88465	2.52840	.254	-2.0796	7.8489
		2	-11.11044	5.85749	.058	-22.6111	.3902
		3	-3.41595	3.69482	.356	-10.6704	3.8385
		5	-2.97005	2.27786	.193	-7.4424	1.5023
	5	1	5.85469*	2.07616	.005	1.7783	9.9310
		2	-8.14040	5.67695	.152	-19.2866	3.0058
		3	-.44591	3.40138	.896	-7.1242	6.2324
		4	2.97005	2.27786	.193	-1.5023	7.4424

Table C-62 UNSA

Dependent Variable	(I) LFeat	(J) LFeat	Mean Difference (I-J)	Std. Error	Sig.	95% Confidence Interval	
						Lower Bound	Upper Bound
dTEC	1	2	42.13636*	4.35004	.000	33.5960	50.6767
		3	-10.36077*	2.57800	.000	-15.4221	-5.2994
		4	9.46042*	1.88270	.000	5.7641	13.1567
		5	13.11463*	1.52746	.000	10.1158	16.1135
	2	1	-42.13636*	4.35004	.000	-50.6767	-33.5960
		3	-52.49713*	4.75553	.000	-61.8336	-43.1606
		4	-32.67594*	4.41742	.000	-41.3486	-24.0033
		5	-29.02173*	4.27810	.000	-37.4209	-20.6226
	3	1	10.36077*	2.57800	.000	5.2994	15.4221
		2	52.49713*	4.75553	.000	43.1606	61.8336
		4	19.82119*	2.69014	.000	14.5397	25.1027
		5	23.47540*	2.45467	.000	18.6562	28.2946
	4	1	-9.46042*	1.88270	.000	-13.1567	-5.7641
		2	32.67594*	4.41742	.000	24.0033	41.3486
		3	-19.82119*	2.69014	.000	-25.1027	-14.5397
		5	3.65421*	1.70994	.033	.2971	7.0113
	5	1	-13.11463*	1.52746	.000	-16.1135	-10.1158
		2	29.02173*	4.27810	.000	20.6226	37.4209
		3	-23.47540*	2.45467	.000	-28.2946	-18.6562
		4	-3.65421*	1.70994	.033	-7.0113	-.2971

Event VI Mean percentage deviation of TECU for each phenomena of Event I from IGS stations.

Table C-63 CONO

Dependent Variable	(I) LFeat	(J) LFeat	Mean Difference (I-J)	Std. Error	Sig.	95% Confidence Interval Lower Bound	95% Confidence Interval Upper Bound
dTEC	1	2	-7.70021*	1.71588	.000	-11.0690	-4.3314
		3	9.12107*	1.66835	.000	5.8456	12.3965
		4	10.70169*	1.80299	.000	7.1619	14.2415
		5	20.96401*	2.77501	.000	15.5158	26.4122
		6	15.54331*	2.24774	.000	11.1303	19.9563
		7	16.66019*	1.69891	.000	13.3247	19.9957
		8	-.85562	1.94389	.660	-4.6721	2.9608
	2	1	7.70021*	1.71588	.000	4.3314	11.0690
		3	16.82128*	1.22803	.000	14.4103	19.2323
		4	18.40190*	1.40551	.000	15.6425	21.1613
		5	28.66422*	2.53483	.000	23.6876	33.6409
		6	23.24353*	1.94346	.000	19.4279	27.0591
		7	24.36040*	1.26924	.000	21.8685	26.8523
		8	6.84460*	1.58221	.000	3.7382	9.9510
	3	1	-9.12107*	1.66835	.000	-12.3965	-5.8456
		2	-16.82128*	1.22803	.000	-19.2323	-14.4103
		4	1.58063	1.34707	.241	-1.0641	4.2253
		5	11.84294*	2.50290	.000	6.9290	16.7569
		6	6.42225*	1.90163	.001	2.6888	10.1557
		7	7.53913*	1.20421	.000	5.1749	9.9033
		8	-9.97668*	1.53053	.000	-12.9816	-6.9718
	4	1	-10.70169*	1.80299	.000	-14.2415	-7.1619
		2	-18.40190*	1.40551	.000	-21.1613	-15.6425
		3	-1.58063	1.34707	.241	-4.2253	1.0641
		5	10.26232*	2.59459	.000	5.1684	15.3563
		6	4.84162*	2.02079	.017	.8742	8.8090
		7	5.95850*	1.38474	.000	3.2398	8.6772
		8	-11.55731*	1.67628	.000	-14.8484	-8.2663
	5	1	-20.96401*	2.77501	.000	-26.4122	-15.5158
		2	-28.66422*	2.53483	.000	-33.6409	-23.6876
		3	-11.84294*	2.50290	.000	-16.7569	-6.9290
		4	-10.26232*	2.59459	.000	-15.3563	-5.1684
		6	-5.42069	2.92121	.064	-11.1559	.3145
		7	-4.30382	2.52337	.089	-9.2580	.6503
		8	-21.81963*	2.69441	.000	-27.1096	-16.5297
	6	1	-15.54331*	2.24774	.000	-19.9563	-11.1303
		2	-23.24353*	1.94346	.000	-27.0591	-19.4279
		3	-6.42225*	1.90163	.001	-10.1557	-2.6888
		4	-4.84162*	2.02079	.017	-8.8090	-.8742
		5	5.42069	2.92121	.064	-.3145	11.1559
		7	1.11688	1.92849	.563	-2.6693	4.9031
		8	-16.39893*	2.14744	.000	-20.6150	-12.1829
	7	1	-16.66019*	1.69891	.000	-19.9957	-13.3247
		2	-24.36040*	1.26924	.000	-26.8523	-21.8685
		3	-7.53913*	1.20421	.000	-9.9033	-5.1749
		4	-5.95850*	1.38474	.000	-8.6772	-3.2398
		5	4.30382	2.52337	.089	-.6503	9.2580
		6	-1.11688	1.92849	.563	-4.9031	2.6693
		8	-17.51581*	1.56379	.000	-20.5860	-14.4456
	8	1	.85562	1.94389	.660	-2.9608	4.6721
		2	-6.84460*	1.58221	.000	-9.9510	-3.7382
		3	9.97668*	1.53053	.000	6.9718	12.9816
		4	11.55731*	1.67628	.000	8.2663	14.8484
		5	21.81963*	2.69441	.000	16.5297	27.1096
		6	16.39893*	2.14744	.000	12.1829	20.6150
		7	17.51581*	1.56379	.000	14.4456	20.5860

Table C-64 COYQ

Dependent Variable	(I) LFeat	(J) LFeat	Mean Difference (I-J)	Std. Error	Sig.	95% Confidence Interval Lower Bound	95% Confidence Interval Upper Bound
dTEC	1	2	37.40851*	4.63195	.000	28.3146	46.5024
		3	86.24207*	4.50363	.000	77.4001	95.0841
		4	56.67588*	4.85847	.000	47.1372	66.2145
		5	126.23553*	7.63281	.000	111.2500	141.2210
		6	137.18011*	6.06770	.000	125.2674	149.0928
		7	104.23510*	4.58614	.000	95.2311	113.2391
		8	120.01458*	5.24745	.000	109.7123	130.3169
	2	1	-37.40851*	4.63195	.000	-46.5024	-28.3146
		3	48.83356*	3.31503	.000	42.3252	55.3420
		4	19.26737*	3.78304	.000	11.8401	26.6946
		5	88.82702*	6.99761	.000	75.0886	102.5654
		6	99.77160*	5.24630	.000	89.4715	110.0717
		7	66.82659*	3.42627	.000	60.0998	73.5534
		8	82.60607*	4.27112	.000	74.2206	90.9916
	3	1	-86.24207*	4.50363	.000	-95.0841	-77.4001
		2	-48.83356*	3.31503	.000	-55.3420	-42.3252
		4	-29.56619*	3.62480	.000	-36.6828	-22.4496
		5	39.99346*	6.91334	.000	26.4205	53.5664
		6	50.93804*	5.13337	.000	40.8597	61.0164
		7	17.99303*	3.25071	.000	11.6109	24.3752
		8	33.77251*	4.13161	.000	25.6609	41.8841
	4	1	-56.67588*	4.85847	.000	-66.2145	-47.1372
		2	-19.26737*	3.78304	.000	-26.6946	-11.8401
		3	29.56619*	3.62480	.000	22.4496	36.6828
		5	69.55965*	7.14957	.000	55.5229	83.5964
		6	80.50423*	5.44733	.000	69.8095	91.1990
		7	47.55922*	3.72681	.000	40.2424	54.8761
		8	63.33870*	4.51577	.000	54.4729	72.2045
	5	1	-126.23553*	7.63281	.000	-141.2210	-111.2500
		2	-88.82702*	6.99761	.000	-102.5654	-75.0886
		3	-39.99346*	6.91334	.000	-53.5664	-26.4205
		4	-69.55965*	7.14957	.000	-83.5964	-55.5229
		6	10.94458	8.02051	.173	-4.8021	26.6913
		7	-22.00043*	6.96737	.002	-35.6795	-8.3214
		8	-6.22095	7.41939	.402	-20.7874	8.3455
	6	1	-137.18011*	6.06770	.000	-149.0928	-125.2674
		2	-99.77160*	5.24630	.000	-110.0717	-89.4715
		3	-50.93804*	5.13337	.000	-61.0164	-40.8597
		4	-80.50423*	5.44733	.000	-91.1990	-69.8095
		5	-10.94458	8.02051	.173	-26.6913	4.8021
		7	-32.94501*	5.20590	.000	-43.1658	-22.7243
		8	-17.16553*	5.79694	.003	-28.5467	-5.7844
	7	1	-104.23510*	4.58614	.000	-113.2391	-95.2311
		2	-66.82659*	3.42627	.000	-73.5534	-60.0998
		3	-17.99303*	3.25071	.000	-24.3752	-11.6109
		4	-47.55922*	3.72681	.000	-54.8761	-40.2424
		5	22.00043*	6.96737	.002	8.3214	35.6795
		6	32.94501*	5.20590	.000	22.7243	43.1658
		8	15.77948*	4.22139	.000	7.4916	24.0673
	8	1	-120.01458*	5.24745	.000	-130.3169	-109.7123
		2	-82.60607*	4.27112	.000	-90.9916	-74.2206
		3	-33.77251*	4.13161	.000	-41.8841	-25.6609
		4	-63.33870*	4.51577	.000	-72.2045	-54.4729
		5	6.22095	7.41939	.402	-8.3455	20.7874
		6	17.16553*	5.79694	.003	5.7844	28.5467
		7	-15.77948*	4.22139	.000	-24.0673	-7.4916

Table C-65 COPO

Dependent Variable	(I) LFeat	(J) LFeat	Mean Difference (I-J)	Std. Error	Sig.	95% Confidence Interval Lower Bound	95% Confidence Interval Upper Bound
dTEC	1	2	1.76431	3.56460	.621	-5.2341	8.7627
		3	-53.63187*	3.46585	.000	-60.4364	-46.8274
		4	-95.41730*	3.73892	.000	-102.7579	-88.0767
		5	-70.27820*	5.87397	.000	-81.8106	-58.7458
		6	-15.87386*	4.66950	.001	-25.0415	-6.7062
		7	-5.27034	3.52934	.136	-12.1995	1.6588
		8	5.40267	4.03827	.181	-2.5257	13.3310
	2	1	-1.76431	3.56460	.621	-8.7627	5.2341
		3	-55.39618*	2.55114	.000	-60.4048	-50.3875
		4	-97.18162*	2.91131	.000	-102.8974	-91.4658
		5	-72.04251*	5.38513	.000	-82.6151	-61.4699
		6	-17.63817*	4.03738	.000	-25.5648	-9.7116
		7	-7.03465*	2.63675	.008	-12.2114	-1.8579
		8	3.63836	3.28691	.269	-2.8148	10.0916
	3	1	53.63187*	3.46585	.000	46.8274	60.4364
		2	55.39618*	2.55114	.000	50.3875	60.4048
		4	-41.78544*	2.78953	.000	-47.2621	-36.3087
		5	-16.64633*	5.32028	.002	-27.0917	-6.2010
		6	37.75801*	3.95047	.000	30.0020	45.5140
		7	48.36153*	2.50164	.000	43.4500	53.2730
		8	59.03454*	3.17956	.000	52.7921	65.2770
	4	1	95.41730*	3.73892	.000	88.0767	102.7579
		2	97.18162*	2.91131	.000	91.4658	102.8974
		3	41.78544*	2.78953	.000	36.3087	47.2621
		5	25.13910*	5.50207	.000	14.3369	35.9413
		6	79.54344*	4.19209	.000	71.3131	87.7738
		7	90.14696*	2.86803	.000	84.5162	95.7778
		8	100.81998*	3.47519	.000	93.9971	107.6428
	5	1	70.27820*	5.87397	.000	58.7458	81.8106
		2	72.04251*	5.38513	.000	61.4699	82.6151
		3	16.64633*	5.32028	.002	6.2010	27.0917
		4	-25.13910*	5.50207	.000	-35.9413	-14.3369
		6	54.40434*	6.17232	.000	42.2862	66.5225
		7	65.00786*	5.36186	.000	54.4809	75.5348
		8	75.68087*	5.70972	.000	64.4710	86.8908
	6	1	15.87386*	4.66950	.001	6.7062	25.0415
		2	17.63817*	4.03738	.000	9.7116	25.5648
		3	-37.75801*	3.95047	.000	-45.5140	-30.0020
		4	-79.54344*	4.19209	.000	-87.7738	-71.3131
		5	-54.40434*	6.17232	.000	-66.5225	-42.2862
		7	10.60352*	4.00629	.008	2.7380	18.4691
		8	21.27653*	4.46113	.000	12.5180	30.0351
	7	1	5.27034	3.52934	.136	-1.6588	12.1995
		2	7.03465*	2.63675	.008	1.8579	12.2114
		3	-48.36153*	2.50164	.000	-53.2730	-43.4500
		4	-90.14696*	2.86803	.000	-95.7778	-84.5162
		5	-65.00786*	5.36186	.000	-75.5348	-54.4809
		6	-10.60352*	4.00629	.008	-18.4691	-2.7380
		8	10.67301*	3.24865	.001	4.2949	17.0511
	8	1	-5.40267	4.03827	.181	-13.3310	2.5257
		2	-3.63836	3.28691	.269	-10.0916	2.8148
		3	-59.03454*	3.17956	.000	-65.2770	-52.7921
		4	-100.81998*	3.47519	.000	-107.6428	-93.9971
		5	-75.68087*	5.70972	.000	-86.8908	-64.4710
		6	-21.27653*	4.46113	.000	-30.0351	-12.5180
		7	-10.67301*	3.24865	.001	-17.0511	-4.2949

Table C-66 GOGA

Dependent Variable	(I) LFeat	(J) LFeat	Mean Difference (I-J)	Std. Error	Sig.	95% Confidence Interval	
						Lower Bound	Upper Bound
dTEC	1	2	-13.41479*	1.90191	.000	-17.1488	-9.6808
		3	25.01846*	1.84922	.000	21.3879	28.6490
		4	31.09064*	1.99492	.000	27.1740	35.0073
		5	47.91247*	3.13408	.000	41.7593	54.0656
		6	38.47755*	2.49144	.000	33.5861	43.3690
		7	26.32320*	1.88310	.000	22.6261	30.0203
		8	-5.25576*	2.15464	.015	-9.4860	-1.0255
	2	1	13.41479*	1.90191	.000	9.6808	17.1488
		3	38.43325*	1.36117	.000	35.7609	41.1056
		4	44.50544*	1.55334	.000	41.4558	47.5551
		5	61.32726*	2.87327	.000	55.6862	66.9683
		6	51.89234*	2.15417	.000	47.6631	56.1216
		7	39.73800*	1.40685	.000	36.9759	42.5001
		8	8.15904*	1.75375	.000	4.7159	11.6022
	3	1	-25.01846*	1.84922	.000	-28.6490	-21.3879
		2	-38.43325*	1.36117	.000	-41.1056	-35.7609
		4	6.07219*	1.48837	.000	3.1501	8.9943
		5	22.89401*	2.83867	.000	17.3209	28.4672
		6	13.45909*	2.10780	.000	9.3209	17.5973
		7	1.30475	1.33476	.329	-1.3158	3.9253
		8	-30.27421*	1.69647	.000	-33.6049	-26.9435
	4	1	-31.09064*	1.99492	.000	-35.0073	-27.1740
		2	-44.50544*	1.55334	.000	-47.5551	-41.4558
		3	-6.07219*	1.48837	.000	-8.9943	-3.1501
		5	16.82183*	2.93566	.000	11.0582	22.5854
		6	7.38691*	2.23671	.001	2.9956	11.7782
		7	-4.76744*	1.53025	.002	-7.7718	-1.7631
		8	-36.34640*	1.85421	.000	-39.9868	-32.7060
	5	1	-47.91247*	3.13408	.000	-54.0656	-41.7593
		2	-61.32726*	2.87327	.000	-66.9683	-55.6862
		3	-22.89401*	2.83867	.000	-28.4672	-17.3209
		4	-16.82183*	2.93566	.000	-22.5854	-11.0582
		6	-9.43492*	3.29328	.004	-15.9006	-2.9692
		7	-21.58927*	2.86085	.000	-27.2060	-15.9726
		8	-53.16823*	3.04645	.000	-59.1493	-47.1871
	6	1	-38.47755*	2.49144	.000	-43.3690	-33.5861
		2	-51.89234*	2.15417	.000	-56.1216	-47.6631
		3	-13.45909*	2.10780	.000	-17.5973	-9.3209
		4	-7.38691*	2.23671	.001	-11.7782	-2.9956
		5	9.43492*	3.29328	.004	2.9692	15.9006
		7	-12.15435*	2.13758	.000	-16.3511	-7.9576
		8	-43.73331*	2.38026	.000	-48.4065	-39.0601
	7	1	-26.32320*	1.88310	.000	-30.0203	-22.6261
		2	-39.73800*	1.40685	.000	-42.5001	-36.9759
		3	-1.30475	1.33476	.329	-3.9253	1.3158
		4	4.76744*	1.53025	.002	1.7631	7.7718
		5	21.58927*	2.86085	.000	15.9726	27.2060
		6	12.15435*	2.13758	.000	7.9576	16.3511
		8	-31.57896*	1.73333	.000	-34.9820	-28.1759
	8	1	5.25576*	2.15464	.015	1.0255	9.4860
		2	-8.15904*	1.75375	.000	-11.6022	-4.7159
		3	30.27421*	1.69647	.000	26.9435	33.6049
		4	36.34640*	1.85421	.000	32.7060	39.9868
		5	53.16823*	3.04645	.000	47.1871	59.1493
		6	43.73331*	2.38026	.000	39.0601	48.4065
		7	31.57896*	1.73333	.000	28.1759	34.9820

Table C-67 IQQE

Dependent Variable	(I) LFeat	(J) LFeat	Mean Difference (I-J)	Std. Error	Sig.	95% Confidence Interval	
						Lower Bound	Upper Bound
dTEC	1	2	-5.99220*	2.25735	.008	-10.4241	-1.5603
		3	12.05078*	2.19482	.000	7.7417	16.3599
		4	-22.76281*	2.36774	.000	-27.4114	-18.1142
		5	21.12213*	3.71980	.000	13.8190	28.4252
		6	30.42712*	2.93489	.000	24.6650	36.1892
		7	-3.84749	2.23713	.086	-8.2396	.5447
		8	24.62195*	2.55731	.000	19.6012	29.6427
	2	1	5.99220*	2.25735	.008	1.5603	10.4241
		3	18.04299*	1.61556	.000	14.8712	21.2148
		4	-16.77060*	1.84364	.000	-20.3902	-13.1510
		5	27.11433*	3.41024	.000	20.4190	33.8097
		6	36.41933*	2.53109	.000	31.4500	41.3886
		7	2.14471	1.67258	.200	-1.1391	5.4285
		8	30.61415*	2.08150	.000	26.5275	34.7008
	3	1	-12.05078*	2.19482	.000	-16.3599	-7.7417
		2	-18.04299*	1.61556	.000	-21.2148	-14.8712
		4	-34.81359*	1.76653	.000	-38.2818	-31.3454
		5	9.07134*	3.36918	.007	2.4566	15.6861
		6	18.37634*	2.47548	.000	13.5162	23.2365
		7	-15.89827*	1.58718	.000	-19.0144	-12.7822
		8	12.57116*	2.01352	.000	8.6180	16.5243
	4	1	22.76281*	2.36774	.000	18.1142	27.4114
		2	16.77060*	1.84364	.000	13.1510	20.3902
		3	34.81359*	1.76653	.000	31.3454	38.2818
		5	43.88493*	3.48430	.000	37.0442	50.7257
		6	53.18993*	2.63001	.000	48.0264	58.3534
		7	18.91531*	1.81882	.000	15.3444	22.4862
		8	47.38475*	2.20073	.000	43.0640	51.7055
	5	1	-21.12213*	3.71980	.000	-28.4252	-13.8190
		2	-27.11433*	3.41024	.000	-33.8097	-20.4190
		3	-9.07134*	3.36918	.007	-15.6861	-2.4566
		4	-43.88493*	3.48430	.000	-50.7257	-37.0442
		6	9.30500*	3.89201	.017	1.6638	16.9462
		7	-24.96962*	3.39689	.000	-31.6387	-18.3005
		8	3.49982	3.61579	.333	-3.5991	10.5987
	6	1	-30.42712*	2.93489	.000	-36.1892	-24.6650
		2	-36.41933*	2.53109	.000	-41.3886	-31.4500
		3	-18.37634*	2.47548	.000	-23.2365	-13.5162
		4	-53.18993*	2.63001	.000	-58.3534	-48.0264
		5	-9.30500*	3.89201	.017	-16.9462	-1.6638
		7	-34.27462*	2.51307	.000	-39.2085	-29.3407
		8	-5.80518*	2.80189	.039	-11.3061	-.3042
	7	1	3.84749	2.23713	.086	-.5447	8.2396
		2	-2.14471	1.67258	.200	-5.4285	1.1391
		3	15.89827*	1.58718	.000	12.7822	19.0144
		4	-18.91531*	1.81882	.000	-22.4862	-15.3444
		5	24.96962*	3.39689	.000	18.3005	31.6387
		6	34.27462*	2.51307	.000	29.3407	39.2085
		8	28.46944*	2.05955	.000	24.4259	32.5130
	8	1	-24.62195*	2.55731	.000	-29.6427	-19.6012
		2	-30.61415*	2.08150	.000	-34.7008	-26.5275
		3	-12.57116*	2.01352	.000	-16.5243	-8.6180
		4	-47.38475*	2.20073	.000	-51.7055	-43.0640
		5	-3.49982	3.61579	.333	-10.5987	3.5991
		6	5.80518*	2.80189	.039	.3042	11.3061
		7	-28.46944*	2.05955	.000	-32.5130	-24.4259

Table C-68 POYE

Dependent Variable	(I) LFeat	(J) LFeat	Mean Difference (I-J)	Std. Error	Sig.	95% Confidence Interval	
						Lower Bound	Upper Bound
dTEC	1	2	7.93782*	1.46914	.000	5.0535	10.8222
		3	8.82112*	1.42844	.000	6.0167	11.6256
		4	-5.16142*	1.54098	.001	-8.1868	-2.1360
		5	23.28950*	2.42094	.000	18.5365	28.0425
		6	27.08700*	1.92452	.000	23.3086	30.8654
		7	12.46155*	1.45461	.000	9.6057	15.3174
		8	12.62827*	1.66436	.000	9.3606	15.8959
	2	1	-7.93782*	1.46914	.000	-10.8222	-5.0535
		3	.88330	1.05144	.401	-1.1810	2.9476
		4	-13.09924*	1.19989	.000	-15.4550	-10.7435
		5	15.35168*	2.21946	.000	10.9942	19.7092
		6	19.14918*	1.66399	.000	15.8823	22.4161
		7	4.52373*	1.08673	.000	2.3902	6.6573
		8	4.69044*	1.35469	.001	2.0308	7.3501
	3	1	-8.82112*	1.42844	.000	-11.6256	-6.0167
		2	-.88330	1.05144	.401	-2.9476	1.1810
		4	-13.98254*	1.14970	.000	-16.2397	-11.7253
		5	14.46838*	2.19274	.000	10.1634	18.7734
		6	18.26588*	1.62817	.000	15.0693	21.4625
		7	3.64043*	1.03104	.000	1.6162	5.6647
		8	3.80714*	1.31044	.004	1.2343	6.3799
	4	1	5.16142*	1.54098	.001	2.1360	8.1868
		2	13.09924*	1.19989	.000	10.7435	15.4550
		3	13.98254*	1.14970	.000	11.7253	16.2397
		5	28.45092*	2.26766	.000	23.9988	32.9030
		6	32.24842*	1.72776	.000	28.8563	35.6405
		7	17.62297*	1.18205	.000	15.3022	19.9437
		8	17.78969*	1.43229	.000	14.9777	20.6017
	5	1	-23.28950*	2.42094	.000	-28.0425	-18.5365
		2	-15.35168*	2.21946	.000	-19.7092	-10.9942
		3	-14.46838*	2.19274	.000	-18.7734	-10.1634
		4	-28.45092*	2.26766	.000	-32.9030	-23.9988
		6	3.79750	2.54390	.136	-1.1969	8.7919
		7	-10.82795*	2.20987	.000	-15.1666	-6.4893
		8	-10.66124*	2.35324	.000	-15.2814	-6.0411
	6	1	-27.08700*	1.92452	.000	-30.8654	-23.3086
		2	-19.14918*	1.66399	.000	-22.4161	-15.8823
		3	-18.26588*	1.62817	.000	-21.4625	-15.0693
		4	-32.24842*	1.72776	.000	-35.6405	-28.8563
		5	-3.79750	2.54390	.136	-8.7919	1.1969
		7	-14.62545*	1.65118	.000	-17.8672	-11.3837
		8	-14.45874*	1.83864	.000	-18.0685	-10.8489
	7	1	-12.46155*	1.45461	.000	-15.3174	-9.6057
		2	-4.52373*	1.08673	.000	-6.6573	-2.3902
		3	-3.64043*	1.03104	.000	-5.6647	-1.6162
		4	-17.62297*	1.18205	.000	-19.9437	-15.3022
		5	10.82795*	2.20987	.000	6.4893	15.1666
		6	14.62545*	1.65118	.000	11.3837	17.8672
		8	.16671	1.33892	.901	-2.4620	2.7954
	8	1	-12.62827*	1.66436	.000	-15.8959	-9.3606
		2	-4.69044*	1.35469	.001	-7.3501	-2.0308
		3	-3.80714*	1.31044	.004	-6.3799	-1.2343
		4	-17.78969*	1.43229	.000	-20.6017	-14.9777
		5	10.66124*	2.35324	.000	6.0411	15.2814
		6	14.45874*	1.83864	.000	10.8489	18.0685
		7	-.16671	1.33892	.901	-2.7954	2.4620

Table C-69 RIOP

Dependent Variable	(I) LFeat	(J) LFeat	Mean Difference (I-J)	Std. Error	Sig.	95% Confidence Interval	
						Lower Bound	Upper Bound
dTEC	1	2	1.08431	1.97697	.584	-2.7971	4.9657
		3	2.18140	1.92296	.257	-1.5940	5.9568
		4	-30.76008*	2.07237	.000	-34.8288	-26.6914
		5	-18.36336*	3.24376	.000	-24.7319	-11.9949
		6	2.29024	2.58242	.375	-2.7798	7.3603
		7	-8.88175*	1.95769	.000	-12.7253	-5.0382
		8	3.29858	2.23631	.141	-1.0920	7.6891
	2	1	-1.08431	1.97697	.584	-4.9657	2.7971
		3	1.09708	1.40525	.435	-1.6618	3.8560
		4	-31.84439*	1.60364	.000	-34.9928	-28.6960
		5	-19.44768*	2.96630	.000	-25.2714	-13.6239
		6	1.20592	2.22392	.588	-3.1603	5.5722
		7	-9.96607*	1.45240	.000	-12.8176	-7.1146
		8	2.21426	1.81053	.222	-1.3404	5.7689
	3	1	-2.18140	1.92296	.257	-5.9568	1.5940
		2	-1.09708	1.40525	.435	-3.8560	1.6618
		4	-32.94147*	1.53656	.000	-35.9582	-29.9247
		5	-20.54476*	2.93058	.000	-26.2984	-14.7911
		6	.10884	2.17604	.960	-4.1634	4.3811
		7	-11.06315*	1.37798	.000	-13.7686	-8.3577
		8	1.11718	1.75140	.524	-2.3213	4.5557
	4	1	30.76008*	2.07237	.000	26.6914	34.8288
		2	31.84439*	1.60364	.000	28.6960	34.9928
		3	32.94147*	1.53656	.000	29.9247	35.9582
		5	12.39671*	3.03071	.000	6.4465	18.3469
		6	33.05031*	2.30913	.000	28.5168	37.5839
		7	21.87832*	1.57980	.000	18.7767	24.9800
		8	34.05866*	1.91424	.000	30.3004	37.8169
	5	1	18.36336*	3.24376	.000	11.9949	24.7319
		2	19.44768*	2.96630	.000	13.6239	25.2714
		3	20.54476*	2.93058	.000	14.7911	26.2984
		4	-12.39671*	3.03071	.000	-18.3469	-6.4465
		6	20.65360*	3.39991	.000	13.9785	27.3287
		7	9.48161*	2.95348	.001	3.6830	15.2802
		8	21.66194*	3.14509	.000	15.4872	27.8367
	6	1	-2.29024	2.58242	.375	-7.3603	2.7798
		2	-1.20592	2.22392	.588	-5.5722	3.1603
		3	-.10884	2.17604	.960	-4.3811	4.1634
		4	-33.05031*	2.30913	.000	-37.5839	-28.5168
		5	-20.65360*	3.39991	.000	-27.3287	-13.9785
		7	-11.17199*	2.20679	.000	-15.5046	-6.8394
		8	1.00834	2.45733	.682	-3.8162	5.8328
	7	1	8.88175*	1.95769	.000	5.0382	12.7253
		2	9.96607*	1.45240	.000	7.1146	12.8176
		3	11.06315*	1.37798	.000	8.3577	13.7686
		4	-21.87832*	1.57980	.000	-24.9800	-18.7767
		5	-9.48161*	2.95348	.001	-15.2802	-3.6830
		6	11.17199*	2.20679	.000	6.8394	15.5046
		8	12.18033*	1.78946	.000	8.6671	15.6936
	8	1	-3.29858	2.23631	.141	-7.6891	1.0920
		2	-2.21426	1.81053	.222	-5.7689	1.3404
		3	-1.11718	1.75140	.524	-4.5557	2.3213
		4	-34.05866*	1.91424	.000	-37.8169	-30.3004
		5	-21.66194*	3.14509	.000	-27.8367	-15.4872
		6	-1.00834	2.45733	.682	-5.8328	3.8162
		7	-12.18033*	1.78946	.000	-15.6936	-8.6671

Table C-70 SCH2

Dependent Variable	(I) LFeat	(J) LFeat	Mean Difference (I-J)	Std. Error	Sig.	95% Confidence Interval Lower Bound	95% Confidence Interval Upper Bound
dTEC	1	2	-9.18403*	3.43692	.008	-15.9317	-2.4363
		3	-32.39930*	3.34171	.000	-38.9601	-25.8385
		4	5.94261	3.60500	.100	-1.1351	13.0203
		5	12.40188*	5.66357	.029	1.2826	23.5212
		6	21.19513*	4.50225	.000	12.3559	30.0344
		7	2.88222	3.40293	.397	-3.7988	9.5632
		8	-8.56134*	3.89362	.028	-16.2057	-.9170
	2	1	9.18403*	3.43692	.008	2.4363	15.9317
		3	-23.21527*	2.45976	.000	-28.0445	-18.3860
		4	15.12664*	2.80703	.000	9.6156	20.6377
		5	21.58591*	5.19225	.000	11.3920	31.7799
		6	30.37916*	3.89277	.000	22.7365	38.0218
		7	12.06625*	2.54230	.000	7.0749	17.0576
		8	.62269	3.16918	.844	-5.5994	6.8448
	3	1	32.39930*	3.34171	.000	25.8385	38.9601
		2	23.21527*	2.45976	.000	18.3860	28.0445
		4	38.34191*	2.68961	.000	33.0614	43.6224
		5	44.80118*	5.12972	.000	34.7300	54.8724
		6	53.59444*	3.80897	.000	46.1163	61.0726
		7	35.28152*	2.41204	.000	30.5460	40.0171
		8	23.83796*	3.06567	.000	17.8191	29.8568
	4	1	-5.94261	3.60500	.100	-13.0203	1.1351
		2	-15.12664*	2.80703	.000	-20.6377	-9.6156
		3	-38.34191*	2.68961	.000	-43.6224	-33.0614
		5	6.45927	5.30500	.224	-3.9560	16.8746
		6	15.25252*	4.04194	.000	7.3170	23.1881
		7	-3.06040	2.76531	.269	-8.4895	2.3687
		8	-14.50395*	3.35072	.000	-21.0824	-7.9255
	5	1	-12.40188*	5.66357	.029	-23.5212	-1.2826
		2	-21.58591*	5.19225	.000	-31.7799	-11.3920
		3	-44.80118*	5.12972	.000	-54.8724	-34.7300
		4	-6.45927	5.30500	.224	-16.8746	3.9560
		6	8.79326	5.95124	.140	-2.8908	20.4773
		7	-9.51966	5.16981	.066	-19.6696	.6302
		8	-20.96321*	5.50521	.000	-31.7716	-10.1548
	6	1	-21.19513*	4.50225	.000	-30.0344	-12.3559
		2	-30.37916*	3.89277	.000	-38.0218	-22.7365
		3	-53.59444*	3.80897	.000	-61.0726	-46.1163
		4	-15.25252*	4.04194	.000	-23.1881	-7.3170
		5	-8.79326	5.95124	.140	-20.4773	2.8908
		7	-18.31292*	3.86279	.000	-25.8967	-10.7291
		8	-29.75647*	4.30134	.000	-38.2013	-21.3116
	7	1	-2.88222	3.40293	.397	-9.5632	3.7988
		2	-12.06625*	2.54230	.000	-17.0576	-7.0749
		3	-35.28152*	2.41204	.000	-40.0171	-30.5460
		4	3.06040	2.76531	.269	-2.3687	8.4895
		5	9.51966	5.16981	.066	-.6302	19.6696
		6	18.31292*	3.86279	.000	10.7291	25.8967
		8	-11.44355*	3.13229	.000	-17.5932	-5.2939
	8	1	8.56134*	3.89362	.028	.9170	16.2057
		2	-.62269	3.16918	.844	-6.8448	5.5994
		3	-23.83796*	3.06567	.000	-29.8568	-17.8191
		4	14.50395*	3.35072	.000	7.9255	21.0824
		5	20.96321*	5.50521	.000	10.1548	31.7716
		6	29.75647*	4.30134	.000	21.3116	38.2013
		7	11.44355*	3.13229	.000	5.2939	17.5932

Table C-71 SCUB

Dependent Variable	(I) LFeat	(J) LFeat	Mean Difference (I-J)	Std. Error	Sig.	95% Confidence Interval	
						Lower Bound	Upper Bound
dTEC	1	2	-17.61754*	2.28509	.000	-22.1039	-13.1312
		3	-23.56099*	2.22342	.000	-27.9263	-19.1957
		4	-12.27802*	2.39684	.000	-16.9838	-7.5723
		5	3.27085	3.76552	.385	-4.1221	10.6638
		6	-2.50673	3.01687	.406	-8.4298	3.4163
		7	-16.00286*	2.26249	.000	-20.4449	-11.5609
		8	-13.11275*	2.59739	.000	-18.2122	-8.0133
	2	1	17.61754*	2.28509	.000	13.1312	22.1039
		3	-5.94346*	1.63763	.000	-9.1586	-2.7283
		4	5.33952*	1.86630	.004	1.6754	9.0037
		5	20.88839*	3.45215	.000	14.1107	27.6661
		6	15.11081*	2.61528	.000	9.9762	20.2454
		7	1.61467	1.69029	.340	-1.7039	4.9333
		8	4.50479*	2.11770	.034	.3471	8.6625
	3	1	23.56099*	2.22342	.000	19.1957	27.9263
		2	5.94346*	1.63763	.000	2.7283	9.1586
		4	11.28298*	1.79026	.000	7.7681	14.7978
		5	26.83185*	3.41164	.000	20.1337	33.5300
		6	21.05427*	2.56157	.000	16.0251	26.0834
		7	7.55813*	1.60594	.000	4.4052	10.7111
		8	10.44825*	2.05100	.000	6.4215	14.4750
	4	1	12.27802*	2.39684	.000	7.5723	16.9838
		2	-5.33952*	1.86630	.004	-9.0037	-1.6754
		3	-11.28298*	1.79026	.000	-14.7978	-7.7681
		5	15.54887*	3.52712	.000	8.6240	22.4737
		6	9.77129*	2.71347	.000	4.4439	15.0987
		7	-3.72485*	1.83856	.043	-7.3345	-.1152
		8	-.83473	2.23782	.709	-5.2283	3.5588
	5	1	-3.27085	3.76552	.385	-10.6638	4.1221
		2	-20.88839*	3.45215	.000	-27.6661	-14.1107
		3	-26.83185*	3.41164	.000	-33.5300	-20.1337
		4	-15.54887*	3.52712	.000	-22.4737	-8.6240
		6	-5.77758	3.97457	.146	-13.5809	2.0258
		7	-19.27372*	3.43724	.000	-26.0221	-12.5253
		8	-16.38360*	3.66635	.000	-23.5818	-9.1854
	6	1	2.50673	3.01687	.406	-3.4163	8.4298
		2	-15.11081*	2.61528	.000	-20.2454	-9.9762
		3	-21.05427*	2.56157	.000	-26.0834	-16.0251
		4	-9.77129*	2.71347	.000	-15.0987	-4.4439
		5	5.77758	3.97457	.146	-2.0258	13.5809
		7	-13.49613*	2.59556	.000	-18.5920	-8.4002
		8	-10.60602*	2.89214	.000	-16.2842	-4.9278
	7	1	16.00286*	2.26249	.000	11.5609	20.4449
		2	-1.61467	1.69029	.340	-4.9333	1.7039
		3	-7.55813*	1.60594	.000	-10.7111	-4.4052
		4	3.72485*	1.83856	.043	.1152	7.3345
		5	19.27372*	3.43724	.000	12.5253	26.0221
		6	13.49613*	2.59556	.000	8.4002	18.5920
		8	2.89011	2.09329	.168	-1.2197	6.9999
	8	1	13.11275*	2.59739	.000	8.0133	18.2122
		2	-4.50479*	2.11770	.034	-8.6625	-.3471
		3	-10.44825*	2.05100	.000	-14.4750	-6.4215
		4	.83473	2.23782	.709	-3.5588	5.2283
		5	16.38360*	3.66635	.000	9.1854	23.5818
		6	10.60602*	2.89214	.000	4.9278	16.2842
		7	-2.89011	2.09329	.168	-6.9999	1.2197

Table C-72 UNSA

Dependent Variable	(I) LFeat	(J) LFeat	Mean Difference (I-J)	Std. Error	Sig.	95% Confidence Interval	
						Lower Bound	Upper Bound
dTEC	1	2	5.57423	3.03287	.066	-.3802	11.5287
		3	9.88729*	2.95102	.001	4.0935	15.6811
		4	-19.72470*	3.18119	.000	-25.9704	-13.4790
		5	31.83418*	4.99775	.000	22.0220	41.6463
		6	27.78256*	4.00411	.000	19.9212	35.6439
		7	-6.87879*	3.00287	.022	-12.7744	-.9832
		8	29.40234*	3.44736	.000	22.6341	36.1706
	2	1	-5.57423	3.03287	.066	-11.5287	.3802
		3	4.31306*	2.17352	.048	.0457	8.5804
		4	-25.29893*	2.47703	.000	-30.1621	-20.4357
		5	26.25995*	4.58184	.000	17.2644	35.2555
		6	22.20833*	3.47111	.000	15.3935	29.0232
		7	-12.45302*	2.24343	.000	-16.8576	-8.0485
		8	23.82811*	2.81070	.000	18.3098	29.3464
	3	1	-9.88729*	2.95102	.001	-15.6811	-4.0935
		2	-4.31306*	2.17352	.048	-8.5804	-.0457
		4	-29.61200*	2.37610	.000	-34.2770	-24.9470
		5	21.94689*	4.52807	.000	13.0569	30.8369
		6	17.89527*	3.39982	.000	11.2203	24.5702
		7	-16.76608*	2.13147	.000	-20.9508	-12.5813
		8	19.51504*	2.72217	.000	14.1706	24.8595
	4	1	19.72470*	3.18119	.000	13.4790	25.9704
		2	25.29893*	2.47703	.000	20.4357	30.1621
		3	29.61200*	2.37610	.000	24.9470	34.2770
		5	51.55888*	4.68133	.000	42.3679	60.7498
		6	47.50726*	3.60142	.000	40.4365	54.5780
		7	12.84591*	2.44021	.000	8.0550	17.6368
		8	49.12704*	2.97013	.000	43.2957	54.9583
	5	1	-31.83418*	4.99775	.000	-41.6463	-22.0220
		2	-26.25995*	4.58184	.000	-35.2555	-17.2644
		3	-21.94689*	4.52807	.000	-30.8369	-13.0569
		4	-51.55888*	4.68133	.000	-60.7498	-42.3679
		6	-4.05162	5.27521	.443	-14.4085	6.3053
		7	-38.71297*	4.56204	.000	-47.6697	-29.7562
		8	-2.43184	4.86613	.617	-11.9856	7.1219
	6	1	-27.78256*	4.00411	.000	-35.6439	-19.9212
		2	-22.20833*	3.47111	.000	-29.0232	-15.3935
		3	-17.89527*	3.39982	.000	-24.5702	-11.2203
		4	-47.50726*	3.60142	.000	-54.5780	-40.4365
		5	4.05162	5.27521	.443	-6.3053	14.4085
		7	-34.66135*	3.44493	.000	-41.4248	-27.8979
		8	1.61978	3.83856	.673	-5.9165	9.1561
	7	1	6.87879*	3.00287	.022	.9832	12.7744
		2	12.45302*	2.24343	.000	8.0485	16.8576
		3	16.76608*	2.13147	.000	12.5813	20.9508
		4	-12.84591*	2.44021	.000	-17.6368	-8.0550
		5	38.71297*	4.56204	.000	29.7562	47.6697
		6	34.66135*	3.44493	.000	27.8979	41.4248
		8	36.28113*	2.77830	.000	30.8264	41.7358
	8	1	-29.40234*	3.44736	.000	-36.1706	-22.6341
		2	-23.82811*	2.81070	.000	-29.3464	-18.3098
		3	-19.51504*	2.72217	.000	-24.8595	-14.1706
		4	-49.12704*	2.97013	.000	-54.9583	-43.2957
		5	2.43184	4.86613	.617	-7.1219	11.9856
		6	-1.61978	3.83856	.673	-9.1561	5.9165
		7	-36.28113*	2.77830	.000	-41.7358	-30.8264

Table C-73 YALP

Dependent Variable	(I) LFeat	(J) LFeat	Mean Difference (I-J)	Std. Error	Sig.	95% Confidence Interval	
						Lower Bound	Upper Bound
dTEC	1	2	13.66198*	1.96454	.000	9.8019	17.5220
		3	27.76054*	2.24067	.000	23.3580	32.1631
		6	10.08680*	2.79641	.000	4.5923	15.5813
		7	2.59925	1.94511	.182	-1.2226	6.4211
		8	14.53395*	2.22560	.000	10.1610	18.9069
	2	1	-13.66198*	1.96454	.000	-17.5220	-9.8019
		3	14.09856*	1.82999	.000	10.5029	17.6942
		6	-3.57518	2.47955	.150	-8.4471	1.2968
		7	-11.06273*	1.45318	.000	-13.9180	-8.2074
		8	.87196	1.81150	.630	-2.6874	4.4313
	3	1	-27.76054*	2.24067	.000	-32.1631	-23.3580
		2	-14.09856*	1.82999	.000	-17.6942	-10.5029
		6	-17.67374*	2.70358	.000	-22.9859	-12.3616
		7	-25.16130*	1.80911	.000	-28.7159	-21.6066
		8	-13.22660*	2.10777	.000	-17.3681	-9.0851
	6	1	-10.08680*	2.79641	.000	-15.5813	-4.5923
		2	3.57518	2.47955	.150	-1.2968	8.4471
		3	17.67374*	2.70358	.000	12.3616	22.9859
		7	-7.48755*	2.46419	.003	-12.3293	-2.6458
		8	4.44714	2.69110	.099	-.8405	9.7348
	7	1	-2.59925	1.94511	.182	-6.4211	1.2226
		2	11.06273*	1.45318	.000	8.2074	13.9180
		3	25.16130*	1.80911	.000	21.6066	28.7159
		6	7.48755*	2.46419	.003	2.6458	12.3293
		8	11.93470*	1.79041	.000	8.4168	15.4526
	8	1	-14.53395*	2.22560	.000	-18.9069	-10.1610
		2	-.87196	1.81150	.630	-4.4313	2.6874
		3	13.22660*	2.10777	.000	9.0851	17.3681
		6	-4.44714	2.69110	.099	-9.7348	.8405
		7	-11.93470*	1.79041	.000	-15.4526	-8.4168

APPENDIX D

FULL MULTIPLE REGRESSION RESULTS FROM SECTION 5.3

Event I

Table D-1 BAIE

Model Summary[b]

Model	R	R Square	Adjusted R Square	Std. Error of the Estimate
1	.688[a]	.474	.419	31.84343

ANOVA[b]

Model		Sum of Squares	df	Mean Square	F	Sig.
1	Regression	78492.834	9	8721.426	8.601	.000[a]
	Residual	87204.356	86	1014.004		
	Total	165697.190	95			

a. Predictors: (Constant), Dst, Bz, Tem, Bx, Speed, Bwai, betta, Density, Bmg

b. Dependent Variable: BAIE1

Coefficients[a]

Model		Unstandardized Coefficients		Standardized Coefficients	t	Sig.	95.0% Confidence Interval for B	
		B	Std. Error	Beta			Lower Bound	Upper Bound
1	(Constant)	107.960	47.199		2.287	.025	14.132	201.789
	B	2.819	1.914	.280	1.473	.145	-.987	6.625
	B_x	1.227	1.072	.122	1.145	.255	-.904	3.359
	B_y	1.741	.602	.288	2.890	.005	.543	2.939
	B_z	-2.187	.782	-.284	-2.798	.006	-3.741	-.633
	T_p	.000	.000	-.333	-2.787	.007	.000	.000
	N_p	2.209	1.126	.323	1.962	.053	-.029	4.447
	V_p	-.207	.108	-.221	-1.918	.058	-.421	.007
	β	-5.569	11.551	-.067	-.482	.631	-28.532	17.394
	Dst	.605	.334	.295	1.815	.073	-.058	1.269

a. Dependent Variable: BAIE1

Table D-2 BOGT

Model Summary[b]

Model	R	R Square	Adjusted R Square	Std. Error of the Estimate
1	.551[a]	.304	.231	30.53367

ANOVA[b]

Model		Sum of Squares	df	Mean Square	F	Sig.
1	Regression	35030.856	9	3892.317	4.175	.000[a]
	Residual	80178.217	86	932.305		
	Total	115209.073	95			

a. Predictors: (Constant), Dst, Bz, Tem, Bx, Speed, Bwai, betta, Density, Bmg

b. Dependent Variable: BOGT1

Coefficients[a]

Model		Unstandardized Coefficients		Standardized Coefficients	t	Sig.	95.0% Confidence Interval for B	
		B	Std. Error	Beta			Lower Bound	Upper Bound
1	(Constant)	67.781	45.258		1.498	.138	-22.188	157.751
	B	3.475	1.836	.414	1.893	.062	-.174	7.124
	B_x	.973	1.028	.116	.946	.347	-1.071	3.016
	B_y	2.136	.578	.424	3.698	.000	.988	3.285
	B_z	-1.952	.750	-.303	-2.604	.011	-3.442	-.462
	T_p	.000	.000	-.180	-1.309	.194	.000	.000
	N_p	-.266	1.079	-.047	-.246	.806	-2.411	1.880
	V_p	-.144	.103	-.185	-1.395	.167	-.350	.061
	β	3.138	11.076	.045	.283	.778	-18.881	25.157
	Dst	.325	.320	.189	1.015	.313	-.311	.961

a. Dependent Variable: BOGT1

Table D-3 BRAZ

Model Summary[b]

Model	R	R Square	Adjusted R Square	Std. Error of the Estimate
1	.597[a]	.356	.289	22.34448

ANOVA[b]

Model		Sum of Squares	df	Mean Square	F	Sig.
1	Regression	23752.190	9	2639.132	5.286	.000[a]
	Residual	42937.706	86	499.276		
	Total	66689.896	95			

a. Predictors: (Constant), Dst, Bz, Tem, Bx, Speed, Bwai, betta, Density, Bmg

b. Dependent Variable: BRAZ1

Coefficients[a]

Model		Unstandardized Coefficients		Standardized Coefficients	t	Sig.	95.0% Confidence Interval for B	
		B	Std. Error	Beta			Lower Bound	Upper Bound
1	(Constant)	109.431	33.120		3.304	.001	43.592	175.271
	B	1.233	1.343	.193	.918	.361	-1.437	3.904
	B_x	-1.188	.752	-.187	-1.579	.118	-2.684	.308
	B_y	-.201	.423	-.052	-.476	.635	-1.042	.639
	B_z	-1.262	.549	-.258	-2.301	.024	-2.352	-.171
	T_p	-6.632E-6	.000	-.009	-.069	.945	.000	.000
	N_p	-.354	.790	-.082	-.449	.655	-1.925	1.216
	V_p	-.263	.076	-.442	-3.471	.001	-.413	-.112
	β	15.377	8.105	.291	1.897	.061	-.736	31.490
	*D*st	.125	.234	.096	.534	.594	-.340	.590

a. Dependent Variable: BRAZ1

Table D-4 COPO

Model Summary[b]

Model	R	R Square	Adjusted R Square	Std. Error of the Estimate
1	.721[a]	.519	.469	20.62632

ANOVA[b]

Model		Sum of Squares	df	Mean Square	F	Sig.
1	Regression	39545.089	9	4393.899	10.328	.000[a]
	Residual	36588.293	86	425.445		
	Total	76133.382	95			

a. Predictors: (Constant), Dst, Bz, Tem, Bx, Speed, Bwai, betta, Density, Bmg

b. Dependent Variable: COPO1

Coefficients[a]

Model		Unstandardized Coefficients		Standardized Coefficients	t	Sig.	95.0% Confidence Interval for B	
		B	Std. Error	Beta			Lower Bound	Upper Bound
1	(Constant)	180.141	30.573		5.892	.000	119.364	240.917
	B	5.254	1.240	.769	4.237	.000	2.789	7.719
	B_x	-1.921	.695	-.282	-2.766	.007	-3.302	-.540
	B_y	1.760	.390	.430	4.511	.000	.984	2.536
	B_z	-1.474	.506	-.282	-2.911	.005	-2.480	-.467
	T_p	8.270E-5	.000	.106	.930	.355	.000	.000
	N_p	1.339	.729	.289	1.837	.070	-.110	2.789
	V_p	-.461	.070	-.725	-6.591	.000	-.600	-.322
	β	-.986	7.482	-.017	-.132	.896	-15.860	13.889
	*D*st	.509	.216	.366	2.357	.021	.080	.939

a. Dependent Variable: COPO1

Table D-5

Model Summary[b]

Model	R	R Square	Adjusted R Square	Std. Error of the Estimate
1	.611[a]	.373	.297	27.13486

ANOVA[b]

Model		Sum of Squares	df	Mean Square	F	Sig.
1	Regression	32430.935	9	3603.437	4.894	.000[a]
	Residual	54486.227	74	736.300		
	Total	86917.162	83			

a. Predictors: (Constant), Dst, Bz, Tem, Bx, Speed, Bwai, betta, Density, Bmg

b. Dependent Variable: IQQE1

Coefficients[a]

Model		Unstandardized Coefficients		Standardized Coefficients	t	Sig.	95.0% Confidence Interval for B	
		B	Std. Error	Beta			Lower Bound	Upper Bound
1	(Constant)	98.638	58.817		1.677	.098	-18.558	215.834
	B	.668	2.047	.090	.326	.745	-3.411	4.748
	B_x	-3.798	1.400	-.448	-2.713	.008	-6.587	-1.009
	B_y	.483	.586	.108	.825	.412	-.685	1.651
	B_z	-.772	.717	-.136	-1.076	.285	-2.200	.657
	T_p	.000	.000	.439	2.470	.016	.000	.001
	N_p	.697	1.012	.139	.689	.493	-1.320	2.714
	V_p	-.265	.142	-.381	-1.862	.067	-.548	.019
	β	-10.797	11.939	-.165	-.904	.369	-34.586	12.992
	Dst	-.868	.363	-.562	-2.393	.019	-1.590	-.145

a. Dependent Variable: IQQE1

Table D-6 LAMT

Model Summary[b]

Model	R	R Square	Adjusted R Square	Std. Error of the Estimate
1	.698[a]	.487	.434	19.19697

ANOVA[b]

Model		Sum of Squares	df	Mean Square	F	Sig.
1	Regression	30124.727	9	3347.192	9.083	.000[a]
	Residual	31693.040	86	368.524		
	Total	61817.766	95			

a. Predictors: (Constant), Dst, Bz, Tem, Bx, Speed, Bwai, betta, Density, Bmg

b. Dependent Variable: LAMT1

Coefficients[a]

Model		Unstandardized Coefficients		Standardized Coefficients	t	Sig.	95.0% Confidence Interval for B	
		B	Std. Error	Beta			Lower Bound	Upper Bound
1	(Constant)	-49.875	28.454		-1.753	.083	-106.440	6.690
	B	3.569	1.154	.580	3.093	.003	1.275	5.864
	B_x	-.266	.646	-.043	-.411	.682	-1.551	1.019
	B_y	-1.024	.363	-.277	-2.820	.006	-1.746	-.302
	B_z	-1.668	.471	-.354	-3.540	.001	-2.605	-.731
	T_p	8.711E-5	.000	.124	1.052	.296	.000	.000
	N_p	-.888	.679	-.212	-1.308	.194	-2.237	.462
	V_p	.052	.065	.091	.801	.425	-.077	.181
	β	11.217	6.964	.221	1.611	.111	-2.627	25.060
	*D*st	.665	.201	.530	3.309	.001	.266	1.065

a. Dependent Variable: LAMT1

Table D-7 SCH2

Model Summary[b]

Model	R	R Square	Adjusted R Square	Std. Error of the Estimate
1	.887[a]	.787	.765	30.41249

ANOVA[b]

Model		Sum of Squares	df	Mean Square	F	Sig.
1	Regression	294294.966	9	32699.441	35.354	.000[a]
	Residual	79543.077	86	924.919		
	Total	373838.043	95			

a. Predictors: (Constant), Dst, Bz, Tem, Bx, Speed, Bwai, betta, Density, Bmg

b. Dependent Variable: SCH21

Coefficients[a]

Model		Unstandardized Coefficients		Standardized Coefficients	t	Sig.	95.0% Confidence Interval for B	
		B	Std. Error	Beta			Lower Bound	Upper Bound
1	(Constant)	14.066	45.078		.312	.756	-75.546	103.679
	B	2.170	1.828	.143	1.187	.239	-1.465	5.805
	B_x	1.243	1.024	.082	1.214	.228	-.792	3.279
	B_y	.859	.575	.095	1.494	.139	-.284	2.003
	B_z	-2.415	.747	-.208	-3.235	.002	-3.899	-.931
	T_p	9.390E-5	.000	.054	.716	.476	.000	.000
	N_p	5.875	1.075	.572	5.464	.000	3.737	8.012
	V_p	-.147	.103	-.104	-1.425	.158	-.352	.058
	β	-16.396	11.032	-.131	-1.486	.141	-38.328	5.535
	Dst	-.441	.319	-.143	-1.384	.170	-1.074	.193

a. Dependent Variable: SCH21

Table D-8 SG05

Model Summary[b]

Model	R	R Square	Adjusted R Square	Std. Error of the Estimate
1	.758[a]	.575	.530	17.80456

ANOVA[b]

Model		Sum of Squares	df	Mean Square	F	Sig.
1	Regression	36862.515	9	4095.835	12.921	.000[a]
	Residual	27262.200	86	317.002		
	Total	64124.714	95			

a. Predictors: (Constant), Dst, Bz, Tem, Bx, Speed, Bwai, betta, Density, Bmg

b. Dependent Variable: SG051

Coefficients[a]

Model		Unstandardized Coefficients		Standardized Coefficients	t	Sig.	95.0% Confidence Interval for B	
		B	Std. Error	Beta			Lower Bound	Upper Bound
1	(Constant)	-8.245	26.390		-.312	.755	-60.708	44.217
	B	3.911	1.070	.624	3.654	.000	1.783	6.039
	B_x	1.874	.600	.300	3.126	.002	.683	3.066
	B_y	1.443	.337	.384	4.285	.000	.774	2.113
	B_z	-.826	.437	-.172	-1.890	.062	-1.695	.043
	T_p	-9.052E-5	.000	-.126	-1.179	.242	.000	.000
	N_p	-.457	.629	-.107	-.726	.470	-1.708	.794
	V_p	-.048	.060	-.082	-.788	.433	-.167	.072
	β	14.598	6.459	.282	2.260	.026	1.759	27.437
	Dst	.064	.187	.050	.345	.731	-.307	.435

a. Dependent Variable: SG05

Table D-9 UNSA

Model Summary

Model	R	R Square	Adjusted R Square	Std. Error of the Estimate
1	.759[a]	.577	.514	13.25038

ANOVA[b]

Model		Sum of Squares	df	Mean Square	F	Sig.
1	Regression	14592.357	9	1621.373	9.235	.000[a]
	Residual	10709.924	61	175.573		
	Total	25302.281	70			

a. Predictors: (Constant), Dst, Speed, Bz, Bwai, betta, Bx, Tem, Bmg, Density

b. Dependent Variable: UNSA1

Coefficients[a]

Model		Unstandardized Coefficients		Standardized Coefficients	t	Sig.	95.0% Confidence Interval for B	
		B	Std. Error	Beta			Lower Bound	Upper Bound
1	(Constant)	186.554	39.038		4.779	.000	108.492	264.615
	Bmg	-.449	1.435	-.075	-.313	.755	-3.318	2.419
	Bx	-2.253	.956	-.432	-2.357	.022	-4.165	-.342
	Bwai	-.799	.444	-.224	-1.801	.077	-1.686	.088
	Bz	-1.110	.494	-.291	-2.248	.028	-2.098	-.123
	Tem	-3.395E-5	.000	-.062	-.298	.766	.000	.000
	Density	1.270	1.085	.295	1.170	.247	-.901	3.440
	Speed	-.371	.094	-.886	-3.949	.000	-.559	-.183
	betta	.337	8.274	.008	.041	.968	-16.208	16.882
	Dst	.507	.275	.298	1.844	.070	-.043	1.056

a. Dependent Variable: UNSA1

Event II

Table D-10

Model Summary[b]

Model	R	R Square	Adjusted R Square	Std. Error of the Estimate
1	.919[a]	.844	.822	30.95143

ANOVA[b]

Model		Sum of Squares	df	Mean Square	F	Sig.
1	Regression	322534.196	9	35837.133	37.409	.000[a]
	Residual	59395.444	62	957.991		
	Total	381929.640	71			

a. Predictors: (Constant), Dst, Bz, Den, Bye, Betta, Speed, Tem, Bx, Bmag

b. Dependent Variable: BAIE2

Coefficients[a]

Model		Unstandardized Coefficients		Standardized Coefficients	t	Sig.	95.0% Confidence Interval for B	
		B	Std. Error	Beta			Lower Bound	Upper Bound
1	(Constant)	-21.410	41.449		-.517	.607	-104.265	61.446
	B	.686	1.952	.142	.351	.727	-3.216	4.587
	B_x	2.282	2.283	.379	1.000	.321	-2.281	6.845
	B_y	2.167	.708	.318	3.062	.003	.753	3.582
	B_z	-3.170	1.193	-.382	-2.656	.010	-5.555	-.785
	T_p	-5.409E-6	.000	-.019	-.086	.932	.000	.000
	N_p	13.136	4.772	.816	2.753	.008	3.597	22.676
	V_p	-.028	.095	-.062	-.300	.765	-.218	.161
	β	-42.058	16.088	-.416	-2.614	.011	-74.217	-9.898
	*D*st	-.496	.293	-.347	-1.693	.096	-1.081	.090

a. Dependent Variable: BAIE2

Table D-11 BOGT

Model Summary[b]

Model	R	R Square	Adjusted R Square	Std. Error of the Estimate
1	.724[a]	.524	.455	31.23835

ANOVA[b]

Model		Sum of Squares	df	Mean Square	F	Sig.
1	Regression	66525.749	9	7391.750	7.575	.000[a]
	Residual	60501.737	62	975.834		
	Total	127027.486	71			

a. Predictors: (Constant), Dst, Bz, Den, Bye, Betta, Speed, Tem, Bx, Bmag

b. Dependent Variable: BOGT2

Coefficients[a]

Model		Unstandardized Coefficients		Standardized Coefficients	t	Sig.	95.0% Confidence Interval for B	
		B	Std. Error	Beta			Lower Bound	Upper Bound
1	(Constant)	72.607	41.833		1.736	.088	-11.017	156.230
	B	-1.023	1.970	-.368	-.519	.605	-4.961	2.914
	B_x	.793	2.304	.228	.344	.732	-3.813	5.398
	B_y	2.284	.714	.581	3.197	.002	.856	3.712
	B_z	-.233	1.204	-.049	-.194	.847	-2.640	2.174
	T_p	9.844E-5	.000	.605	1.555	.125	.000	.000
	N_p	-5.268	4.816	-.567	-1.094	.278	-14.896	4.359
	V_p	.044	.096	.168	.464	.644	-.147	.235
	β	-35.054	16.237	-.601	-2.159	.035	-67.512	-2.597
	Dst	.418	.296	.507	1.415	.162	-.173	1.009

a. Dependent Variable: BOGT2

Table D-12 BRAZ

Model Summary[b]

Model	R	R Square	Adjusted R Square	Std. Error of the Estimate
1	.463[a]	.214	.100	27.54303

ANOVA[b]

Model		Sum of Squares	df	Mean Square	F	Sig.
1	Regression	12804.283	9	1422.698	1.875	.072[a]
	Residual	47034.346	62	758.618		
	Total	59838.628	71			

a. Predictors: (Constant), Dst, Bz, Den, Bye, Betta, Speed, Tem, Bx, Bmag

b. Dependent Variable: BRAZ2

Coefficients[a]

Model	Unstandardized Coefficients		Standardized Coefficients	t	Sig.	95.0% Confidence Interval for B	
	B	Std. Error	Beta			Lower Bound	Upper Bound
1 (Constant)	13.878	36.885		.376	.708	-59.853	87.610
B	-1.390	1.737	-.729	-.800	.427	-4.861	2.082
B_x	-2.215	2.031	-.930	-1.090	.280	-6.275	1.846
B_y	-.290	.630	-.108	-.461	.646	-1.550	.969
B_z	-.489	1.062	-.149	-.461	.647	-2.612	1.633
T_p	4.656E-5	.000	.417	.834	.407	.000	.000
N_p	-3.777	4.247	-.593	-.889	.377	-12.266	4.712
V_p	.073	.084	.404	.867	.389	-.095	.242
β	1.039	14.316	.026	.073	.942	-27.580	29.657
*D*st	.361	.261	.638	1.385	.171	-.160	.882

a. Dependent Variable: BRAZ2

Table D-13 COYQ

Model Summary[b]

Model	R	R Square	Adjusted R Square	Std. Error of the Estimate
1	.707[a]	.500	.427	38.18983

ANOVA[b]

Model		Sum of Squares	df	Mean Square	F	Sig.
1	Regression	90402.298	9	10044.700	6.887	.000[a]
	Residual	90424.704	62	1458.463		
	Total	180827.002	71			

a. Predictors: (Constant), Dst, Bz, Den, Bye, Betta, Speed, Tem, Bx, Bmag

b. Dependent Variable: COYQ2

Coefficients[a]

Model	Unstandardized Coefficients		Standardized Coefficients	t	Sig.	95.0% Confidence Interval for B	
	B	Std. Error	Beta			Lower Bound	Upper Bound
1 (Constant)	42.814	51.143		.837	.406	-59.419	145.046
B	.773	2.408	.233	.321	.749	-4.041	5.587
B_x	-1.536	2.816	-.371	-.545	.588	-7.166	4.094
B_y	-2.797	.873	-.596	-3.203	.002	-4.543	-1.052
B_z	2.481	1.472	.434	1.685	.097	-.462	5.424
T_p	-8.961E-5	.000	-.462	-1.158	.251	.000	.000
N_p	9.409	5.888	.849	1.598	.115	-2.360	21.179
V_p	-.101	.117	-.322	-.866	.390	-.335	.132
β	-5.430	19.851	-.078	-.274	.785	-45.111	34.251
Dst	-.026	.361	-.026	-.071	.944	-.748	.697

a. Dependent Variable: COYQ2

Table D-14 IQQE

Model Summary[b]

Model	R	R Square	Adjusted R Square	Std. Error of the Estimate
1	.732[a]	.536	.469	30.20465

ANOVA[b]

Model		Sum of Squares	df	Mean Square	F	Sig.
1	Regression	65315.699	9	7257.300	7.955	.000[a]
	Residual	56563.880	62	912.321		
	Total	121879.579	71			

a. Predictors: (Constant), Dst, Bz, Den, Bye, Betta, Speed, Tem, Bx, Bmag

b. Dependent Variable: IQQE2

Coefficients[a]

Model		Unstandardized Coefficients		Standardized Coefficients	t	Sig.	95.0% Confidence Interval for B	
		B	Std. Error	Beta			Lower Bound	Upper Bound
1	(Constant)	56.696	40.449		1.402	.166	-24.161	137.552
	B	4.358	1.905	1.602	2.288	.026	.551	8.165
	B_x	-1.304	2.228	-.384	-.585	.560	-5.757	3.149
	B_y	-2.103	.691	-.546	-3.044	.003	-3.483	-.722
	B_z	.248	1.164	.053	.213	.832	-2.080	2.575
	T_p	.000	.000	.677	1.762	.083	.000	.000
	N_p	-7.917	4.657	-.870	-1.700	.094	-17.226	1.392
	V_p	-.093	.092	-.361	-1.009	.317	-.278	.091
	β	10.277	15.700	.180	.655	.515	-21.106	41.661
	Dst	.644	.286	.797	2.253	.028	.073	1.215

a. Dependent Variable: IQQE2

Table D-15 LAMT

Model Summary[b]

Model	R	R Square	Adjusted R Square	Std. Error of the Estimate
1	.640[a]	.409	.323	29.51661

ANOVA[b]

Model		Sum of Squares	df	Mean Square	F	Sig.
1	Regression	37396.356	9	4155.151	4.769	.000[a]
	Residual	54016.278	62	871.230		
	Total	91412.634	71			

a. Predictors: (Constant), Dst, Bz, Den, Bye, Betta, Speed, Tem, Bx, Bmag

b. Dependent Variable: LAMT2

Coefficients[a]

Model	Unstandardized Coefficients		Standardized Coefficients	t	Sig.	95.0% Confidence Interval for B	
	B	Std. Error	Beta			Lower Bound	Upper Bound
1 (Constant)	66.041	39.528		1.671	.100	-12.974	145.056
B	-1.617	1.861	-.686	-.869	.388	-5.337	2.104
B_x	.084	2.177	.029	.039	.969	-4.267	4.436
B_y	1.091	.675	.327	1.617	.111	-.258	2.440
B_z	.297	1.138	.073	.261	.795	-1.977	2.572
T_p	2.951E-5	.000	.214	.493	.624	.000	.000
N_p	4.517	4.551	.573	.993	.325	-4.580	13.614
V_p	-.145	.090	-.647	-1.602	.114	-.325	.036
β	-21.984	15.342	-.445	-1.433	.157	-52.653	8.685
*D*st	-.453	.279	-.647	-1.621	.110	-1.011	.105

a. Dependent Variable: LAMT2

Table D-16 PARC

Model Summary[b]

Model	R	R Square	Adjusted R Square	Std. Error of the Estimate
1	.754[a]	.568	.505	37.34467

ANOVA[b]

Model		Sum of Squares	df	Mean Square	F	Sig.
1	Regression	113683.532	9	12631.504	9.057	.000[a]
	Residual	86466.732	62	1394.625		
	Total	200150.264	71			

a. Predictors: (Constant), Dst, Bz, Den, Bye, Betta, Speed, Tem, Bx, Bmag

b. Dependent Variable: PARC2

Coefficients[a]

Model		Unstandardized Coefficients		Standardized Coefficients	t	Sig.	95.0% Confidence Interval for B	
		B	Std. Error	Beta			Lower Bound	Upper Bound
1	(Constant)	-143.244	50.011		-2.864	.006	-243.215	-43.274
	B	-6.138	2.355	-1.761	-2.607	.011	-10.845	-1.431
	B_x	-5.294	2.754	-1.216	-1.922	.059	-10.800	.211
	B_y	-1.788	.854	-.362	-2.093	.040	-3.495	-.080
	B_z	-.186	1.440	-.031	-.129	.898	-3.063	2.692
	T_p	.000	.000	-.523	-1.412	.163	.000	.000
	N_p	3.828	5.758	.328	.665	.509	-7.682	15.337
	V_p	.337	.114	1.017	2.948	.005	.108	.565
	β	6.647	19.411	.091	.342	.733	-32.156	45.449
	Dst	-.052	.353	-.050	-.147	.884	-.758	.654

a. Dependent Variable: PARC2

Table D-17 SCH2

Model Summary[b]

Model	R	R Square	Adjusted R Square	Std. Error of the Estimate
1	.833[a]	.694	.650	27.50877

ANOVA[b]

Model		Sum of Squares	df	Mean Square	F	Sig.
1	Regression	106553.737	9	11839.304	15.645	.000[a]
	Residual	46917.422	62	756.733		
	Total	153471.159	71			

a. Predictors: (Constant), Dst, Bz, Den, Bye, Betta, Speed, Tem, Bx, Bmag

b. Dependent Variable: SCH22

Coefficients[a]

Model		Unstandardized Coefficients		Standardized Coefficients	t	Sig.	95.0% Confidence Interval for B	
		B	Std. Error	Beta			Lower Bound	Upper Bound
1	(Constant)	-36.023	36.839		-.978	.332	-109.663	37.616
	B	.266	1.735	.087	.153	.879	-3.201	3.733
	B_x	4.331	2.029	1.136	2.135	.037	.276	8.387
	B_y	1.477	.629	.342	2.349	.022	.220	2.735
	B_z	-.254	1.060	-.048	-.240	.811	-2.374	1.866
	T_p	-6.458E-5	.000	-.361	-1.158	.251	.000	.000
	N_p	12.486	4.241	1.223	2.944	.005	4.008	20.964
	V_p	.018	.084	.063	.216	.830	-.150	.186
	β	-13.492	14.299	-.211	-.944	.349	-42.075	15.090
	*D*st	-.663	.260	-.731	-2.548	.013	-1.183	-.143

a. Dependent Variable: SCH22

Table D-18 SCUB

Model Summary[b]

Model	R	R Square	Adjusted R Square	Std. Error of the Estimate
1	.586[a]	.343	.246	31.38168

ANOVA[b]

Model		Sum of Squares	df	Mean Square	F	Sig.
1	Regression	31348.331	9	3483.148	3.537	.001[a]
	Residual	60073.403	61	984.810		
	Total	91421.734	70			

a. Predictors: (Constant), Dst, Bz, Den, Bye, Betta, Speed, Tem, Bx, Bmag

b. Dependent Variable: SCUB2

Coefficients[a]

Model		Unstandardized Coefficients		Standardized Coefficients	t	Sig.	95.0% Confidence Interval for B	
		B	Std. Error	Beta			Lower Bound	Upper Bound
1	(Constant)	-86.749	42.054		-2.063	.043	-170.840	-2.657
	B	-4.116	1.981	-1.744	-2.078	.042	-8.078	-.155
	B_x	-2.179	2.314	-.738	-.941	.350	-6.807	2.449
	B_y	1.668	.719	.500	2.321	.024	.231	3.105
	B_z	-2.128	1.213	-.522	-1.753	.085	-4.554	.299
	T_p	2.180E-5	.000	.158	.342	.733	.000	.000
	N_p	-7.614	4.867	-.965	-1.565	.123	-17.346	2.118
	V_p	.266	.096	1.183	2.769	.007	.074	.458
	β	3.281	16.312	.066	.201	.841	-29.336	35.899
	Dst	.270	.299	.385	.902	.370	-.328	.868

a. Dependent Variable: SCUB2

Table D-19 SG05

Model Summary[b]

Model	R	R Square	Adjusted R Square	Std. Error of the Estimate
1	.555[a]	.308	.208	35.75513

ANOVA[b]

Model		Sum of Squares	df	Mean Square	F	Sig.
1	Regression	35342.604	9	3926.956	3.072	.004[a]
	Residual	79262.625	62	1278.429		
	Total	114605.229	71			

a. Predictors: (Constant), Dst, Bz, Den, Bye, Betta, Speed, Tem, Bx, Bmag

b. Dependent Variable: SG052

Coefficients[a]

Model		Unstandardized Coefficients		Standardized Coefficients	t	Sig.	95.0% Confidence Interval for B	
		B	Std. Error	Beta			Lower Bound	Upper Bound
1	(Constant)	-87.616	47.882		-1.830	.072	-183.331	8.098
	B	-4.822	2.255	-1.828	-2.139	.036	-9.328	-.315
	B_x	-2.974	2.637	-.903	-1.128	.264	-8.245	2.297
	B_y	1.009	.818	.270	1.234	.222	-.626	2.643
	B_z	-1.934	1.378	-.425	-1.403	.166	-4.689	.822
	T_p	1.313E-5	.000	.085	.181	.857	.000	.000
	N_p	-5.652	5.513	-.641	-1.025	.309	-16.671	5.368
	V_p	.255	.109	1.018	2.330	.023	.036	.474
	β	.518	18.585	.009	.028	.978	-36.633	37.669
	*D*st	.237	.338	.302	.700	.486	-.439	.913

Table D-20 SCUB

Model Summary[b]

Model	R	R Square	Adjusted R Square	Std. Error of the Estimate
1	.586[a]	.343	.246	31.38168

ANOVA[b]

Model		Sum of Squares	df	Mean Square	F	Sig.
1	Regression	31348.331	9	3483.148	3.537	.001[a]
	Residual	60073.403	61	984.810		
	Total	91421.734	70			

a. Predictors: (Constant), Dst, Bz, Den, Bye, Betta, Speed, Tem, Bx, Bmag

b. Dependent Variable: SCUB2

Coefficients[a]

Model		Unstandardized Coefficients		Standardized Coefficients	t	Sig.	95.0% Confidence Interval for B	
		B	Std. Error	Beta			Lower Bound	Upper Bound
1	(Constant)	-86.749	42.054		-2.063	.043	-170.840	-2.657
	B	-4.116	1.981	-1.744	-2.078	.042	-8.078	-.155
	B_x	-2.179	2.314	-.738	-.941	.350	-6.807	2.449
	B_y	1.668	.719	.500	2.321	.024	.231	3.105
	B_z	-2.128	1.213	-.522	-1.753	.085	-4.554	.299
	T_p	2.180E-5	.000	.158	.342	.733	.000	.000
	N_p	-7.614	4.867	-.965	-1.565	.123	-17.346	2.118
	V_p	.266	.096	1.183	2.769	.007	.074	.458
	β	3.281	16.312	.066	.201	.841	-29.336	35.899
	*D*st	.270	.299	.385	.902	.370	-.328	.868

a. Dependent Variable: SCUB2

Table D-21 SG05

Model Summary[b]

Model	R	R Square	Adjusted R Square	Std. Error of the Estimate
1	.555[a]	.308	.208	35.75513

ANOVA[b]

Model		Sum of Squares	df	Mean Square	F	Sig.
1	Regression	35342.604	9	3926.956	3.072	.004[a]
	Residual	79262.625	62	1278.429		
	Total	114605.229	71			

a. Predictors: (Constant), Dst, Bz, Den, Bye, Betta, Speed, Tem, Bx, Bmag

b. Dependent Variable: SG052

Coefficients[a]

Model		Unstandardized Coefficients		Standardized Coefficients	t	Sig.	95.0% Confidence Interval for B	
		B	Std. Error	Beta			Lower Bound	Upper Bound
1	(Constant)	-87.616	47.882		-1.830	.072	-183.331	8.098
	B	-4.822	2.255	-1.828	-2.139	.036	-9.328	-.315
	B_x	-2.974	2.637	-.903	-1.128	.264	-8.245	2.297
	B_y	1.009	.818	.270	1.234	.222	-.626	2.643
	B_z	-1.934	1.378	-.425	-1.403	.166	-4.689	.822
	T_p	1.313E-5	.000	.085	.181	.857	.000	.000
	N_p	-5.652	5.513	-.641	-1.025	.309	-16.671	5.368
	V_p	.255	.109	1.018	2.330	.023	.036	.474
	β	.518	18.585	.009	.028	.978	-36.633	37.669
	Dst	.237	.338	.302	.700	.486	-.439	.913

Table D-22 UNSA

Model Summary[b]

Model	R	R Square	Adjusted R Square	Std. Error of the Estimate
1	.239[a]	.057	-.080	42.86585

ANOVA[b]

Model		Sum of Squares	df	Mean Square	F	Sig.
1	Regression	6889.011	9	765.446	.417	.922[a]
	Residual	113923.847	62	1837.481		
	Total	120812.858	71			

a. Predictors: (Constant), Dst, Bz, Den, Bye, Betta, Speed, Tem, Bx, Bmag

b. Dependent Variable: UNSA

Coefficients[a]

Model		Unstandardized Coefficients		Standardized Coefficients	t	Sig.	95.0% Confidence Interval for B	
		B	Std. Error	Beta			Lower Bound	Upper Bound
1	(Constant)	100.260	57.405		1.747	.086	-14.490	215.010
	B	3.024	2.703	1.117	1.119	.268	-2.379	8.427
	B_x	4.067	3.161	1.202	1.286	.203	-2.253	10.386
	B_y	-1.262	.980	-.329	-1.288	.203	-3.222	.697
	B_z	2.503	1.652	.536	1.515	.135	-.800	5.807
	T_p	8.037E-6	.000	.051	.093	.927	.000	.000
	N_p	6.020	6.609	.665	.911	.366	-7.191	19.231
	V_p	-.139	.131	-.542	-1.062	.292	-.402	.123
	β	-22.719	22.281	-.400	-1.020	.312	-67.258	21.820
	Dst	-.378	.406	-.470	-.932	.355	-1.189	.433

a. Dependent Variable: UNSA

Event III

Table D-23 BAIE

Model Summary[b]

Model	R	R Square	Adjusted R Square	Std. Error of the Estimate
1	.649[a]	.421	.337	22.02561

ANOVA[b]

Model		Sum of Squares	df	Mean Square	F	Sig.
1	Regression	21901.376	9	2433.486	5.016	.000[a]
	Residual	30077.909	62	485.128		
	Total	51979.285	71			

a. Predictors: (Constant), Dst, Betta, Bx, Speed, Den, Bz, Bmag, Bye, Tem

b. Dependent Variable: BAIE3

Coefficients[a]

Model		Unstandardized Coefficients		Standardized Coefficients	t	Sig.	95.0% Confidence Interval for B	
		B	Std. Error	Beta			Lower Bound	Upper Bound
1	(Constant)	26.106	37.883		.689	.493	-49.622	101.834
	B	2.280	.974	.454	2.342	.022	.334	4.226
	B_x	-.629	1.340	-.077	-.469	.641	-3.307	2.050
	B_y	.817	.993	.179	.822	.414	-1.169	2.802
	B_z	-1.045	.784	-.222	-1.333	.187	-2.613	.522
	T_p	-2.081E-5	.000	-.087	-.369	.713	.000	.000
	N_p	.215	1.395	.027	.154	.878	-2.573	3.004
	V_p	-.089	.069	-.249	-1.284	.204	-.226	.049
	β	-2.279	4.272	-.093	-.534	.596	-10.819	6.261
	Dst	.147	.194	.166	.762	.449	-.239	.534

a. Dependent Variable: BAIE3

Table D-24 BOGT

Model Summary[b]

Model	R	R Square	Adjusted R Square	Std. Error of the Estimate
1	.760[a]	.577	.516	29.08375

ANOVA[b]

Model		Sum of Squares	df	Mean Square	F	Sig.
1	Regression	71597.285	9	7955.254	9.405	.000[a]
	Residual	52443.608	62	845.865		
	Total	124040.893	71			

a. Predictors: (Constant), Dst, Betta, Bx, Speed, Den, Bz, Bmag, Bye, Tem

b. Dependent Variable: BOGT3

Coefficients[a]

Model		Unstandardized Coefficients		Standardized Coefficients	t	Sig.	95.0% Confidence Interval for B	
		B	Std. Error	Beta			Lower Bound	Upper Bound
1	(Constant)	-107.458	50.023		-2.148	.036	-207.453	-7.463
	B	1.479	1.285	.191	1.150	.254	-1.091	4.048
	B_x	-1.346	1.769	-.107	-.761	.450	-4.883	2.191
	B_y	-1.627	1.311	-.231	-1.240	.220	-4.248	.995
	B_z	-3.774	1.035	-.520	-3.646	.001	-5.843	-1.705
	T_p	-4.367E-5	.000	-.118	-.587	.559	.000	.000
	N_p	-2.683	1.842	-.217	-1.457	.150	-6.365	.999
	V_p	.262	.091	.477	2.877	.006	.080	.444
	β	-4.804	5.641	-.127	-.852	.398	-16.081	6.472
	Dst	.249	.256	.182	.976	.333	-.261	.760

a. Dependent Variable: BOGT3

Table D-25 LAMT

Model Summary[b]

Model	R	R Square	Adjusted R Square	Std. Error of the Estimate
1	.782[a]	.611	.555	13.40877

ANOVA[b]

Model		Sum of Squares	df	Mean Square	F	Sig.
1	Regression	17530.278	9	1947.809	10.833	.000[a]
	Residual	11147.300	62	179.795		
	Total	28677.578	71			

a. Predictors: (Constant), Dst, Betta, Bx, Speed, Den, Bz, Bmag, Bye, Tem

b. Dependent Variable: LAMT3

Coefficients[a]

Model		Unstandardized Coefficients		Standardized Coefficients	t	Sig.	95.0% Confidence Interval for B	
		B	Std. Error	Beta			Lower Bound	Upper Bound
1	(Constant)	13.252	23.063		.575	.568	-32.850	59.354
	B	-.445	.593	-.119	-.751	.456	-1.630	.740
	B_x	.239	.816	.039	.293	.770	-1.391	1.870
	B_y	-.902	.605	-.267	-1.493	.141	-2.111	.306
	B_z	1.798	.477	.515	3.768	.000	.844	2.752
	T_p	-9.727E-6	.000	-.055	-.284	.778	.000	.000
	N_p	.019	.849	.003	.022	.982	-1.679	1.716
	V_p	-.038	.042	-.146	-.916	.363	-.122	.045
	β	-2.035	2.601	-.112	-.782	.437	-7.233	3.164
	Dst	.206	.118	.312	1.746	.086	-.030	.441

a. Dependent Variable: LAMT3

Table D-26 SCH2

Model Summary[b]

Model	R	R Square	Adjusted R Square	Std. Error of the Estimate
1	.478[a]	.229	.046	32.08454

ANOVA[b]

Model		Sum of Squares	df	Mean Square	F	Sig.
1	Regression	11597.914	9	1288.657	1.252	.294[a]
	Residual	39117.867	38	1029.418		
	Total	50715.781	47			

a. Predictors: (Constant), Dst, Betta, Bx, Tem, Bz, Bmag, Den, Bye, Speed

b. Dependent Variable: SCH23

Coefficients[a]

Model		Unstandardized Coefficients		Standardized Coefficients	t	Sig.	95.0% Confidence Interval for B	
		B	Std. Error	Beta			Lower Bound	Upper Bound
1	(Constant)	52.470	74.724		.702	.487	-98.802	203.742
	B	-.078	2.817	-.007	-.028	.978	-5.781	5.625
	B_x	2.899	2.926	.297	.991	.328	-3.024	8.823
	B_y	1.890	2.754	.230	.686	.497	-3.684	7.465
	B_z	-1.922	2.316	-.213	-.830	.412	-6.610	2.766
	T_p	-7.227E-5	.000	-.232	-.543	.590	.000	.000
	N_p	-1.197	2.550	-.140	-.469	.641	-6.358	3.965
	V_p	-.008	.157	-.023	-.051	.959	-.326	.310
	β	-3.747	8.035	-.112	-.466	.644	-20.012	12.518
	Dst	.472	.497	.376	.950	.348	-.534	1.478

a. Dependent Variable: SCH23

SCUB

Table D-27 SCUB

Model Summary[b]

Model	R	R Square	Adjusted R Square	Std. Error of the Estimate
1	.792[a]	.627	.573	24.31375

ANOVA[b]

Model		Sum of Squares	df	Mean Square	F	Sig.
	Regression	61683.440	9	6853.716	11.594	.000[a]
1	Residual	36651.827	62	591.159		
	Total	98335.267	71			

a. Predictors: (Constant), Dst, Betta, Bx, Speed, Den, Bz, Bmag, Bye, Tem

b. Dependent Variable: SCUB3

Coefficients[a]

Model		Unstandardized Coefficients		Standardized Coefficients	t	Sig.	95.0% Confidence Interval for B	
		B	Std. Error	Beta			Lower Bound	Upper Bound
1	(Constant)	-103.186	41.819		-2.467	.016	-186.781	-19.591
	B	1.064	1.075	.154	.990	.326	-1.084	3.212
	B_x	-.106	1.479	-.009	-.072	.943	-3.063	2.850
	B_y	-4.258	1.096	-.680	-3.884	.000	-6.450	-2.066
	B_z	-1.359	.865	-.210	-1.570	.122	-3.088	.371
	T_p	.000	.000	-.472	-2.503	.015	.000	.000
	N_p	.020	1.540	.002	.013	.990	-3.058	3.098
	V_p	.222	.076	.453	2.912	.005	.069	.374
	β	8.224	4.716	.244	1.744	.086	-1.203	17.651
	Dst	.249	.214	.203	1.164	.249	-.178	.676

a. Dependent Variable: SCUB3

Table D-28 SG05

Model Summary[b]

Model	R	R Square	Adjusted R Square	Std. Error of the Estimate
1	.806[a]	.650	.599	21.20249

ANOVA[b]

Model		Sum of Squares	df	Mean Square	F	Sig.
1	Regression	51673.150	9	5741.461	12.772	.000[a]
	Residual	27871.828	62	449.546		
	Total	79544.978	71			

a. Predictors: (Constant), Dst, Betta, Bx, Speed, Den, Bz, Bmag, Bye, Tem

b. Dependent Variable: SG053

Coefficients[a]

Model		Unstandardized Coefficients		Standardized Coefficients	t	Sig.	95.0% Confidence Interval for B	
		B	Std. Error	Beta			Lower Bound	Upper Bound
1	(Constant)	-33.436	36.468		-.917	.363	-106.334	39.462
	B	.006	.937	.001	.006	.995	-1.867	1.879
	B_x	1.681	1.290	.166	1.303	.197	-.898	4.259
	B_y	-2.193	.956	-.390	-2.294	.025	-4.105	-.282
	B_z	.636	.755	.109	.843	.403	-.873	2.145
	T_p	.000	.000	-.632	-3.457	.001	.000	.000
	N_p	2.438	1.343	.246	1.815	.074	-.246	5.122
	V_p	.057	.066	.129	.858	.394	-.076	.190
	β	2.480	4.112	.082	.603	.549	-5.741	10.700
	Dst	-.056	.186	-.051	-.298	.766	-.428	.317

a. Dependent Variable: SG053

Table D-29 UNSA

Model Summary[b]

Model	R	R Square	Adjusted R Square	Std. Error of the Estimate
1	.728[a]	.530	.462	34.19861

ANOVA[b]

Model		Sum of Squares	df	Mean Square	F	Sig.
1	Regression	81885.912	9	9098.435	7.779	.000[a]
	Residual	72511.774	62	1169.545		
	Total	154397.686	71			

Coefficients[a]

Model		Unstandardized Coefficients		Standardized Coefficients	t	Sig.	95.0% Confidence Interval for B	
		B	Std. Error	Beta			Lower Bound	Upper Bound
1	(Constant)	-105.738	58.821		-1.798	.077	-223.319	11.843
	B	1.039	1.512	.120	.687	.495	-1.983	4.060
	B_x	4.254	2.081	.302	2.044	.045	.095	8.413
	B_y	1.726	1.542	.220	1.120	.267	-1.356	4.809
	B_z	-2.499	1.217	-.308	-2.053	.044	-4.932	-.066
	T_p	4.012E-5	.000	.097	.459	.648	.000	.000
	N_p	-.352	2.166	-.025	-.162	.871	-4.682	3.978
	V_p	.221	.107	.361	2.065	.043	.007	.435
	β	-3.683	6.633	-.087	-.555	.581	-16.943	9.577
	Dst	-.205	.300	-.134	-.681	.499	-.805	.396

a. Dependent Variable: UNSA3

Event IV

Table D-30 BAIE

Model Summary[b]

Model	R	R Square	Adjusted R Square	Std. Error of the Estimate
1	.933[a]	.871	.852	35.64261

ANOVA[b]

Model		Sum of Squares	df	Mean Square	F	Sig.
1	Regression	531378.857	9	59042.095	46.475	.000[a]
	Residual	78764.521	62	1270.395		
	Total	610143.378	71			

a. Predictors: (Constant), Dst, Speed, Bx, Betta, Bz, Density, Bye, Tem, Bmag

b. Dependent Variable: BAIE4

Coefficients[a]

Model		Unstandardized Coefficients		Standardized Coefficients	t	Sig.
		B	Std. Error	Beta		
1	(Constant)	-359.018	87.293		-4.113	.000
	B	22.676	3.666	1.100	6.185	.000
	B_x	-8.071	3.393	-.243	-2.379	.020
	B_y	-2.055	2.315	-.103	-.888	.378
	B_z	4.844	1.486	.251	3.260	.002
	T_p	.000	.000	-.692	-5.766	.000
	N_p	-12.034	2.829	-.429	-4.253	.000
	V_p	.484	.149	.587	3.248	.002
	β	41.469	10.973	.362	3.779	.000
	*D*st	-.054	.243	-.025	-.221	.826

a. Dependent Variable: BAIE4

Table D-31 BOGT

Model Summary[b]

Model	R	R Square	Adjusted R Square	Std. Error of the Estimate
1	.619[a]	.384	.294	60.22907

ANOVA[b]

Model		Sum of Squares	df	Mean Square	F	Sig.
1	Regression	140030.725	9	15558.969	4.289	.000[a]
	Residual	224907.551	62	3627.541		
	Total	364938.276	71			

a. Predictors: (Constant), Dst, Speed, Bx, Betta, Bz, Density, Bye, Tem, Bmag

b. Dependent Variable: BOGT4

Coefficients[a]

Model		Unstandardized Coefficients		Standardized Coefficients	t	Sig.
		B	Std. Error	Beta		
1	(Constant)	-45.963	147.508		-.312	.756
	B	8.078	6.196	.507	1.304	.197
	B_x	-15.039	5.734	-.585	-2.623	.011
	B_y	3.223	3.911	.209	.824	.413
	B_z	2.072	2.510	.139	.825	.412
	T_p	-6.609E-5	.000	-.292	-1.116	.269
	N_p	-6.835	4.781	-.315	-1.430	.158
	V_p	.139	.252	.218	.551	.584
	β	3.903	18.542	.044	.210	.834
	Dst	-.159	.410	-.094	-.387	.700

a. Dependent Variable: BOGT4

Table D-32 BRAZ

Model Summary[b]

Model	R	R Square	Adjusted R Square	Std. Error of the Estimate
1	.727[a]	.529	.460	39.82498

ANOVA[b]

Model		Sum of Squares	df	Mean Square	F	Sig.
1	Regression	110306.470	9	12256.274	7.728	.000[a]
	Residual	98333.789	62	1586.029		
	Total	208640.259	71			

a. Predictors: (Constant), Dst, Speed, Bx, Betta, Bz, Density, Bye, Tem, Bmag

b. Dependent Variable: BRAZ4

Coefficients[a]

Model		Unstandardized Coefficients		Standardized Coefficients	t	Sig.
		B	Std. Error	Beta		
1	(Constant)	-57.026	97.536		-.585	.561
	B	-10.074	4.097	-.836	-2.459	.017
	B_x	1.739	3.791	.089	.459	.648
	B_y	-6.693	2.586	-.575	-2.588	.012
	B_z	3.927	1.660	.349	2.366	.021
	T_p	5.270E-5	.000	.308	1.345	.183
	N_p	.284	3.162	.017	.090	.929
	V_p	.060	.166	.124	.358	.722
	β	-28.457	12.260	-.425	-2.321	.024
	Dst	-1.898	.271	-1.490	-6.997	.000

a. Dependent Variable: BRAZ4

CONO

Table D-33 CONO

Model Summary[b]

Model	R	R Square	Adjusted R Square	Std. Error of the Estimate
1	.900[a]	.809	.782	22.20507

ANOVA[b]

Model		Sum of Squares	df	Mean Square	F	Sig.
1	Regression	129897.779	9	14433.087	29.272	.000[a]
	Residual	30570.040	62	493.065		
	Total	160467.819	71			

a. Predictors: (Constant), Dst, Speed, Bx, Betta, Bz, Density, Bye, Tem, Bmag

b. Dependent Variable: CONO4

Coefficients[a]

Model		Unstandardized Coefficients		Standardized Coefficients	t	Sig.
		B	Std. Error	Beta		
1	(Constant)	-16.899	54.383		-.311	.757
	B	7.004	2.284	.663	3.066	.003
	B_x	-3.810	2.114	-.223	-1.803	.076
	B_y	-2.902	1.442	-.284	-2.013	.049
	B_z	-.135	.926	-.014	-.145	.885
	T_p	-3.106E-5	.000	-.207	-1.422	.160
	N_p	4.404	1.763	.306	2.498	.015
	V_p	.001	.093	.002	.008	.994
	β	-3.713	6.836	-.063	-.543	.589
	*D*st	.633	.151	.567	4.188	.000

a. Dependent Variable: CONO4

Table D-34 COPO

Model Summary[b]

Model	R	R Square	Adjusted R Square	Std. Error of the Estimate
1	.670[a]	.449	.369	19.19932

ANOVA[b]

Model		Sum of Squares	df	Mean Square	F	Sig.
1	Regression	18625.884	9	2069.543	5.614	.000[a]
	Residual	22854.062	62	368.614		
	Total	41479.946	71			

a. Predictors: (Constant), Dst, Speed, Bx, Betta, Bz, Density, Bye, Tem, Bmag

b. Dependent Variable: COPO4

Coefficients[a]

Model		Unstandardized Coefficients		Standardized Coefficients	t	Sig.
		B	Std. Error	Beta		
1	(Constant)	-85.388	47.021		-1.816	.074
	B	1.411	1.975	.263	.714	.478
	B_x	-3.526	1.828	-.407	-1.929	.058
	B_y	-.710	1.247	-.137	-.569	.571
	B_z	1.885	.800	.375	2.355	.022
	T_p	-5.508E-5	.000	-.723	-2.917	.005
	N_p	-2.113	1.524	-.289	-1.387	.171
	V_p	.160	.080	.744	1.993	.051
	β	4.085	5.911	.137	.691	.492
	Dst	.080	.131	.141	.613	.542

a. Dependent Variable: COPO4

Table D-35 GOGA

Model Summary[b]

Model	R	R Square	Adjusted R Square	Std. Error of the Estimate
1	.879[a]	.773	.741	20.92325

ANOVA[b]

Model		Sum of Squares	df	Mean Square	F	Sig.
1	Regression	92637.742	9	10293.082	23.512	.000[a]
	Residual	27142.498	62	437.782		
	Total	119780.240	71			

a. Predictors: (Constant), Dst, Speed, Bx, Betta, Bz, Density, Bye, Tem, Bmag

b. Dependent Variable: GOGA4

Coefficients[a]

Model		Unstandardized Coefficients		Standardized Coefficients	t	Sig.
		B	Std. Error	Beta		
1	(Constant)	-258.215	51.243		-5.039	.000
	B	2.855	2.152	.313	1.327	.189
	B_x	-1.781	1.992	-.121	-.894	.375
	B_y	-4.421	1.359	-.501	-3.254	.002
	B_z	5.510	.872	.646	6.318	.000
	T_p	.000	.000	-.923	-5.809	.000
	N_p	-3.647	1.661	-.293	-2.196	.032
	V_p	.386	.087	1.058	4.420	.000
	β	13.532	6.441	.267	2.101	.040
	Dst	-.383	.142	-.397	-2.685	.009

a. Dependent Variable: GOGA4

Table D-36 PARC

Model Summary[b]

Model	R	R Square	Adjusted R Square	Std. Error of the Estimate
1	.933[a]	.871	.852	18.70173

ANOVA[b]

Model		Sum of Squares	df	Mean Square	F	Sig.
1	Regression	146295.444	9	16255.049	46.476	.000[a]
	Residual	21684.795	62	349.755		
	Total	167980.239	71			

a. Predictors: (Constant), Dst, Speed, Bx, Betta, Bz, Density, Bye, Tem, Bmag

b. Dependent Variable: PARC4

Coefficients[a]

Model		Unstandardized Coefficients		Standardized Coefficients	t	Sig.
		B	Std. Error	Beta		
1	(Constant)	-53.668	45.803		-1.172	.246
	B	6.361	1.924	.588	3.306	.002
	B_x	-2.032	1.780	-.116	-1.141	.258
	B_y	-5.341	1.214	-.511	-4.398	.000
	B_z	3.558	.780	.352	4.565	.000
	T_p	-5.099E-5	.000	-.332	-2.772	.007
	N_p	3.012	1.485	.204	2.029	.047
	V_p	.071	.078	.164	.909	.367
	β	-2.034	5.757	-.034	-.353	.725
	Dst	.299	.127	.262	2.350	.022

a. Dependent Variable: PARC4

Table D-37 SCH2

Model Summary[b]

Model	R	R Square	Adjusted R Square	Std. Error of the Estimate
1	.939[a]	.881	.864	42.00834

ANOVA[b]

Model		Sum of Squares	df	Mean Square	F	Sig.
1	Regression	812384.523	9	90264.947	51.150	.000[a]
	Residual	109411.433	62	1764.701		
	Total	921795.956	71			

a. Predictors: (Constant), Dst, Speed, Bx, Betta, Bz, Density, Bye, Tem, Bmag

b. Dependent Variable: SCH24

Coefficients[a]

Model		Unstandardized Coefficients		Standardized Coefficients	t	Sig.
		B	Std. Error	Beta		
1	(Constant)	42.555	102.883		.414	.681
	B	10.558	4.321	.417	2.443	.017
	B_x	-11.818	3.999	-.289	-2.955	.004
	B_y	5.753	2.728	.235	2.109	.039
	B_z	-7.076	1.751	-.299	-4.041	.000
	T_p	9.940E-5	.000	.277	2.406	.019
	N_p	6.014	3.335	.174	1.803	.076
	V_p	-.174	.176	-.171	-.990	.326
	β	-21.721	12.933	-.154	-1.680	.098
	Dst	-.842	.286	-.314	-2.943	.005

a. Dependent Variable: SCH24

Table D-38 SG05

Model Summary[b]

Model	R	R Square	Adjusted R Square	Std. Error of the Estimate
1	.837[a]	.701	.656	30.54863

ANOVA[b]

Model		Sum of Squares	df	Mean Square	F	Sig.
1	Regression	131390.472	9	14598.941	15.644	.000[a]
	Residual	55993.132	60	933.219		
	Total	187383.604	69			

a. Predictors: (Constant), Dst, Speed, Bx, Betta, Bz, Density, Bye, Tem, Bmag

b. Dependent Variable: SG05

Coefficients[a]

Model		Unstandardized Coefficients		Standardized Coefficients	t	Sig.
		B	Std. Error	Beta		
1	(Constant)	56.204	75.515		.744	.460
	B	10.792	3.207	.929	3.366	.001
	B_x	-5.420	2.915	-.287	-1.859	.068
	B_y	-1.664	1.996	-.151	-.834	.408
	B_z	-3.367	1.274	-.315	-2.642	.010
	T_p	-4.095E-5	.000	-.252	-1.356	.180
	N_p	3.243	2.437	.208	1.330	.188
	V_p	-.088	.129	-.193	-.683	.497
	β	1.963	9.457	.031	.208	.836
	Dst	1.066	.210	.883	5.079	.000

a. Dependent Variable: SG05

Event V

Table D-39 BAIE

Model Summary[b]

Model	R	R Square	Adjusted R Square	Std. Error of the Estimate
1	.557[a]	.310	.210	10.24399

ANOVA[b]

Model		Sum of Squares	df	Mean Square	F	Sig.
1	Regression	2921.262	9	324.585	3.093	.004[a]
	Residual	6506.236	62	104.939		
	Total	9427.499	71			

a. Predictors: (Constant), Dst, Betta, Bz, Speed, Bmag, Density, Tem, Byi, Bx

b. Dependent Variable: BAIE5

Coefficients[a]

Model		Unstandardized Coefficients		Standardized Coefficients	t	Sig.	95.0% Confidence Interval for B	
		B	Std. Error	Beta			Lower Bound	Upper Bound
1	(Constant)	45.122	11.674		3.865	.000	21.787	68.457
	B	.201	.734	.090	.274	.785	-1.267	1.669
	B_x	-.579	.946	-.202	-.611	.543	-2.470	1.313
	B_y	.390	.524	.219	.745	.459	-.657	1.437
	B_z	-.020	.611	-.008	-.033	.974	-1.241	1.201
	T_p	-1.639E-5	.000	-.151	-.569	.571	.000	.000
	N_p	-.480	.378	-.338	-1.270	.209	-1.236	.276
	V_p	-.061	.022	-.559	-2.787	.007	-.105	-.017
	β	-.078	2.130	-.008	-.037	.971	-4.336	4.181
	Dst	.048	.137	.107	.349	.728	-.226	.322

a. Dependent Variable: BAIE5

Table D-40 BOGT

Model Summary[b]

Model	R	R Square	Adjusted R Square	Std. Error of the Estimate
1	.814[a]	.662	.613	28.13511

ANOVA[b]

Model		Sum of Squares	df	Mean Square	F	Sig.
1	Regression	96231.511	9	10692.390	13.508	.000[a]
	Residual	49078.223	62	791.584		
	Total	145309.734	71			

a. Predictors: (Constant), Dst, Betta, Bz, Speed, Bmag, Density, Tem, Byi, Bx

b. Dependent Variable: BOGT5

Coefficients[a]

Model		Unstandardized Coefficients		Standardized Coefficients	t	Sig.	95.0% Confidence Interval for B	
		B	Std. Error	Beta			Lower Bound	Upper Bound
1	(Constant)	111.544	32.062		3.479	.001	47.454	175.635
	B	4.955	2.017	.563	2.457	.017	.923	8.987
	B_x	-3.296	2.599	-.293	-1.268	.210	-8.492	1.900
	B_y	1.136	1.439	.162	.789	.433	-1.740	4.012
	B_z	2.530	1.677	.239	1.508	.137	-.823	5.883
	T_p	.000	.000	-.636	-3.430	.001	.000	.000
	N_p	-.277	1.039	-.050	-.267	.790	-2.353	1.799
	V_p	-.297	.060	-.694	-4.945	.000	-.418	-.177
	β	7.617	5.851	.208	1.302	.198	-4.078	19.313
	Dst	-2.010	.377	-1.140	-5.335	.000	-2.763	-1.257

a. Dependent Variable: BOGT5

Table D-41 BRAZ

Model Summary[b]

Model	R	R Square	Adjusted R Square	Std. Error of the Estimate
1	.456[a]	.208	.093	18.19849

ANOVA[b]

Model		Sum of Squares	df	Mean Square	F	Sig.
1	Regression	5385.657	9	598.406	1.807	.085[a]
	Residual	20533.471	62	331.185		
	Total	25919.129	71			

a. Predictors: (Constant), Dst, Betta, Bz, Speed, Bmag, Density, Tem, Byi, Bx

b. Dependent Variable: BRAZ5

Coefficients[a]

Model		Unstandardized Coefficients		Standardized Coefficients	t	Sig.	95.0% Confidence Interval for B	
		B	Std. Error	Beta			Lower Bound	Upper Bound
1	(Constant)	-9.047	20.738		-.436	.664	-50.502	32.408
	B	.405	1.305	.109	.311	.757	-2.203	3.013
	B_x	2.944	1.681	.620	1.751	.085	-.417	6.305
	B_y	1.050	.931	.355	1.128	.263	-.810	2.910
	B_z	-1.891	1.085	-.422	-1.742	.086	-4.060	.278
	T_p	.000	.000	-.580	-2.042	.045	.000	.000
	N_p	.060	.672	.025	.089	.929	-1.283	1.402
	V_p	.028	.039	.152	.708	.482	-.050	.105
	β	4.231	3.784	.273	1.118	.268	-3.334	11.796
	Dst	-.699	.244	-.938	-2.868	.006	-1.186	-.212

a. Dependent Variable: BRAZ5

Table D-42 CONO

Model Summary[b]

Model	R	R Square	Adjusted R Square	Std. Error of the Estimate
1	.766[a]	.587	.526	9.39962

ANOVA[b]

Model		Sum of Squares	df	Mean Square	F	Sig.
1	Regression	7769.957	9	863.329	9.771	.000[a]
	Residual	5477.879	62	88.353		
	Total	13247.836	71			

a. Predictors: (Constant), Dst, Betta, Bz, Speed, Bmag, Density, Tem, Byi, Bx

b. Dependent Variable: CONO5

Coefficients[a]

Model		Unstandardized Coefficients		Standardized Coefficients	t	Sig.	95.0% Confidence Interval for B	
		B	Std. Error	Beta			Lower Bound	Upper Bound
1	(Constant)	45.805	10.711		4.276	.000	24.394	67.217
	B	-.927	.674	-.349	-1.375	.174	-2.274	.420
	B_x	.174	.868	.051	.201	.842	-1.562	1.910
	B_y	.180	.481	.085	.375	.709	-.781	1.141
	B_z	-1.294	.560	-.404	-2.309	.024	-2.415	-.174
	T_p	1.556E-5	.000	.121	.589	.558	.000	.000
	N_p	.502	.347	.298	1.448	.153	-.191	1.196
	V_p	-.077	.020	-.597	-3.845	.000	-.117	-.037
	β	-4.279	1.955	-.387	-2.189	.032	-8.186	-.372
	Dst	.036	.126	.068	.286	.776	-.216	.288

a. Dependent Variable: CONO5

Table D-43 COPO

Model Summary[b]

Model	R	R Square	Adjusted R Square	Std. Error of the Estimate
1	.795[a]	.632	.579	24.24588

ANOVA[b]

Model		Sum of Squares	df	Mean Square	F	Sig.
1	Regression	62703.518	9	6967.058	11.852	.000[a]
	Residual	36447.493	62	587.863		
	Total	99151.010	71			

Coefficients[a]

Model		Unstandardized Coefficients		Standardized Coefficients	t	Sig.	95.0% Confidence Interval for B	
		B	Std. Error	Beta			Lower Bound	Upper Bound
1	(Constant)	-22.501	27.630		-.814	.419	-77.732	32.730
	B	-1.169	1.738	-.161	-.672	.504	-4.643	2.306
	B_x	6.499	2.240	.700	2.901	.005	2.021	10.976
	B_y	2.386	1.240	.413	1.925	.059	-.092	4.865
	B_z	-4.193	1.446	-.479	-2.900	.005	-7.083	-1.303
	T_p	.000	.000	-.653	-3.375	.001	.000	.000
	N_p	.679	.895	.147	.759	.451	-1.110	2.468
	V_p	.060	.052	.169	1.153	.253	-.044	.163
	β	5.234	5.042	.173	1.038	.303	-4.844	15.313
	Dst	-1.943	.325	-1.334	-5.983	.000	-2.592	-1.293

a. Dependent Variable: COPO5

Table D-44 COYQ

Model Summary[b]

Model	R	R Square	Adjusted R Square	Std. Error of the Estimate
1	.741[a]	.549	.484	18.65127

ANOVA[b]

Model		Sum of Squares	df	Mean Square	F	Sig.
1	Regression	26285.626	9	2920.625	8.396	.000[a]
	Residual	21567.923	62	347.870		
	Total	47853.550	71			

a. Predictors: (Constant), Dst, Betta, Bz, Speed, Bmag, Density, Tem, Byi, Bx

b. Dependent Variable: COYQ5

Coefficients[a]

Model		Unstandardized Coefficients		Standardized Coefficients	t	Sig.	95.0% Confidence Interval for B	
		B	Std. Error	Beta			Lower Bound	Upper Bound
1	(Constant)	60.490	21.254		2.846	.006	18.004	102.977
	B	4.366	1.337	.864	3.265	.002	1.693	7.039
	B_x	-5.396	1.723	-.836	-3.131	.003	-8.840	-1.951
	B_y	2.440	.954	.607	2.558	.013	.533	4.346
	B_z	2.598	1.112	.427	2.336	.023	.375	4.821
	T_p	5.220E-6	.000	.021	.100	.921	.000	.000
	N_p	-.527	.688	-.165	-.766	.447	-1.903	.849
	V_p	-.175	.040	-.711	-4.391	.000	-.255	-.095
	β	5.063	3.879	.241	1.305	.197	-2.690	12.816
	*D*st	.374	.250	.369	1.496	.140	-.126	.873

a. Dependent Variable: COYQ5

Table D-45 GOGA

Model Summary[b]

Model	R	R Square	Adjusted R Square	Std. Error of the Estimate
1	.917[a]	.841	.818	16.76233

ANOVA[b]

Model		Sum of Squares	df	Mean Square	F	Sig.
1	Regression	92211.464	9	10245.718	36.465	.000[a]
	Residual	17420.490	62	280.976		
	Total	109631.954	71			

a. Predictors: (Constant), Dst, Betta, Bz, Speed, Bmag, Density, Tem, Byi, Bx

b. Dependent Variable: GOGA5

Coefficients[a]

Model		Unstandardized Coefficients		Standardized Coefficients	t	Sig.	95.0% Confidence Interval for B	
		B	Std. Error	Beta			Lower Bound	Upper Bound
1	(Constant)	51.174	19.102		2.679	.009	12.990	89.358
	B	2.641	1.202	.345	2.197	.032	.238	5.043
	B_x	3.481	1.549	.356	2.248	.028	.386	6.577
	B_y	-1.577	.857	-.259	-1.840	.071	-3.290	.137
	B_z	-.620	.999	-.067	-.621	.537	-2.618	1.378
	T_p	.000	.000	.382	3.001	.004	.000	.000
	N_p	1.294	.619	.267	2.092	.041	.057	2.531
	V_p	-.185	.036	-.497	-5.166	.000	-.257	-.113
	β	-3.098	3.486	-.097	-.889	.378	-10.066	3.870
	*D*st	-.239	.224	-.156	-1.063	.292	-.687	.210

a. Dependent Variable: GOGA5

Table D-46 HUGO

Model Summary[b]

Model	R	R Square	Adjusted R Square	Std. Error of the Estimate
1	.553[a]	.306	.205	10.35892

ANOVA[b]

Model		Sum of Squares	df	Mean Square	F	Sig.
1	Regression	2934.666	9	326.074	3.039	.004[a]
	Residual	6653.042	62	107.307		
	Total	9587.708	71			

a. Predictors: (Constant), Dst, Betta, Bz, Speed, Bmag, Density, Tem, Byi, Bx

b. Dependent Variable: HUGO5

Coefficients[a]

Model		Unstandardized Coefficients		Standardized Coefficients	t	Sig.	95.0% Confidence Interval for B	
		B	Std. Error	Beta			Lower Bound	Upper Bound
1	(Constant)	15.288	11.805		1.295	.200	-8.309	38.885
	B	.590	.743	.261	.795	.430	-.894	2.075
	B_x	-2.007	.957	-.695	-2.097	.040	-3.920	-.094
	B_y	.820	.530	.456	1.548	.127	-.239	1.879
	B_z	.748	.618	.275	1.210	.231	-.487	1.982
	T_p	-6.901E-5	.000	-.630	-2.370	.021	.000	.000
	N_p	-.382	.382	-.266	-.999	.322	-1.146	.382
	V_p	.003	.022	.031	.152	.880	-.041	.048
	β	-.118	2.154	-.013	-.055	.956	-4.424	4.188
	Dst	.251	.139	.554	1.810	.075	-.026	.528

a. Dependent Variable: HUGO5

Table D- 47 IQQE

Model Summary[b]

Model	R	R Square	Adjusted R Square	Std. Error of the Estimate
1	.695[a]	.482	.407	19.15126

ANOVA[b]

Model		Sum of Squares	df	Mean Square	F	Sig.
	Regression	21188.429	9	2354.270	6.419	.000[a]
1	Residual	22739.791	62	366.771		
	Total	43928.220	71			

a. Predictors: (Constant), Dst, Betta, Bz, Speed, Bmag, Density, Tem, Byi, Bx

b. Dependent Variable: IQQE5

Coefficients[a]

Model		Unstandardized Coefficients		Standardized Coefficients			95.0% Confidence Interval for B	
		B	Std. Error	Beta	t	Sig.	Lower Bound	Upper Bound
1	(Constant)	-55.682	21.824		-2.551	.013	-99.308	-12.056
	B	-.223	1.373	-.046	-.162	.872	-2.967	2.522
	B_x	1.816	1.769	.294	1.026	.309	-1.721	5.353
	B_y	.437	.979	.114	.447	.657	-1.520	2.395
	B_z	-.231	1.142	-.040	-.202	.841	-2.513	2.052
	T_p	-1.723E-5	.000	-.073	-.320	.750	.000	.000
	N_p	1.287	.707	.419	1.820	.074	-.126	2.700
	V_p	.102	.041	.432	2.487	.016	.020	.184
	β	-2.996	3.983	-.149	-.752	.455	-10.957	4.965
	*D*st	-.706	.256	-.728	-2.753	.008	-1.219	-.193

a. Dependent Variable: IQQE5

Table D-48 LAFE

Model Summary[b]

Model	R	R Square	Adjusted R Square	Std. Error of the Estimate
1	.659[a]	.434	.352	16.49118

ANOVA[b]

Model		Sum of Squares	df	Mean Square	F	Sig.
1	Regression	12946.265	9	1438.474	5.289	.000[a]
	Residual	16861.464	62	271.959		
	Total	29807.728	71			

a. Predictors: (Constant), Dst, Betta, Bz, Speed, Bmag, Density, Tem, Byi, Bx

b. Dependent Variable: LAFE5

Coefficients[a]

Model		Unstandardized Coefficients		Standardized Coefficients	t	Sig.	95.0% Confidence Interval for B	
		B	Std. Error	Beta			Lower Bound	Upper Bound
1	(Constant)	-.070	18.793		-.004	.997	-37.636	37.496
	B	3.889	1.182	.976	3.289	.002	1.526	6.252
	B_x	-1.110	1.524	-.218	-.729	.469	-4.156	1.935
	B_y	1.288	.843	.406	1.528	.132	-.397	2.974
	B_z	.700	.983	.146	.712	.479	-1.265	2.666
	T_p	-1.407E-5	.000	-.073	-.304	.762	.000	.000
	N_p	-.712	.609	-.282	-1.170	.247	-1.929	.505
	V_p	-.042	.035	-.219	-1.205	.233	-.113	.028
	β	.634	3.429	.038	.185	.854	-6.221	7.489
	Dst	-.159	.221	-.199	-.720	.474	-.600	.283

a. Dependent Variable: LAFE5

Table D-49 LAMT

Model Summary[b]

Model	R	R Square	Adjusted R Square	Std. Error of the Estimate
1	.719[a]	.517	.447	19.576492

ANOVA[b]

Model		Sum of Squares	df	Mean Square	F	Sig.
1	Regression	25450.109	9	2827.790	7.379	.000[a]
	Residual	23760.820	62	383.239		
	Total	49210.929	71			

a. Predictors: (Constant), Dst, Betta, Bz, Speed, Bmag, Density, Tem, Byi, Bx

b. Dependent Variable: LAMT5

Coefficients[a]

Model		Unstandardized Coefficients		Standardized Coefficients	t	Sig.	95.0% Confidence Interval for B	
		B	Std. Error	Beta			Lower Bound	Upper Bound
1	(Constant)	47.234	22.309		2.117	.038	2.640	91.829
	B	-4.967	1.403	-.970	-3.539	.001	-7.773	-2.162
	B_x	.207	1.809	.032	.114	.909	-3.408	3.822
	B_y	.218	1.001	.054	.218	.828	-1.783	2.219
	B_z	-2.003	1.167	-.325	-1.716	.091	-4.337	.330
	T_p	2.335E-5	.000	.094	.424	.673	.000	.000
	N_p	.137	.723	.042	.190	.850	-1.307	1.582
	V_p	.046	.042	.183	1.091	.279	-.038	.129
	β	-10.501	4.071	-.492	-2.579	.012	-18.638	-2.363
	Dst	.372	.262	.362	1.418	.161	-.152	.896

a. Dependent Variable: LAMT5

Table D-50 POVE

Model Summary[b]

Model	R	R Square	Adjusted R Square	Std. Error of the Estimate
1	.784[a]	.615	.559	20.76950

ANOVA[b]

Model		Sum of Squares	df	Mean Square	F	Sig.
1	Regression	42648.354	9	4738.706	10.985	.000[a]
	Residual	26745.078	62	431.372		
	Total	69393.433	71			

a. Predictors: (Constant), Dst, Betta, Bz, Speed, Bmag, Density, Tem, Byi, Bx

b. Dependent Variable: POVE5

Coefficients[a]

Model		Unstandardized Coefficients		Standardized Coefficients	t	Sig.	95.0% Confidence Interval for B	
		B	Std. Error	Beta			Lower Bound	Upper Bound
1	(Constant)	139.960	23.668		5.913	.000	92.649	187.272
	B	-3.344	1.489	-.550	-2.246	.028	-6.321	-.368
	B_x	2.526	1.919	.325	1.317	.193	-1.309	6.362
	B_y	-.752	1.062	-.155	-.708	.482	-2.875	1.371
	B_z	-1.514	1.238	-.207	-1.223	.226	-3.989	.961
	T_p	3.201E-5	.000	.109	.548	.585	.000	.000
	N_p	.230	.767	.060	.300	.765	-1.302	1.763
	V_p	-.187	.044	-.632	-4.218	.000	-.276	-.098
	β	-7.495	4.319	-.296	-1.735	.088	-16.129	1.139
	Dst	-.025	.278	-.021	-.091	.928	-.581	.531

a. Dependent Variable: POVE5

Table D-51 RIOP

Model Summary[b]

Model	R	R Square	Adjusted R Square	Std. Error of the Estimate
1	.663[a]	.439	.358	19.20951

ANOVA[b]

Model		Sum of Squares	df	Mean Square	F	Sig.
1	Regression	17916.852	9	1990.761	5.395	.000[a]
	Residual	22878.336	62	369.005		
	Total	40795.188	71			

a. Predictors: (Constant), Dst, Betta, Bz, Speed, Bmag, Density, Tem, Byi, Bx

b. Dependent Variable: RIOP5

Coefficients[a]

Model		Unstandardized Coefficients		Standardized Coefficients	t	Sig.	95.0% Confidence Interval for B	
		B	Std. Error	Beta			Lower Bound	Upper Bound
1	(Constant)	63.018	21.890		2.879	.005	19.260	106.777
	B	1.053	1.377	.226	.765	.447	-1.700	3.806
	B_x	-2.163	1.775	-.363	-1.219	.228	-5.710	1.385
	B_y	1.556	.982	.420	1.584	.118	-.407	3.520
	B_z	.262	1.145	.047	.229	.820	-2.028	2.551
	T_p	.000	.000	-.526	-2.202	.031	.000	.000
	N_p	.108	.709	.037	.153	.879	-1.309	1.526
	V_p	-.123	.041	-.542	-3.000	.004	-.205	-.041
	β	1.702	3.995	.088	.426	.672	-6.284	9.687
	Dst	-.524	.257	-.560	-2.036	.046	-1.038	-.009

a. Dependent Variable: RIOP5

Table D-52 SCUB

Model Summary[b]

Model	R	R Square	Adjusted R Square	Std. Error of the Estimate
1	.492[a]	.242	.132	10.95532

ANOVA[b]

Model		Sum of Squares	df	Mean Square	F	Sig.
1	Regression	2379.300	9	264.367	2.203	.034[a]
	Residual	7441.177	62	120.019		
	Total	9820.477	71			

a. Predictors: (Constant), Dst, Betta, Bz, Speed, Bmag, Density, Tem, Byi, Bx

b. Dependent Variable: SCUB5

Coefficients[a]

Model		Unstandardized Coefficients		Standardized Coefficients	t	Sig.	95.0% Confidence Interval for B	
		B	Std. Error	Beta			Lower Bound	Upper Bound
1	(Constant)	26.640	12.484		2.134	.037	1.685	51.596
	B	-1.268	.785	-.554	-1.615	.111	-2.838	.302
	B_x	.569	1.012	.195	.562	.576	-1.454	2.592
	B_y	-.069	.560	-.038	-.124	.902	-1.189	1.051
	B_z	-.150	.653	-.055	-.230	.819	-1.456	1.155
	T_p	8.148E-6	.000	.073	.265	.792	.000	.000
	N_p	.122	.404	.084	.302	.763	-.686	.931
	V_p	-.021	.023	-.191	-.907	.368	-.068	.026
	β	-4.441	2.278	-.466	-1.949	.056	-8.995	.113
	Dst	-.031	.147	-.067	-.209	.835	-.324	.263

a. Dependent Variable: SCUB5

Table D-53 UNSA

Model Summary[b]

Model	R	R Square	Adjusted R Square	Std. Error of the Estimate
1	.728[a]	.530	.462	20.84830

ANOVA[b]

Model		Sum of Squares	df	Mean Square	F	Sig.
1	Regression	30413.775	9	3379.308	7.775	.000[a]
	Residual	26948.410	62	434.652		
	Total	57362.184	71			

a. Predictors: (Constant), Dst, Betta, Bz, Speed, Bmag, Density, Tem, Byi, Bx

b. Dependent Variable: UNSA5

Coefficients[a]

Model		Unstandardized Coefficients		Standardized Coefficients	t	Sig.	95.0% Confidence Interval for B	
		B	Std. Error	Beta			Lower Bound	Upper Bound
1	(Constant)	-34.837	23.758		-1.466	.148	-82.328	12.655
	B	.666	1.495	.121	.446	.657	-2.321	3.654
	B_x	3.152	1.926	.446	1.636	.107	-.698	7.002
	B_y	1.686	1.066	.383	1.581	.119	-.446	3.817
	B_z	-1.640	1.243	-.246	-1.319	.192	-4.125	.845
	T_p	.000	.000	-.464	-2.121	.038	.000	.000
	N_p	.178	.770	.051	.232	.818	-1.360	1.717
	V_p	.064	.045	.237	1.435	.156	-.025	.153
	β	2.986	4.335	.130	.689	.494	-5.681	11.652
	Dst	-1.184	.279	-1.068	-4.240	.000	-1.742	-.626

a. Dependent Variable: UNSA5

Event VI

Table D-54 BAIE

Model Summary[b]

Model	R	R Square	Adjusted R Square	Std. Error of the Estimate
1	.522[a]	.272	.166	33.63780

ANOVA[b]

Model		Sum of Squares	df	Mean Square	F	Sig.
1	Regression	26221.230	9	2913.470	2.575	.014[a]
	Residual	70153.087	62	1131.501		
	Total	96374.317	71			

a. Predictors: (Constant), Dst, Bz, Bye, Betta, Bx, Density, Tem, Bmag, Speed

b. Dependent Variable: BAIE6

Coefficients[a]

Model		Unstandardized Coefficients		Standardized Coefficients	t	Sig.
		B	Std. Error	Beta		
1	(Constant)	125.558	72.040		1.743	.086
	B	-.156	3.050	-.014	-.051	.959
	B_x	4.188	2.777	.278	1.508	.137
	B_y	2.675	2.040	.197	1.311	.195
	B_z	2.306	1.584	.225	1.455	.151
	T_p	.000	.000	-.531	-2.237	.029
	N_p	-.151	1.279	-.031	-.118	.906
	V_p	-.101	.102	-.350	-.989	.327
	β	-2.797	2.286	-.279	-1.223	.226
	Dst	-.386	.402	-.218	-.959	.341

a. Dependent Variable: BAIE6

Table D-55 BOGT

Model Summary

Model	R	R Square	Adjusted R Square	Std. Error of the Estimate	Change Statistics				
					R Square Change	F Change	df1	df2	Sig. F Change
1	.522[a]	.272	.166	19.41323	.272	2.573	9	62	.014

ANOVA[b]

Model		Sum of Squares	df	Mean Square	F	Sig.
1	Regression	8728.745	9	969.861	2.573	.014[a]
	Residual	23366.162	62	376.874		
	Total	32094.907	71			

a. Predictors: (Constant), Dst, Bz, Bye, Betta, Bx, Density, Tem, Bmag, Speed

b. Dependent Variable: BOGT6

Coefficients[a]

Model		Unstandardized Coefficients		Standardized Coefficients	t	Sig.	95.0% Confidence Interval for B	
		B	Std. Error	Beta			Lower Bound	Upper Bound
1	(Constant)	7.795	41.576		.187	.852	-75.314	90.905
	B	1.064	1.760	.163	.605	.548	-2.454	4.583
	B_x	-1.017	1.603	-.117	-.635	.528	-4.222	2.187
	B_y	-.079	1.177	-.010	-.067	.947	-2.433	2.274
	B_z	-.223	.914	-.038	-.244	.808	-2.051	1.605
	T_p	5.183E-5	.000	.301	1.267	.210	.000	.000
	N_p	-.409	.738	-.146	-.554	.581	-1.885	1.066
	V_p	-.045	.059	-.271	-.765	.447	-.163	.073
	β	2.256	1.319	.390	1.710	.092	-.382	4.893
	Dst	-.190	.232	-.186	-.819	.416	-.654	.274

a. Dependent Variable: BOGT6

Table D-56 BRAZ

Model Summary[b]

Model	R	R Square	Adjusted R Square	Std. Error of the Estimate
1	.646[a]	.417	.332	23.20270

ANOVA[b]

Model		Sum of Squares	df	Mean Square	F	Sig.
1	Regression	23881.427	9	2653.492	4.929	.000[a]
	Residual	33378.638	62	538.365		
	Total	57260.065	71			

a. Predictors: (Constant), Dst, Bz, Bye, Betta, Bx, Density, Tem, Bmag, Speed

b. Dependent Variable: BRAZ6

Coefficients[a]

Model		Unstandardized Coefficients		Standardized Coefficients	t	Sig.
		B	Std. Error	Beta		
1	(Constant)	-48.772	49.692		-.981	.330
	B	-1.882	2.104	-.215	-.895	.374
	B_x	-2.891	1.916	-.249	-1.509	.136
	B_y	1.480	1.407	.141	1.051	.297
	B_z	-2.453	1.093	-.310	-2.244	.028
	T_p	1.112E-5	.000	.048	.227	.821
	N_p	.072	.882	.019	.082	.935
	V_p	.062	.071	.277	.874	.386
	β	-.240	1.577	-.031	-.152	.880
	*D*st	-.419	.277	-.307	-1.513	.135

a. Dependent Variable: BRAZ6

Table D-57 CONO

Model Summary[b]

Model	R	R Square	Adjusted R Square	Std. Error of the Estimate
1	.635[a]	.403	.317	13.91696

ANOVA[b]

Model		Sum of Squares	df	Mean Square	F	Sig.
1	Regression	8117.512	9	901.946	4.657	.000[a]
	Residual	12008.268	62	193.682		
	Total	20125.780	71			

a. Predictors: (Constant), Dst, Bz, Bye, Betta, Bx, Density, Tem, Bmag, Speed

b. Dependent Variable: CONO6

Coefficients[a]

Model		Unstandardized Coefficients		Standardized Coefficients	t	Sig.
		B	Std. Error	Beta		
1	(Constant)	-32.416	29.805		-1.088	.281
	B	1.463	1.262	.282	1.160	.251
	B_x	-.488	1.149	-.071	-.425	.672
	B_y	.774	.844	.125	.917	.363
	B_z	-.139	.656	-.030	-.211	.833
	T_p	-3.164E-5	.000	-.232	-1.079	.285
	N_p	.449	.529	.202	.848	.400
	V_p	.051	.042	.386	1.204	.233
	β	-.476	.946	-.104	-.503	.617
	Dst	-.313	.166	-.386	-1.881	.065

a. Dependent Variable: CONO6

Table D-58 COYQ

Model Summary[b]

Model	R	R Square	Adjusted R Square	Std. Error of the Estimate
1	.783[a]	.613	.556	24.21477

ANOVA[b]

Model		Sum of Squares	df	Mean Square	F	Sig.
1	Regression	57509.943	9	6389.994	10.898	.000[a]
	Residual	36354.030	62	586.355		
	Total	93863.973	71			

a. Predictors: (Constant), Dst, Bz, Bye, Betta, Bx, Density, Tem, Bmag, Speed

b. Dependent Variable: COYQ6

Coefficients[a]

Model		Unstandardized Coefficients		Standardized Coefficients	t	Sig.
		B	Std. Error	Beta		
1	(Constant)	153.206	51.859		2.954	.004
	B	-.195	2.195	-.017	-.089	.930
	B_x	-2.676	1.999	-.180	-1.338	.186
	B_y	-2.125	1.468	-.158	-1.447	.153
	B_z	-.981	1.141	-.097	-.860	.393
	T_p	-4.121E-5	.000	-.140	-.808	.422
	N_p	-1.890	.921	-.395	-2.053	.044
	V_p	-.220	.074	-.769	-2.980	.004
	β	-6.211	1.646	-.628	-3.774	.000
	Dst	-.568	.289	-.325	-1.962	.054

a. Dependent Variable: COYQ6

Table D-59 LAMT

Model Summary[b]

Model	R	R Square	Adjusted R Square	Std. Error of the Estimate
1	.520[a]	.270	.164	11.63399

ANOVA[b]

Model		Sum of Squares	df	Mean Square	F	Sig.
1	Regression	3105.211	9	345.023	2.549	.015[a]
	Residual	8391.680	62	135.350		
	Total	11496.892	71			

a. Predictors: (Constant), Dst, Bz, Bye, Betta, Bx, Density, Tem, Bmag, Speed

b. Dependent Variable: LAMT6

Coefficients[a]

Model		Unstandardized Coefficients		Standardized Coefficients	t	Sig.
		B	Std. Error	Beta		
1	(Constant)	6.197	24.916		.249	.804
	B	.803	1.055	.205	.761	.449
	B_x	-.911	.961	-.175	-.948	.347
	B_y	-1.107	.706	-.236	-1.569	.122
	B_z	-.357	.548	-.101	-.651	.517
	T_p	3.930E-5	.000	.381	1.603	.114
	N_p	-.070	.442	-.042	-.157	.876
	V_p	-.024	.035	-.236	-.665	.509
	β	-.590	.791	-.170	-.747	.458
	Dst	.014	.139	.023	.102	.919

a. Dependent Variable: LAMT6

Table D-60 PARC

Model Summary[b]

Model	R	R Square	Adjusted R Square	Std. Error of the Estimate
1	.602[a]	.363	.270	25.23994

ANOVA[b]

Model		Sum of Squares	df	Mean Square	F	Sig.
1	Regression	22488.740	9	2498.749	3.922	.001[a]
	Residual	39497.382	62	637.055		
	Total	61986.122	71			

a. Predictors: (Constant), Dst, Bz, Bye, Betta, Bx, Density, Tem, Bmag, Speed

b. Dependent Variable: PARC6

Coefficients[a]

Model		Unstandardized Coefficients		Standardized Coefficients	t	Sig.
		B	Std. Error	Beta		
1	(Constant)	16.603	54.055		.307	.760
	B	.029	2.288	.003	.013	.990
	B_x	.874	2.084	.072	.419	.676
	B_y	2.400	1.531	.220	1.568	.122
	B_z	1.680	1.189	.204	1.413	.163
	T_p	.000	.000	-.852	-3.832	.000
	N_p	.070	.960	.018	.073	.942
	V_p	.032	.077	.139	.418	.677
	β	-2.351	1.715	-.292	-1.370	.175
	Dst	-.764	.302	-.538	-2.533	.014

a. Dependent Variable: PARC6

Table D-61 SCH2

Model Summary[b]

Model	R	R Square	Adjusted R Square	Std. Error of the Estimate
1	.452[a]	.204	.089	41.92212

ANOVA[b]

Model		Sum of Squares	df	Mean Square	F	Sig.
1	Regression	27953.432	9	3105.937	1.767	.093[a]
	Residual	108962.765	62	1757.464		
	Total	136916.197	71			

a. Predictors: (Constant), Dst, Bz, Bye, Betta, Bx, Density, Tem, Bmag, Speed

b. Dependent Variable: SCH26

Coefficients[a]

Model		Unstandardized Coefficients		Standardized Coefficients	t	Sig.
		B	Std. Error	Beta		
1	(Constant)	-57.666	89.782		-.642	.523
	B	-.616	3.801	-.046	-.162	.872
	B_x	1.149	3.461	.064	.332	.741
	B_y	5.241	2.542	.323	2.061	.043
	B_z	-2.927	1.975	-.239	-1.482	.143
	T_p	.000	.000	-.350	-1.408	.164
	N_p	-.084	1.594	-.015	-.053	.958
	V_p	.162	.128	.469	1.266	.210
	β	.308	2.849	.026	.108	.914
	*D*st	-.210	.501	-.099	-.419	.677

a. Dependent Variable: SCH26

SCUB

Table D-62 SCUB

Model Summary[b]

Model	R	R Square	Adjusted R Square	Std. Error of the Estimate
1	.504[a]	.254	.145	22.58999

ANOVA[b]

Model		Sum of Squares	df	Mean Square	F	Sig.
1	Regression	10754.632	9	1194.959	2.342	.024[a]
	Residual	31639.075	62	510.308		
	Total	42393.707	71			

a. Predictors: (Constant), Dst, Bz, Bye, Betta, Bx, Density, Tem, Bmag, Speed

b. Dependent Variable: SCUB6

Coefficients[a]

Model		Unstandardized Coefficients		Standardized Coefficients	t	Sig.
		B	Std. Error	Beta		
1	(Constant)	8.018	48.380		.166	.869
	B	-.620	2.048	-.082	-.303	.763
	B_x	-1.848	1.865	-.185	-.991	.326
	B_y	.441	1.370	.049	.322	.749
	B_z	-.070	1.064	-.010	-.066	.948
	T_p	.000	.000	-.514	-2.135	.037
	N_p	.629	.859	.195	.733	.467
	V_p	-.013	.069	-.069	-.194	.847
	β	-.387	1.535	-.058	-.252	.802
	Dst	-.700	.270	-.595	-2.592	.012

a. Dependent Variable: SCUB6

Table D-63 SG05

Model Summary[b]

Model	R	R Square	Adjusted R Square	Std. Error of the Estimate
1	.564[a]	.318	.219	18.26151

ANOVA[b]

Model		Sum of Squares	df	Mean Square	F	Sig.
1	Regression	9631.174	9	1070.130	3.209	.003[a]
	Residual	20675.931	62	333.483		
	Total	30307.105	71			

a. Predictors: (Constant), Dst, Bz, Bye, Betta, Bx, Density, Tem, Bmag, Speed

b. Dependent Variable: SG056

Coefficients[a]

Model		Unstandardized Coefficients		Standardized Coefficients	t	Sig.
		B	Std. Error	Beta		
1	(Constant)	-46.257	39.110		-1.183	.241
	B	1.192	1.656	.187	.720	.474
	B_x	-.193	1.508	-.023	-.128	.899
	B_y	1.584	1.107	.208	1.431	.158
	B_z	.894	.860	.156	1.040	.303
	T_p	.000	.000	-.927	-4.031	.000
	N_p	1.053	.694	.387	1.517	.134
	V_p	.102	.056	.627	1.830	.072
	β	-.442	1.241	-.079	-.356	.723
	Dst	-.465	.218	-.468	-2.130	.037

a. Dependent Variable: SG056

Table D-64 UNSA

Model Summary[b]

Model	R	R Square	Adjusted R Square	Std. Error of the Estimate
1	.663[a]	.439	.357	14.17691

ANOVA[b]

Model		Sum of Squares	df	Mean Square	F	Sig.
1	Regression	9748.802	9	1083.200	5.389	.000[a]
	Residual	12461.053	62	200.985		
	Total	22209.855	71			

a. Predictors: (Constant), Dst, Bz, Bye, Betta, Bx, Density, Tem, Bmag, Speed

b. Dependent Variable: UNSA6

Coefficients[a]

Model		Unstandardized Coefficients		Standardized Coefficients	t	Sig.
		B	Std. Error	Beta		
1	(Constant)	-5.615	30.362		-.185	.854
	B	1.153	1.285	.212	.897	.373
	B_x	-3.212	1.171	-.443	-2.744	.008
	B_y	1.745	.860	.267	2.029	.047
	B_z	-2.361	.668	-.480	-3.536	.001
	T_p	-2.730E-5	.000	-.191	-.914	.364
	N_p	-.756	.539	-.324	-1.403	.166
	V_p	.028	.043	.205	.659	.512
	β	1.819	.964	.378	1.888	.064
	Dst	.499	.169	.587	2.949	.004

a. Dependent Variable: UNSA6

Event VII

Table D-65 CONO

Model Summary[b]

Model	R	R Square	Adjusted R Square	Std. Error of the Estimate
1	.729[a]	.532	.464	9.66811

ANOVA[b]

Model		Sum of Squares	df	Mean Square	F	Sig.
1	Regression	6592.178	9	732.464	7.836	.000[a]
	Residual	5795.289	62	93.472		
	Total	12387.467	71			

a. Predictors: (Constant), Dst, Density, Bx, Betta, Bz, Tem, Bye, Speed, Bmag

b. Dependent Variable: CONO7

Coefficients[a]

Model		Unstandardized Coefficients		Standardized Coefficients	t	Sig.
		B	Std. Error	Beta		
1	(Constant)	-1.182	18.795		-.063	.950
	B	1.731	1.227	.389	1.411	.163
	B_x	-1.111	.718	-.158	-1.548	.127
	B_y	1.602	.490	.601	3.267	.002
	B_z	.151	.409	.044	.370	.713
	T_p	4.702E-5	.000	.268	1.338	.186
	N_p	-.253	.454	-.141	-.557	.580
	V_p	-.012	.038	-.072	-.307	.760
	β	3.005	2.396	.253	1.254	.215
	Dst	.106	.109	.197	.973	.335

a. Dependent Variable: CONO7

Table D-66 COPO

Model Summary[b]

Model	R	R Square	Adjusted R Square	Std. Error of the Estimate
1	.813[a]	.661	.612	25.72876

ANOVA[b]

Model		Sum of Squares	df	Mean Square	F	Sig.
	Regression	80120.961	9	8902.329	13.448	.000[a]
1	Residual	41042.095	62	661.969		
	Total	121163.057	71			

a. Predictors: (Constant), Dst, Density, Bx, Betta, Bz, Tem, Bye, Speed, Bmag

Coefficients[a]

Model		Unstandardized Coefficients		Standardized Coefficients	t	Sig.
		B	Std. Error	Beta		
1	(Constant)	87.145	50.017		1.742	.086
	B	-4.828	3.264	-.347	-1.479	.144
	B_x	-3.483	1.910	-.159	-1.823	.073
	B_y	-3.288	1.305	-.394	-2.520	.014
	B_z	-3.699	1.089	-.344	-3.398	.001
	T_p	.000	.000	-.296	-1.740	.087
	N_p	-.253	1.209	-.045	-.209	.835
	V_p	-.177	.102	-.347	-1.732	.088
	β	-5.036	6.376	-.136	-.790	.433
	*D*st	-1.043	.290	-.620	-3.600	.001

a. Dependent Variable: COPO7

Table D-67 COQY

Model Summary[b]

Model	R	R Square	Adjusted R Square	Std. Error of the Estimate
1	.776[a]	.603	.545	30.96496

ANOVA[b]

Model		Sum of Squares	df	Mean Square	F	Sig.
1	Regression	90226.100	9	10025.122	10.456	.000[a]
	Residual	59447.392	62	958.829		
	Total	149673.493	71			

a. Predictors: (Constant), Dst, Density, Bx, Betta, Bz, Tem, Bye, Speed, Bmag

b. Dependent Variable: COYQ7

Coefficients[a]

Model		Unstandardized Coefficients		Standardized Coefficients	t	Sig.
		B	Std. Error	Beta		
1	(Constant)	233.351	60.197		3.876	.000
	B	-4.724	3.928	-.306	-1.203	.234
	B_x	-8.801	2.299	-.360	-3.828	.000
	B_y	1.427	1.570	.154	.909	.367
	B_z	1.698	1.310	.142	1.296	.200
	T_p	7.480E-6	.000	.012	.066	.947
	N_p	-.456	1.455	-.073	-.314	.755
	V_p	-.458	.123	-.805	-3.714	.000
	β	4.042	7.674	.098	.527	.600
	Dst	-.506	.349	-.271	-1.451	.152

a. Dependent Variable: COYQ7

Table D-68 GOGA

Model Summary[b]

Model	R	R Square	Adjusted R Square	Std. Error of the Estimate
1	.870[a]	.757	.722	11.14770

ANOVA[b]

Model		Sum of Squares	df	Mean Square	F	Sig.
1	Regression	24016.828	9	2668.536	21.473	.000[a]
	Residual	7704.816	62	124.271		
	Total	31721.644	71			

a. Predictors: (Constant), Dst, Density, Bx, Betta, Bz, Tem, Bye, Speed, Bmag

b. Dependent Variable: GOGA7

Coefficients[a]

Model		Unstandardized Coefficients		Standardized Coefficients	t	Sig.
		B	Std. Error	Beta		
1	(Constant)	-65.436	21.671		-3.019	.004
	B	3.862	1.414	.543	2.731	.008
	B_x	-2.184	.828	-.194	-2.638	.011
	B_y	4.273	.565	1.001	7.559	.000
	B_z	2.325	.472	.422	4.930	.000
	T_p	8.950E-5	.000	.318	2.208	.031
	N_p	.764	.524	.266	1.460	.149
	V_p	.069	.044	.263	1.551	.126
	β	3.319	2.763	.175	1.201	.234
	Dst	-.067	.125	-.078	-.536	.594

a. Dependent Variable: GOGA7

Table D-69 IQQE

Model Summary[b]

Model	R	R Square	Adjusted R Square	Std. Error of the Estimate
1	.466[a]	.217	.104	18.97641

ANOVA[b]

Model		Sum of Squares	df	Mean Square	F	Sig.
1	Regression	6203.577	9	689.286	1.914	.066[a]
	Residual	22326.446	62	360.104		
	Total	28530.023	71			

a. Predictors: (Constant), Dst, Density, Bx, Betta, Bz, Tem, Bye, Speed, Bmag

b. Dependent Variable: IQQE7

Coefficients[a]

Model		Unstandardized Coefficients		Standardized Coefficients	t	Sig.
		B	Std. Error	Beta		
1	(Constant)	33.446	36.891		.907	.368
	B	-.257	2.407	-.038	-.107	.915
	B_x	-3.787	1.409	-.355	-2.688	.009
	B_y	1.125	.962	.278	1.169	.247
	B_z	-.040	.803	-.008	-.049	.961
	T_p	1.069E-5	.000	.040	.155	.877
	N_p	-.643	.892	-.236	-.721	.473
	V_p	-.069	.076	-.280	-.918	.362
	β	2.378	4.703	.132	.506	.615
	Dst	-.471	.214	-.578	-2.206	.031

a. Dependent Variable: IQQE7

Table D-70 POVE

Model Summary[b]

Model	R	R Square	Adjusted R Square	Std. Error of the Estimate
1	.476[a]	.226	.114	10.13470

ANOVA[b]

Model		Sum of Squares	df	Mean Square	F	Sig.
1	Regression	1861.498	9	206.833	2.014	.053[a]
	Residual	6368.156	62	102.712		
	Total	8229.654	71			

a. Predictors: (Constant), Dst, Density, Bx, Betta, Bz, Tem, Bye, Speed, Bmag

b. Dependent Variable: POVE7

Coefficients[a]

Model		Unstandardized Coefficients		Standardized Coefficients	t	Sig.
		B	Std. Error	Beta		
1	(Constant)	46.326	19.702		2.351	.022
	B	-1.335	1.286	-.368	-1.038	.303
	B_x	-2.263	.752	-.395	-3.008	.004
	B_y	-.196	.514	-.090	-.382	.704
	B_z	.077	.429	.027	.179	.858
	T_p	3.436E-5	.000	.240	.933	.355
	N_p	.094	.476	.064	.198	.844
	V_p	-.092	.040	-.688	-2.273	.027
	β	-.335	2.512	-.035	-.133	.894
	*D*st	-.164	.114	-.373	-1.433	.157

a. Dependent Variable: POVE7

Table D-71 RIOP

Model Summary[b]

Model	R	R Square	Adjusted R Square	Std. Error of the Estimate
1	.693[a]	.481	.405	11.62572

ANOVA[b]

Model		Sum of Squares	df	Mean Square	F	Sig.
1	Regression	7756.651	9	861.850	6.377	.000[a]
	Residual	8379.752	62	135.157		
	Total	16136.403	71			

a. Predictors: (Constant), Dst, Density, Bx, Betta, Bz, Tem, Bye, Speed, Bmag

b. Dependent Variable: RIOP7

Coefficients[a]

Model		Unstandardized Coefficients		Standardized Coefficients	t	Sig.
		B	Std. Error	Beta		
1	(Constant)	36.853	22.601		1.631	.108
	B	-3.106	1.475	-.612	-2.106	.039
	B_x	-1.726	.863	-.215	-2.000	.050
	B_y	-.842	.590	-.277	-1.429	.158
	B_z	-1.074	.492	-.273	-2.184	.033
	T_p	.000	.000	-.530	-2.515	.014
	N_p	-.468	.546	-.229	-.857	.395
	V_p	.000	.046	-.005	-.019	.985
	β	-1.236	2.881	-.091	-.429	.669
	Dst	-.306	.131	-.499	-2.336	.023

a. Dependent Variable: RIOP7

Table D-72 SCH2

Model Summary[b]

Model	R	R Square	Adjusted R Square	Std. Error of the Estimate
1	.855[a]	.731	.692	14.22651

ANOVA[b]

Model		Sum of Squares	df	Mean Square	F	Sig.
1	Regression	34057.999	9	3784.222	18.697	.000[a]
	Residual	12548.395	62	202.393		
	Total	46606.394	71			

a. Predictors: (Constant), Dst, Density, Bx, Betta, Bz, Tem, Bye, Speed, Bmag

b. Dependent Variable: SCH27

Coefficients[a]

Model		Unstandardized Coefficients		Standardized Coefficients	t	Sig.
		B	Std. Error	Beta		
1	(Constant)	-86.970	27.657		-3.145	.003
	B	6.511	1.805	.755	3.607	.001
	B_x	-2.378	1.056	-.175	-2.251	.028
	B_y	1.796	.721	.347	2.490	.015
	B_z	.461	.602	.069	.766	.446
	T_p	5.026E-5	.000	.148	.972	.335
	N_p	1.250	.668	.359	1.871	.066
	V_p	.042	.057	.133	.742	.461
	β	8.418	3.526	.366	2.388	.020
	Dst	-.352	.160	-.338	-2.201	.031

a. Dependent Variable: SCH27

Table D-73 SCUB

Model Summary[b]

Model	R	R Square	Adjusted R Square	Std. Error of the Estimate
1	.470[a]	.221	.108	12.31271

ANOVA[b]

Model		Sum of Squares	df	Mean Square	F	Sig.
1	Regression	2664.430	9	296.048	1.953	.061[a]
	Residual	9399.370	62	151.603		
	Total	12063.800	71			

a. Predictors: (Constant), Dst, Density, Bx, Betta, Bz, Tem, Bye, Speed, Bmag

b. Dependent Variable: SCUB7

Coefficients[a]

Model		Unstandardized Coefficients		Standardized Coefficients	t	Sig.
		B	Std. Error	Beta		
1	(Constant)	-23.457	23.936		-.980	.331
	B	2.114	1.562	.482	1.354	.181
	B_x	1.910	.914	.275	2.089	.041
	B_y	.487	.624	.185	.779	.439
	B_z	-.905	.521	-.266	-1.737	.087
	T_p	2.819E-5	.000	.163	.630	.531
	N_p	-.582	.578	-.329	-1.005	.319
	V_p	-.003	.049	-.019	-.062	.951
	β	2.940	3.051	.251	.964	.339
	*D*st	.123	.139	.232	.887	.379

a. Dependent Variable: SCUB7

Table D-74 UNSA

Model Summary[b]

Model	R	R Square	Adjusted R Square	Std. Error of the Estimate
1	.478[a]	.228	.116	21.55069

ANOVA[b]

Model		Sum of Squares	df	Mean Square	F	Sig.
1	Regression	8505.140	9	945.016	2.035	.050[a]
	Residual	28794.803	62	464.432		
	Total	37299.943	71			

a. Predictors: (Constant), Dst, Density, Bx, Betta, Bz, Tem, Bye, Speed, Bmag

b. Dependent Variable: UNSA7

Coefficients[a]

Model		Unstandardized Coefficients		Standardized Coefficients	t	Sig.
		B	Std. Error	Beta		
1	(Constant)	7.934	41.895		.189	.850
	B	-.413	2.734	-.054	-.151	.880
	B_x	-4.943	1.600	-.405	-3.089	.003
	B_y	.896	1.093	.194	.820	.415
	B_z	-.527	.912	-.088	-.578	.565
	T_p	-2.072E-6	.000	-.007	-.026	.979
	N_p	.558	1.012	.179	.551	.583
	V_p	.033	.086	.116	.384	.702
	β	-1.778	5.341	-.086	-.333	.740
	Dst	-.331	.243	-.355	-1.364	.178

a. Dependent Variable: UNSA7

Table D-75 VALP

Model Summary[b]

Model	R	R Square	Adjusted R Square	Std. Error of the Estimate
1	.732[a]	.536	.432	11.14404

ANOVA[b]

Model		Sum of Squares	df	Mean Square	F	Sig.
1	Regression	5744.904	9	638.323	5.140	.000[a]
	Residual	4967.581	40	124.190		
	Total	10712.485	49			

a. Predictors: (Constant), Dst, Bz, Bmag, Bx, Bye, Tem, Betta, Density, Speed

b. Dependent Variable: VALP7

Coefficients[a]

Model		Unstandardized Coefficients		Standardized Coefficients	t	Sig.
		B	Std. Error	Beta		
1	(Constant)	46.046	29.980		1.536	.132
	B	1.617	3.075	.199	.526	.602
	B_x	-2.281	1.199	-.311	-1.903	.064
	B_y	-1.303	.905	-.397	-1.440	.158
	B_z	1.485	.940	.252	1.581	.122
	T_p	-3.515E-5	.000	-.196	-.482	.633
	N_p	-3.678	1.389	-1.054	-2.647	.012
	V_p	-.058	.073	-.361	-.803	.427
	β	7.158	4.570	.595	1.566	.125
	*D*st	.013	.449	.013	.030	.976

a. Dependent Variable: VALP7

VITA

Sorasit Thanomponkrang was born on March 5, 1987 in Bangkok, Thailand. He was a graduate student of Earth sciences program at Chulalongkorn university, Thailand. He received his B.Sc. in Marine sciences from Kasetsart university.

Presentation

Sorasit Thanomponkrung (2013) The Total Electron Content Deviation During Magnetic Clouds Transtent. The 27th National Graduate Research Conference, Naresuan University, Pitsanulok, Thailand.